An Evaluation of the Model Potential and Pseudopotential Methods for the Calculation of Interatomic Potentials

by

Colin Raymond Mason

Volume 2 : Annexes A - F and References

Thesis submitted for the degree of Doctor of Philosophy
in the Faculty of Science of the University of London

University College London
November 1990

Annex A

Coordinate Transformations

Appendix A1 Coordinate Transformation 1

A1.1 Introduction

The purpose of this appendix is to transform the coordinates $\mathbf{r}_{oe}$, $\mathbf{R}_A$ and $\mathbf{R}_B$ of the Schrödinger equation

$$\left[-\frac{\hbar^2}{2m_e}\nabla^2_{\mathbf{r}_{oe}} - \frac{\hbar^2}{2M_A}\nabla^2_{\mathbf{R}_A} - \frac{\hbar^2}{2M_B}\nabla^2_{\mathbf{R}_B} + V(\mathbf{r}_{oe}, \mathbf{R}_A, \mathbf{R}_B) - E_T \right] \Psi_T = 0 \qquad \text{(A1.1.1)}$$

to the coordinates $\mathbf{r}_{Ae}$, $\mathbf{R'}_A$, $\mathbf{R'}_B$ given by

$$\mathbf{r}_{Ae} = \mathbf{r}_{oe} - \mathbf{R}_A \,, \qquad \text{(A1.1.2)}$$

$$\mathbf{R'}_A = \frac{M_A\mathbf{R}_A + m_e\mathbf{r}_{oe}}{M_A + m_e} \,, \qquad \text{(A1.1.3)}$$

$$\mathbf{R'}_B = \mathbf{R}_B. \qquad \text{(A1.1.4)}$$

A1.2 The Transformation

The kinetic energy terms

$$\left[-\frac{\hbar^2}{2m_e}\nabla^2_{\mathbf{r}_{oe}} - \frac{\hbar^2}{2M_A}\nabla^2_{\mathbf{R}_A} \right] \Psi_T \qquad \text{(A1.2.1)}$$

are treated first. The eigenfunction Ψ_T may be considered to be a function of coordinates $(\mathbf{r}_{oe}, \mathbf{R}_A)$ or of coordinates $(\mathbf{r}_{Ae}, \mathbf{R'}_A)$. With the latter, and considering just the x-component of each vector, denoted (x_{Ae}, X'_A), the total differential $d\Psi_T$ is

$$d\Psi_T = \frac{\partial\Psi_T}{\partial x_{Ae}}\, dx_{Ae} + \frac{\partial\Psi_T}{\partial X'_A}\, dX'_A \,. \qquad \text{(A1.2.2)}$$

From Eqs.A1.1.2 and A1.1.3, the differentials dx_{Ae} and dX'_A are

$$dx_{Ae} = dx_{oe} - dX_A \,, \qquad \text{(A1.2.3)}$$

$$dX'_A = \left\{\frac{M_A}{M_A + m_e}\right\} dX_A + \left\{\frac{m_e}{M_A + m_e}\right\} dx_{oe} \qquad \text{(A1.2.4)}$$

where (x_{oe}, X_A) are the x-components of coordinates $(\mathbf{r}_{oe}, \mathbf{R}_A)$. With these, Eq.A1.2.2 becomes

$$d\Psi_T = \left[\left\{\frac{M_A}{M_A + m_e}\right\} \frac{\partial \Psi_T}{\partial X'_A} - \frac{\partial \Psi_T}{\partial x_{Ae}} \right] dX_A + \left[\left\{\frac{m_e}{M_A + m_e}\right\} \frac{\partial \Psi_T}{\partial X'_A} + \frac{\partial \Psi_T}{\partial x_{Ae}} \right] dx_{oe}. \qquad \text{(A1.2.5)}$$

Considering Ψ_T now to be a function of coordinates $(\mathbf{r}_{oe}, \mathbf{R}_A)$, the differential in Eq.A1.2.5 yields the transformation of the first derivatives:

$$\frac{\partial \Psi_T}{\partial X_A} = \left\{\frac{M_A}{M_A + m_e}\right\} \frac{\partial \Psi_T}{\partial X'_A} - \frac{\partial \Psi_T}{\partial x_{Ae}}, \qquad \text{(A1.2.6)}$$

$$\frac{\partial \Psi_T}{\partial x_{oe}} = \left\{\frac{m_e}{M_A + m_e}\right\} \frac{\partial \Psi_T}{\partial X'_A} + \frac{\partial \Psi_T}{\partial x_{Ae}}. \qquad \text{(A1.2.7)}$$

In order to obtain the transformation of the second derivatives of Ψ_T, the functions

$$G(x_{Ae}, X'_A) = \frac{\partial \Psi_T}{\partial X_A}, \qquad \text{(A1.2.8)}$$

$$H(x_{Ae}, X'_A) = \frac{\partial \Psi_T}{\partial x_{oe}} \qquad \text{(A1.2.9)}$$

are defined so that

$$\frac{\partial^2 \Psi_T}{\partial X_A^2} = \frac{\partial G}{\partial X_A} \quad ; \quad \frac{\partial^2 \Psi_T}{\partial x_{oe}^2} = \frac{\partial H}{\partial x_{oe}}. \qquad \text{(A1.2.10)}$$

Since Eqs.A1.2.6 and A1.2.7 are true for any function Ψ_T, they must hold also for the functions $G(x_{Ae}, X'_A)$ and $H(x_{Ae}, X'_A)$. Replacing Ψ_T in Eq.A1.2.6 by G and Ψ_T in Eq.A1.2.7 by H gives

$$\frac{\partial G}{\partial X_A} = \left\{\frac{M_A}{M_A + m_e}\right\} \frac{\partial G}{\partial X'_A} - \frac{\partial G}{\partial x_{Ae}} = \frac{\partial^2 \Psi_T}{\partial X_A^2}, \qquad \text{(A1.2.11)}$$

$$\frac{\partial H}{\partial x_{oe}} = \left\{\frac{m_e}{M_A + m_e}\right\} \frac{\partial H}{\partial X'_A} + \frac{\partial H}{\partial x_{Ae}} = \frac{\partial^2 \Psi_T}{\partial x_{oe}^2}. \qquad \text{(A1.2.12)}$$

The partial derivatives of functions G and H with respect to x_{Ae} and X'_A are obtained from Eqs.A1.2.6 and A1.2.7 and leads to the transformation of the second derivatives :

$$\frac{\partial^2 \Psi_T}{\partial X_A^2} = \left\{\frac{M_A}{M_A + m_e}\right\}^2 \frac{\partial^2 \Psi_T}{\partial X'^2_A} - \left\{\frac{M_A}{M_A + m_e}\right\} \left[\frac{\partial^2 \Psi_T}{\partial X'_A \partial x_{Ae}} + \frac{\partial^2 \Psi_T}{\partial x_{Ae} \partial X'_A}\right] + \frac{\partial^2 \Psi_T}{\partial x_{Ae}^2}, \qquad \text{(A1.2.13)}$$

$$\frac{\partial^2 \Psi_T}{\partial x_{oe}^2} = \left\{\frac{m_e}{M_A + m_e}\right\}^2 \frac{\partial^2 \Psi_T}{\partial X'^2_A} + \left\{\frac{m_e}{M_A + m_e}\right\} \left[\frac{\partial^2 \Psi_T}{\partial X'_A \partial x_{Ae}} + \frac{\partial^2 \Psi_T}{\partial x_{Ae} \partial X'_A}\right] + \frac{\partial^2 \Psi_T}{\partial x_{Ae}^2}. \qquad \text{(A1.2.14)}$$

These expressions allow the x-components of the terms in Eq.A1.2.1 to be written

$$-\frac{\hbar^2}{2m_e} \frac{\partial^2 \Psi_T}{\partial x_{oe}^2} - \frac{\hbar^2}{2M_A} \frac{\partial^2 \Psi_T}{\partial X_A^2} = -\frac{\hbar^2}{2} \left\{\frac{1}{m_e} + \frac{1}{M_A}\right\} \frac{\partial^2 \Psi_T}{\partial x_{Ae}^2} - \frac{\hbar^2}{2(M_A + m_e)} \frac{\partial^2 \Psi_T}{\partial X'^2_A}. \qquad \text{(A1.2.15)}$$

In the first term on the rhs of Eq.A1.2.15, $\left\{\frac{1}{M_A}\right\}$ is negligible in comparison with $\left\{\frac{1}{m_e}\right\}$ and is ignored. The y- and z-components of (r_{oe}, R_A) transform in exactly the same way, leading to the transformation of the kinetic energy terms of Eq.A1.2.1 as follows :

$$\left[-\frac{\hbar^2}{2m_e} \nabla^2_{r_{oe}} - \frac{\hbar^2}{2M_A} \nabla^2_{R_A}\right] \Psi_T \rightarrow \left[-\frac{\hbar^2}{2m_e} \nabla^2_{r_{Ae}} - \frac{\hbar^2}{2(M_A + m_e)} \nabla^2_{R'_A}\right] \Psi_T. \qquad \text{(A1.2.16)}$$

The transformation of the kinetic energy term for the rare gas atom is straight forward, since the vectors R'_B and R_B are identical; thus

$$\left[-\frac{\hbar^2}{2M_B} \nabla^2_{R_B}\right] \Psi_T \rightarrow \left[-\frac{\hbar^2}{2M_B} \nabla^2_{R'_B}\right] \Psi_T. \qquad \text{(A1.2.17)}$$

Applying the transformations of Eqs.A1.2.16 and A1.2.17 to Eq.A1.1.1 yields the Schrödinger equation in terms of coordinates (r_{Ae}, R'_A, R'_B), completing the required transformation:

$$\left[-\frac{\hbar^2}{2m_e} \nabla^2_{r_{Ae}} - \frac{\hbar^2}{2(M_A + m_e)} \nabla^2_{R'_A} - \frac{\hbar^2}{2M_B} \nabla^2_{R'_B} + V(r_{Ae}, R'_A, R'_B) - E_T\right] \Psi_T = 0. \qquad \text{(A1.2.18)}$$

Appendix A2 Coordinate Transformation 2

A2.1 Introduction

The purpose of this appendix is to transform the coordinates $\mathbf{R'}_A$ and $\mathbf{R'}_B$ of the Schrödinger equation

$$\left[-\frac{\hbar^2}{2m_e}\nabla^2_{r_{Ae}} - \frac{\hbar^2}{2(M_A+m_e)}\nabla^2_{R'_A} - \frac{\hbar^2}{2M_B}\nabla^2_{R'_B} + V(r_{Ae}, R'_A, R'_B) - E_T \right] \Psi_T = 0 \qquad \text{(A2.1.1)}$$

to the coordinates $\mathbf{R'}$, $\mathbf{R}_{cm}$ given by

$$\mathbf{R'} = \mathbf{R'}_B - \mathbf{R'}_A\,, \qquad \text{(A2.1.2)}$$

$$\mathbf{R}_{cm} = \left\{\frac{M_A+m_e}{M}\right\}\mathbf{R'}_A + \left\{\frac{M_B}{M}\right\}\mathbf{R'}_B\,. \qquad \text{(A2.1.3)}$$

A2.2 The Transformation

The kinetic energy terms to be transformed are

$$\left[-\frac{\hbar^2}{2(M_A+m_e)}\nabla^2_{R'_A} - \frac{\hbar^2}{2M_B}\nabla^2_{R'_B} \right] \Psi_T\,. \qquad \text{(A2.2.1)}$$

The eigenfunction Ψ_T may be considered to be a function of coordinates $(\mathbf{R'}_A, \mathbf{R'}_B)$ or of coordinates $(\mathbf{R'}, \mathbf{R}_{cm})$. With the latter, and considering just the x-component of each vector, denoted (X', X'_{cm}), the total differential $d\Psi_T$ is

$$d\Psi_T = \frac{\partial\Psi_T}{\partial X'}\,dX' + \frac{\partial\Psi_T}{\partial X_{cm}}\,dX_{cm}\,. \qquad \text{(A2.2.2)}$$

From Eqs.A2.1.2 and A2.1.3, the differentials dX' and dX_{cm} are

$$dX' = dX'_B - dX'_A\,, \qquad \text{(A2.2.3)}$$

$$dX_{cm} = \left\{\frac{M_A+m_e}{M}\right\}dX'_A + \left\{\frac{M_B}{M}\right\}dX'_B \qquad \text{(A2.2.4)}$$

where (X'_A, X'_B) are the x-components of coordinates (R'_A, R'_B). With these, Eq.A2.2.2 becomes

$$d\Psi_T = \left[\left\{\frac{M_A + m_e}{M}\right\} \frac{\partial \Psi_T}{\partial X_{cm}} - \frac{\partial \Psi_T}{\partial X'} \right] dX'_A + \left[\left\{\frac{M_B}{M}\right\} \frac{\partial \Psi_T}{\partial X_{cm}} + \frac{\partial \Psi_T}{\partial X'} \right] dX'_B . \tag{A2.2.5}$$

Considering Ψ_T now to be a function of coordinates (R'_A, R'_B), the differential in Eq.A2.2.5 yields the transformation of the first derivatives:

$$\frac{\partial \Psi_T}{\partial X'_A} = \left\{\frac{M_A + m_e}{M}\right\} \frac{\partial \Psi_T}{\partial X_{cm}} - \frac{\partial \Psi_T}{\partial X'}, \tag{A2.2.6}$$

$$\frac{\partial \Psi_T}{\partial X'_B} = \left\{\frac{M_B}{M}\right\} \frac{\partial \Psi_T}{\partial X_{cm}} + \frac{\partial \Psi_T}{\partial X'} . \tag{A2.2.7}$$

In order to obtain the transformation of the second derivatives of Ψ_T, the functions

$$G(X', X_{cm}) = \frac{\partial \Psi_T}{\partial X'_A}, \tag{A2.2.8}$$

$$H(X', X_{cm}) = \frac{\partial \Psi_T}{\partial X'_B} \tag{A2.2.9}$$

are defined so that

$$\frac{\partial^2 \Psi_T}{\partial X'^2_A} = \frac{\partial G}{\partial X'_A} \quad ; \quad \frac{\partial^2 \Psi_T}{\partial X'^2_B} = \frac{\partial H}{\partial X'_B} . \tag{A2.2.10}$$

Since Eqs.A2.2.6 and A2.2.7 are true for any function Ψ_T, they must hold also for the functions $G(X', X_{cm})$ and $H(X', X_{cm})$. Replacing Ψ_T in Eq.A2.2.6 by G and Ψ_T in Eq.A2.2.7 by H gives

$$\frac{\partial G}{\partial X'_A} = \left\{\frac{M_A + m_e}{M}\right\} \frac{\partial G}{\partial X_{cm}} - \frac{\partial G}{\partial X'} = \frac{\partial^2 \Psi_T}{\partial X'^2_A}, \tag{A2.2.11}$$

$$\frac{\partial H}{\partial X'_B} = \left\{\frac{M_B}{M}\right\} \frac{\partial H}{\partial X_{cm}} + \frac{\partial H}{\partial X'} = \frac{\partial^2 \Psi_T}{\partial X'^2_B} . \tag{A2.2.12}$$

The partial derivatives of functions G and H with respect to X' and X_{cm} are obtained from Eqs.A2.2.6 and A2.2.7 and leads to the transformation of the second derivatives :

$$\frac{\partial^2\Psi_T}{\partial X'^2_A} = \left\{\frac{M_A + m_e}{M}\right\}^2 \frac{\partial^2\Psi_T}{\partial X^2_{cm}} - \left\{\frac{M_A + m_e}{M}\right\}\left[\frac{\partial^2\Psi_T}{\partial X_{cm}\partial X'} + \frac{\partial^2\Psi_T}{\partial X'\partial X_{cm}}\right] + \frac{\partial^2\Psi_T}{\partial X'^2}, \qquad \text{(A2.2.13)}$$

$$\frac{\partial^2\Psi_T}{\partial X'^2_B} = \left\{\frac{M_B}{M}\right\}^2 \frac{\partial^2\Psi_T}{\partial X^2_{cm}} + \left\{\frac{M_B}{M}\right\}\left[\frac{\partial^2\Psi_T}{\partial X_{cm}\partial X'} + \frac{\partial^2\Psi_T}{\partial X'\partial X_{cm}}\right] + \frac{\partial^2\Psi_T}{\partial X'^2}. \qquad \text{(A2.2.14)}$$

These expressions allow the x-components of the terms in Eq.A2.2.1 to be written

$$-\frac{\hbar^2}{2(M_A + m_e)}\frac{\partial^2\Psi_T}{\partial X'^2_A} - \frac{\hbar^2}{2M_B}\frac{\partial^2\Psi_T}{\partial X'^2_B} = -\frac{\hbar^2}{2M}\frac{\partial^2\Psi_T}{\partial X^2_{cm}} - \frac{\hbar^2}{2\mu}\frac{\partial^2\Psi_T}{\partial X'^2} \qquad \text{(A2.2.15)}$$

where μ is the reduced mass of the two atoms, defined by

$$\mu = \frac{(M_A + m_e)\,M_B}{M}. \qquad \text{(A2.2.16)}$$

The y- and z-components of $(\mathbf{R'}_A, \mathbf{R'}_B)$ transform in exactly the same way, leading to the transformation of the kinetic energy terms of Eq.A2.2.1 as follows :

$$\left[-\frac{\hbar^2}{2(M_A + m_e)}\nabla^2_{\mathbf{R'}_A} - \frac{\hbar^2}{2M_B}\nabla^2_{\mathbf{R'}_B}\right]\Psi_T \rightarrow \left[-\frac{\hbar^2}{2M}\nabla^2_{\mathbf{R}_{cm}} - \frac{\hbar^2}{2\mu}\nabla^2_{\mathbf{R'}}\right]\Psi_T. \qquad \text{(A2.2.17)}$$

Applying the transformation of Eq.A2.2.17 to Eq.A2.1.1 yields the Schrödinger equation in terms of coordinates $(\mathbf{r}_{Ae}, \mathbf{R'}, \mathbf{R}_{cm})$, completing the required transformation:

$$\left[-\frac{\hbar^2}{2m_e}\nabla^2_{\mathbf{r}_{Ae}} - \frac{\hbar^2}{2M}\nabla^2_{\mathbf{R}_{cm}} - \frac{\hbar^2}{2\mu}\nabla^2_{\mathbf{R'}} + V(\mathbf{r}_{Ae}, \mathbf{R'}) - E_T\right]\Psi_T = 0. \qquad \text{(A2.2.18)}$$

Annex B

The Theoretical Alkali-Rare Gas Interatomic Potentials

Appendix B1 The Alkali-Rare Gas Interatomic Potentials of Peach

B1.1 Introduction

This appendix lists, in numerical form, the theoretical alkali-rare gas interatomic potentials calculated by Peach (1988). On the following pages are eight tables, each one containing data for one alkali-rare gas system and one type of interatomic potential (model potential or pseudopotential). The data presented in each table consist of the following quantities:

(i) R - the internuclear separation;

(ii) $V(X^2\Sigma)$ - the $X^2\Sigma$ interatomic potential as a function of R;

(iii) $V(B^2\Sigma)$ - the $B^2\Sigma$ interatomic potential as a function of R;

(iv) $V(A^2\Pi)$ - the $A^2\Pi$ interatomic potential as a function of R;

(v) $D_{\Lambda',\Lambda}(B^2\Sigma - X^2\Sigma)$ - the dipole transition moment for $B^2\Sigma - X^2\Sigma$ electronic transitions as a function of R;

(vi) $D_{\Lambda',\Lambda}(A^2\Pi - X^2\Sigma)$ - the dipole transition moment for $A^2\Pi - X^2\Sigma$ electronic transitions as a function of R.

All the tabulated quantities are measured in atomic units; the potentials $V(X^2\Sigma)$, $V(B^2\Sigma)$ and $V(A^2\Pi)$ are measured relative to their respective separated atom limits.

Table B1.1 : LiHe Model Potentials

R	$V(X^2\Sigma)$	$V(B^2\Sigma)$	$V(A^2\Pi)$	$D_{\Lambda'\Lambda}(B^2\Sigma\text{-}X^2\Sigma)$	$D_{\Lambda'\Lambda}(A^2\Pi\text{-}X^2\Sigma)$
2.00	9.88104E-02	1.09475E-01	7.16323E-02	1.81263E+00	2.32273E+00
2.10	8.15282E-02	9.33426E-02	5.49247E-02	1.73610E+00	2.30054E+00
2.20	6.73344E-02	8.03187E-02	4.13793E-02	1.67221E+00	2.28151E+00
2.30	5.57357E-02	6.98832E-02	3.04806E-02	1.62024E+00	2.26531E+00
2.40	4.63168E-02	6.16046E-02	2.17984E-02	1.57938E+00	2.25164E+00
2.50	3.87194E-02	5.51134E-02	1.49637E-02	1.54886E+00	2.24017E+00
2.60	3.26308E-02	5.00886E-02	9.65626E-03	1.52804E+00	2.23063E+00
2.70	2.77787E-02	4.62505E-02	5.59817E-03	1.51643E+00	2.22278E+00
2.80	2.39281E-02	4.33571E-02	2.55037E-03	1.51367E+00	2.21638E+00
2.90	2.08790E-02	4.11998E-02	3.09509E-04	1.51951E+00	2.21126E+00
3.00	1.84636E-02	3.96010E-02	-1.29505E-03	1.53370E+00	2.20725E+00
3.10	1.65428E-02	3.84101E-02	-2.40453E-03	1.55599E+00	2.20421E+00
3.20	1.50037E-02	3.75005E-02	-3.13424E-03	1.58592E+00	2.20203E+00
3.30	1.37552E-02	3.67663E-02	-3.57706E-03	1.62279E+00	2.20058E+00
3.40	1.27256E-02	3.61201E-02	-3.80684E-03	1.66549E+00	2.19979E+00
3.50	1.18588E-02	3.54912E-02	-3.88156E-03	1.71247E+00	2.19958E+00
3.60	1.11119E-02	3.48249E-02	-3.84616E-03	1.76184E+00	2.19986E+00
3.70	1.04524E-02	3.40823E-02	-3.73502E-03	1.81153E+00	2.20059E+00
3.80	9.85621E-03	3.32396E-02	-3.57413E-03	1.85963E+00	2.20170E+00
3.90	9.30602E-03	3.22874E-02	-3.38279E-03	1.90460E+00	2.20315E+00
4.00	8.78948E-03	3.12282E-02	-3.17516E-03	1.94547E+00	2.20490E+00
4.10	8.29819E-03	3.00740E-02	-2.96139E-03	1.98186E+00	2.20691E+00
4.20	7.82668E-03	2.88425E-02	-2.74862E-03	2.01378E+00	2.20916E+00
4.30	7.37158E-03	2.75543E-02	-2.54167E-03	2.04157E+00	2.21161E+00
4.40	6.93106E-03	2.62304E-02	-2.34370E-03	2.06569E+00	2.21424E+00
4.50	6.50434E-03	2.48905E-02	-2.15660E-03	2.08664E+00	2.21704E+00
4.60	6.09133E-03	2.35521E-02	-1.98137E-03	2.10491E+00	2.21997E+00
4.70	5.69237E-03	2.22301E-02	-1.81839E-03	2.12093E+00	2.22303E+00
4.80	5.30798E-03	2.09363E-02	-1.66758E-03	2.13506E+00	2.22621E+00
4.90	4.93876E-03	1.96802E-02	-1.52860E-03	2.14761E+00	2.22948E+00
5.00	4.58531E-03	1.84687E-02	-1.40088E-03	2.15884E+00	2.23283E+00
5.10	4.24814E-03	1.73066E-02	-1.28379E-03	2.16897E+00	2.23626E+00
5.20	3.92761E-03	1.61973E-02	-1.17661E-03	2.17817E+00	2.23974E+00
5.30	3.62395E-03	1.51425E-02	-1.07861E-03	2.18658E+00	2.24327E+00
5.40	3.33724E-03	1.41428E-02	-9.89079E-04	2.19433E+00	2.24683E+00
5.50	3.06739E-03	1.31981E-02	-9.07320E-04	2.20152E+00	2.25042E+00
5.60	2.81421E-03	1.23075E-02	-8.32678E-04	2.20822E+00	2.25402E+00
5.80	2.35642E-03	1.06824E-02	-7.02326E-04	2.22047E+00	2.26121E+00
6.00	1.96007E-03	9.25279E-03	-5.93624E-04	2.23149E+00	2.26832E+00
6.20	1.62026E-03	8.00102E-03	-5.02860E-04	2.24157E+00	2.27526E+00
6.40	1.33146E-03	6.90880E-03	-4.26944E-04	2.25090E+00	2.28198E+00
6.60	1.08794E-03	5.95823E-03	-3.63325E-04	2.25961E+00	2.28843E+00
6.80	8.84032E-04	5.13259E-03	-3.09898E-04	2.26777E+00	2.29455E+00
7.00	7.14394E-04	4.41660E-03	-2.64937E-04	2.27543E+00	2.30031E+00
7.25	5.43066E-04	3.65494E-03	-2.18496E-04	2.28434E+00	2.30699E+00
7.50	4.09060E-04	3.01961E-03	-1.80838E-04	2.29252E+00	2.31305E+00
7.75	3.05074E-04	2.49038E-03	-1.50199E-04	2.30000E+00	2.31851E+00
8.00	2.24991E-04	2.05017E-03	-1.25190E-04	2.30680E+00	2.32339E+00
8.25	1.63773E-04	1.68446E-03	-1.04709E-04	2.31292E+00	2.32769E+00
8.50	1.17329E-04	1.38106E-03	-8.78820E-05	2.31840E+00	2.33147E+00
8.75	8.23715E-05	1.12975E-03	-7.40132E-05	2.32327E+00	2.33477E+00
9.00	5.62846E-05	9.21897E-04	-6.25455E-05	2.32757E+00	2.33763E+00
9.25	3.70035E-05	7.50297E-04	-5.30331E-05	2.33134E+00	2.34009E+00
9.50	2.29104E-05	6.08890E-04	-4.51175E-05	2.33463E+00	2.34219E+00

Table B1.1 - continued

R	$V(X^2\Sigma)$	$V(B^2\Sigma)$	$V(A^2\Pi)$	$D_{\Lambda'\Lambda}(B^2\Sigma\text{-}X^2\Sigma)$	$D_{\Lambda'\Lambda}(A^2\Pi\text{-}X^2\Sigma)$
9.75	1.27452E-05	4.92597E-04	-3.85102E-05	2.33747E+00	2.34399E+00
10.00	5.53300E-06	3.97166E-04	-3.29772E-05	2.33993E+00	2.34551E+00
10.25	5.23944E-07	3.19036E-04	-2.83296E-05	2.34203E+00	2.34679E+00
10.50	-2.85513E-06	2.55233E-04	-2.44136E-05	2.34382E+00	2.34786E+00
10.75	-5.04037E-06	2.03270E-04	-2.11038E-05	2.34534E+00	2.34875E+00
11.00	-6.36117E-06	1.61072E-04	-1.82978E-05	2.34662E+00	2.34949E+00
11.25	-7.06498E-06	1.26911E-04	-1.59119E-05	2.34770E+00	2.35011E+00
11.50	-7.33619E-06	9.93468E-05	-1.38771E-05	2.34860E+00	2.35062E+00
11.75	-7.31125E-06	7.71852E-05	-1.21366E-05	2.34936E+00	2.35103E+00
12.00	-7.09022E-06	5.94357E-05	-1.06435E-05	2.34998E+00	2.35137E+00
12.25	-6.74564E-06	4.52793E-05	-9.35912E-06	2.35050E+00	2.35164E+00
12.50	-6.32949E-06	3.40405E-05	-8.25106E-06	2.35092E+00	2.35186E+00
12.75	-5.87841E-06	2.51634E-05	-7.29256E-06	2.35127E+00	2.35204E+00
13.00	-5.41770E-06	1.81912E-05	-6.46120E-06	2.35155E+00	2.35218E+00
13.50	-4.52938E-06	8.53614E-06	-5.10783E-06	2.35197E+00	2.35238E+00
14.00	-3.73782E-06	2.84175E-06	-4.07407E-06	2.35225E+00	2.35250E+00
14.50	-3.06476E-06	-3.63576E-07	-3.27677E-06	2.35242E+00	2.35257E+00
15.00	-2.50733E-06	-2.03618E-06	-2.65618E-06	2.35252E+00	2.35261E+00
16.00	-1.68425E-06	-3.00935E-06	-1.78321E-06	2.35262E+00	2.35264E+00
17.00	-1.14736E-06	-2.71637E-06	-1.22825E-06	2.35265E+00	2.35264E+00
18.00	-7.96481E-07	-2.13935E-06	-8.65292E-07	2.35264E+00	2.35263E+00
20.00	-4.06974E-07	-1.17525E-06	-4.54911E-07	2.35263E+00	2.35261E+00
22.00	-2.23004E-07	-6.35879E-07	-2.54900E-07	2.35262E+00	2.35261E+00
24.00	-1.29437E-07	-3.57716E-07	-1.50441E-07	2.35261E+00	2.35260E+00
26.00	-7.87623E-08	-2.11180E-07	-9.27174E-08	2.35260E+00	2.35260E+00
30.00	-3.26225E-08	-8.36132E-08	-3.91062E-08	2.35260E+00	2.35260E+00
35.00	-1.27110E-08	-3.14651E-08	-1.54844E-08	2.35260E+00	2.35260E+00
40.00	-5.64129E-09	-1.36634E-08	-6.95601E-09	2.35260E+00	2.35260E+00

Table B1.2 : LiHe Pseudopotentials

R	$V(X^2\Sigma)$	$V(B^2\Sigma)$	$V(A^2\Pi)$	$D_{\Lambda'\Lambda}(B^2\Sigma\text{-}X^2\Sigma)$	$D_{\Lambda'\Lambda}(A^2\Pi\text{-}X^2\Sigma)$
2.00	1.06044E-01	1.15145E-01	7.16323E-02	1.27098E+00	2.17570E+00
2.10	8.77363E-02	9.88506E-02	5.49247E-02	1.21223E+00	2.15772E+00
2.20	7.27352E-02	8.56921E-02	4.13793E-02	1.16456E+00	2.14275E+00
2.30	6.05014E-02	7.51576E-02	3.04806E-02	1.12571E+00	2.13014E+00
2.40	5.05839E-02	6.68203E-02	2.17984E-02	1.09409E+00	2.11938E+00
2.50	4.25967E-02	6.03140E-02	1.49637E-02	1.06859E+00	2.11011E+00
2.60	3.62057E-02	5.53200E-02	9.65626E-03	1.04849E+00	2.10205E+00
2.70	3.11214E-02	5.15614E-02	5.59817E-03	1.03336E+00	2.09499E+00
2.80	2.70954E-02	4.87992E-02	2.55037E-03	1.02304E+00	2.08878E+00
2.90	2.39168E-02	4.68292E-02	3.09509E-04	1.01762E+00	2.08331E+00
3.00	2.14085E-02	4.54785E-02	-1.29505E-03	1.01736E+00	2.07849E+00
3.10	1.94242E-02	4.46026E-02	-2.40453E-03	1.02278E+00	2.07426E+00
3.20	1.78445E-02	4.40810E-02	-3.13424E-03	1.03460E+00	2.07057E+00
3.30	1.65729E-02	4.38140E-02	-3.57706E-03	1.05380E+00	2.06742E+00
3.40	1.55329E-02	4.37178E-02	-3.80684E-03	1.08156E+00	2.06477E+00
3.50	1.46643E-02	4.37211E-02	-3.88156E-03	1.11920E+00	2.06262E+00
3.60	1.39204E-02	4.37614E-02	-3.84616E-03	1.16799E+00	2.06096E+00
3.70	1.32657E-02	4.37808E-02	-3.73502E-03	1.22870E+00	2.05981E+00
3.80	1.26733E-02	4.37247E-02	-3.57413E-03	1.30096E+00	2.05916E+00
3.90	1.21235E-02	4.35413E-02	-3.38279E-03	1.38243E+00	2.05903E+00
4.00	1.16018E-02	4.31847E-02	-3.17516E-03	1.46852E+00	2.05941E+00
4.10	1.10984E-02	4.26220E-02	-2.96139E-03	1.55338E+00	2.06031E+00
4.20	1.06064E-02	4.18392E-02	-2.74862E-03	1.63185E+00	2.06173E+00
4.30	1.01218E-02	4.08423E-02	-2.54167E-03	1.70116E+00	2.06367E+00
4.40	9.64210E-03	3.96529E-02	-2.34370E-03	1.76100E+00	2.06613E+00
4.50	9.16652E-03	3.83017E-02	-2.15660E-03	1.81248E+00	2.06910E+00
4.60	8.69511E-03	3.68221E-02	-1.98137E-03	1.85706E+00	2.07257E+00
4.70	8.22866E-03	3.52474E-02	-1.81839E-03	1.89607E+00	2.07652E+00
4.80	7.76842E-03	3.36087E-02	-1.66758E-03	1.93052E+00	2.08092E+00
4.90	7.31588E-03	3.19338E-02	-1.52860E-03	1.96115E+00	2.08576E+00
5.00	6.87268E-03	3.02471E-02	-1.40088E-03	1.98852E+00	2.09101E+00
5.10	6.44047E-03	2.85696E-02	-1.28379E-03	2.01304E+00	2.09663E+00
5.20	6.02079E-03	2.69184E-02	-1.17661E-03	2.03505E+00	2.10259E+00
5.30	5.61506E-03	2.53076E-02	-1.07861E-03	2.05484E+00	2.10886E+00
5.40	5.22453E-03	2.37480E-02	-9.89079E-04	2.07267E+00	2.11539E+00
5.50	4.85021E-03	2.22477E-02	-9.07320E-04	2.08876E+00	2.12216E+00
5.60	4.49291E-03	2.08124E-02	-8.32678E-04	2.10332E+00	2.12911E+00
5.80	3.83145E-03	1.81496E-02	-7.02326E-04	2.12859E+00	2.14343E+00
6.00	3.24224E-03	1.57701E-02	-5.93624E-04	2.14975E+00	2.15807E+00
6.20	2.72437E-03	1.36669E-02	-5.02860E-04	2.16781E+00	2.17274E+00
6.40	2.27456E-03	1.18222E-02	-4.26944E-04	2.18357E+00	2.18721E+00
6.60	1.88799E-03	1.02132E-02	-3.63325E-04	2.19760E+00	2.20129E+00
6.80	1.55878E-03	8.81527E-03	-3.09898E-04	2.21032E+00	2.21482E+00
7.00	1.28069E-03	7.60391E-03	-2.64937E-04	2.22202E+00	2.22769E+00
7.25	9.95387E-04	6.31711E-03	-2.18496E-04	2.23549E+00	2.24271E+00
7.50	7.68489E-04	5.24538E-03	-1.80838E-04	2.24788E+00	2.25648E+00
7.75	5.89500E-04	4.35349E-03	-1.50199E-04	2.25932E+00	2.26896E+00
8.00	4.49295E-04	3.61153E-03	-1.25190E-04	2.26988E+00	2.28017E+00
8.25	3.40155E-04	2.99430E-03	-1.04709E-04	2.27957E+00	2.29017E+00
8.50	2.55679E-04	2.48080E-03	-8.78820E-05	2.28843E+00	2.29901E+00
8.75	1.90650E-04	2.05356E-03	-7.40132E-05	2.29649E+00	2.30680E+00
9.00	1.40844E-04	1.69809E-03	-6.25455E-05	2.30376E+00	2.31360E+00
9.25	1.02910E-04	1.40236E-03	-5.30331E-05	2.31028E+00	2.31953E+00
9.50	7.41770E-05	1.15642E-03	-4.51175E-05	2.31610E+00	2.32466E+00

Table B1.2 - continued

R	$V(X^2\Sigma)$	$V(B^2\Sigma)$	$V(A^2\Pi)$	$D_{\Lambda'\Lambda}(B^2\Sigma\text{-}X^2\Sigma)$	$D_{\Lambda'\Lambda}(A^2\Pi\text{-}X^2\Sigma)$
9.75	5.25421E-05	9.52004E-04	-3.85102E-05	2.32125E+00	2.32908E+00
10.00	3.63644E-05	7.82201E-04	-3.29772E-05	2.32579E+00	2.33288E+00
10.25	2.43634E-05	6.41319E-04	-2.83296E-05	2.32978E+00	2.33613E+00
10.50	1.55397E-05	5.24568E-04	-2.44136E-05	2.33325E+00	2.33889E+00
10.75	9.12338E-06	4.27954E-04	-2.11038E-05	2.33626E+00	2.34124E+00
11.00	4.52225E-06	3.48149E-04	-1.82978E-05	2.33885E+00	2.34322E+00
11.25	1.28177E-06	2.82361E-04	-1.59119E-05	2.34109E+00	2.34489E+00
11.50	-9.47781E-07	2.28244E-04	-1.38771E-05	2.34300E+00	2.34629E+00
11.75	-2.43137E-06	1.83831E-04	-1.21366E-05	2.34462E+00	2.34745E+00
12.00	-3.36976E-06	1.47480E-04	-1.06435E-05	2.34600E+00	2.34842E+00
12.25	-3.91444E-06	1.17811E-04	-9.35912E-06	2.34716E+00	2.34922E+00
12.50	-4.17863E-06	9.36642E-05	-8.25106E-06	2.34814E+00	2.34988E+00
12.75	-4.24689E-06	7.40755E-05	-7.29256E-06	2.34896E+00	2.35043E+00
13.00	-4.18204E-06	5.82362E-05	-6.46120E-06	2.34964E+00	2.35087E+00
13.50	-3.82385E-06	3.52259E-05	-5.10783E-06	2.35068E+00	2.35153E+00
14.00	-3.33697E-06	2.05099E-05	-4.07407E-06	2.35138E+00	2.35196E+00
14.50	-2.83790E-06	1.12629E-05	-3.27677E-06	2.35186E+00	2.35223E+00
15.00	-2.37947E-06	5.57547E-06	-2.65618E-06	2.35217E+00	2.35240E+00
16.00	-1.64394E-06	2.12659E-07	-1.78321E-06	2.35249E+00	2.35257E+00
17.00	-1.13476E-06	-1.36990E-06	-1.22825E-06	2.35261E+00	2.35262E+00
18.00	-7.92561E-07	-1.58215E-06	-8.65292E-07	2.35264E+00	2.35263E+00
20.00	-4.06583E-07	-1.08205E-06	-4.54911E-07	2.35264E+00	2.35262E+00
22.00	-2.22945E-07	-6.20739E-07	-2.54900E-07	2.35262E+00	2.35262E+00
24.00	-1.29405E-07	-3.55350E-07	-1.50441E-07	2.35261E+00	2.35261E+00
26.00	-7.87340E-08	-2.10854E-07	-9.27174E-08	2.35261E+00	2.35261E+00
30.00	-3.25936E-08	-8.36613E-08	-3.91062E-08	2.35261E+00	2.35261E+00
35.00	-1.26833E-08	-3.15303E-08	-1.54844E-08	2.35261E+00	2.35261E+00
40.00	-5.61512E-09	-1.37183E-08	-6.95601E-09	2.35261E+00	2.35261E+00

Table B1.3 : LiNe Model Potentials

R	$V(X^2\Sigma)$	$V(B^2\Sigma)$	$V(A^2\Pi)$	$D_{\Lambda'\Lambda}(B^2\Sigma\text{-}X^2\Sigma)$	$D_{\Lambda'\Lambda}(A^2\Pi\text{-}X^2\Sigma)$
2.00	2.44159E-01	2.46730E-01	2.38188E-01	2.27355E+00	2.55052E+00
2.10	1.87136E-01	1.90791E-01	1.80156E-01	2.19435E+00	2.52078E+00
2.20	1.46616E-01	1.51415E-01	1.38776E-01	2.12536E+00	2.49406E+00
2.30	1.16817E-01	1.22769E-01	1.08246E-01	2.06703E+00	2.47025E+00
2.40	9.42343E-02	1.01320E-01	8.50484E-02	2.01906E+00	2.44912E+00
2.50	7.67121E-02	8.48926E-02	6.70165E-02	1.98077E+00	2.43039E+00
2.60	6.28862E-02	7.21110E-02	5.27790E-02	1.95132E+00	2.41381E+00
2.70	5.18586E-02	6.20701E-02	4.14321E-02	1.92990E+00	2.39915E+00
2.80	4.30096E-02	5.41450E-02	3.23500E-02	1.91573E+00	2.38619E+00
2.90	3.58889E-02	4.78807E-02	2.50772E-02	1.90812E+00	2.37474E+00
3.00	3.01540E-02	4.29304E-02	1.92656E-02	1.90642E+00	2.36464E+00
3.10	2.55355E-02	3.90201E-02	1.46404E-02	1.91005E+00	2.35574E+00
3.20	2.18165E-02	3.59280E-02	1.09790E-02	1.91843E+00	2.34790E+00
3.30	1.88197E-02	3.34718E-02	8.09865E-03	1.93099E+00	2.34100E+00
3.40	1.64002E-02	3.15011E-02	5.84869E-03	1.94714E+00	2.33496E+00
3.50	1.44394E-02	2.98925E-02	4.10492E-03	1.96624E+00	2.32966E+00
3.60	1.28406E-02	2.85456E-02	2.76496E-03	1.98763E+00	2.32502E+00
3.70	1.15256E-02	2.73796E-02	1.74528E-03	2.01059E+00	2.32097E+00
3.80	1.04318E-02	2.63311E-02	9.77720E-04	2.03441E+00	2.31745E+00
3.90	9.50930E-03	2.53519E-02	4.07320E-04	2.05841E+00	2.31440E+00
4.00	8.71926E-03	2.44073E-02	-9.94115E-06	2.08196E+00	2.31176E+00
4.10	8.03129E-03	2.34735E-02	-3.09262E-04	2.10455E+00	2.30949E+00
4.20	7.42216E-03	2.25363E-02	-5.18466E-04	2.12578E+00	2.30756E+00
4.30	6.87425E-03	2.15882E-02	-6.59385E-04	2.14537E+00	2.30593E+00
4.40	6.37453E-03	2.06279E-02	-7.49064E-04	2.16318E+00	2.30459E+00
4.50	5.91344E-03	1.96580E-02	-8.00732E-04	2.17918E+00	2.30350E+00
4.60	5.48393E-03	1.86831E-02	-8.24578E-04	2.19341E+00	2.30265E+00
4.70	5.08124E-03	1.77097E-02	-8.28355E-04	2.20598E+00	2.30202E+00
4.80	4.70198E-03	1.67445E-02	-8.17940E-04	2.21702E+00	2.30161E+00
4.90	4.34378E-03	1.57938E-02	-7.97807E-04	2.22671E+00	2.30140E+00
5.00	4.00513E-03	1.48637E-02	-7.71248E-04	2.23521E+00	2.30137E+00
5.10	3.68507E-03	1.39593E-02	-7.40669E-04	2.24266E+00	2.30153E+00
5.20	3.38286E-03	1.30848E-02	-7.07881E-04	2.24923E+00	2.30185E+00
5.30	3.09803E-03	1.22433E-02	-6.74145E-04	2.25504E+00	2.30233E+00
5.40	2.83020E-03	1.14375E-02	-6.40345E-04	2.26022E+00	2.30296E+00
5.50	2.57900E-03	1.06687E-02	-6.07108E-04	2.26486E+00	2.30373E+00
5.60	2.34405E-03	9.93793E-03	-5.74846E-04	2.26906E+00	2.30462E+00
5.80	1.92129E-03	8.59126E-03	-5.14167E-04	2.27643E+00	2.30674E+00
6.00	1.55799E-03	7.39465E-03	-4.59252E-04	2.28280E+00	2.30922E+00
6.20	1.24946E-03	6.34028E-03	-4.10140E-04	2.28850E+00	2.31197E+00
6.40	9.90389E-04	5.41745E-03	-3.66445E-04	2.29372E+00	2.31490E+00
6.60	7.75227E-04	4.61428E-03	-3.27634E-04	2.29862E+00	2.31792E+00
6.80	5.98349E-04	3.91834E-03	-2.93162E-04	2.30325E+00	2.32095E+00
7.00	4.54408E-04	3.31766E-03	-2.62504E-04	2.30765E+00	2.32395E+00
7.25	3.13259E-04	2.68366E-03	-2.28849E-04	2.31285E+00	2.32755E+00
7.50	2.07143E-04	2.16084E-03	-1.99670E-04	2.31771E+00	2.33094E+00
7.75	1.28661E-04	1.73147E-03	-1.74326E-04	2.32220E+00	2.33406E+00
8.00	7.16526E-05	1.38026E-03	-1.52280E-04	2.32632E+00	2.33689E+00
8.25	3.10997E-05	1.09406E-03	-1.33088E-04	2.33006E+00	2.33941E+00
8.50	2.98724E-06	8.61708E-04	-1.16369E-04	2.33341E+00	2.34163E+00
8.75	-1.58476E-05	6.73755E-04	-1.01802E-04	2.33639E+00	2.34357E+00
9.00	-2.78571E-05	5.22364E-04	-8.91068E-05	2.33900E+00	2.34524E+00
9.25	-3.49272E-05	4.00962E-04	-7.80416E-05	2.34128E+00	2.34666E+00
9.50	-3.84864E-05	3.04081E-04	-6.83967E-05	2.34325E+00	2.34786E+00

Table B1.3 - continued

R	$V(X^2\Sigma)$	$V(B^2\Sigma)$	$V(A^2\Pi)$	$D_{\Lambda'\Lambda}(B^2\Sigma\text{-}X^2\Sigma)$	$D_{\Lambda'\Lambda}(A^2\Pi\text{-}X^2\Sigma)$
9.75	-3.96081E-05	2.27172E-04	-5.99899E-05	2.34494E+00	2.34887E+00
10.00	-3.90869E-05	1.66471E-04	-5.26614E-05	2.34638E+00	2.34971E+00
10.25	-3.75036E-05	1.18882E-04	-4.62717E-05	2.34759E+00	2.35040E+00
10.50	-3.52774E-05	8.18543E-05	-4.06992E-05	2.34860E+00	2.35096E+00
10.75	-3.27056E-05	5.33021E-05	-3.58373E-05	2.34945E+00	2.35141E+00
11.00	-2.99947E-05	3.15172E-05	-3.15938E-05	2.35014E+00	2.35177E+00
11.25	-2.72842E-05	1.51101E-05	-2.78876E-05	2.35071E+00	2.35206E+00
11.50	-2.46660E-05	2.93175E-06	-2.46487E-05	2.35118E+00	2.35228E+00
11.75	-2.21939E-05	-5.89284E-06	-2.18160E-05	2.35156E+00	2.35246E+00
12.00	-1.99001E-05	-1.21181E-05	-1.93363E-05	2.35186E+00	2.35259E+00
12.25	-1.77981E-05	-1.63349E-05	-1.71637E-05	2.35210E+00	2.35268E+00
12.50	-1.58903E-05	-1.90143E-05	-1.52581E-05	2.35228E+00	2.35275E+00
12.75	-1.41712E-05	-2.05302E-05	-1.35849E-05	2.35243E+00	2.35280E+00
13.00	-1.26307E-05	-2.11787E-05	-1.21140E-05	2.35254E+00	2.35283E+00
13.50	-1.00330E-05	-2.07502E-05	-9.67832E-06	2.35269E+00	2.35285E+00
14.00	-7.98566E-06	-1.90310E-05	-7.78150E-06	2.35276E+00	2.35285E+00
14.50	-6.38059E-06	-1.67885E-05	-6.29608E-06	2.35279E+00	2.35283E+00
15.00	-5.12393E-06	-1.44529E-05	-5.12606E-06	2.35279E+00	2.35280E+00
16.00	-3.36364E-06	-1.02781E-05	-3.45997E-06	2.35276E+00	2.35275E+00
17.00	-2.26439E-06	-7.12946E-06	-2.38930E-06	2.35272E+00	2.35270E+00
18.00	-1.56236E-06	-4.92409E-06	-1.68498E-06	2.35269E+00	2.35267E+00
20.00	-7.94409E-07	-2.41256E-06	-8.85923E-07	2.35264E+00	2.35263E+00
22.00	-4.34583E-07	-1.25642E-06	-4.96060E-07	2.35262E+00	2.35262E+00
24.00	-2.52038E-07	-6.97990E-07	-2.92547E-07	2.35261E+00	2.35261E+00
26.00	-1.53282E-07	-4.10382E-07	-1.80156E-07	2.35261E+00	2.35261E+00
30.00	-6.34420E-08	-1.62142E-07	-7.58619E-08	2.35260E+00	2.35260E+00
35.00	-2.47059E-08	-6.09703E-08	-2.99381E-08	2.35260E+00	2.35260E+00
40.00	-1.09609E-08	-2.64647E-08	-1.33945E-08	2.35260E+00	2.35260E+00

Table B1.4 : LiNe Pseudopotentials

R	$V(X^2\Sigma)$	$V(B^2\Sigma)$	$V(A^2\Pi)$	$D_{\Lambda'\Lambda}(B^2\Sigma\text{-}X^2\Sigma)$	$D_{\Lambda'\Lambda}(A^2\Pi\text{-}X^2\Sigma)$
2.00	2.53530E-01	2.56702E-01	2.42008E-01	1.86175E+00	2.49090E+00
2.10	1.95353E-01	2.00371E-01	1.83685E-01	1.76506E+00	2.44883E+00
2.20	1.53851E-01	1.60675E-01	1.42030E-01	1.68604E+00	2.41311E+00
2.30	1.23220E-01	1.31786E-01	1.11241E-01	1.62206E+00	2.38266E+00
2.40	9.99365E-02	1.10167E-01	8.78000E-02	1.57079E+00	2.35657E+00
2.50	8.18253E-02	9.36374E-02	6.95400E-02	1.53022E+00	2.33407E+00
2.60	6.75066E-02	8.08188E-02	5.50896E-02	1.49874E+00	2.31457E+00
2.70	5.60687E-02	7.08014E-02	4.35447E-02	1.47508E+00	2.29757E+00
2.80	4.68798E-02	6.29561E-02	3.42791E-02	1.45829E+00	2.28268E+00
2.90	3.94789E-02	5.68244E-02	2.68367E-02	1.44769E+00	2.26960E+00
3.00	3.35147E-02	5.20565E-02	2.08688E-02	1.44279E+00	2.25807E+00
3.10	2.87097E-02	4.83750E-02	1.60997E-02	1.44331E+00	2.24789E+00
3.20	2.48399E-02	4.55547E-02	1.23063E-02	1.44910E+00	2.23889E+00
3.30	2.17221E-02	4.34095E-02	9.30494E-03	1.46012E+00	2.23095E+00
3.40	1.92059E-02	4.17841E-02	6.94436E-03	1.47637E+00	2.22396E+00
3.50	1.71679E-02	4.05482E-02	5.09947E-03	1.49787E+00	2.21783E+00
3.60	1.55070E-02	3.95924E-02	3.66733E-03	1.52455E+00	2.21248E+00
3.70	1.41413E-02	3.88242E-02	2.56356E-03	1.55625E+00	2.20786E+00
3.80	1.30047E-02	3.81663E-02	1.71948E-03	1.59256E+00	2.20391E+00
3.90	1.20445E-02	3.75538E-02	1.07950E-03	1.63284E+00	2.20059E+00
4.00	1.12191E-02	3.69336E-02	5.98950E-04	1.67617E+00	2.19787E+00
4.10	1.04959E-02	3.62638E-02	2.42134E-04	1.72139E+00	2.19570E+00
4.20	9.84997E-03	3.55136E-02	-1.92388E-05	1.76722E+00	2.19406E+00
4.30	9.26217E-03	3.46632E-02	-2.07498E-04	1.81242E+00	2.19293E+00
4.40	8.71831E-03	3.37036E-02	-3.40112E-04	1.85590E+00	2.19228E+00
4.50	8.20808E-03	3.26352E-02	-4.30705E-04	1.89684E+00	2.19208E+00
4.60	7.72406E-03	3.14666E-02	-4.89809E-04	1.93474E+00	2.19231E+00
4.70	7.26126E-03	3.02121E-02	-5.25531E-04	1.96935E+00	2.19296E+00
4.80	6.81639E-03	2.88902E-02	-5.44071E-04	2.00064E+00	2.19400E+00
4.90	6.38748E-03	2.75206E-02	-5.50138E-04	2.02876E+00	2.19541E+00
5.00	5.97351E-03	2.61233E-02	-5.47287E-04	2.05392E+00	2.19717E+00
5.10	5.57412E-03	2.47169E-02	-5.38187E-04	2.07637E+00	2.19925E+00
5.20	5.18940E-03	2.33180E-02	-5.24820E-04	2.09639E+00	2.20164E+00
5.30	4.81962E-03	2.19409E-02	-5.08652E-04	2.11425E+00	2.20432E+00
5.40	4.46526E-03	2.05972E-02	-4.90753E-04	2.13020E+00	2.20725E+00
5.50	4.12675E-03	1.92960E-02	-4.71899E-04	2.14448E+00	2.21041E+00
5.60	3.80450E-03	1.80443E-02	-4.52643E-04	2.15730E+00	2.21379E+00
5.80	3.20995E-03	1.57066E-02	-4.14362E-04	2.17928E+00	2.22107E+00
6.00	2.68260E-03	1.36040E-02	-3.77761E-04	2.19740E+00	2.22890E+00
6.20	2.22131E-03	1.17375E-02	-3.43612E-04	2.21263E+00	2.23708E+00
6.40	1.82299E-03	1.00966E-02	-3.12146E-04	2.22571E+00	2.24545E+00
6.60	1.48319E-03	8.66433E-03	-2.83329E-04	2.23718E+00	2.25384E+00
6.80	1.19643E-03	7.42076E-03	-2.57014E-04	2.24744E+00	2.26211E+00
7.00	9.56849E-04	6.34533E-03	-2.33019E-04	2.25674E+00	2.27015E+00
7.25	7.14683E-04	5.20718E-03	-2.06002E-04	2.26733E+00	2.27973E+00
7.50	5.25897E-04	4.26480E-03	-1.81971E-04	2.27694E+00	2.28868E+00
7.75	3.80489E-04	3.48645E-03	-1.60618E-04	2.28573E+00	2.29692E+00
8.00	2.69765E-04	2.84483E-03	-1.41668E-04	2.29376E+00	2.30442E+00
8.25	1.86398E-04	2.31672E-03	-1.24875E-04	2.30107E+00	2.31115E+00
8.50	1.24350E-04	1.88263E-03	-1.10015E-04	2.30770E+00	2.31714E+00
8.75	7.87435E-05	1.52627E-03	-9.68862E-05	2.31369E+00	2.32244E+00
9.00	4.56853E-05	1.23410E-03	-8.53045E-05	2.31904E+00	2.32708E+00
9.25	2.21242E-05	9.94881E-04	-7.51014E-05	2.32380E+00	2.33112E+00
9.50	5.67800E-06	7.99323E-04	-6.61239E-05	2.32801E+00	2.33461E+00

Table B1.4 - continued

R	$V(X^2\Sigma)$	$V(B^2\Sigma)$	$V(A^2\Pi)$	$D_{\Lambda'\Lambda}(B^2\Sigma\text{-}X^2\Sigma)$	$D_{\Lambda'\Lambda}(A^2\Pi\text{-}X^2\Sigma)$
9.75	-5.49041E-06	6.39740E-04	-5.82334E-05	2.33171E+00	2.33760E+00
10.00	-1.27821E-05	5.09755E-04	-5.13040E-05	2.33494E+00	2.34017E+00
10.25	-1.72603E-05	4.04135E-04	-4.52230E-05	2.33774E+00	2.34235E+00
10.50	-1.97284E-05	3.18526E-04	-3.98889E-05	2.34016E+00	2.34419E+00
10.75	-2.07850E-05	2.49338E-04	-3.52114E-05	2.34223E+00	2.34574E+00
11.00	-2.08726E-05	1.93608E-04	-3.11102E-05	2.34400E+00	2.34703E+00
11.25	-2.03156E-05	1.48889E-04	-2.75142E-05	2.34551E+00	2.34811E+00
11.50	-1.93509E-05	1.13155E-04	-2.43603E-05	2.34679E+00	2.34901E+00
11.75	-1.81476E-05	8.47350E-05	-2.15932E-05	2.34786E+00	2.34975E+00
12.00	-1.68246E-05	6.22571E-05	-1.91643E-05	2.34876E+00	2.35035E+00
12.25	-1.54643E-05	4.45888E-05	-1.70308E-05	2.34950E+00	2.35085E+00
12.50	-1.41219E-05	3.07985E-05	-1.51555E-05	2.35012E+00	2.35125E+00
12.75	-1.28330E-05	2.01262E-05	-1.35056E-05	2.35064E+00	2.35157E+00
13.00	-1.16193E-05	1.19480E-05	-1.20527E-05	2.35106E+00	2.35183E+00
13.50	-9.45769E-06	1.13541E-06	-9.64171E-06	2.35168E+00	2.35220E+00
14.00	-7.65979E-06	-4.65639E-06	-7.75961E-06	2.35209E+00	2.35243E+00
14.50	-6.19669E-06	-7.39579E-06	-6.28299E-06	2.35235E+00	2.35256E+00
15.00	-5.02054E-06	-8.34311E-06	-5.11821E-06	2.35251E+00	2.35263E+00
16.00	-3.33119E-06	-7.72158E-06	-3.45714E-06	2.35266E+00	2.35268E+00
17.00	-2.25430E-06	-6.07233E-06	-2.38827E-06	2.35269E+00	2.35268E+00
18.00	-1.55923E-06	-4.49095E-06	-1.68461E-06	2.35268E+00	2.35267E+00
20.00	-7.94099E-07	-2.34140E-06	-8.85897E-07	2.35265E+00	2.35264E+00
22.00	-4.34534E-07	-1.24502E-06	-4.96094E-07	2.35263E+00	2.35262E+00
24.00	-2.52007E-07	-6.96222E-07	-2.92593E-07	2.35262E+00	2.35261E+00
26.00	-1.53254E-07	-4.10143E-07	-1.80210E-07	2.35261E+00	2.35261E+00
30.00	-6.34134E-08	-1.62188E-07	-7.59197E-08	2.35261E+00	2.35261E+00
35.00	-2.46783E-08	-6.10339E-08	-3.00035E-08	2.35261E+00	2.35261E+00
40.00	-1.09348E-08	-2.65189E-08	-1.34494E-08	2.35261E+00	2.35261E+00

Table B1.5 : NaHe Model Potentials

R	$V(X^2\Sigma)$	$V(B^2\Sigma)$	$V(A^2\Pi)$	$D_{\Lambda'\Lambda}(B^2\Sigma\text{-}X^2\Sigma)$	$D_{\Lambda'\Lambda}(A^2\Pi\text{-}X^2\Sigma)$
2.00	2.68377E-01	2.54311E-01	2.41650E-01	2.23907E+00	2.58657E+00
2.10	2.10239E-01	1.97904E-01	1.83809E-01	2.16842E+00	2.56582E+00
2.20	1.67407E-01	1.56816E-01	1.41334E-01	2.09953E+00	2.54446E+00
2.30	1.34906E-01	1.26053E-01	1.09263E-01	2.03524E+00	2.52337E+00
2.40	1.09681E-01	1.02545E-01	8.45424E-02	1.97740E+00	2.50312E+00
2.50	8.97957E-02	8.43395E-02	6.52297E-02	1.92715E+00	2.48409E+00
2.60	7.39620E-02	7.01381E-02	5.00302E-02	1.88503E+00	2.46649E+00
2.70	6.12820E-02	5.90349E-02	3.80367E-02	1.85119E+00	2.45041E+00
2.80	5.10968E-02	5.03659E-02	2.85817E-02	1.82551E+00	2.43586E+00
2.90	4.29037E-02	4.36232E-02	2.11535E-02	1.80772E+00	2.42280E+00
3.00	3.63070E-02	3.84078E-02	1.53488E-02	1.79744E+00	2.41116E+00
3.10	3.09898E-02	3.43992E-02	1.08434E-02	1.79423E+00	2.40086E+00
3.20	2.66961E-02	3.13377E-02	7.37465E-03	1.79760E+00	2.39181E+00
3.30	2.32184E-02	2.90123E-02	4.72915E-03	1.80701E+00	2.38393E+00
3.40	2.03887E-02	2.72508E-02	2.73358E-03	1.82184E+00	2.37713E+00
3.50	1.80717E-02	2.59140E-02	1.24784E-03	1.84141E+00	2.37133E+00
3.60	1.61588E-02	2.48896E-02	1.59235E-04	1.86493E+00	2.36646E+00
3.70	1.45638E-02	2.40881E-02	-6.22343E-04	1.89152E+00	2.36245E+00
3.80	1.32184E-02	2.34386E-02	-1.16846E-03	1.92025E+00	2.35923E+00
3.90	1.20690E-02	2.28862E-02	-1.53558E-03	1.95019E+00	2.35676E+00
4.00	1.10739E-02	2.23894E-02	-1.76799E-03	1.98044E+00	2.35497E+00
4.10	1.02007E-02	2.19173E-02	-1.90012E-03	2.01026E+00	2.35382E+00
4.20	9.42453E-03	2.14486E-02	-1.95862E-03	2.03902E+00	2.35326E+00
4.30	8.72646E-03	2.09690E-02	-1.96396E-03	2.06631E+00	2.35325E+00
4.40	8.09203E-03	2.04703E-02	-1.93170E-03	2.09189E+00	2.35375E+00
4.50	7.51033E-03	1.99482E-02	-1.87363E-03	2.11566E+00	2.35471E+00
4.60	6.97313E-03	1.94019E-02	-1.79859E-03	2.13767E+00	2.35611E+00
4.70	6.47427E-03	1.88330E-02	-1.71311E-03	2.15801E+00	2.35790E+00
4.80	6.00907E-03	1.82441E-02	-1.62200E-03	2.17683E+00	2.36006E+00
4.90	5.57399E-03	1.76388E-02	-1.52874E-03	2.19429E+00	2.36254E+00
5.00	5.16632E-03	1.70212E-02	-1.43579E-03	2.21054E+00	2.36532E+00
5.10	4.78397E-03	1.63955E-02	-1.34486E-03	2.22574E+00	2.36837E+00
5.20	4.42526E-03	1.57657E-02	-1.25710E-03	2.24001E+00	2.37165E+00
5.30	4.08881E-03	1.51356E-02	-1.17323E-03	2.25346E+00	2.37514E+00
5.40	3.77342E-03	1.45085E-02	-1.09367E-03	2.26619E+00	2.37881E+00
5.50	3.47807E-03	1.38876E-02	-1.01865E-03	2.27829E+00	2.38264E+00
5.60	3.20180E-03	1.32755E-02	-9.48191E-04	2.28981E+00	2.38660E+00
5.80	2.70301E-03	1.20867E-02	-8.20691E-04	2.31136E+00	2.39481E+00
6.00	2.27029E-03	1.09562E-02	-7.09964E-04	2.33116E+00	2.40327E+00
6.20	1.89721E-03	9.89311E-03	-6.14300E-04	2.34946E+00	2.41182E+00
6.40	1.57755E-03	8.90268E-03	-5.31875E-04	2.36641E+00	2.42033E+00
6.60	1.30527E-03	7.98692E-03	-4.60944E-04	2.38212E+00	2.42870E+00
6.80	1.07472E-03	7.14558E-03	-3.99920E-04	2.39668E+00	2.43682E+00
7.00	8.80554E-04	6.37679E-03	-3.47404E-04	2.41013E+00	2.44461E+00
7.25	6.81635E-04	5.51312E-03	-2.91883E-04	2.42548E+00	2.45383E+00
7.50	5.23438E-04	4.75059E-03	-2.45756E-04	2.43928E+00	2.46239E+00
7.75	3.98559E-04	4.08088E-03	-2.07371E-04	2.45161E+00	2.47023E+00
8.00	3.00693E-04	3.49536E-03	-1.75370E-04	2.46256E+00	2.47737E+00
8.25	2.24533E-04	2.98552E-03	-1.48641E-04	2.47222E+00	2.48379E+00
8.50	1.65678E-04	2.54321E-03	-1.26275E-04	2.48067E+00	2.48950E+00
8.75	1.20525E-04	2.16071E-03	-1.07521E-04	2.48802E+00	2.49457E+00
9.00	8.61430E-05	1.83099E-03	-9.17666E-05	2.49437E+00	2.49903E+00
9.25	6.01721E-05	1.54762E-03	-7.85052E-05	2.49982E+00	2.50292E+00
9.50	4.07280E-05	1.30476E-03	-6.73197E-05	2.50445E+00	2.50630E+00

Table B1.5 - continued

R	$V(X^2\Sigma)$	$V(B^2\Sigma)$	$V(A^2\Pi)$	$D_{\Lambda'\Lambda}(B^2\Sigma\text{-}X^2\Sigma)$	$D_{\Lambda'\Lambda}(A^2\Pi\text{-}X^2\Sigma)$
9.75	2.63160E-05	1.09717E-03	-5.78653E-05	2.50836E+00	2.50921E+00
10.00	1.57587E-05	9.20209E-04	-4.98582E-05	2.51165E+00	2.51171E+00
10.25	8.13383E-06	7.69752E-04	-4.30626E-05	2.51438E+00	2.51384E+00
10.50	2.72420E-06	6.42162E-04	-3.72831E-05	2.51665E+00	2.51566E+00
10.75	-1.02537E-06	5.34236E-04	-3.23570E-05	2.51850E+00	2.51720E+00
11.00	-3.54173E-06	4.43174E-04	-2.81490E-05	2.52000E+00	2.51849E+00
11.25	-5.15119E-06	3.66543E-04	-2.45470E-05	2.52121E+00	2.51957E+00
11.50	-6.10175E-06	3.02221E-04	-2.14569E-05	2.52218E+00	2.52047E+00
11.75	-6.58055E-06	2.48372E-04	-1.88001E-05	2.52294E+00	2.52123E+00
12.00	-6.72797E-06	2.03407E-04	-1.65108E-05	2.52353E+00	2.52185E+00
12.25	-6.64826E-06	1.65961E-04	-1.45337E-05	2.52399E+00	2.52237E+00
12.50	-6.41827E-06	1.34862E-04	-1.28225E-05	2.52433E+00	2.52279E+00
12.75	-6.09403E-06	1.09106E-04	-1.13382E-05	2.52458E+00	2.52313E+00
13.00	-5.71591E-06	8.78378E-05	-1.00479E-05	2.52475E+00	2.52341E+00
13.50	-4.90360E-06	5.59549E-05	-7.94225E-06	2.52495E+00	2.52382E+00
14.00	-4.11825E-06	3.46136E-05	-6.33035E-06	2.52501E+00	2.52409E+00
14.50	-3.41795E-06	2.05332E-05	-5.08594E-06	2.52499E+00	2.52426E+00
15.00	-2.81992E-06	1.14003E-05	-4.11722E-06	2.52493E+00	2.52436E+00
16.00	-1.91248E-06	2.01497E-06	-2.75596E-06	2.52478E+00	2.52445E+00
17.00	-1.30789E-06	-1.30926E-06	-1.89285E-06	2.52466E+00	2.52447E+00
18.00	-9.08777E-07	-2.14564E-06	-1.33013E-06	2.52457E+00	2.52448E+00
20.00	-4.63691E-07	-1.71255E-06	-6.96589E-07	2.52448E+00	2.52446E+00
22.00	-2.53527E-07	-1.02232E-06	-3.89295E-07	2.52445E+00	2.52445E+00
24.00	-1.46890E-07	-5.87667E-07	-2.29362E-07	2.52444E+00	2.52444E+00
26.00	-8.92625E-08	-3.45703E-07	-1.41163E-07	2.52444E+00	2.52444E+00
30.00	-3.69057E-08	-1.34133E-07	-5.93930E-08	2.52444E+00	2.52444E+00
35.00	-1.43611E-08	-4.95298E-08	-2.34222E-08	2.52444E+00	2.52444E+00
40.00	-6.36847E-09	-2.12580E-08	-1.04678E-08	2.52444E+00	2.52444E+00

Table B1.6 : NaHe Pseudopotentials

R	$V(X^2\Sigma)$	$V(B^2\Sigma)$	$V(A^2\Pi)$	$D_{\Lambda'\Lambda}(B^2\Sigma\text{-}X^2\Sigma)$	$D_{\Lambda'\Lambda}(A^2\Pi\text{-}X^2\Sigma)$
2.00	2.79112E-01	2.65300E-01	2.41650E-01	1.25442E+00	2.30699E+00
2.10	2.20125E-01	2.08312E-01	1.83809E-01	1.21663E+00	2.28973E+00
2.20	1.76505E-01	1.66626E-01	1.41334E-01	1.18626E+00	2.27418E+00
2.30	1.43290E-01	1.35285E-01	1.09263E-01	1.16251E+00	2.26018E+00
2.40	1.17431E-01	1.11239E-01	8.45424E-02	1.14468E+00	2.24756E+00
2.50	9.69854E-02	9.25494E-02	6.52297E-02	1.13221E+00	2.23617E+00
2.60	8.06609E-02	7.79255E-02	5.00302E-02	1.12463E+00	2.22587E+00
2.70	6.75523E-02	6.64628E-02	3.80367E-02	1.12163E+00	2.21655E+00
2.80	5.69928E-02	5.74967E-02	2.85817E-02	1.12294E+00	2.20812E+00
2.90	4.84728E-02	5.05172E-02	2.11535E-02	1.12849E+00	2.20051E+00
3.00	4.15897E-02	4.51227E-02	1.53488E-02	1.13825E+00	2.19366E+00
3.10	3.60207E-02	4.09896E-02	1.08434E-02	1.15232E+00	2.18752E+00
3.20	3.15045E-02	3.78552E-02	7.37465E-03	1.17089E+00	2.18206E+00
3.30	2.78285E-02	3.55054E-02	4.72915E-03	1.19418E+00	2.17725E+00
3.40	2.48207E-02	3.37649E-02	2.73358E-03	1.22252E+00	2.17308E+00
3.50	2.23418E-02	3.24909E-02	1.24784E-03	1.25619E+00	2.16953E+00
3.60	2.02803E-02	3.15669E-02	1.59235E-04	1.29546E+00	2.16660E+00
3.70	1.85469E-02	3.08975E-02	-6.22343E-04	1.34039E+00	2.16429E+00
3.80	1.70710E-02	3.04049E-02	-1.16846E-03	1.39079E+00	2.16258E+00
3.90	1.57971E-02	3.00255E-02	-1.53558E-03	1.44601E+00	2.16148E+00
4.00	1.46817E-02	2.97076E-02	-1.76799E-03	1.50483E+00	2.16099E+00
4.10	1.36911E-02	2.94093E-02	-1.90012E-03	1.56549E+00	2.16111E+00
4.20	1.27994E-02	2.90990E-02	-1.95862E-03	1.62584E+00	2.16182E+00
4.30	1.19868E-02	2.87535E-02	-1.96396E-03	1.68375E+00	2.16313E+00
4.40	1.12382E-02	2.83582E-02	-1.93170E-03	1.73748E+00	2.16503E+00
4.50	1.05424E-02	2.79057E-02	-1.87363E-03	1.78606E+00	2.16750E+00
4.60	9.89092E-03	2.73947E-02	-1.79859E-03	1.82924E+00	2.17054E+00
4.70	9.27754E-03	2.68275E-02	-1.71311E-03	1.86739E+00	2.17412E+00
4.80	8.69766E-03	2.62095E-02	-1.62200E-03	1.90121E+00	2.17823E+00
4.90	8.14792E-03	2.55470E-02	-1.52874E-03	1.93146E+00	2.18285E+00
5.00	7.62586E-03	2.48469E-02	-1.43579E-03	1.95890E+00	2.18794E+00
5.10	7.12967E-03	2.41160E-02	-1.34486E-03	1.98411E+00	2.19349E+00
5.20	6.65802E-03	2.33610E-02	-1.25710E-03	2.00760E+00	2.19946E+00
5.30	6.20989E-03	2.25879E-02	-1.17323E-03	2.02972E+00	2.20582E+00
5.40	5.78447E-03	2.18025E-02	-1.09367E-03	2.05072E+00	2.21254E+00
5.50	5.38108E-03	2.10099E-02	-1.01865E-03	2.07079E+00	2.21959E+00
5.60	4.99911E-03	2.02148E-02	-9.48191E-04	2.09007E+00	2.22693E+00
5.80	4.29718E-03	1.86336E-02	-8.20691E-04	2.12658E+00	2.24233E+00
6.00	3.67408E-03	1.70870E-02	-7.09964E-04	2.16069E+00	2.25847E+00
6.20	3.12490E-03	1.55968E-02	-6.14300E-04	2.19263E+00	2.27507E+00
6.40	2.64438E-03	1.41783E-02	-5.31875E-04	2.22254E+00	2.29187E+00
6.60	2.22681E-03	1.28421E-02	-4.60944E-04	2.25051E+00	2.30864E+00
6.80	1.86638E-03	1.15942E-02	-3.99920E-04	2.27661E+00	2.32517E+00
7.00	1.55720E-03	1.04373E-02	-3.47404E-04	2.30089E+00	2.34127E+00
7.25	1.23412E-03	9.11908E-03	-2.91883E-04	2.32880E+00	2.36060E+00
7.50	9.71627E-04	7.93886E-03	-2.45756E-04	2.35409E+00	2.37883E+00
7.75	7.60029E-04	6.88933E-03	-2.07371E-04	2.37689E+00	2.39581E+00
8.00	5.90709E-04	5.96124E-03	-1.75370E-04	2.39734E+00	2.41146E+00
8.25	4.56133E-04	5.14445E-03	-1.48641E-04	2.41557E+00	2.42573E+00
8.50	3.49852E-04	4.42858E-03	-1.26275E-04	2.43171E+00	2.43863E+00
8.75	2.66429E-04	3.80333E-03	-1.07521E-04	2.44594E+00	2.45020E+00
9.00	2.01332E-04	3.25900E-03	-9.17666E-05	2.45839E+00	2.46051E+00
9.25	1.50817E-04	2.78646E-03	-7.85052E-05	2.46922E+00	2.46961E+00
9.50	1.11859E-04	2.37732E-03	-6.73197E-05	2.47860E+00	2.47762E+00

Table B1.7 : NaNe Model Potentials

R	$V(X^2\Sigma)$	$V(B^2\Sigma)$	$V(A^2\Pi)$	$D_{\Lambda'\Lambda}(B^2\Sigma\text{-}X^2\Sigma)$	$D_{\Lambda'\Lambda}(A^2\Pi\text{-}X^2\Sigma)$
2.00	1.12278E+00	1.10452E+00	1.10354E+00	2.81049E+00	2.86474E+00
2.10	8.01232E-01	7.83710E-01	7.82177E-01	2.76208E+00	2.82953E+00
2.20	5.81959E-01	5.65514E-01	5.63073E-01	2.69927E+00	2.79666E+00
2.30	4.30498E-01	4.15346E-01	4.11825E-01	2.63149E+00	2.76615E+00
2.40	3.24213E-01	3.10475E-01	3.05803E-01	2.56417E+00	2.73799E+00
2.50	2.48275E-01	2.36012E-01	2.30178E-01	2.50063E+00	2.71212E+00
2.60	1.92979E-01	1.82209E-01	1.75237E-01	2.44280E+00	2.68846E+00
2.70	1.51948E-01	1.42660E-01	1.34601E-01	2.39163E+00	2.66680E+00
2.80	1.20964E-01	1.13130E-01	1.04047E-01	2.34743E+00	2.64695E+00
2.90	9.72044E-02	9.07813E-02	8.07485E-02	2.31019E+00	2.62875E+00
3.00	7.87469E-02	7.36841E-02	6.27801E-02	2.27960E+00	2.61201E+00
3.10	6.42581E-02	6.04988E-02	4.88049E-02	2.25524E+00	2.59659E+00
3.20	5.27912E-02	5.02740E-02	3.78725E-02	2.23661E+00	2.58238E+00
3.30	4.36578E-02	4.23180E-02	2.92914E-02	2.22319E+00	2.56926E+00
3.40	3.63463E-02	3.61161E-02	2.25463E-02	2.21444E+00	2.55714E+00
3.50	3.04687E-02	3.12777E-02	1.72457E-02	2.20982E+00	2.54597E+00
3.60	2.57256E-02	2.75013E-02	1.30866E-02	2.20878E+00	2.53566E+00
3.70	2.18832E-02	2.45510E-02	9.83191E-03	2.21083E+00	2.52619E+00
3.80	1.87573E-02	2.22413E-02	7.29397E-03	2.21545E+00	2.51749E+00
3.90	1.62018E-02	2.04250E-02	5.32362E-03	2.22217E+00	2.50954E+00
4.00	1.41008E-02	1.89859E-02	3.80191E-03	2.23054E+00	2.50231E+00
4.10	1.23619E-02	1.78317E-02	2.63373E-03	2.24013E+00	2.49575E+00
4.20	1.09117E-02	1.68904E-02	1.74319E-03	2.25056E+00	2.48984E+00
4.30	9.69187E-03	1.61052E-02	1.06984E-03	2.26151E+00	2.48456E+00
4.40	8.65641E-03	1.54325E-02	5.65639E-04	2.27269E+00	2.47987E+00
4.50	7.76894E-03	1.48392E-02	1.92505E-04	2.28387E+00	2.47576E+00
4.60	7.00065E-03	1.43003E-02	-7.96165E-05	2.29487E+00	2.47219E+00
4.70	6.32917E-03	1.37974E-02	-2.74320E-04	2.30558E+00	2.46914E+00
4.80	5.73688E-03	1.33176E-02	-4.10077E-04	2.31588E+00	2.46658E+00
4.90	5.20992E-03	1.28517E-02	-5.01324E-04	2.32575E+00	2.46448E+00
5.00	4.73753E-03	1.23938E-02	-5.59218E-04	2.33514E+00	2.46282E+00
5.10	4.31131E-03	1.19403E-02	-5.92345E-04	2.34407E+00	2.46158E+00
5.20	3.92461E-03	1.14893E-02	-6.07350E-04	2.35253E+00	2.46071E+00
5.30	3.57222E-03	1.10402E-02	-6.09262E-04	2.36057E+00	2.46020E+00
5.40	3.25002E-03	1.05932E-02	-6.01887E-04	2.36820E+00	2.46001E+00
5.50	2.95467E-03	1.01490E-02	-5.88108E-04	2.37545E+00	2.46012E+00
5.60	2.68347E-03	9.70870E-03	-5.70073E-04	2.38237E+00	2.46051E+00
5.80	2.20500E-03	8.84481E-03	-5.27145E-04	2.39529E+00	2.46200E+00
6.00	1.80055E-03	8.01160E-03	-4.81260E-04	2.40718E+00	2.46428E+00
6.20	1.45945E-03	7.21793E-03	-4.36548E-04	2.41820E+00	2.46717E+00
6.40	1.17306E-03	6.47051E-03	-3.94870E-04	2.42846E+00	2.47050E+00
6.60	9.33993E-04	5.77389E-03	-3.56887E-04	2.43803E+00	2.47412E+00
6.80	7.35734E-04	5.13031E-03	-3.22663E-04	2.44696E+00	2.47792E+00
7.00	5.72482E-04	4.54039E-03	-2.91960E-04	2.45528E+00	2.48177E+00
7.25	4.09847E-04	3.87718E-03	-2.58017E-04	2.46484E+00	2.48655E+00
7.50	2.85030E-04	3.29280E-03	-2.28365E-04	2.47350E+00	2.49116E+00
7.75	1.90502E-04	2.78201E-03	-2.02380E-04	2.48128E+00	2.49549E+00
8.00	1.19957E-04	2.33868E-03	-1.79524E-04	2.48820E+00	2.49951E+00
8.25	6.81684E-05	1.95631E-03	-1.59363E-04	2.49430E+00	2.50317E+00
8.50	3.08774E-05	1.62841E-03	-1.41539E-04	2.49962E+00	2.50644E+00
8.75	4.66002E-06	1.34864E-03	-1.25751E-04	2.50423E+00	2.50935E+00
9.00	-1.31978E-05	1.11116E-03	-1.11752E-04	2.50818E+00	2.51190E+00
9.25	-2.48324E-05	9.10522E-04	-9.93311E-05	2.51153E+00	2.51411E+00
9.50	-3.18987E-05	7.41795E-04	-8.83058E-05	2.51434E+00	2.51600E+00

Table B1.7 - continued

R	$V(X^2\Sigma)$	$V(B^2\Sigma)$	$V(A^2\Pi)$	$D_{\Lambda'\Lambda}(B^2\Sigma\text{-}X^2\Sigma)$	$D_{\Lambda'\Lambda}(A^2\Pi\text{-}X^2\Sigma)$
9.75	-3.56710E-05	6.00532E-04	-7.85192E-05	2.51668E+00	2.51762E+00
10.00	-3.71169E-05	4.82800E-04	-6.98334E-05	2.51861E+00	2.51898E+00
10.25	-3.69622E-05	3.85132E-04	-6.21264E-05	2.52018E+00	2.52013E+00
10.50	-3.57461E-05	3.04486E-04	-5.52894E-05	2.52144E+00	2.52108E+00
10.75	-3.38630E-05	2.38225E-04	-4.92250E-05	2.52245E+00	2.52186E+00
11.00	-3.15978E-05	1.84061E-04	-4.38471E-05	2.52324E+00	2.52250E+00
11.25	-2.91521E-05	1.40037E-04	-3.90787E-05	2.52384E+00	2.52302E+00
11.50	-2.66667E-05	1.04417E-04	-3.48513E-05	2.52430E+00	2.52343E+00
11.75	-2.42322E-05	7.58647E-05	-3.11033E-05	2.52464E+00	2.52376E+00
12.00	-2.19098E-05	5.31158E-05	-2.77800E-05	2.52489E+00	2.52402E+00
12.25	-1.97350E-05	3.51418E-05	-2.48328E-05	2.52506E+00	2.52423E+00
12.50	-1.77260E-05	2.10779E-05	-2.22183E-05	2.52516E+00	2.52438E+00
12.75	-1.58894E-05	1.02009E-05	-1.98981E-05	2.52522E+00	2.52449E+00
13.00	-1.42236E-05	1.90649E-06	-1.78384E-05	2.52524E+00	2.52457E+00
13.50	-1.13745E-05	-8.85409E-06	-1.43827E-05	2.52521E+00	2.52467E+00
14.00	-9.09544E-06	-1.42556E-05	-1.16491E-05	2.52514E+00	2.52471E+00
14.50	-7.28944E-06	-1.63538E-05	-9.48006E-06	2.52504E+00	2.52471E+00
15.00	-5.86446E-06	-1.65033E-05	-7.75285E-06	2.52494E+00	2.52469E+00
16.00	-3.85423E-06	-1.41302E-05	-5.26352E-06	2.52476E+00	2.52463E+00
17.00	-2.59274E-06	-1.08553E-05	-3.64527E-06	2.52463E+00	2.52458E+00
18.00	-1.78617E-06	-7.95245E-06	-2.57350E-06	2.52456E+00	2.52454E+00
20.00	-9.05149E-07	-4.08805E-06	-1.35257E-06	2.52448E+00	2.52448E+00
22.00	-4.93841E-07	-2.13345E-06	-7.56308E-07	2.52445E+00	2.52446E+00
24.00	-2.85858E-07	-1.16867E-06	-4.45447E-07	2.52445E+00	2.52445E+00
26.00	-1.73612E-07	-6.75765E-07	-2.74037E-07	2.52444E+00	2.52445E+00
30.00	-7.17270E-08	-2.60084E-07	-1.15240E-07	2.52444E+00	2.52444E+00
35.00	-2.78953E-08	-9.59019E-08	-4.54356E-08	2.52444E+00	2.52444E+00
40.00	-1.23659E-08	-4.11408E-08	-2.03169E-08	2.52444E+00	2.52444E+00

Table B1.8 : NaNe Pseudopotentials

R	$V(X^2\Sigma)$	$V(B^2\Sigma)$	$V(A^2\Pi)$	$D_{\Lambda'\Lambda}(B^2\Sigma\text{-}X^2\Sigma)$	$D_{\Lambda'\Lambda}(A^2\Pi\text{-}X^2\Sigma)$
2.00	1.13821E+00	1.11419E+00	1.10704E+00	2.24372E+00	2.71087E+00
2.10	8.15276E-01	7.94143E-01	7.85283E-01	2.10565E+00	2.66364E+00
2.20	5.94668E-01	5.76267E-01	5.65838E-01	1.99338E+00	2.62418E+00
2.30	4.41996E-01	4.26164E-01	4.14295E-01	1.90365E+00	2.59098E+00
2.40	3.34632E-01	3.21207E-01	3.08018E-01	1.83284E+00	2.56273E+00
2.50	2.57744E-01	2.46574E-01	2.32170E-01	1.77764E+00	2.53833E+00
2.60	2.01611E-01	1.92561E-01	1.77037E-01	1.73529E+00	2.51696E+00
2.70	1.59847E-01	1.52791E-01	1.36232E-01	1.70357E+00	2.49798E+00
2.80	1.28222E-01	1.23047E-01	1.05531E-01	1.68068E+00	2.48093E+00
2.90	1.03900E-01	1.00503E-01	8.21016E-02	1.66530E+00	2.46544E+00
3.00	8.49499E-02	8.32354E-02	6.40178E-02	1.65632E+00	2.45126E+00
3.10	7.00290E-02	6.99077E-02	4.99397E-02	1.65293E+00	2.43819E+00
3.20	5.81822E-02	5.95692E-02	3.89150E-02	1.65453E+00	2.42611E+00
3.30	4.87141E-02	5.15277E-02	3.02508E-02	1.66060E+00	2.41490E+00
3.40	4.11065E-02	4.52664E-02	2.34305E-02	1.67077E+00	2.40449E+00
3.50	3.49654E-02	4.03923E-02	1.80614E-02	1.68471E+00	2.39485E+00
3.60	2.99868E-02	3.66002E-02	1.38398E-02	1.70212E+00	2.38593E+00
3.70	2.59322E-02	3.36505E-02	1.05278E-02	1.72271E+00	2.37771E+00
3.80	2.26136E-02	3.13532E-02	7.93723E-03	1.74613E+00	2.37019E+00
3.90	1.98816E-02	2.95564E-02	5.91839E-03	1.77201E+00	2.36335E+00
4.00	1.76173E-02	2.81387E-02	4.35191E-03	1.79988E+00	2.35718E+00
4.10	1.57259E-02	2.70028E-02	3.14233E-03	1.82925E+00	2.35169E+00
4.20	1.41319E-02	2.60716E-02	2.21348E-03	1.85955E+00	2.34686E+00
4.30	1.27755E-02	2.52837E-02	1.50466E-03	1.89021E+00	2.34270E+00
4.40	1.16090E-02	2.45918E-02	9.67562E-04	1.92070E+00	2.33919E+00
4.50	1.05950E-02	2.39593E-02	5.63925E-04	1.95054E+00	2.33632E+00
4.60	9.70403E-03	2.33592E-02	2.63539E-04	1.97935E+00	2.33409E+00
4.70	8.91291E-03	2.27721E-02	4.26199E-05	2.00688E+00	2.33248E+00
4.80	8.20361E-03	2.21845E-02	-1.17470E-04	2.03296E+00	2.33146E+00
4.90	7.56205E-03	2.15882E-02	-2.31259E-04	2.05756E+00	2.33103E+00
5.00	6.97730E-03	2.09783E-02	-3.10039E-04	2.08070E+00	2.33116E+00
5.10	6.44088E-03	2.03530E-02	-3.62537E-04	2.10244E+00	2.33181E+00
5.20	5.94622E-03	1.97126E-02	-3.95469E-04	2.12289E+00	2.33298E+00
5.30	5.48820E-03	1.90586E-02	-4.13975E-04	2.14216E+00	2.33462E+00
5.40	5.06279E-03	1.83936E-02	-4.21965E-04	2.16037E+00	2.33671E+00
5.50	4.66685E-03	1.77206E-02	-4.22400E-04	2.17761E+00	2.33921E+00
5.60	4.29784E-03	1.70430E-02	-4.17506E-04	2.19398E+00	2.34210E+00
5.80	3.63273E-03	1.56876E-02	-3.97942E-04	2.22442E+00	2.34888E+00
6.00	3.05464E-03	1.43525E-02	-3.71985E-04	2.25221E+00	2.35679E+00
6.20	2.55380E-03	1.30593E-02	-3.44231E-04	2.27772E+00	2.36556E+00
6.40	2.12208E-03	1.18245E-02	-3.16969E-04	2.30124E+00	2.37496E+00
6.60	1.75212E-03	1.06595E-02	-2.91224E-04	2.32296E+00	2.38474E+00
6.80	1.43718E-03	9.57166E-03	-2.67365E-04	2.34305E+00	2.39470E+00
7.00	1.17081E-03	8.56461E-03	-2.45435E-04	2.36161E+00	2.40467E+00
7.25	8.97114E-04	7.42039E-03	-2.20576E-04	2.38280E+00	2.41690E+00
7.50	6.79228E-04	6.40056E-03	-1.98270E-04	2.40191E+00	2.42866E+00
7.75	5.07513E-04	5.49884E-03	-1.78216E-04	2.41905E+00	2.43977E+00
8.00	3.73534E-04	4.70680E-03	-1.60146E-04	2.43436E+00	2.45012E+00
8.25	2.70029E-04	4.01507E-03	-1.43838E-04	2.44794E+00	2.45964E+00
8.50	1.90875E-04	3.41394E-03	-1.29111E-04	2.45990E+00	2.46828E+00
8.75	1.30986E-04	2.89373E-03	-1.15810E-04	2.47038E+00	2.47606E+00
9.00	8.61927E-05	2.44534E-03	-1.03807E-04	2.47949E+00	2.48299E+00
9.25	5.31110E-05	2.06023E-03	-9.29852E-05	2.48735E+00	2.48912E+00
9.50	2.90499E-05	1.73055E-03	-8.32414E-05	2.49410E+00	2.49449E+00

Table B1.8 - continued

R	$V(X^2\Sigma)$	$V(B^2\Sigma)$	$V(A^2\Pi)$	$D_{\Lambda'\Lambda}(B^2\Sigma\text{-}X^2\Sigma)$	$D_{\Lambda'\Lambda}(A^2\Pi\text{-}X^2\Sigma)$
9.75	1.18591E-05	1.44919E-03	-7.44796E-05	2.49983E+00	2.49918E+00
10.00	-1.44114E-07	1.20980E-03	-6.66132E-05	2.50468E+00	2.50323E+00
10.25	-8.26726E-06	1.00670E-03	-5.95605E-05	2.50875E+00	2.50672E+00
10.50	-1.35222E-05	8.34904E-04	-5.32457E-05	2.51214E+00	2.50971E+00
10.75	-1.66858E-05	6.89992E-04	-4.75981E-05	2.51494E+00	2.51225E+00
11.00	-1.83466E-05	5.68107E-04	-4.25524E-05	2.51723E+00	2.51440E+00
11.25	-1.89477E-05	4.65893E-04	-3.80489E-05	2.51908E+00	2.51621E+00
11.50	-1.88198E-05	3.80438E-04	-3.40325E-05	2.52059E+00	2.51774E+00
11.75	-1.82085E-05	3.09208E-04	-3.04525E-05	2.52178E+00	2.51901E+00
12.00	-1.72926E-05	2.50024E-04	-2.72629E-05	2.52272E+00	2.52007E+00
12.25	-1.62009E-05	2.01009E-04	-2.44220E-05	2.52345E+00	2.52094E+00
12.50	-1.50246E-05	1.60559E-04	-2.18920E-05	2.52401E+00	2.52166E+00
12.75	-1.38270E-05	1.27299E-04	-1.96391E-05	2.52442E+00	2.52225E+00
13.00	-1.26507E-05	1.00053E-04	-1.76328E-05	2.52473E+00	2.52273E+00
13.50	-1.04628E-05	5.97718E-05	-1.42532E-05	2.52508E+00	2.52343E+00
14.00	-8.56918E-06	3.34482E-05	-1.15676E-05	2.52522E+00	2.52389E+00
14.50	-6.98671E-06	1.66304E-05	-9.42887E-06	2.52523E+00	2.52417E+00
15.00	-5.69092E-06	6.19000E-06	-7.72070E-06	2.52517E+00	2.52435E+00
16.00	-3.79770E-06	-3.52935E-06	-5.25085E-06	2.52497E+00	2.52450E+00
17.00	-2.57453E-06	-5.97796E-06	-3.64029E-06	2.52479E+00	2.52454E+00
18.00	-1.78037E-06	-5.73745E-06	-2.57155E-06	2.52467E+00	2.52454E+00
20.00	-9.04592E-07	-3.64577E-06	-1.35227E-06	2.52453E+00	2.52450E+00
22.00	-4.93800E-07	-2.04821E-06	-7.56245E-07	2.52448E+00	2.52448E+00
24.00	-2.85869E-07	-1.15272E-06	-4.45433E-07	2.52447E+00	2.52447E+00
26.00	-1.73620E-07	-6.72847E-07	-2.74029E-07	2.52447E+00	2.52447E+00
30.00	-7.17384E-08	-2.59977E-07	-1.15223E-07	2.52446E+00	2.52447E+00
35.00	-2.78982E-08	-9.58865E-08	-4.54206E-08	2.52446E+00	2.52446E+00
40.00	-1.23730E-08	-4.11249E-08	-2.03006E-08	2.52446E+00	2.52446E+00

Annex C

Details of the Quantum Mechanical Line Wing Broadening Model

Appendix C1 The Core Eigenfunction

C1.1 Introduction

The purpose of this appendix is to obtain the functional form of the eigenfunction $\chi_i(R)$ describing the relative motion of the alkali and rare gas cores in the initial (excited) state.

C1.2 The Core Schrödinger Equation

The eigenfunction $\chi_i(R)$ satisfies the core Schrödinger equation obtained in §3.3.2 (cf. Eq.3.3.24):

$$\left[-\frac{\hbar^2}{2\mu}\nabla_R^2 + V_i(R) - E_i \right] \chi_i(R) = 0 \qquad \text{(C1.2.1)}$$

where $V_i(R)$ is the excited state interatomic potential. In spherical polar coordinates, this equation becomes (Schiff (1968), Eqs.14.1 and 14.21)

$$\left[-\frac{\hbar^2}{2\mu R^2}\frac{\partial}{\partial R}\left(R^2\frac{\partial}{\partial R}\right)+\frac{K^2}{2\mu R^2} \right] \chi_i(R) = (E_i - V_i(R))\,\chi_i(R) \qquad \text{(C1.2.2)}$$

where K^2 is the operator for the total angular momentum (i.e., that of the cores *and* the valence electron) given by (cf. Edmonds (1957), Eq.4.8.5)

$$K^2 = -\hbar^2\left[\frac{\partial^2}{\partial\beta^2} + \cot(\beta)\frac{\partial}{\partial\beta} + \frac{1}{\sin^2(\beta)}\left(\frac{\partial^2}{\partial\alpha^2} + \cos^2(\beta)\frac{\partial^2}{\partial\gamma^2}\right) - \frac{2\cos(\beta)}{\sin^2(\beta)}\frac{\partial^2}{\partial\alpha\partial\gamma} \right] \qquad \text{(C1.2.3)}$$

where (α, β, γ) are the Euler angles. The radial and angular parts of Eq.C1.2.2 are now separated by writing $\chi_i(R)$ in the product form

$$\chi_i(R) = \frac{1}{R}\,g_i(R)\,Y_i(\alpha,\beta,\gamma) \qquad \text{(C1.2.4)}$$

and substituting this into Eq.C1.2.2 giving

$$\left[\frac{1}{R}g_i(R)\right]^{-1}\left\{\frac{\partial}{\partial R}\left[R^2\frac{\partial}{\partial R}\left(\frac{1}{R}g_i(R)\right)\right]\right\} - \left[\hbar^2 Y_i(\alpha,\beta,\gamma)\right]^{-1} K^2 Y_i(\alpha,\beta,\gamma) = -\frac{2\mu R^2}{\hbar^2}(E_i - V_i(R)).$$

(C1.2.5)

Setting the radial and angular parts of this equation equal to the same constant yields the radial equation

$$\frac{1}{g_i(R)}\frac{d^2 g_i(R)}{dR^2} + \frac{2\mu}{\hbar^2}\left[E_i - V_i(R) \right] = \frac{c}{R^2} \qquad \text{(C1.2.6)}$$

and the angular equation

$$K^2\, Y_i(\alpha,\beta,\gamma) = \hbar^2\, c\, Y_i(\alpha,\beta,\gamma) \qquad \text{(C1.2.7)}$$

where c is the separation constant to be determined. This constant is found by considering the angular equation, Eq.C1.2.7.

C1.3 The Separation Constant

The angular function $Y_i(\alpha,\beta,\gamma)$ is written as a product of functions of the Euler angles α, β and γ:

$$Y_i(\alpha,\beta,\gamma) = \exp(iM\alpha)\, B(\beta)\, \exp(iM_L\gamma). \qquad \text{(C1.3.1)}$$

This form is used because the dependence of $Y_i(\alpha,\beta,\gamma)$ on γ is just a rotation about the internuclear axis corresponding to a function $\exp(iM_L\gamma)$, where $|M_L| = \Lambda$, the projection of the electron orbital angular momentum on the internuclear axis. Similarly, the dependence of $Y_i(\alpha,\beta,\gamma)$ on α is a rotation about the z'-axis of the space-fixed frame of reference corresponding to a function $\exp(iM\alpha)$, where M is the projection of the total angular momentum on this axis.

Substituting Eq.C1.3.1 into Eq.C1.2.7 and using Eq.C1.2.3 for K^2 leads to the equation satisfied by $B(\beta)$:

$$\left[\frac{\partial^2}{\partial\beta^2} + \cot(\beta)\frac{\partial}{\partial\beta} - \frac{1}{\sin^2(\beta)}\left[M^2 + M_L^2\cos^2(\beta)\right] + \frac{2\cos(\beta)}{\sin^2(\beta)} MM_L \right] \quad B(\beta) = -cB(\beta). \qquad \text{(C1.3.2)}$$

The function $B(\beta)$ is thus closely related to the matrix elements of the rotation matrix since (see Edmonds (1957), Eq.4.7.6)

$$\left[\frac{\partial^2}{\partial\beta^2} + \cot(\beta)\frac{\partial}{\partial\beta} - \frac{m^2 + k^2 - 2mk\cos(\beta)}{\sin^2(\beta)} + l(l+1) \right] \quad d^{(l)}_{mk}(\beta) = 0 \qquad \text{(C1.3.3)}$$

and comparing this with Eq.C1.3.2 shows that, to within a constant,

$$B(\beta) = d^{(K)}_{M M_L}(\beta) \qquad \text{(C1.3.4)}$$

provided that

$$c = K(K + 1) - \Lambda^2. \qquad \text{(C1.3.5)}$$

The rotational eigenfunction $Y_i(\alpha,\beta,\gamma)$ is thus (Edmonds (1957), Eq.4.1.12)

$$Y_i(\alpha,\beta,\gamma) = \exp(iM\alpha)\, d^{(K)}_{M M_L}(\beta)\, \exp(iM_L\gamma) \qquad \text{(C1.3.6)}$$
$$= D^{(K)}_{M M_L}(\alpha,\beta,\gamma).$$

The required normalisation of $Y_i(\alpha,\beta,\gamma)$ is such that

$$\int Y_i^*(\alpha,\beta,\gamma)\; Y_i(\alpha,\beta,\gamma)\; d\omega = 1\,; \quad d\omega \equiv d\alpha \sin(\beta) d\beta\, d\gamma \qquad \text{(C1.3.7)}$$

but as it stands, the function of Eq.C1.3.6 is not normalised in this way. The function $D^{(K)}_{M M_L}(\alpha,\beta,\gamma)$ satisfies (Edmonds (1957), Eq.4.6.1)

$$\frac{1}{8\pi^2}\int_0^{2\pi}\int_0^{\pi}\int_0^{2\pi} D^{(j_1)*}_{m'_1 m_1}(\alpha,\beta,\gamma)\; D^{(j_2)}_{m'_2 m_2}(\alpha,\beta,\gamma)\, d\alpha \sin(\beta) d\beta\, d\gamma$$
$$= \delta_{m'_1 m'_2}\delta_{m_1 m_2}\delta_{j_1 j_2}\frac{1}{(2j_1 + 1)} \qquad \text{(C1.3.8)}$$

so that the correctly normalised angular function is

$$Y_i(\alpha,\beta,\gamma) = \left[\frac{(2K+1)}{8\pi^2}\right]^{1/2} D^{(K)}_{M M_L}(\alpha,\beta,\gamma). \qquad \text{(C1.3.9)}$$

From Eq.C1.2.4, the required form of the eigenfunction $\chi_i(R)$ is then

$$\chi_i(R) = \frac{1}{R} g_i(R)\left[\frac{(2K+1)}{8\pi^2}\right]^{1/2} D^{(K)}_{M M_L}(\alpha,\beta,\gamma). \qquad \text{(C1.3.10)}$$

C1.4 The Radial Equation

With the separation constant c defined by Eq.C1.3.5, the radial Schrödinger equation, Eq.C1.2.6, is

$$\frac{d^2 g_i(R)}{dR^2} + \frac{2\mu}{\hbar^2}\left[E_i - V_i(R) - \frac{\hbar^2(K(K+1) - \Lambda^2)}{2\mu R^2} \right] g_i(R) = 0. \qquad \text{(C1.4.1)}$$

The centrifugal term involves the total angular momentum of the alkali - rare gas system (i.e., that of the cores *and* the valence electron), as indicated by the quantum number K, minus a contribution from the valence electron, as indicated by the quantum number Λ. It is assumed now that the electronic contribution to the total angular momentum is negligible in comparison with the angular momentum of the two cores and Eq.C1.4.1 then becomes

$$\frac{d^2 g_i(R)}{dR^2} + \frac{2\mu}{\hbar^2}\left[E_i - V_i(R) - \frac{\hbar^2 K(K+1)}{2\mu R^2} \right] g_i(R) = 0. \qquad \text{(C1.4.2)}$$

Appendix C2 The Bound-Free Transition Probability Function

C2.1 Introduction

The purpose of this appendix is to obtain an expression for the quantity $\left\{\frac{A_{if}}{\omega_i}\right\}dk_f$ appearing in the bound-free contribution $I_{BF}(\nu)$ given by Eq.5.2.1. This quantity is defined by

$$\frac{A_{if}}{\omega_i}dk_f = \frac{64\pi^4\nu^3}{3hc^3\omega_i}\left|\int \Psi_i(r',R)\, er'\, \Psi_f^*(k_f,r',R)\; dr'dR\;\right|^2 dk_f \qquad \text{(C2.1.1)}$$

with all quantities as defined in §5.2.1.

C2.2 The Substitutions

For convenience, the quantity R_{if} is defined via

$$R_{if} = \frac{1}{\omega_i}\left|\int \Psi_i(r',R)\, er'\, \Psi_f^*(k_f,r',R)\, dr'dR\;\right|^2 dk_f \qquad \text{(C2.2.1)}$$

so that

$$\frac{A_{if}}{\omega_i}dk_f = \frac{64\pi^4\nu^3}{3hc^3}R_{if}\,. \qquad \text{(C2.2.2)}$$

The form of the eigenfunctions $\Psi_i(r',R)$ and $\Psi_f(k_f,r',R)$ is given in §5.2.1 by Eqs.5.2.5

and 5.2.6, together with Eqs.5.2.10 and 5.2.16. With these functions, and with the electron coordinates r' expressed in their spherical components defined in Eq.5.2.18, R_{if} may be written

Table B1.6 - continued

R	$V(X^2\Sigma)$	$V(B^2\Sigma)$	$V(A^2\Pi)$	$D_{\Lambda'\Lambda}(B^2\Sigma\text{-}X^2\Sigma)$	$D_{\Lambda'\Lambda}(A^2\Pi\text{-}X^2\Sigma)$
9.75	8.19814E-05	2.02392E-03	-5.78653E-05	2.48665E+00	2.48462E+00
10.00	5.92096E-05	1.71941E-03	-4.98582E-05	2.49352E+00	2.49069E+00
10.25	4.19721E-05	1.45760E-03	-4.30626E-05	2.49936E+00	2.49595E+00
10.50	2.90201E-05	1.23303E-03	-3.72831E-05	2.50429E+00	2.50048E+00
10.75	1.93661E-05	1.04081E-03	-3.23570E-05	2.50841E+00	2.50436E+00
11.00	1.22394E-05	8.76625E-04	-2.81490E-05	2.51183E+00	2.50767E+00
11.25	7.03927E-06	7.36702E-04	-2.45470E-05	2.51466E+00	2.51047E+00
11.50	3.29958E-06	6.17725E-04	-2.14569E-05	2.51699E+00	2.51286E+00
11.75	6.57602E-07	5.16772E-04	-1.88001E-05	2.51888E+00	2.51487E+00
12.00	-1.16420E-06	4.31301E-04	-1.65108E-05	2.52040E+00	2.51656E+00
12.25	-2.37809E-06	3.59099E-04	-1.45337E-05	2.52161E+00	2.51797E+00
12.50	-3.14571E-06	2.98245E-04	-1.28225E-05	2.52257E+00	2.51915E+00
12.75	-3.58924E-06	2.47074E-04	-1.13382E-05	2.52332E+00	2.52013E+00
13.00	-3.80090E-06	2.04139E-04	-1.00479E-05	2.52389E+00	2.52094E+00
13.50	-3.78839E-06	1.38176E-04	-7.94225E-06	2.52464E+00	2.52217E+00
14.00	-3.47175E-06	9.23715E-05	-6.33035E-06	2.52502E+00	2.52299E+00
14.50	-3.04453E-06	6.08705E-05	-5.08594E-06	2.52517E+00	2.52354E+00
15.00	-2.60499E-06	3.94167E-05	-4.11722E-06	2.52520E+00	2.52390E+00
16.00	-1.84195E-06	1.53333E-05	-2.75596E-06	2.52505E+00	2.52427E+00
17.00	-1.28501E-06	4.91517E-06	-1.89285E-06	2.52487E+00	2.52442E+00
18.00	-9.01441E-07	7.20757E-07	-1.33013E-06	2.52471E+00	2.52447E+00
20.00	-4.62970E-07	-1.12707E-06	-6.96589E-07	2.52454E+00	2.52448E+00
22.00	-2.53466E-07	-9.07651E-07	-3.89295E-07	2.52448E+00	2.52447E+00
24.00	-1.46897E-07	-5.65992E-07	-2.29362E-07	2.52447E+00	2.52447E+00
26.00	-8.92692E-08	-3.41710E-07	-1.41163E-07	2.52446E+00	2.52446E+00
30.00	-3.69164E-08	-1.33991E-07	-5.93930E-08	2.52446E+00	2.52446E+00
35.00	-1.43637E-08	-4.95134E-08	-2.34222E-08	2.52446E+00	2.52446E+00
40.00	-6.37543E-09	-2.12418E-08	-1.04678E-08	2.52446E+00	2.52446E+00

$$R_{if} = \frac{e^2}{\omega_i} \sum_{m'} \int \Psi_i^* \, r'^*_{m'} \, \Psi_f \, dr' \, dR \int \Psi_i \, r'_{m'} \, \Psi_f^* \, dr' \, dR \, dk_f$$

$$= \frac{e^2}{\omega_i} \sum_{\substack{m' m_1 m_2 \\ M M_L M'_L}} \int \psi_{M'_L} \left(\frac{4\pi}{3}\right)^{1/2} r \, D^{(1)*}_{m' m_1}(\omega) \, Y^*_{1 m_1}(\theta,\phi) \, \psi^*_{M_L} dr$$

$$\times \frac{1}{R} g_i(R) \left[\frac{(2K+1)}{8\pi^2}\right]^{1/2} D^{(K)*}_{M M_L}(\omega)$$

$$\times \frac{1}{(2\pi)^2} \sum_{K_1 M_1} i^{K_1} \frac{1}{k_f R} g_f(R) \, (4\pi)^{1/2} (2K_1+1)^{1/2} \, Y^*_{K_1 M_1}(\theta_{k_f}, \phi_{k_f}) \, D^{(K_1)}_{M_1 M'_L}(\omega) \, R^2 \, dR \, d\omega$$

$$\times \int \psi^*_{M'_L} \left(\frac{4\pi}{3}\right)^{1/2} r \, D^{(1)}_{m' m_2}(\omega') \, Y_{1 m_2}(\theta,\phi) \, \psi_{M_L} dr$$

$$\times \frac{1}{R'} g_i(R') \left[\frac{(2K+1)}{8\pi^2}\right]^{1/2} D^{(K)}_{M M_L}(\omega')$$

$$\times \frac{1}{(2\pi)^2} \sum_{K_2 M_2} (-i)^{K_2} \frac{1}{k_f R'} g_f(R') \, (4\pi)^{1/2} (2K_2+1)^{1/2} \, Y_{K_2 M_2}(\theta_{k_f}, \phi_{k_f}) \, D^{(K_2)*}_{M_2 M'_L}(\omega') \, R'^2 \, dR' \, d\omega'$$

$$\times k_f^2 \, dk_f \, d\hat{k}_f \qquad \text{(C2.2.3)}$$

where the electron eigenfunctions have been labelled with M_L and M'_L, the projections of the electron orbital angular momentum on the internuclear axis in the initial and final state respectively, and the arguments ω and ω' of the rotation matrix elements denote the Euler angles ($\alpha \, \beta \, \gamma$).

The normalisation of the spherical harmonics requires that (Merzbacher (1970), Eq.9.69)

$$\int Y^*_{K_1 M_1}(\theta_{k_f}, \phi_{k_f}) \, Y_{K_2 M_2}(\theta_{k_f}, \phi_{k_f}) \, d\hat{k}_f = \delta_{K_1 K_2} \delta_{M_1 M_2} \qquad \text{(C2.2.4)}$$

and with this result R_{if} becomes

$$R_{if} = \frac{e^2(2K+1)}{24\pi^4\omega_i} \sum_{\substack{m' m_1 m_2 \\ M M_L M'_L}} \sum_{K' M'} (2K'+1) \int \psi_{M'_L}\ r\ Y^*_{1m_1}(\theta,\phi)\, \psi^*_{M_L} dr\, g_i(R)\, g_f(R)\, dR$$

$$\times \int \psi^*_{M'_L}\ r\ Y_{1m_2}(\theta,\phi)\, \psi_{M_L} dr\, g_i(R')\, g_f(R')\, dR'$$

$$\times \int D^{(1)*}_{m'm_1}(\omega)\, D^{(K)*}_{M M_L}(\omega)\, D^{(K')}_{M' M'_L}(\omega)\, d\omega$$

$$\times \int D^{(1)}_{m'm_2}(\omega')\, D^{(K)}_{M M_L}(\omega')\, D^{(K')*}_{M' M'_L}(\omega')\, d\omega'\, dk_f \qquad \text{(C2.2.5)}$$

The complex conjugates of the rotation matrix elements transform according to (Edmonds (1957), Eq.4.2.7)

$$D^{(1)*}_{m'm_1}(\omega) = (-1)^{m'-m_1} D^{(1)}_{-m'-m_1}(\omega),$$

$$D^{(K)*}_{M M_L}(\omega) = (-1)^{M-M_L} D^{(K)}_{-M-M_L}(\omega), \qquad \text{(C2.2.6)}$$

$$D^{(K')*}_{M' M'_L}(\omega') = (-1)^{M'-M'_L} D^{(K')}_{-M'-M'_L}(\omega').$$

These relations allow the integrals involving the rotation matrix elements in Eq.C2.2.5 to be written (cf. Edmonds (1957), Eq.4.6.2)

$$\int D^{(1)*}_{m'm_1}(\omega)\, D^{(K)*}_{M M_L}(\omega)\, D^{(K')}_{M' M'_L}(\omega)\, d\omega$$

$$= (-1)^{m'-m_1+M-M_L} 8\pi^2 \begin{pmatrix} 1 & K & K' \\ -m' & -M & M' \end{pmatrix} \begin{pmatrix} 1 & K & K' \\ -m_1 & -M_L & M'_L \end{pmatrix} \qquad \text{(C2.2.7)}$$

and

$$\int D^{(1)}_{m'm_2}(\omega')\, D^{(K)}_{M M_L}(\omega')\, D^{(K')*}_{M' M'_L}(\omega')\, d\omega'$$

$$= (-1)^{M'-M'_L} 8\pi^2 \begin{pmatrix} 1 & K & K' \\ m' & M & -M' \end{pmatrix} \begin{pmatrix} 1 & K & K' \\ m_2 & M_L & -M'_L \end{pmatrix}. \qquad \text{(C2.2.8)}$$

The symmetry properties of the 3-j symbols (see Edmonds (1957), Eq.3.7.6) show that

$$\begin{pmatrix} 1 & K & K' \\ -m' & -M & M' \end{pmatrix} = (-1)^{1+K+K'} \begin{pmatrix} 1 & K & K' \\ m' & M & -M' \end{pmatrix} \qquad \text{(C2.2.9)}$$

and

$$\begin{pmatrix} 1 & K & K' \\ -m_1 & -M_L & M'_L \end{pmatrix} = (-1)^{1+K+K'} \begin{pmatrix} 1 & K & K' \\ m_1 & M_L & -M'_L \end{pmatrix}. \qquad \text{(C2.2.10)}$$

The product of Eqs.C2.2.7 and C2.2.8 is then

$$(-1)^{m' - m_1 + M - M_L + M' - M'_L} 64\pi^4 \begin{pmatrix} 1 & K & K' \\ m' & M & -M' \end{pmatrix}^2 \begin{pmatrix} 1 & K & K' \\ m_1 & M_L & -M'_L \end{pmatrix} \begin{pmatrix} 1 & K & K' \\ m_2 & M_L & -M'_L \end{pmatrix}. \qquad \text{(C2.2.11)}$$

The 3-j symbols are zero unless the following conditions hold :

$$\begin{aligned} &m' + M - M' = 0, \\ &m_1 + M_L - M'_L = 0, \\ &m_2 + M_L - M'_L = 0, \end{aligned} \qquad \text{(C2.2.12)}$$

from which it is clear that

$$m_1 = m_2 = M'_L - M_L \equiv m. \qquad \text{(C2.2.13)}$$

These conditions reduce the expression C2.2.11 to

$$64\pi^4 \left\{ \begin{pmatrix} 1 & K & K' \\ m' & M & -M' \end{pmatrix} \begin{pmatrix} 1 & K & K' \\ m & M_L & -M'_L \end{pmatrix} \right\}^2 \qquad \text{(C2.2.14)}$$

and Eq.C2.2.5 then becomes

$$\begin{aligned} R_{if} = \frac{8e^2(2K+1)}{3\omega_i} \sum_{\substack{m' m \\ M M_L M'_L}} \sum_{K' M'} (2K'+1) &\int \psi_{M'_L} \; r \; Y^*_{1m}(\theta,\phi) \, \psi^*_{M_L} dr \, g_i(R) \, g_f(R) \, dR \\ &\times \int \psi^*_{M'_L} \; r \; Y_{1m}(\theta,\phi) \, \psi_{M_L} dr \, g_i(R') \, g_f(R') \, dR' \\ &\times \left\{ \begin{pmatrix} 1 & K & K' \\ m' & M & -M' \end{pmatrix} \begin{pmatrix} 1 & K & K' \\ m & M_L & -M'_L \end{pmatrix} \right\}^2 dk_f . \end{aligned} \qquad \text{(C2.2.15)}$$

The first term to consider is the sum

$$\sum_{M\,M'} \begin{pmatrix} 1 & K & K' \\ m' & M & -M' \end{pmatrix}^2 \qquad \text{(C2.2.16)}$$

appearing in Eq.C2.2.15. The sum over M' is taken from M' = -K' to M' = K', i.e., from -M' = K' to -M' = -K', and this may be written (Edmonds (1957), Eq, 3.7.4)

$$\sum_{M\,M'} \begin{pmatrix} 1 & K & K' \\ m' & M & -M' \end{pmatrix}^2 = \sum_{M\,-M'} \begin{pmatrix} 1 & K & K' \\ m' & M & -M' \end{pmatrix}^2 = \sum_{M\,-M'} \begin{pmatrix} K & K' & 1 \\ M & -M' & m' \end{pmatrix}^2. \qquad \text{(C2.2.17)}$$

This last form of the sum is given by (Edmonds (1957), Eq.3.7.8)

$$\sum_{M\,-M'} \begin{pmatrix} K & K' & 1 \\ M & -M' & m' \end{pmatrix}^2 = \frac{1}{3}\,\delta(K\,K'\,1) \qquad \text{(C2.2.18)}$$

where $\delta(K\,K'\,1) = 1$ if K, K', 1 satisfy the triangular condition and is zero otherwise.

Summing the expression of Eq.C2.2.16 over m' then yields

$$\sum_{m'}\sum_{M\,M'} \begin{pmatrix} 1 & K & K' \\ m' & M & -M' \end{pmatrix}^2 = \frac{3\,\delta(K\,K'\,1)}{3} = \delta(K\,K'\,1) \qquad \text{(C2.2.19)}$$

since the sum over m' runs for $m' = 0, \pm 1$. The sum of Eq.C2.2.19 is therefore unity if the triangular condition is satisfied, i.e.,

$$|\,K - K'\,| \le 1 \qquad \text{(C2.2.20)}$$

and is zero otherwise.

From Eq.5.2.18 of §5.2.1, the electron coordinate, r, may be written in terms of its spherical components as

$$r\,Y_{1m}(\theta,\phi) \equiv r\,Y^{*}_{1m}(\theta,\phi) = \left(\frac{3}{4\pi}\right)^{1/2} r_m\,. \qquad \text{(C2.2.21)}$$

Substituting these expressions, together with the result in Eq.C2.2.19, into Eq.C2.2.15 gives

$$R_{if} = \frac{8e^2(2K+1)}{3\omega_i} \sum_{\substack{m \\ M_L M'_L}} \sum_{K'} (2K'+1) \int \psi_{M'_L} \left(\frac{3}{4\pi}\right)^{1/2} r_m \ \psi^*_{M_L} dr\, g_i(R)\, g_f(R)\, dR$$

$$\times \int \psi^*_{M'_L} \left(\frac{3}{4\pi}\right)^{1/2} r_m \ \psi_{M_L} dr\, g_i(R')\, g_f(R')\, dR'$$

$$\times \begin{pmatrix} 1 & K & K' \\ m & M_L & -M'_L \end{pmatrix}^2 \delta(K\, K'\, 1)\ dk_f$$

$$= \frac{2(2K+1)}{\pi\omega_i} \sum_{\substack{m \\ M_L M'_L}} \sum_{K'} (2K'+1) \begin{pmatrix} K & 1 & K' \\ M_L & m & -M'_L \end{pmatrix}^2$$

$$\times \left| \int \psi_{M'_L} e r_m \psi^*_{M_L} dr \int g_i(R)\, g_f(R)\, dR \right|^2 \delta(K\, K'\, 1)\ dk_f \qquad \text{(C2.2.22)}$$

where the symmetry relation (Edmonds (1957), Eq.3.7.5),

$$\begin{pmatrix} 1 & K & K' \\ m & M_L & -M'_L \end{pmatrix} = (-1)^{1+K+K'} \begin{pmatrix} K & 1 & K' \\ M_L & m & -M'_L \end{pmatrix} \qquad \text{(C2.2.23)}$$

has been used.

The next term to consider is the sum

$$\frac{1}{\omega_i} \sum_{\substack{m \\ M_L M'_L}} \begin{pmatrix} K & 1 & K' \\ M_L & m & -M'_L \end{pmatrix}^2 \left| \int \psi_{M'_L} e r_m \psi^*_{M_L} dr \right|^2 \qquad \text{(C2.2.24)}$$

where (see Eq.C2.2.13)

$$m = M'_L - M_L\ ; \quad |M_L| = \Lambda. \qquad \text{(C2.2.25)}$$

For the $A^2\Pi - X^2\Sigma$ transition,

$$\begin{aligned} &\Lambda = 1 \ \ (M_L = \pm 1); \\ &\Lambda' = 0 \ \ (M'_L = 0); \\ &\omega_i = 2 \end{aligned} \qquad \text{(C2.2.26)}$$

and the sum (C2.2.24) becomes

$$\frac{1}{2}\left\{ \begin{pmatrix} K & 1 & K' \\ 1 & -1 & 0 \end{pmatrix}^2 \left| \int \psi_0 \, er_{-1} \, \psi_1^* dr \right|^2 + \begin{pmatrix} K & 1 & K' \\ -1 & 1 & 0 \end{pmatrix}^2 \left| \int \psi_0 \, er_1 \, \psi_{-1}^* dr \right|^2 \right\}. \qquad \text{(C2.2.27)}$$

By symmetry (Edmonds (1957), Eq.3.7.6)

$$\begin{pmatrix} K & 1 & K' \\ -1 & 1 & 0 \end{pmatrix} = (-1)^{1+K+K'} \begin{pmatrix} K & 1 & K' \\ 1 & -1 & 0 \end{pmatrix} \qquad \text{(C2.2.28)}$$

so that

$$\begin{pmatrix} K & 1 & K' \\ -1 & 1 & 0 \end{pmatrix}^2 = \begin{pmatrix} K & 1 & K' \\ 1 & -1 & 0 \end{pmatrix}^2. \qquad \text{(C2.2.29)}$$

Also

$$\left| \int \psi_0 \, er_{-1} \, \psi_1^* dr \right|^2 = \left| \int \psi_0 \, er_1 \, \psi_{-1}^* dr \right|^2 \qquad \text{(C2.2.30)}$$

so that the sum C2.2.27 reduces to

$$\begin{pmatrix} K & 1 & K' \\ 1 & -1 & 0 \end{pmatrix}^2 \left| \int \psi_{\Lambda'} \, er_{\Lambda' - \Lambda} \, \psi_\Lambda^* dr \right|^2. \qquad \text{(C2.2.31)}$$

For the $B^2\Sigma - X^2\Sigma$ transition,

$$\begin{aligned} &\Lambda = 0 \;\; (M_L = 0); \\ &\Lambda' = 0 \;\; (M'_L = 0); \\ &\omega_i = 1 \end{aligned} \qquad \text{(C2.2.32)}$$

and the sum (C2.2.24) comprises the single term

$$\begin{pmatrix} K & 1 & K' \\ 0 & 0 & 0 \end{pmatrix}^2 \left| \int \psi_{\Lambda'} \, er_{\Lambda' - \Lambda} \, \psi_\Lambda^* dr \right|^2. \qquad \text{(C2.2.33)}$$

Thus Eq.C2.2.22 becomes, for the $A^2\Pi - X^2\Sigma$ transition,

$$R_{if}(\Lambda = 1, \Lambda' = 0) = \frac{2}{\pi}(2K + 1) \sum_{K'} (2K' + 1) \begin{pmatrix} K & 1 & K' \\ 1 & -1 & 0 \end{pmatrix}^2 S_{if}\ \delta(K\ K'\ 1)\ dk_f \quad (C2.2.34)$$

and for the $B^2\Sigma - X^2\Sigma$ transition,

$$R_{if}(\Lambda = 0, \Lambda' = 0) = \frac{2}{\pi}(2K + 1) \sum_{K'} (2K' + 1) \begin{pmatrix} K & 1 & K' \\ 0 & 0 & 0 \end{pmatrix}^2 S_{if}\ \delta(K\ K'\ 1)\ dk_f \quad (C2.2.35)$$

where

$$S_{if} = \left| \int_0^\infty g_i(R)\, D_{\Lambda'\Lambda}(R)\, g_f(R)\, dR \right|^2 \quad (C2.2.36)$$

and $D_{\Lambda'\Lambda}(R)$, defined by

$$D_{\Lambda'\Lambda}(R) = \int \psi_{\Lambda'}\, er_{\Lambda' - \Lambda}\, \psi_{\Lambda}^{*} dr, \quad (C2.2.37)$$

is the dipole transition moment. The radial dependence of $D_{\Lambda'\Lambda}(R)$ is through the parametric dependence of the electron eigenfunctions on R (see Eqs.5.2.5 and 5.2.6 of §5).

The final sum to be considered is that over K'. The matrix element S_{if} depends on K' through the radial eigenfunction $g_f(R)$ (see §5, Eq.5.2.17). Since the only non-zero contributions to R_{if} are those for which $\delta(K\ K'\ 1)$ is non-zero (i.e., K' = K - 1, K, K + 1), so that the change in K for the transition is at most unity, the approximation is now made that the S_{if} for the K' = K - 1 and K' = K + 1 transitions are equal in magnitude to the S_{if} for the K' = K transition. The S_{if} are then independent of K', with $g_f(R)$ satisfying

$$\frac{d^2 g_f(R)}{dR^2} + \frac{2\mu}{\hbar^2}\left[E_f - V_f(R) - \frac{\hbar^2 K(K+1)}{2\mu R^2} \right] g_f(R) = 0. \quad (C2.2.38)$$

With this approximation, the sum over K' to be evaluated for the $A^2\Pi - X^2\Sigma$ transition is (see Eq.C2.2.34)

$$S = \sum_{K'} (2K' + 1) \begin{pmatrix} K & 1 & K' \\ 1 & -1 & 0 \end{pmatrix}^2 \delta(K\, K'\, 1). \qquad \text{(C2.2.39)}$$

The only non-zero contributions to the sum S are those for which $\delta(K\, K'\, 1)$ is non-zero, i.e., K' = K - 1, K or K + 1. Hence,

$$S = (2(K + 1) + 1) \begin{pmatrix} K & 1 & K+1 \\ 1 & -1 & 0 \end{pmatrix}^2 + (2K + 1) \begin{pmatrix} K & 1 & K \\ 1 & -1 & 0 \end{pmatrix}^2$$
$$+ (2(K - 1) + 1) \begin{pmatrix} K & 1 & K-1 \\ 1 & -1 & 0 \end{pmatrix}^2. \qquad \text{(C2.2.40)}$$

Using the symmetry properties of the 3-j symbols and their explicit forms (see Edmonds (1957), Appendix 2, Table 2) the terms in the sum are

$$\begin{pmatrix} K & 1 & K+1 \\ 1 & -1 & 0 \end{pmatrix}^2 \equiv \begin{pmatrix} K+1 & K & 1 \\ 0 & -1 & 1 \end{pmatrix}^2 = \frac{K(K+1)}{(2K+3)(2K+2)(2K+1)}, \qquad \text{(C2.2.41)}$$

$$\begin{pmatrix} K & 1 & K \\ 1 & -1 & 0 \end{pmatrix}^2 \equiv \begin{pmatrix} K & K & 1 \\ 0 & -1 & 1 \end{pmatrix}^2 = \frac{2K(K+1)}{(2K+2)(2K+1)(2K)}, \qquad \text{(C2.2.42)}$$

$$\begin{pmatrix} K & 1 & K-1 \\ 1 & -1 & 0 \end{pmatrix}^2 = \frac{K(K+1)}{(2K+1)(2K)(2K-1)} \qquad \text{(C2.2.43)}$$

so that

$$S = \frac{(2K+3)K(K+1)}{(2K+3)(2K+2)(2K+1)} + \frac{(2K+1)(2K)(K+1)}{(2K+2)(2K+1)(2K)} + \frac{(2K-1)(K)(K+1)}{(2K+1)(2K)(2K-1)}$$

$$= \frac{K + (2K+1) + K + 1}{2(2K+1)} \qquad \text{(C2.2.44)}$$

$$= 1.$$

The sum over K' to be evaluated for the $B^2\Sigma - X^2\Sigma$ transition is (see Eq.C2.2.35)

$$S = \sum_{K'} (2K' + 1) \begin{pmatrix} K & 1 & K' \\ 0 & 0 & 0 \end{pmatrix}^2 \delta(K\, K'\, 1). \qquad \text{(C2.2.45)}$$

As with the $A^2\Pi - X^2\Sigma$ transition, the only non-zero contributions to S are those for which K' = K - 1, K or K + 1. Hence,

$$S = (2(K+1)+1)\begin{pmatrix} K & 1 & K+1 \\ 0 & 0 & 0 \end{pmatrix}^2 + (2K+1)\begin{pmatrix} K & 1 & K \\ 0 & 0 & 0 \end{pmatrix}^2$$
$$+ (2(K-1)+1)\begin{pmatrix} K & 1 & K-1 \\ 0 & 0 & 0 \end{pmatrix}^2. \qquad \text{(C2.2.46)}$$

The second term in this sum is zero since (K + 1 + K) is odd (see Edmonds (1957), Eq.3.7.14); the remaining two terms may be written (see Edmonds (1957), Appendix 2, Table 2)

$$\begin{pmatrix} K & 1 & K+1 \\ 0 & 0 & 0 \end{pmatrix}^2 \equiv \begin{pmatrix} K+1 & K & 1 \\ 0 & 0 & 0 \end{pmatrix}^2 = \frac{2(K+1)(K+1)}{(2K+3)(2K+2)(2K+1)}, \qquad \text{(C2.2.47)}$$

$$\begin{pmatrix} K & 1 & K-1 \\ 0 & 0 & 0 \end{pmatrix}^2 = \frac{2K^2}{(2K+1)(2K)(2K-1)} \qquad \text{(C2.2.48)}$$

so that

$$S = \frac{(2K+3)2(K+1)(K+1)}{(2K+3)(2K+2)(2K+1)} + \frac{(2K-1)(2K^2)}{(2K+1)(2K)(2K-1)}$$

$$= \frac{K+1}{(2K+1)} + \frac{K}{(2K+1)} \qquad \text{(C2.2.49)}$$

$$= 1.$$

The sums over K' for the $A^2\Pi - X^2\Sigma$ and $B^2\Sigma - X^2\Sigma$ transitions are thus identical and are equal to unity, resulting in the final form of R_{if}, applicable to both transitions:

$$R_{if} = \frac{2}{\pi}(2K+1)\, S_{if}\, dk_f\,. \qquad \text{(C2.2.50)}$$

Thus, from Eq.C2.2.2,

$$\frac{A_{if}}{\omega_i} dk_f = \frac{128\pi^3\nu^3}{3hc^3}(2K+1)\, S_{if}\, dk_f\,, \qquad \text{(C2.2.51)}$$

and this result completes the analysis of this appendix.

Appendix C3 The Free-Free Transition Probability Function

C3.1 Introduction

The purpose of this appendix is to obtain an expression for the quantity $\left\{\frac{A_{if}}{\omega_i}\right\} dk_i\, dk_f$ appearing in the free-free contribution $I_{FF}(\nu)$ given by Eq.5.2.38. This quantity is defined by

$$\frac{A_{if}}{\omega_i} dk_i\, dk_f = \frac{64\pi^4\nu^3}{3hc^3\omega_i} \left| \int \Psi_i(k_i,r',R)\, er'\, \Psi_f^*(k_f,r',R)\, dr'dR \right|^2 dk_i\, dk_f \qquad \text{(C3.1.1)}$$

with all quantities as defined in §5.2.1 and §5.2.3.

C3.2 The Substitutions

For convenience, the quantity R_{if} is defined via

$$R_{if} = \frac{1}{\omega_i} \left| \int \Psi_i(k_i,r',R)\, er'\, \Psi_f^*(k_f,r',R)\, dr'dR \right|^2 dk_i\, dk_f \qquad \text{(C3.2.1)}$$

so that

$$\frac{A_{if}}{\omega_i} dk_i\, dk_f = \frac{64\pi^4\nu^3}{3hc^3} R_{if}\,. \qquad \text{(C3.2.2)}$$

The form of the eigenfunctions $\Psi_i(k_i,r',R)$ and $\Psi_f(k_f,r',R)$ is given in §5.2.3 by Eqs.5.2.39 and 5.2.40, together with Eqs.5.2.41 and 5.2.42. With these functions, and with the electron coordinates r' expressed in their spherical components defined in Eq.5.2.18, R_{if} may be written

$$R_{if} = \frac{e^2}{\omega_i} \sum_{m'} \int \Psi_i^* \, r'^*_{m'} \, \Psi_f \, dr' \, dR \int \Psi_i \, r'_{m'} \, \Psi_f^* \, dr' \, dR \, dk_i \, dk_f$$

$$= \frac{e^2}{\omega_i} \sum_{\substack{m' m_1 m_2 \\ M_L M'_L}} \int \psi_{M'_L} \left(\frac{4\pi}{3}\right)^{1/2} r \, D^{(1)*}_{m' m_1}(\omega) \, Y^*_{1 m_1}(\theta,\phi) \, \psi^*_{M_L} \, dr$$

$$\times \frac{1}{(2\pi)^2} \sum_{K_1 M_1} i^{K_1} \frac{1}{k_f R} g_f(R) \, (4\pi)^{1/2} (2K_1+1)^{1/2} \, Y^*_{K_1 M_1}(\theta_{k_f}, \phi_{k_f}) \, D^{(K_1)}_{M_1 M'_L}(\omega)$$

$$\times \frac{1}{(2\pi)^2} \sum_{K_2 M_2} (-i)^{K_2} \frac{1}{k_i R} g_i(R) \, (4\pi)^{1/2} (2K_2+1)^{1/2} \, Y_{K_2 M_2}(\theta_{k_i}, \phi_{k_i}) \, D^{(K_2)*}_{M_2 M_L}(\omega) \, R^2 \, dR \, d\omega$$

$$\times \int \psi^*_{M'_L} \left(\frac{4\pi}{3}\right)^{1/2} r \, D^{(1)}_{m' m_2}(\omega') \, Y_{1 m_2}(\theta,\phi) \, \psi_{M_L} \, dr$$

$$\times \frac{1}{(2\pi)^2} \sum_{K_3 M_3} (-i)^{K_3} \frac{1}{k_f R'} g_f(R') \, (4\pi)^{1/2} (2K_3+1)^{1/2} \, Y_{K_3 M_3}(\theta_{k_f}, \phi_{k_f}) \, D^{(K_3)*}_{M_3 M'_L}(\omega')$$

$$\times \frac{1}{(2\pi)^2} \sum_{K_4 M_4} i^{K_4} \frac{1}{k_i R'} g_i(R') \, (4\pi)^{1/2} (2K_4+1)^{1/2} \, Y^*_{K_4 M_4}(\theta_{k_i}, \phi_{k_i}) \, D^{(K_4)}_{M_4 M_L}(\omega') \, R'^2 \, dR' \, d\omega'$$

$$\times k_i^2 \, dk_i \, d\hat{k}_i \, k_f^2 \, dk_f \, d\hat{k}_f \qquad \text{(C3.2.3)}$$

where the electron eigenfunctions have been labelled with M_L and M'_L, the projections of the electron orbital angular momentum on the internuclear axis in the initial and final state respectively, and the arguments ω and ω' of the rotation matrix elements denote the Euler angles ($\alpha\,\beta\,\gamma$).

Application of the normalisation condition for spherical harmonics (see Eq.C2.2.4) shows that the only non-zero contributions to R_{if} are from terms for which

$$\begin{aligned} K_2 &= K_4 \;(\equiv K) \\ M_2 &= M_4 \;(\equiv M) \\ K_1 &= K_3 \;(\equiv K') \\ M_1 &= M_3 \;(\equiv M') \end{aligned} \qquad \text{(C3.2.4)}$$

so that R_{if} may be simplified to

$$R_{if} = \frac{e^2}{12\pi^5\omega_i} \sum_{\substack{m' m_1 m_2 \\ M_L M'_L}} \sum_{\substack{K M \\ K' M'}} (2K+1)\ (2K'+1) \int \psi_{M'_L}\ r\ Y^*_{1m_1}(\theta,\phi)\ \psi^*_{M_L} dr\ g_i(R)\ g_f(R)\ dR$$

$$\times \int \psi^*_{M'_L}\ r\ Y_{1m_2}(\theta,\phi)\ \psi_{M_L} dr\ g_i(R')\ g_f(R')\ dR'$$

$$\times \int D^{(1)*}_{m' m_1}(\omega)\ D^{(K)*}_{M M_L}(\omega)\ D^{(K')}_{M' M'_L}(\omega)\ d\omega$$

$$\times \int D^{(1)}_{m' m_2}(\omega')\ D^{(K)}_{M M_L}(\omega')\ D^{(K')*}_{M' M'_L}(\omega')\ d\omega'\ dk_i\ dk_f$$

(C3.2.5)

The integrals involving the rotation matrix elements are identical to those arising in the bound-free case (see Eq.C2.2.5). The product of these integrals is thus given by Eq.C2.2.14 and the above expression for R_{if} may be written

$$R_{if} = \frac{16e^2}{3\pi\omega_i} \sum_{\substack{m m' \\ M_L M'_L}} \sum_{\substack{K M \\ K' M'}} (2K+1)\ (2K'+1) \int \psi_{M'_L}\ r\ Y^*_{1m}(\theta,\phi)\ \psi^*_{M_L} dr\ g_i(R)\ g_f(R)\ dR$$

$$\times \int \psi^*_{M'_L}\ r\ Y_{1m}(\theta,\phi)\ \psi_{M_L} dr\ g_i(R')\ g_f(R')\ dR'$$

$$\times \left\{ \begin{pmatrix} 1 & K & K' \\ m' & M & -M' \end{pmatrix} \begin{pmatrix} 1 & K & K' \\ m & M_L & -M'_L \end{pmatrix} \right\}^2 dk_i\ dk_f$$

(C3.2.6)

where

$$m_1 = m_2 = M'_L - M_L \equiv m. \qquad \text{(C3.2.7)}$$

The sum of the 3-j symbols over M, M' and m' is given by Eq.C2.2.19, and using Eq.C2.2.21, the above expression for R_{if} becomes

$$R_{if} = \frac{4}{\pi^2\omega_i} \sum_{\substack{m \\ M_L M'_L}} \sum_{K K'} (2K+1)\,(2K'+1) \begin{pmatrix} K & 1 & K' \\ M_L & m & -M'_L \end{pmatrix}^2$$

$$\times \left| \int \psi_{M'_L}\, er_m\, \psi^*_{M_L} dr \int g_i(R)\, g_f(R)\, dR \right|^2 \delta(K\,K'\,1)\ dk_i\, dk_f \qquad \text{(C3.2.8)}$$

which is the free-free equivalent of Eq.C2.2.22. The sum of the 3-j symbols over m, M_L and M'_L (see Eq.C2.2.24) is performed as in the bound-free case and results in, for the $A^2\Pi - X^2\Sigma$ transition,

$$R_{if}(\Lambda = 1, \Lambda' = 0) = \frac{4}{\pi^2} \sum_{K\,K'} (2K + 1)\,(2K' + 1) \begin{pmatrix} K & 1 & K' \\ 1 & -1 & 0 \end{pmatrix}^2 S_{if}\ \delta(K\,K'\,1)\ dk_i\,dk_f \qquad \text{(C3.2.9)}$$

and for the $B^2\Sigma - X^2\Sigma$ transition,

$$R_{if}(\Lambda = 0, \Lambda' = 0) = \frac{4}{\pi^2} \sum_{K\,K'} (2K + 1)\,(2K' + 1) \begin{pmatrix} K & 1 & K' \\ 0 & 0 & 0 \end{pmatrix}^2 S_{if}\ \delta(K\,K'\,1)\ dk_i\,dk_f \qquad \text{(C3.2.10)}$$

where

$$S_{if} = \left| \int_0^\infty g_i(R)\, D_{\Lambda'\,\Lambda}(R)\, g_f(R)\, dR \right|^2 \qquad \text{(C3.2.11)}$$

and $D_{\Lambda'\,\Lambda}(R)$, is the dipole transition moment defined by Eq.C2.2.37.

The final sum to be considered is that over K'. The matrix element S_{if} is again made independent of K' using the same assumptions as in the bound-free case, so that the radial eigenfunction $g_f(R)$ now satisfies Eq.C2.2.38. The 3-j symbols of Eqs.C3.2.9 and C3.2.10 are identical to those appearing in the bound-free case (see Eqs.C2.2.34 and C2.2.35) and the sums over K' are equal to unity in both cases. The final form of R_{if}, applicable to both $A^2\Pi - X^2\Sigma$ and $B^2\Sigma - X^2\Sigma$ transitions, is therefore

$$R_{if} = \frac{4}{\pi^2} \sum_K (2K + 1)\, S_{if}\ dk_i\,dk_f\ . \qquad \text{(C3.2.12)}$$

Thus, from Eq.C3.2.2,

$$\frac{A_{if}}{\omega_i}\, dk_i\,dk_f = \frac{256\pi^2\nu^3}{3hc^3} \sum_K (2K + 1)\, S_{if}\, dk_i\,dk_f\,, \qquad \text{(C3.2.13)}$$

and this result completes the analysis of this appendix.

Annex D

Details of the Line Core Broadening Model

Appendix D1 The Equations of Motion for Alkali States

D1.1 Introduction

In §6.4 the equations governing the time development of the excited and ground states of the alkali valence electron under perturbation by a rare gas atom were obtained in the form

$$i\frac{da_n(t)}{dt} = \sum_k a_k(t) < j_n\, m_n \mid V_i \mid j_k\, m_k > e^{i\omega_{nk}t}; \quad n = 1, 6, \tag{D1.1.1}$$

$$i\frac{db_n(t)}{dt} = \sum_k b_k(t) < j_n\, m_n \mid V_f \mid j_k\, m_k >; \quad n = 1, 2. \tag{D1.1.2}$$

These equations contain perturbation matrices expressed in an atomic representation relative to the space-fixed (collision) frame of reference. The purpose of this appendix is to re-write these matrices in terms of a molecular representation relative to the body-fixed (rotating) frame of reference and to obtain the above equations in this representation. The excited state equations (Eq.D1.1.1) are considered first, in §D1.2, followed by the ground state equations (Eq.D1.1.2) in §D1.3.

D1.2 The Excited State Equations

The elements of the perturbation matrix in the atomic representation of Eq.D1.1.1 are related to those in the molecular representation by Eq.6.4.11 of §6.4:

$$< j_n\, m_n \mid V_i \mid j'_n\, m'_n > = \sum_{\substack{m_l m'_l \\ m_s \Lambda}} < l\, s\, m_l\, m_s \mid j_n\, m_n >< l\, s\, m'_l\, m_s \mid j'_n\, m'_n > \times D^{(l)}_{m_l \Lambda}(\phi, \pi/2, \pi/2)\, D^{-1\,(l)}_{\Lambda m'_l}(\phi, \pi/2, \pi/2) < \Lambda \mid V_i \mid \Lambda > \tag{D1.2.1}$$

The first step in the re-formulation of Eq.D1.1.1 is to consider the rotation matrices of Eq.D1.2.1. The general form of the rotation matrix is given by (Edmonds (1957), Eq.4.1.12)

$$D^{(l)}_{m'm}(\alpha,\beta,\gamma) = e^{im'\alpha}\, d^{(l)}_{m'm}(\beta)\, e^{im\gamma} \tag{D1.2.2}$$

so that the first rotation matrix of Eq.D1.2.1 is

$$D^{(l)}_{m_l \Lambda}(\phi, \pi/2, \pi/2) = e^{im_l\phi}\, d^{(l)}_{m_l \Lambda}(\pi/2)\, e^{i\Lambda\pi/2}. \qquad \text{(D1.2.3)}$$

For the excited alkali state, $l = 1$ and in this case (Edmonds (1957), §4.1) the second component of Eq.D1.2.3 has the general form

$$d^{(1)}_{m_l \Lambda}(\beta) = \begin{array}{c|ccc} & \Lambda & & \\ m_l & +1 & 0 & -1 \\ \hline +1 & \frac{1}{2}(1+\cos(\beta)) & \frac{1}{\sqrt{2}}\sin(\beta) & \frac{1}{2}(1-\cos(\beta)) \\ 0 & -\frac{1}{\sqrt{2}}\sin(\beta) & \cos(\beta) & \frac{1}{\sqrt{2}}\sin(\beta) \\ -1 & \frac{1}{2}(1-\cos(\beta)) & -\frac{1}{\sqrt{2}}\sin(\beta) & \frac{1}{2}(1+\cos(\beta)) \end{array} \qquad \text{(D1.2.4)}$$

so that, for $\beta = \pi/2$,

$$d^{(1)}_{m_l \Lambda}(\pi/2) = \begin{array}{c|ccc} & \Lambda & & \\ m_l & +1 & 0 & -1 \\ \hline +1 & \frac{1}{2} & \frac{1}{\sqrt{2}} & \frac{1}{2} \\ 0 & -\frac{1}{\sqrt{2}} & 0 & \frac{1}{\sqrt{2}} \\ -1 & \frac{1}{2} & -\frac{1}{\sqrt{2}} & \frac{1}{2} \end{array} \qquad \text{(D1.2.5)}$$

The third component of Eq.D1.2.3 has the values

$$\begin{aligned} e^{i\Lambda\pi/2} &= i \quad (\Lambda = +1), \\ &= 1 \quad (\Lambda = 0), \\ &= -i \quad (\Lambda = -1). \end{aligned} \qquad \text{(D1.2.6)}$$

Using Eqs.D1.2.5 and D1.2.6, the first rotation matrix of Eq.D1.2.1 becomes

$$D^{(1)}_{m_l \Lambda}(\phi, \pi/2, \pi/2) =$$

m_l \ Λ	+1	0	-1
+1	$\frac{i}{2}e^{i\phi}$	$\frac{1}{\sqrt{2}}e^{i\phi}$	$-\frac{i}{2}e^{i\phi}$
0	$-\frac{i}{\sqrt{2}}$	0	$-\frac{i}{\sqrt{2}}$
-1	$\frac{i}{2}e^{-i\phi}$	$-\frac{1}{\sqrt{2}}e^{-i\phi}$	$-\frac{i}{2}e^{-i\phi}$

(D1.2.7)

To obtain the form of the second rotation matrix of Eq.D1.2.1, the non-inverse matrix $D^{(1)}_{\Lambda m'_l}(\phi, \pi/2, \pi/2)$ is considered first. This is equivalent to Eq.D1.2.7 with the row and column labels interchanged, and with m_l replaced by m'_l:

$$D^{(1)}_{\Lambda m'_l}(\phi, \pi/2, \pi/2) =$$

Λ \ m'_l	+1	0	-1
+1	$\frac{i}{2}e^{i\phi}$	$\frac{1}{\sqrt{2}}e^{i\phi}$	$-\frac{i}{2}e^{i\phi}$
0	$-\frac{i}{\sqrt{2}}$	0	$-\frac{i}{\sqrt{2}}$
-1	$\frac{i}{2}e^{-i\phi}$	$-\frac{1}{\sqrt{2}}e^{-i\phi}$	$-\frac{i}{2}e^{-i\phi}$

(D1.2.8)

Since the rotation matrices are unitary (Edmonds (1957), p55) the inverse of the above matrix is simply its transpose conjugate, i.e.,

$$D^{-1\,(1)}_{\Lambda m'_l}(\phi, \pi/2, \pi/2) =$$

Λ \ m'_l	+1	0	-1
+1	$-\frac{i}{2}e^{-i\phi}$	$\frac{i}{\sqrt{2}}$	$-\frac{i}{2}e^{i\phi}$
0	$\frac{1}{\sqrt{2}}e^{-i\phi}$	0	$-\frac{1}{\sqrt{2}}e^{i\phi}$
-1	$\frac{i}{2}e^{-i\phi}$	$\frac{i}{\sqrt{2}}$	$\frac{i}{2}e^{i\phi}$

(D1.2.9)

Both rotation matrices appearing in Eq.D1.2.1 have now been obtained in explicit form. The next step is to consider the perturbation matrix elements $< \Lambda \mid V_i \mid \Lambda >$. In the molecular representation, these elements are the adiabatic interatomic potentials connecting to the excited atomic states of the alkali atom and form a diagonal matrix:

$$V_i = \begin{array}{c|ccc} & \Lambda & & \\ \Lambda & +1 & 0 & -1 \\ \hline +1 & V_{A^2\Pi} & 0 & 0 \\ 0 & 0 & V_{B^2\Sigma} & 0 \\ -1 & 0 & 0 & V_{A^2\Pi} \end{array} \qquad \text{(D1.2.10)}$$

The sum over Λ appearing in Eq.D1.2.1 may now be evaluated. This sum forms a matrix denoted $D^{(1)}_{m_l m'_l}$ and given by

$$D^{(1)}_{m_l m'_l} = \sum_{\Lambda} D^{(1)}_{m_l \Lambda}(\phi, \pi/2, \pi/2)\, D^{-1\,(1)}_{\Lambda\, m'_l}(\phi, \pi/2, \pi/2) < \Lambda \mid V_i \mid \Lambda >. \qquad \text{(D1.2.11)}$$

Using Eqs.D1.2.7, D1.2.9 and D1.2.10, this matrix has the form

$$D^{(1)}_{m_l m'_l} = \begin{array}{c|ccc} & m'_l & & \\ m_l & +1 & 0 & -1 \\ \hline +1 & \frac{1}{2}(V_{A^2\Pi} + V_{B^2\Sigma}) & 0 & \frac{1}{2}(V_{A^2\Pi} - V_{B^2\Sigma})\, e^{2i\phi} \\ 0 & 0 & V_{A^2\Pi} & 0 \\ -1 & \frac{1}{2}(V_{A^2\Pi} - V_{B^2\Sigma})\, e^{-2i\phi} & 0 & \frac{1}{2}(V_{A^2\Pi} + V_{B^2\Sigma}) \end{array} \qquad \text{(D1.2.12)}$$

With this matrix, Eq.D1.2.1 becomes

$$< j_n\, m_n \mid V_i \mid j'_n\, m'_n > = \sum_{\substack{m_l m'_l \\ m_s}} < l\, s\, m_l\, m_s \mid j_n\, m_n >< l\, s\, m'_l\, m_s \mid j'_n\, m'_n > D^{(1)}_{m_l m'_l} \qquad \text{(D1.2.13)}$$

The $\mid j\ m >$ states to be considered for the excited state of the valence electron (see §6.4, Eq.6.4.3) are $\mid \frac{1}{2}\ -\frac{1}{2} >, \mid \frac{3}{2}\ -\frac{1}{2} >, \mid \frac{3}{2}\ \frac{3}{2} >, \mid \frac{1}{2}\ \frac{1}{2} >, \mid \frac{3}{2}\ \frac{1}{2} >$ and $\mid \frac{3}{2}\ -\frac{3}{2} >$. As indicated by Roueff (1972), the only states $\mid j\ m >, \mid j'\ m' >$ connected are those for which $m - m' = 0, \pm 2$, so that

$m = -\frac{1}{2}$ connects only with $m' = -\frac{1}{2}, \frac{3}{2}$;
$m = \frac{3}{2}$ connects only with $m' = -\frac{1}{2}, \frac{3}{2}$;
$m = \frac{1}{2}$ connects only with $m' = \frac{1}{2}, -\frac{3}{2}$;
$m = -\frac{3}{2}$ connects only with $m' = \frac{1}{2}, -\frac{3}{2}$.

This selection rule partitions the six atomic states into two sets of three coupled states denoted Set A and Set B:

Set A = $\{ \mid \frac{1}{2}\ \frac{1}{2} >, \mid \frac{3}{2}\ \frac{1}{2} >, \mid \frac{3}{2}\ -\frac{3}{2} > \}$,
Set B = $\{ \mid \frac{1}{2}\ -\frac{1}{2} >, \mid \frac{3}{2}\ -\frac{1}{2} >, \mid \frac{3}{2}\ \frac{3}{2} > \}$,

and the perturbation matrix of Eq.D1.2.13 is evaluated for each set separately. For the states of Set A, the perturbation matrix in the atomic representation is denoted as follows:

$$V_i = \begin{array}{c|ccc} & \mid j'\ m' > & & \\ < j\ m \mid & \mid \frac{1}{2}\ \frac{1}{2} > & \mid \frac{3}{2}\ \frac{1}{2} > & \mid \frac{3}{2}\ -\frac{3}{2} > \\ \hline < \frac{1}{2}\ \frac{1}{2} \mid & V_{11} & V_{12} & V_{13} \\ < \frac{3}{2}\ \frac{1}{2} \mid & V_{21} & V_{22} & V_{23} \\ < \frac{3}{2}\ -\frac{3}{2} \mid & V_{31} & V_{32} & V_{33} \end{array} \qquad \text{(D1.2.14)}$$

where the subscripts on $< j_n\, m_n \mid$ and $\mid j'_n\, m'_n >$ have been dropped for clarity. Noting that the generic vector coupling coefficient $< j_1\, j_2\, m_1\, m_2 \mid j\ m >$ is zero unless $m = m_1 + m_2$, and using the values

$$\begin{aligned} l &= 1, & m_l &= 0, \pm 1, \\ s &= \tfrac{1}{2}, & m_s &= \pm \tfrac{1}{2}, \\ j &= \tfrac{1}{2}, \tfrac{3}{2}, & m &= m_l + m_s \end{aligned} \qquad \text{(D1.2.15)}$$

appropriate to the excited state of the valence electron, the elements of Eq.D1.2.14 are given via Eq.D1.2.13 as follows:

Element V_{11}:

$$\begin{aligned} &<j\,m| = <\tfrac{1}{2}\,\tfrac{1}{2}|; && m = \tfrac{1}{2} \;\Rightarrow\; && m_l = 0 && \text{for } m_s = \tfrac{1}{2}; \\ & && && m_l = 1 && \text{for } m_s = -\tfrac{1}{2}; \\ &|j'\,m'> = |\tfrac{1}{2}\,\tfrac{1}{2}>; && m' = \tfrac{1}{2} \;\Rightarrow\; && m'_l = 0 && \text{for } m_s = \tfrac{1}{2}; \\ & && && m'_l = 1 && \text{for } m_s = -\tfrac{1}{2}; \end{aligned}$$

and hence

$$V_{11} = <1\,\tfrac{1}{2}\,0\,\tfrac{1}{2}|\tfrac{1}{2}\,\tfrac{1}{2}><1\,\tfrac{1}{2}\,0\,\tfrac{1}{2}|\tfrac{1}{2}\,\tfrac{1}{2}>D^{(1)}_{0\,0} + <1\,\tfrac{1}{2}\,1\,-\tfrac{1}{2}|\tfrac{1}{2}\,\tfrac{1}{2}><1\,\tfrac{1}{2}\,1\,-\tfrac{1}{2}|\tfrac{1}{2}\,\tfrac{1}{2}>D^{(1)}_{1\,1}.$$

(D1.2.16)

Element V_{12}:

$$\begin{aligned} &<j\,m| = <\tfrac{1}{2}\,\tfrac{1}{2}|; && m = \tfrac{1}{2} \;\Rightarrow\; && m_l = 0 && \text{for } m_s = \tfrac{1}{2}; \\ & && && m_l = 1 && \text{for } m_s = -\tfrac{1}{2}; \\ &|j'\,m'> = |\tfrac{3}{2}\,\tfrac{1}{2}>; && m' = \tfrac{1}{2} \;\Rightarrow\; && m'_l = 0 && \text{for } m_s = \tfrac{1}{2}; \\ & && && m'_l = 1 && \text{for } m_s = -\tfrac{1}{2}; \end{aligned}$$

and hence

$$V_{12} = <1\,\tfrac{1}{2}\,0\,\tfrac{1}{2}|\tfrac{1}{2}\,\tfrac{1}{2}><1\,\tfrac{1}{2}\,0\,\tfrac{1}{2}|\tfrac{3}{2}\,\tfrac{1}{2}>D^{(1)}_{0\,0} + <1\,\tfrac{1}{2}\,1\,-\tfrac{1}{2}|\tfrac{1}{2}\,\tfrac{1}{2}><1\,\tfrac{1}{2}\,1\,-\tfrac{1}{2}|\tfrac{3}{2}\,\tfrac{1}{2}>D^{(1)}_{1\,1}.$$

(D1.2.17)

Element V_{13}:

$$\begin{aligned} &<j\,m| = <\tfrac{1}{2}\,\tfrac{1}{2}|; && m = \tfrac{1}{2} \;\Rightarrow\; && m_l = 0 && \text{for } m_s = \tfrac{1}{2}; \\ & && && m_l = 1 && \text{for } m_s = -\tfrac{1}{2}; \\ &|j'\,m'> = |\tfrac{3}{2}\,-\tfrac{3}{2}>; && m' = -\tfrac{3}{2} \Rightarrow && m'_l = -1 && \text{for } m_s = -\tfrac{1}{2}; \end{aligned}$$

and hence

$$V_{13} = <1\,\tfrac{1}{2}\,1\,-\tfrac{1}{2}\,|\,\tfrac{1}{2}\,\tfrac{1}{2}> <1\,\tfrac{1}{2}\,-1\,-\tfrac{1}{2}\,|\,\tfrac{3}{2}\,-\tfrac{3}{2}> D^{(1)}_{1\,-1}\,. \qquad \text{(D1.2.18)}$$

Element V_{21}:

$<j\,m\,| = <\tfrac{3}{2}\,\tfrac{1}{2}\,|$;	$m = \tfrac{1}{2} \Rightarrow$	$m_l = 0$	for $m_s = \tfrac{1}{2}$;
		$m_l = 1$	for $m_s = -\tfrac{1}{2}$;
$|\,j'\,m'> = |\,\tfrac{1}{2}\,\tfrac{1}{2}>$;	$m' = \tfrac{1}{2} \Rightarrow$	$m'_l = 0$	for $m_s = \tfrac{1}{2}$;
		$m'_l = 1$	for $m_s = -\tfrac{1}{2}$;

and hence

$$V_{21} = <1\,\tfrac{1}{2}\,0\,\tfrac{1}{2}\,|\,\tfrac{3}{2}\,\tfrac{1}{2}> <1\,\tfrac{1}{2}\,0\,\tfrac{1}{2}\,|\,\tfrac{1}{2}\,\tfrac{1}{2}> D^{(1)}_{0\,0} + <1\,\tfrac{1}{2}\,1\,-\tfrac{1}{2}\,|\,\tfrac{3}{2}\,\tfrac{1}{2}> <1\,\tfrac{1}{2}\,1\,-\tfrac{1}{2}\,|\,\tfrac{1}{2}\,\tfrac{1}{2}> D^{(1)}_{1\,1}\,. \qquad \text{(D1.2.19)}$$

Element V_{22}:

$<j\,m\,| = <\tfrac{3}{2}\,\tfrac{1}{2}\,|$;	$m = \tfrac{1}{2} \Rightarrow$	$m_l = 0$	for $m_s = \tfrac{1}{2}$;
		$m_l = 1$	for $m_s = -\tfrac{1}{2}$;
$|\,j'\,m'> = |\,\tfrac{3}{2}\,\tfrac{1}{2}>$;	$m' = \tfrac{1}{2} \Rightarrow$	$m'_l = 0$	for $m_s = \tfrac{1}{2}$;
		$m'_l = 1$	for $m_s = -\tfrac{1}{2}$;

and hence

$$V_{22} = <1\,\tfrac{1}{2}\,0\,\tfrac{1}{2}\,|\,\tfrac{3}{2}\,\tfrac{1}{2}> <1\,\tfrac{1}{2}\,0\,\tfrac{1}{2}\,|\,\tfrac{3}{2}\,\tfrac{1}{2}> D^{(1)}_{0\,0} + <1\,\tfrac{1}{2}\,1\,-\tfrac{1}{2}\,|\,\tfrac{3}{2}\,\tfrac{1}{2}> <1\,\tfrac{1}{2}\,1\,-\tfrac{1}{2}\,|\,\tfrac{3}{2}\,\tfrac{1}{2}> D^{(1)}_{1\,1}\,. \qquad \text{(D1.2.20)}$$

Element V_{23}:

$<j\,m\,| = <\tfrac{3}{2}\,\tfrac{1}{2}\,|$;	$m = \tfrac{1}{2} \Rightarrow$	$m_l = 0$	for $m_s = \tfrac{1}{2}$;
		$m_l = 1$	for $m_s = -\tfrac{1}{2}$;
$|\,j'\,m'> = |\,\tfrac{3}{2}\,-\tfrac{3}{2}>$;	$m' = -\tfrac{3}{2} \Rightarrow$	$m'_l = -1$	for $m_s = -\tfrac{1}{2}$;

and hence

$$V_{23} = <1\,\tfrac{1}{2}\,1\,-\tfrac{1}{2}\,|\,\tfrac{3}{2}\,\tfrac{1}{2}> <1\,\tfrac{1}{2}\,-1\,-\tfrac{1}{2}\,|\,\tfrac{3}{2}\,-\tfrac{3}{2}> D^{(1)}_{1\,-1}\,. \qquad \text{(D1.2.21)}$$

Element V_{31}:

$$<j\,m\,| = <\tfrac{3}{2}\ -\tfrac{3}{2}|; \qquad m = -\tfrac{3}{2} \Rightarrow \qquad m_l = -1 \qquad \text{for } m_s = -\tfrac{1}{2};$$
$$|j'\,m'> = |\tfrac{1}{2}\ \tfrac{1}{2}>; \qquad m' = \tfrac{1}{2} \Rightarrow \qquad m'_l = 0 \qquad \text{for } m_s = \tfrac{1}{2};$$
$$m'_l = 1 \qquad \text{for } m_s = -\tfrac{1}{2};$$

and hence

$$V_{31} = <1\,\tfrac{1}{2}\ -1\ -\tfrac{1}{2}|\tfrac{3}{2}\ -\tfrac{3}{2}><1\,\tfrac{1}{2}\ 1\ -\tfrac{1}{2}|\tfrac{1}{2}\ \tfrac{1}{2}>\mathrm{D}^{(1)}_{-1\,1}. \qquad \text{(D1.2.22)}$$

Element V_{32}:

$$<j\,m\,| = <\tfrac{3}{2}\ -\tfrac{3}{2}|; \qquad m = -\tfrac{3}{2} \Rightarrow \qquad m_l = -1 \qquad \text{for } m_s = -\tfrac{1}{2};$$
$$|j'\,m'> = |\tfrac{3}{2}\ \tfrac{1}{2}>; \qquad m' = \tfrac{1}{2} \Rightarrow \qquad m'_l = 0 \qquad \text{for } m_s = \tfrac{1}{2};$$
$$m'_l = 1 \qquad \text{for } m_s = -\tfrac{1}{2};$$

and hence

$$V_{32} = <1\,\tfrac{1}{2}\ -1\ -\tfrac{1}{2}|\tfrac{3}{2}\ -\tfrac{3}{2}><1\,\tfrac{1}{2}\ 1\ -\tfrac{1}{2}|\tfrac{3}{2}\ \tfrac{1}{2}>\mathrm{D}^{(1)}_{-1\,1}. \qquad \text{(D1.2.23)}$$

Element V_{33}:

$$<j\,m\,| = <\tfrac{3}{2}\ -\tfrac{3}{2}|; \qquad m = -\tfrac{3}{2} \Rightarrow \qquad m_l = -1 \qquad \text{for } m_s = -\tfrac{1}{2};$$
$$|j'\,m'> = |\tfrac{3}{2}\ -\tfrac{3}{2}>; \qquad m' = -\tfrac{3}{2} \Rightarrow \qquad m'_l = -1 \qquad \text{for } m_s = -\tfrac{1}{2};$$

and hence

$$V_{33} = <1\,\tfrac{1}{2}\ -1\ -\tfrac{1}{2}|\tfrac{3}{2}\ -\tfrac{3}{2}><1\,\tfrac{1}{2}\ -1\ -\tfrac{1}{2}|\tfrac{3}{2}\ -\tfrac{3}{2}>\mathrm{D}^{(1)}_{-1\,-1}. \qquad \text{(D1.2.24)}$$

The next step is to evaluate the vector coupling coefficients. These are written in terms of 3-j symbols via (Edmonds (1957), Eq.3.7.3)

$$<l\,s\,m_l\,m_s\,|\,j\,m> = (-1)^{-l+s-m}(2j+1)^{1/2}\begin{pmatrix} l & s & j \\ m_l & m_s & -m \end{pmatrix}. \qquad \text{(D1.2.25)}$$

In this form, together with the symmetry relation for even permutations of columns,

$$\begin{pmatrix} j_1 & j_2 & j_3 \\ m_1 & m_2 & m_3 \end{pmatrix} = \begin{pmatrix} j_2 & j_3 & j_1 \\ m_2 & m_3 & m_1 \end{pmatrix} = \begin{pmatrix} j_3 & j_1 & j_2 \\ m_3 & m_1 & m_2 \end{pmatrix}, \qquad \text{(D1.2.26)}$$

the symmetry relation for odd permutations of columns,

$$(-1)^{j_1+j_2+j_3} \begin{pmatrix} j_1 & j_2 & j_3 \\ m_1 & m_2 & m_3 \end{pmatrix} = \begin{pmatrix} j_2 & j_1 & j_3 \\ m_2 & m_1 & m_3 \end{pmatrix} = \begin{pmatrix} j_1 & j_3 & j_2 \\ m_1 & m_3 & m_2 \end{pmatrix} = \begin{pmatrix} j_3 & j_2 & j_1 \\ m_3 & m_2 & m_1 \end{pmatrix}, \qquad \text{(D1.2.27)}$$

and the relation

$$\begin{pmatrix} j_1 & j_2 & j_3 \\ m_1 & m_2 & m_3 \end{pmatrix} = (-1)^{j_1+j_2+j_3} \begin{pmatrix} j_1 & j_2 & j_3 \\ -m_1 & -m_2 & -m_3 \end{pmatrix}, \qquad \text{(D1.2.28)}$$

the vector coupling coefficients of Eqs.D1.2.16 - D1.2.24 may be obtained from standard tables (Edmonds (1957), Appendix 2, Table 2). The coefficients required evaluate as follows:

$$\begin{aligned} &\langle 1\tfrac{1}{2}\,0\,\tfrac{1}{2} | \tfrac{1}{2}\tfrac{1}{2}\rangle = -\frac{1}{\sqrt{3}}, && \langle 1\tfrac{1}{2}\,1\,-\tfrac{1}{2} | \tfrac{1}{2}\tfrac{1}{2}\rangle = \frac{2}{\sqrt{6}}, \\ &\langle 1\tfrac{1}{2}\,0\,\tfrac{1}{2} | \tfrac{3}{2}\tfrac{1}{2}\rangle = \frac{2}{\sqrt{6}}, && \langle 1\tfrac{1}{2}\,1\,-\tfrac{1}{2} | \tfrac{3}{2}\tfrac{1}{2}\rangle = \frac{1}{\sqrt{3}}, \\ &\langle 1\tfrac{1}{2}\,-1\,-\tfrac{1}{2} | \tfrac{3}{2}\,-\tfrac{3}{2}\rangle = 1. \end{aligned} \qquad \text{(D1.2.29)}$$

The elements of the perturbation matrix (Eq.D1.2.14) are then given by

$$\begin{aligned} V_{11} &= \frac{2}{3} V_{A^2\Pi} + \frac{1}{3} V_{B^2\Sigma}, & V_{12} &= -\frac{1}{3\sqrt{2}} (V_{A^2\Pi} - V_{B^2\Sigma}), \\ V_{13} &= \frac{1}{\sqrt{6}} (V_{A^2\Pi} - V_{B^2\Sigma})\, e^{2i\phi}, & V_{21} &= -\frac{1}{3\sqrt{2}} (V_{A^2\Pi} - V_{B^2\Sigma}), \\ V_{22} &= \frac{1}{6} (5V_{A^2\Pi} + V_{B^2\Sigma}), & V_{23} &= \frac{1}{2\sqrt{3}} (V_{A^2\Pi} - V_{B^2\Sigma})\, e^{2i\phi}, \\ V_{31} &= \frac{1}{\sqrt{6}} (V_{A^2\Pi} - V_{B^2\Sigma})\, e^{-2i\phi}, & V_{32} &= \frac{1}{2\sqrt{3}} (V_{A^2\Pi} - V_{B^2\Sigma})\, e^{-2i\phi}, \\ V_{33} &= \frac{1}{2} (V_{A^2\Pi} + V_{B^2\Sigma}). \end{aligned} \qquad \text{(D1.2.30)}$$

Defining the quantities

$$\begin{aligned} \tilde{V} &= \frac{2}{3} V_{A^2\Pi} + \frac{1}{3} V_{B^2\Sigma}, \\ f &= V_{B^2\Sigma} - V_{A^2\Pi}, \end{aligned} \qquad \text{(D1.2.31)}$$

gives the final form of the perturbation matrix for the atomic states of Set A:

$$
\mathbf{V_I} = \begin{array}{c|ccc}
 & |j'\,m'> & & \\
<j\,m| & |\tfrac{1}{2}\ \tfrac{1}{2}> & |\tfrac{3}{2}\ \tfrac{1}{2}> & |\tfrac{3}{2}\ -\tfrac{3}{2}> \\
\hline
<\tfrac{1}{2}\ \tfrac{1}{2}| & \tilde{V} & \frac{f}{3\sqrt{2}} & -\frac{f}{\sqrt{6}}e^{2i\phi} \\
<\tfrac{3}{2}\ \tfrac{1}{2}| & \frac{f}{3\sqrt{2}} & \tilde{V}-\frac{f}{6} & -\frac{f}{2\sqrt{3}}e^{2i\phi} \\
<\tfrac{3}{2}\ -\tfrac{3}{2}| & -\frac{f}{\sqrt{6}}e^{-2i\phi} & -\frac{f}{2\sqrt{3}}e^{-2i\phi} & \tilde{V}+\frac{f}{6}
\end{array}
\qquad \text{(D1.2.32)}
$$

The equivalent matrix for atomic states of Set B is obtained from Eq.D1.2.32 using the symmetry relation (see §6.4, Eq.6.4.14)

$$
<j\,m\,|\,V_i\,|\,j'\,m'> = (-1)^{j+j'-1}\,<j\,-m\,|\,V_i\,|\,j'\,-m'>^{*}. \qquad \text{(D1.2.33)}
$$

Thus, for the states of Set B, the perturbation matrix has the form

$$
\mathbf{V_I} = \begin{array}{c|ccc}
 & |j'\,m'> & & \\
<j\,m| & |\tfrac{1}{2}\ -\tfrac{1}{2}> & |\tfrac{3}{2}\ -\tfrac{1}{2}> & |\tfrac{3}{2}\ \tfrac{3}{2}> \\
\hline
<\tfrac{1}{2}\ -\tfrac{1}{2}| & \tilde{V} & -\frac{f}{3\sqrt{2}} & \frac{f}{\sqrt{6}}e^{-2i\phi} \\
<\tfrac{3}{2}\ -\tfrac{1}{2}| & -\frac{f}{3\sqrt{2}} & \tilde{V}-\frac{f}{6} & -\frac{f}{2\sqrt{3}}e^{-2i\phi} \\
<\tfrac{3}{2}\ \tfrac{3}{2}| & \frac{f}{\sqrt{6}}e^{2i\phi} & -\frac{f}{2\sqrt{3}}e^{2i\phi} & \tilde{V}+\frac{f}{6}
\end{array}
\qquad \text{(D1.2.34)}
$$

With Eqs.D1.2.32 and D1.2.34, the equations for the expansion coefficients $\{a_n(t)\}$, Eq.D1.1.1, may now be written in the molecular representation. The correspondence between expansion coefficients and atomic states is given by (see §6.4, Eq.6.4.3)

$$
\begin{aligned}
&a_1(t) \Leftrightarrow |\tfrac{1}{2}\ -\tfrac{1}{2}>, && a_2(t) \Leftrightarrow |\tfrac{3}{2}\ -\tfrac{1}{2}>, \\
&a_3(t) \Leftrightarrow |\tfrac{3}{2}\ \tfrac{3}{2}>, && a_4(t) \Leftrightarrow |\tfrac{1}{2}\ \tfrac{1}{2}>, \\
&a_5(t) \Leftrightarrow |\tfrac{3}{2}\ \tfrac{1}{2}>, && a_6(t) \Leftrightarrow |\tfrac{3}{2}\ -\tfrac{3}{2}>,
\end{aligned}
\qquad \text{(D1.2.35)}
$$

and Eq.D1.1.1 may then be written in its final form as two sets of three coupled equations:

$$i\frac{da_1(t)}{dt} = \tilde{V}a_1(t) - \frac{f}{3\sqrt{2}}e^{-i\omega t}a_2(t) + \frac{f}{\sqrt{6}}e^{-i\omega t-2i\phi}a_3(t)$$

$$i\frac{da_2(t)}{dt} = -\frac{f}{3\sqrt{2}}e^{i\omega t}a_1(t) + (\tilde{V} - \frac{f}{6})a_2(t) - \frac{f}{2\sqrt{3}}e^{-2i\phi}a_3(t) \qquad \text{(D1.2.36)}$$

$$i\frac{da_3(t)}{dt} = \frac{f}{\sqrt{6}}e^{i\omega t+2i\phi}a_1(t) - \frac{f}{2\sqrt{3}}e^{2i\phi}a_2(t) + (\tilde{V} + \frac{f}{6})a_3(t)$$

$$i\frac{da_4(t)}{dt} = \tilde{V}a_4(t) + \frac{f}{3\sqrt{2}}e^{-i\omega t}a_5(t) - \frac{f}{\sqrt{6}}e^{-i\omega t+2i\phi}a_6(t)$$

$$i\frac{da_5(t)}{dt} = \frac{f}{3\sqrt{2}}e^{i\omega t}a_4(t) + (\tilde{V} - \frac{f}{6})a_5(t) - \frac{f}{2\sqrt{3}}e^{2i\phi}a_6(t) \qquad \text{(D1.2.37)}$$

$$i\frac{da_6(t)}{dt} = -\frac{f}{\sqrt{6}}e^{i\omega t-2i\phi}a_4(t) - \frac{f}{2\sqrt{3}}e^{-2i\phi}a_5(t) + (\tilde{V} + \frac{f}{6})a_6(t)$$

where ω is the fine structure splitting of the alkali excited state.

D1.3 The Ground State Equations

The elements of the perturbation matrix in the atomic representation of Eq.D1.1.2 are related to those in the molecular representation by Eq.6.4.11 of §6.4. However, for the ground state of the alkali valence electron, $l = 0$ and the rotation matrices of this equation are both unity, reflecting the spherical symmetry of the state and its consequent invariance under rotation. In addition, the perturbation matrix in the molecular representation, $< \Lambda \mid V_f \mid \Lambda >$, consists of just a single element ($\Lambda = 0$ only) equal to the ground state interatomic potential, $V_{X^2\Sigma}$. Thus the relation between the atomic and molecular representations is

$$< j_n\, m_n \mid V_f \mid j'_n\, m'_n > = \sum_{\substack{m_l, m'_l \\ m_s}} < l\, s\, m_l\, m_s \mid j_n\, m_n >< l\, s\, m'_l\, m_s \mid j'_n\, m'_n >\, V_{X^2\Sigma}\,. \qquad \text{(D1.3.1)}$$

The $\mid j\ m >$ states to be considered for the ground state of the valence electron (see §6.4, Eq.6.4.8) are $\mid \frac{1}{2}\ \frac{1}{2} >$ and $\mid \frac{1}{2}\ -\frac{1}{2} >$. The only states $\mid j\ m >, \mid j'\ m' >$ connected are those for which $m - m' = 0, \pm 2$ (Roueff (1972)), so that

$m = \frac{1}{2}$ connects only with $m' = \frac{1}{2}$;
$m = -\frac{1}{2}$ connects only with $m' = -\frac{1}{2}$.

The perturbation matrix in the atomic representation is therefore diagonal and is denoted as follows:

$$V_f = \begin{array}{c|cc} & |j'\,m'> & \\ & |\tfrac{1}{2}\,\tfrac{1}{2}> & |\tfrac{1}{2}\,-\tfrac{1}{2}> \\ \hline <j\,m| & & \\ <\tfrac{1}{2}\,\tfrac{1}{2}| & V_{11} & 0 \\ <\tfrac{1}{2}\,-\tfrac{1}{2}| & 0 & V_{22} \end{array} \qquad \text{(D1.3.2)}$$

where the subscripts on $< j_n\, m_n |$ and $| j'_n\, m'_n >$ have been dropped for clarity. Noting that the generic vector coupling coefficient $< j_1\, j_2\, m_1\, m_2 \,|\, j\, m >$ is zero unless $m = m_1 + m_2$, and using the values

$$\begin{aligned} l &= 0, & m_l &= 0, \\ s &= \tfrac{1}{2}, & m_s &= \pm\tfrac{1}{2}, \\ j &= \tfrac{1}{2}, & m &= m_l + m_s \end{aligned} \qquad \text{(D1.3.3)}$$

appropriate to the ground state of the valence electron, the elements of Eq.D1.3.2 are given via Eq.D1.3.1 as follows:

Element V_{11}:

$$\begin{aligned} &< j\,m| = <\tfrac{1}{2}\,\tfrac{1}{2}|; && m = \tfrac{1}{2} \;\Rightarrow\; && m_l = 0 && \text{for } m_s = \tfrac{1}{2}; \\ &|j'\,m'> = |\tfrac{1}{2}\,\tfrac{1}{2}>; && m' = \tfrac{1}{2} \;\Rightarrow\; && m'_l = 0 && \text{for } m_s = \tfrac{1}{2}; \end{aligned}$$

and hence

$$V_{11} = <0\,\tfrac{1}{2}\,0\,\tfrac{1}{2}|\tfrac{1}{2}\,\tfrac{1}{2}><0\,\tfrac{1}{2}\,0\,\tfrac{1}{2}|\tfrac{1}{2}\,\tfrac{1}{2}>\, V_{X^2\Sigma}\,. \qquad \text{(D1.3.4)}$$

Element V_{22}:

$$\begin{aligned} &< j\,m| = <\tfrac{1}{2}\,-\tfrac{1}{2}|; && m = -\tfrac{1}{2} \Rightarrow && m_l = 0 && \text{for } m_s = -\tfrac{1}{2}; \\ &|j'\,m'> = |\tfrac{1}{2}\,-\tfrac{1}{2}>; && m' = -\tfrac{1}{2} \Rightarrow && m'_l = 0 && \text{for } m_s = -\tfrac{1}{2}; \end{aligned}$$

and hence

$$V_{22} = <0\,\tfrac{1}{2}\,0\,-\tfrac{1}{2}|\tfrac{1}{2}\,-\tfrac{1}{2}><0\,\tfrac{1}{2}\,0\,-\tfrac{1}{2}|\tfrac{1}{2}\,-\tfrac{1}{2}>\, V_{X^2\Sigma}\,. \qquad \text{(D1.3.5)}$$

The vector coupling coefficients of Eqs.D1.3.4 and D1.3.5 are evaluated in the same way as for the excited state of the alkali atom considered in §D1.2. They are written in terms of 3-j symbols via Eq.D1.2.25 and using the symmetry relations of Eqs.D1.2.26 - D1.2.28 the vector coupling coefficients are then obtained from standard tables (Edmonds (1957), Appendix 2, Table 2). The coefficients required evaluate as follows:

$$<0\tfrac{1}{2}0\tfrac{1}{2}|\tfrac{1}{2}\tfrac{1}{2}>=1, \qquad <0\tfrac{1}{2}0\ -\tfrac{1}{2}|\tfrac{1}{2}\ -\tfrac{1}{2}>=1. \tag{D1.3.6}$$

The elements of the perturbation matrix are then given by

$$V_{11}=V_{22}=V_{X^2\Sigma}, \qquad V_{12}=V_{21}=0, \tag{D1.3.7}$$

so that Eq.D1.3.2 becomes

$$V_f = \begin{array}{c|cc} & |j'\ m'> & \\ <j\ m| & |\frac{1}{2}\ \frac{1}{2}> & |\frac{1}{2}\ -\frac{1}{2}> \\ \hline <\frac{1}{2}\ \frac{1}{2}| & V_{X^2\Sigma} & 0 \\ <\frac{1}{2}\ -\frac{1}{2}| & 0 & V_{X^2\Sigma} \end{array} \tag{D1.3.8}$$

With Eq.D1.3.8, the equations for the expansion coefficients $\{b_n(t)\}$, Eq.D1.1.2 may now be written in the molecular representation. The correspondence between expansion coefficients and atomic states is given by (see §6.4, Eq.6.4.8)

$$b_1(t) \Leftrightarrow |\tfrac{1}{2}\ \tfrac{1}{2}>, \qquad b_2(t) \Leftrightarrow |\tfrac{1}{2}\ -\tfrac{1}{2}>, \tag{D1.3.9}$$

and Eq.D1.1.2 may then be written in its final form as a pair of uncoupled equations:

$$i\frac{db_1(t)}{dt} = V_{X^2\Sigma}\, b_1(t), \tag{D1.3.10}$$

$$i\frac{db_2(t)}{dt} = V_{X^2\Sigma}\, b_2(t). \tag{D1.3.11}$$

The equations governing the time development of the excited and ground states of the alkali valence electron, Eq.D1.1.1 and Eq.D1.1.2 respectively, have now been transformed into the required molecular representation, yielding Eqs. D1.2.36 and

D1.2.37 for the excited state and Eqs.D1.3.10 and D1.3.11 for the ground state. These results complete the analysis of this appendix.

Annex E

The Implementation of the Line Wing Broadening Models

Appendix E1 Functional Description of Program PROF_BF

E1.1 Introduction

PROF_BF is a computer program written in FORTRAN-77 and running on an HP9050 computer under the HP-UX (UNIX) operating system. It consists of 1124 lines of source code occupying 30.9K of storage; the executable module occupies 133.6K.

The purpose of PROF_BF is to calculate the contribution to the alkali resonance line wing emission intensity arising from bound-free transitions given by (see §7.2, Eq.7.2.5)

$$I_{BF}(\lambda,T) = 1.76526\times10^{14}\,\omega\lambda_A^{-4}\,T^{-3/2}\mu^{-1}\sum_{V\,K}(2K+1)\,E_f^{-1/2}S_{if}(V,K)\exp(-E_{V,K}/kT). \qquad \text{(E1.1.1)}$$

The dependence of $I_{BF}(\lambda,T)$ on the alkali-rare gas interatomic potentials is through the eigenvalues $E_{V,K}$ and E_f, and the eigenfunctions contained in the matrix element $S_{if}(V,K)$:

$$S_{if}(V,K) = \left|\int_0^\infty g_i^{V,K}(R)\,D_{\Lambda'\Lambda}(R)\,g_f^{K}(R)\,dR\right|^2. \qquad \text{(E1.1.2)}$$

The eigenfunctions $g_i^{V,K}(R)$ and $g_f^{K}(R)$ describe the relative radial motion of the alkali and rare gas cores under the influence of the excited and ground state interatomic potentials respectively. In the context of bound-free transitions, the eigenfunction $g_i^{V,K}(R)$ describes the initial state of core motion - a discrete bound state of energy $E_{V,K}$ - and the eigenfunction $g_f^{K}(R)$ describes the final state of core motion - a continuum state of energy E_f. The bound-free contribution $I_{BF}(\lambda,T)$ is obtained by summing functions of matrix elements connecting all bound states supported by the excited state interatomic potential with the continuum of the ground state.

A single run of PROF_BF performs this summation for a combination of

(i) one alkali-rare gas system (one of LiHe, LiNe, NaHe or NaNe in the present study);

(ii) one type of interatomic potential (either model potential or pseudopotential);

(iii) one type of electronic transition (either $A^2\Pi - X^2\Sigma$ or $B^2\Sigma - X^2\Sigma$)

at a given set of wavelengths and temperatures. The current implementation of PROF_BF has restrictions on the last two quantities, namely, a maximum of 60 wavelengths and 5 temperatures.

E1.2 Input/Output Data Files

E1.2.1 Overview of Input Files

The input data required by PROF_BF are organised physically into a number of datasets, each stored in a separate disc file on the HP9050 computer system. For the present study, four pairs of datasets were created for PROF_BF, each pair relating to one of the alkali-rare gas systems under investigation. Within each pair, one dataset includes interatomic potentials calculated by the model potential method, the other includes interatomic potentials calculated by the pseudopotential method. To identify the datasets, each is named according to the system and potential type to which the data refer, using the following convention:

Dataset File Name = system | potential type | .dat (E1.2.1)

where

system = one of {LiHe, LiNe, NaHe, NaNe},
potential type = M for model potentials
= P for pseudopotentials.

Thus, for example, the PROF_BF dataset including model potentials for LiHe is named LiHeM.dat.

E1.2.2 Content of Input Files

There are eight input files created for PROF_BF, each file holding one of the datasets described in the previous section, and, on any single run of the program, PROF_BF reads data from just one of these files. All eight input files have the same basic data structure containing the following quantities:

(i) the number of input values, denoted NIV, used to specify each of the interatomic potentials and dipole transition moments, and the radial grid on which these are represented;

(ii) the internuclear separations R(I), I = 1, NIV, at which the interatomic potentials and dipole transition moments have been calculated by Peach;

(iii) the $A^2\Pi$, $B^2\Sigma$ and $X^2\Sigma$ interatomic potentials at each R(I);

(iv) the dipole transition moments for $A^2\Pi - X^2\Sigma$ and $B^2\Sigma - X^2\Sigma$ transitions at each R(I);

(v) the number of wavelengths, denoted NLAMDA, at which the emission intensity is to be calculated;

(vi) the NLAMDA wavelengths;

(vii) the number of temperatures, denoted NTEMP, at which the emission intensity is to be calculated;

(viii) the NTEMP temperatures;

(ix) the energies of the atomic alkali states connecting to the $A^2\Pi$, $B^2\Sigma$ and $X^2\Sigma$ molecular states;

(x) the reduced mass of the alkali-rare gas system.

The wavelengths and temperatures are measured in Å and degrees Kelvin respectively; all other data are expressed in atomic units. In addition, the interatomic potentials are measured relative to their respective separated atom limits (the alkali atomic state energies).

E1.2.3 Overview of Output Files

A single run of PROF_BF creates one output disc file holding the results of the calculation for a particular combination of system, interatomic potential type and electronic transition (see §E1.1). To identify the output files, each is named using the following convention:

Output File Name = system | potential type | transition | bf.out (E1.2.2)

where

system = one of {LiHe, LiNe, NaHe, NaNe},
potential type = M for model potentials
= P for pseudopotentials,
transition = A for $A^2\Pi - X^2\Sigma$
= B for $B^2\Sigma - X^2\Sigma$.

Thus, for example, the PROF_BF output file containing the bound-free intensity contribution arising from $A^2\Pi - X^2\Sigma$ transitions in LiHe, calculated using model potential interaction curves, is named LiHeMAbf.out.

The content of the output file is given in §E1.11 following a description of the calculation performed by PROF_BF.

E1.3 Computational Procedure of PROF_BF

The computational procedure for evaluating Eq.E1.1.1 consists of eight major steps as follows:

Step 1 Read appropriate input data.

Define a set of wavelengths $\{\lambda_n\}$ and temperatures $\{T_m\}$ at which to calculate the bound-free emission intensity.

Determine if bound states are supported by the excited state interatomic potential.

Step 2 Initialise the main tote:

FOR each wavelength in $\{\lambda_n\}$
  FOR each temperature in $\{T_m\}$
    $I_{BF}(\lambda_n, T_m) \leftarrow 0.0$
  ENDFOR
ENDFOR

Step 3 Define a suitable solution grid upon which to construct the eigenfunctions $g_i^{V,K}(R)$ and $g_f^{K}(R)$.

Step 4 Interpolate the interatomic potentials and dipole transition moments read in Step 1 for values on the solution grid defined in Step 3.

Step 5 Calculate the energies $E_{V,K}$ of all bound states of core motion supported by the excited state interatomic potential.

Step 6 **FOR** each bound state of core motion located

Calculate the normalised eigenfunction $g_i^{V,K}(R)$ corresponding to the energy $E_{V,K}$.

FOR each wavelength in $\{\lambda_n\}$

Calculate the energy of the free state, $E_f(\lambda_n)$, supported by the ground state interatomic potential appropriate for emission of radiation at wavelength λ_n.

Calculate the normalised eigenfunction $g_f^K(R)$ corresponding to the energy $E_f(\lambda_n)$.

Calculate the matrix element $S_{if}(V,K)$.

Increment the main tote:

FOR each temperature in $\{T_m\}$

$$I_{BF}(\lambda_n,T_m) \leftarrow I_{BF}(\lambda_n,T_m) + \lambda_n^{-4} T_m^{-3/2} (2K+1) E_f^{-1/2}(\lambda_n) S_{if}(V,K) \exp(-E_{V,K}/kT_m).$$

ENDFOR

ENDFOR

ENDFOR

Step 7 Calculate the bound-free contribution:

FOR each wavelength in $\{\lambda_n\}$

FOR each temperature in $\{T_m\}$

$$I_{BF}(\lambda_n,T_m) \leftarrow 1.76526\times10^{14}\omega\mu^{-1} I_{BF}(\lambda_n,T_m).$$

ENDFOR

ENDFOR

Step 8 Write the results of the calculation to the output file.

The details of how each of these steps is implemented in PROF_BF are described in the remaining sections of this appendix.

E1.4 Step 1 : Read Input Data

On starting program PROF_BF three items are requested from the user:

(i) the alkali-rare gas system for which the bound-free contribution is to be calculated (LiHe, LiNe, NaHe or NaNe);

(ii) a single character denoting the type of interatomic potentials to be used (M for model potentials, P for pseudopotentials);

(iii) a single character denoting the electronic transition to be used (A for $A^2\Pi - X^2\Sigma$, B for $B^2\Sigma - X^2\Sigma$).

The first two items are used to construct, in accordance with the convention given in Eq.E1.2.1, the name of the file holding the input dataset; the file is then opened for reading. Next, all three items are used to construct, in accordance with the convention given in Eq.E1.2.2, the name of the output file which will hold the results of the calculation performed by PROF_BF; this file is then created and opened for writing.

PROF_BF then reads the main input data from the open dataset. The content of the dataset is specified in §E1.2.2; for future reference, the program variables used to hold these data are listed in Table E1.1. The interatomic potentials and dipole transition moments used by PROF_BF are listed in Annex B, Appendix B1; each curve is specified at 82 values of the internuclear separation covering the range 2 - 40 au. The wavelengths and temperatures appropriate to each alkali-rare gas system are given in Table 7.4 of §7.2. The energies of the alkali atomic states (EAUP, EBUP and EXUP) and the reduced masses of the alkali-rare gas systems are listed below in Tables E1.2 and E1.3 respectively.

Having read the input data, the first action is to check whether or not the relevant excited state interatomic potential can possibly support bound states of alkali-rare gas core motion. To be capable of supporting bound states, the excited state potential must possess a negative potential well (recall that the potentials are measured relative to their respective separated atom limits) indicated by a potential extremum (minimum) at negative energy. Hence, if the requested electronic transition is $A^2\Pi - X^2\Sigma$, the array of interatomic potential energies, VAI, is searched for an element VAI(I) satisfying

$$VAI(I-1) > VAI(I) < VAI(I+1) ; \quad VAI(I) < 0. \qquad \text{(E1.4.1)}$$

Table E1.1 Input Data for Program PROF_BF

FORTRAN Variable Name	Description of Data Held
NIV	Number of input values for internuclear separations, interatomic potentials and dipole transition moments.
RI(I)	Array of NIV values specifying the internuclear separations at which the interatomic potentials and dipole transition moments are available.
VAI(I)	Array of NIV values, one value for each RI(I), specifying the $A^2\Pi$ interatomic potential.
VBI(I)	Array of NIV values, one value for each RI(I), specifying the $B^2\Sigma$ interatomic potential.
VXI(I)	Array of NIV values, one value for each RI(I), specifying the $X^2\Sigma$ interatomic potential.
DTMAI(I)	Array of NIV values, one value for each RI(I), specifying the dipole transition moment for the $A^2\Pi - X^2\Sigma$ electronic transition.
DTMBI(I)	Array of NIV values, one value for each RI(I), specifying the dipole transition moment for the $B^2\Sigma - X^2\Sigma$ electronic transition.
NLAMDA	Number of wavelengths at which $I_{BF}(\lambda,T)$ is to be calculated.
FLAMDA(n)	Array of NLAMDA values specifying the wavelengths $\{\lambda_n\}$ at which $I_{BF}(\lambda,T)$ is to be calculated.
NTEMP	Number of temperatures at which $I_{BF}(\lambda,T)$ is to be calculated.
TEMP(m)	Array of NTEMP values specifying the temperatures $\{T_m\}$ at which $I_{BF}(\lambda,T)$ is to be calculated.
EAUP	Energy of the alkali atomic state connected to the $A^2\Pi$ molecular state.
EBUP	Energy of the alkali atomic state connected to the $B^2\Sigma$ molecular state.
EXUP	Energy of the alkali atomic state connected to the $X^2\Sigma$ molecular state.
FMU	Reduced mass of the alkali-rare gas system.

If such an element is found, it is possible that the $A^2\Pi$ potential might support bound states; the minimum of the potential well, V_{min}, is taken to be the value of VAI(I). If no such element is found satisfying condition E1.4.1, then no potential well exists and no bound states can be supported; PROF_BF terminates in this case.

A similar check is performed if the requested electronic transition is $B^2\Sigma - X^2\Sigma$. The array of interatomic potential energies, VBI, is searched for an element VBI(I) satisfying

Table E1.2 : Alkali Atomic State Energies		
	Atomic State Energy (au)	
Alkali	EAUP, EBUP	EXUP
Li	$-1.30245260 \times 10^{-1}$	$-1.97951990 \times 10^{-1}$
Na	$-1.11550011 \times 10^{-1}$	$-1.88862058 \times 10^{-1}$

Table E1.3 : Alkali-Rare Gas Reduced Masses	
System	Reduced Mass (au)
LiHe	4.64585×10^{3}
LiNe	9.46708×10^{3}
NaHe	6.21435×10^{3}
NaNe	1.94927×10^{4}

$$VBI(I-1) > VBI(I) < VBI(I+1); \quad VBI(I) < 0. \tag{E1.4.2}$$

The minimum of the potential well, V_{min}, is taken to be the value of VBI(I) if condition E1.4.2 is satisfied, otherwise PROF_BF terminates.

If an excited state potential well does exist, the final action of Step 1 is to set the statistical weight ω to the value appropriate for the requested electronic transition, i.e.,

$$\begin{aligned} \omega &= \frac{2}{3} \text{ for } A^2\Pi - X^2\Sigma \\ &= \frac{1}{3} \text{ for } B^2\Sigma - X^2\Sigma. \end{aligned} \tag{E1.4.3}$$

E1.5 Step 2 : Initialise Tote

PROF_BF uses a single tote in which to accumulate the contributions to the total bound-free emission intensity arising from each of the bound states of core motion supported by the excited state interatomic potential. This tote is a matrix with generic element

$I_{BF}(\lambda_n, T_m)$ which, on completion of PROF_BF execution, will hold the bound-free emission intensity at wavelength λ_n and temperature T_m. The tote is implemented as a FORTRAN array FIBF(n,m) with index n running from 1 to NLAMDA and index m running from 1 to NTEMP. In this step, the matrix is initialised by setting each element to zero.

E1.6 Step 3 : Define the Solution Grid

The next step in the PROF_BF procedure is to create the solution grid upon which the radial eigenfunctions $g_q^{VK}(R)$ and $g_f^K(R)$ are to be generated. One possibility would have been to use the radial grid defined by the input data {RI(I)} but, as shown in Annex B, Appendix B1, this is a rather coarse grid, especially at large R, and it was considered necessary to use a much finer grid in order to obtain an accurate representation of the radial eigenfunctions.

The solution grid adopted is defined by a set of radial points held in a FORTRAN array R(I) with the index I running from 0 to a maximum value N. The limits of the grid are defined by variables RMIN and RMAX chosen to coincide with the limits of the grid {RI(I)} :

$$\begin{aligned} &RMIN = RI(1) \\ &RMAX = RI(NIV). \end{aligned} \qquad \text{(E1.6.1)}$$

Intermediate grid points are arranged at a constant separation, denoted by s, so that the quantity N is calculated by

$$N = \left[\frac{RMAX - RMIN}{s} \right]_{nint} \qquad \text{(E1.6.2)}$$

where 'nint' denotes conversion to the nearest integer. The solution grid {R(I)} is then generated by the scheme

$$\begin{aligned} &R(0) = RMIN = RI(1), \\ &R(I) = R(0) + (s \times I) ; \quad I = 1, N - 1, \\ &R(N) = RMAX = RI(NIV). \end{aligned} \qquad \text{(E1.6.3)}$$

These are thus a total of (N + 1) radial points defining the solution grid. Extensive numerical experiments, carried out to determine the sensitivity of the eigenfunction representation to the magnitude of s, showed a value of s = 0.02 au to be satisfactory.

E1.7 Step 4 : Interpolate Interatomic Potential Data

Having generated the solution grid {R(I)} it is now necessary to obtain the appropriate interatomic potentials and dipole transition moment, defined as input data on the grid {RI(I)}, on this new grid. This is achieved using 4-point Lagrange interpolation.

To interpolate a general function F, defined on the grid {RI(I)}, for a value at a point R(I), four successive grid points, denoted RI(K) ... RI(K+3), are taken such that

$$RI(K) \le R(I) \le RI(K+3). \qquad \text{(E1.7.1)}$$

These four points define the interpolation grid. The interpolated value of F at R(I) is then given in terms of the function values at the interpolation grid points via (Abramowitz and Stegun (1972), Eq.25.2.1)

$$F(R(I)) = \sum_{m=K}^{K+3} l_m(R(I))\ F(RI(m)) + O(s^4) \qquad \text{(E1.7.2)}$$

where (Abramowitz and Stegun (1972), Eq.25.2.2)

$$l_m(R(I)) = \prod_{\substack{j=K \\ j\neq m}}^{K+3} \left\{ \frac{R(I) - RI(j)}{RI(m) - RI(j)} \right\}. \qquad \text{(E1.7.3)}$$

The error term $O(s^4)$ of Eq.E1.7.2 is neglected. Note also that the denominator of $l_m(R(I))$ is a constant for any particular interpolation grid. The steps for carrying out the interpolation of the appropriate interatomic potentials and dipole transition moment for their values on the solution grid {R(I)} are then as follows:

Step 1 Initialise the interpolation grid:

K = 1.

Step 2 Calculate the initial grid constants:

$$C_m = \prod_{\substack{j=K \\ j\neq m}}^{K+3} (RI(m) - RI(j)) ; \qquad m = K, K+3.$$

Step 3 **FOR** each radial point R(I), I = 0, N

Ensure R(I) is on the interpolation grid:

IF R(I) > RI(K+3) **THEN**

Reset interpolation grid: K ← K + 3.

Ensure interpolation grid wholly contained within{RI(I)}:

IF K > NIV-3 **THEN**

K ← NIV-3.

ENDIF

Update the grid constants:

$$C_m = \prod_{\substack{j=K \\ j\neq m}}^{K+3} (RI(m) - RI(j)) ; \qquad m = K, K+3.$$

ENDIF

Calculate differences and $l_m(R(I))$:

$$D_m = \prod_{\substack{j=K \\ j\neq m}}^{K+3} (R(I) - RI(j)) ; \qquad m = K, K+3.$$

$$l_m(R(I)) = \frac{D_m}{C_m}; \qquad m = K, K+3.$$

Calculate the interpolated functions:

IF requested transition is $A^2\Pi - X^2\Sigma$ **THEN**

$$VEX(I) = \sum_{m=K}^{K+3} l_m(R(I))\, VAI(m).$$

$$DTM(I) = \sum_{m=K}^{K+3} l_m(R(I))\, DTMAI(m).$$

ELSE

$$VEX(I) = \sum_{m=K}^{K+3} l_m(R(I))\, VBI(m).$$

$$DTM(I) = \sum_{m=K}^{K+3} l_m(R(I))\, DTMBI(m).$$

ENDIF

$$VGR(I) = \sum_{m=K}^{K+3} l_m(R(I))\, VXI(m).$$

ENDFOR

The output of the interpolation procedure is an excited state interatomic potential held in array VEX, a ground state interatomic potential held in array VGR and a dipole transition moment held in array DTM. All three arrays contain values corresponding to the radial points of the solution grid {R(I)}. Note that if the transition requested on starting PROF_BF is $A^2\Pi - X^2\Sigma$, the array VEX will hold the $A^2\Pi$ interatomic potential and array DTM will hold the dipole transition moment for this transition. Similarly, if the requested transition is $B^2\Sigma - X^2\Sigma$, the array VEX will hold the $B^2\Sigma$ interatomic potential and array DTM will hold the dipole transition moment for this transition. The array VGR always holds the $X^2\Sigma$ interatomic potential.

E1.8 Step 5 : Location of Bound States

The next step in the computational procedure of PROF_BF is to determine the set of bound states of alkali-rare gas core motion that are supported by the excited state interatomic potential. In the following sections, a method for locating the energies of these bound states is described.

E1.8.1 D(E) - An Indicator of Bound States

The relative radial motion of the alkali-rare gas cores in a bound state supported by the excited state interatomic potential is described by a solution of the Schrödinger equation

$$\frac{d^2 g_i^{V,K}(R)}{dR^2} + \frac{2\mu}{\hbar^2}\left[E_{V,K} - V_i(R) - \frac{\hbar^2 K(K+1)}{2\mu R^2} \right] g_i^{V,K}(R) = 0 \qquad \text{(E1.8.1)}$$

where $V_i(R)$ is the initial (excited) state interatomic potential and $E_{V,K}$ is the (negative) energy of the bound state. To be an acceptable wavefunction, the solution value and first derivative must be continuous, finite and single-valued at every point in space, with boundary conditions

$$g_i^{V,K}(R) \to 0\,; \quad R \to 0, \qquad \text{(E1.8.2)}$$

$$g_i^{V,K}(R) \to 0\,; \quad R \to \infty. \qquad \text{(E1.8.3)}$$

Such solutions are the eigenfunctions. These conditions are satisfied only for a discrete set of energies $E_{V,K}$ (the eigenvalues) within the range $[V_{min},0]$ where V_{min} is the (negative) minimum of the excited state interatomic potential well.

The condition of solution continuity for the eigenfunctions is the key to locating the eigenvalues $E_{V,K}$. To illustrate this, suppose that a solution of Eq.E1.8.1 is obtained via numerical integration for an arbitrary energy E in the range $[V_{min},0]$ on the solution grid {R(I)}. In order to satisfy both boundary conditions E1.8.2 and E1.8.3, the solution is generated in two parts. Firstly, Eq.E1.8.1 is integrated in the inward direction (direction of decreasing R), with the boundary condition E1.8.3, from R(N) to some point R(m), with index $m > 0$. This generates a set of solution values denoted

$$g_i^{in}(I) \equiv g_i^{in}(R(I)) ; \qquad I = m, N. \tag{E1.8.4}$$

Since the Schrödinger equation (Eq.E1.8.1) is homogeneous in g(R), the values $g_i^{in}(I)$ may be scaled arbitrarily. In particular, they may be scaled thus:

$$g_i^{in}(I) \leftarrow \frac{g_i^{in}(I)}{g_i^{in}(m)}; \qquad I = m, N \tag{E1.8.5}$$

so that

$$g_i^{in}(m) \equiv g_i^{in}(R(m)) = 1. \tag{E1.8.6}$$

The solution derivative at R(m) may be scaled in the same way, so that

$$g_i'^{in}(m) \equiv g_i'^{in}(R(m)) = \frac{g_i'^{in}(m)}{g_i^{in}(m)} . \tag{E1.8.7}$$

Following these scalings, Eq.E1.8.1 is integrated in the outward direction (direction of increasing R), with the boundary condition E1.8.2, from R(0) to the same point R(m). This generates a second set of solution values denoted

$$g_i^{out}(I) \equiv g_i^{out}(R(I)) ; \qquad I = 0, m \tag{E1.8.8}$$

which may be scaled in a similar way as for the inward integration:

$$g_i^{out}(I) \leftarrow \frac{g_i^{out}(I)}{g_i^{out}(m)}; \quad I = 0, m \tag{E1.8.9}$$

so that

$$g_i^{out}(m) \equiv g_i^{out}(R(m)) = 1. \tag{E1.8.10}$$

The solution derivative at R(m) may be similarly scaled:

$$g_i'^{out}(m) \equiv g_i'^{out}(R(m)) = \frac{g_i'^{out}(m)}{g_i^{out}(m)}. \tag{E1.8.11}$$

Continuity conditions may now be invoked at the matching point of the two integrations, R(m), to determine the acceptability of the solution $\{g_i(R(I)\}$ as an eigenfunction. The scalings of Eqs.E1.8.5 and E1.8.9 ensure that the solution value is continuous at R(m):

$$g_i^{out}(R(m)) - g_i^{in}(R(m)) = 0. \tag{E1.8.12}$$

This will always be true, whether or not the solution represents an eigenfunction. However, a similar condition on the solution derivatives,

$$g_i'^{out}(R(m)) - g_i'^{in}(R(m)) = 0 \tag{E1.8.13}$$

will only hold if the solution is an eigenfunction. This latter condition thus provides a test for identifying eigenfunctions and the corresponding energy eigenvalues: denoting the difference in first derivatives, obtained from a pair of inward and outward integrations of the Schrödinger equation, by D(E), i.e.,

$$D(E) = g_i'^{out}(R(m)) - g_i'^{in}(R(m)), \tag{E1.8.14}$$

this quantity is zero for a solution $\{g_i(R(I))\}$ which represents an eigenfunction $g_i^{V,K}(R)$, the energy E being the corresponding eigenvalue $E_{V,K}$. For energies E which are not eigenvalues, D(E) must be non-zero.

The quantity D(E) forms the basis of the procedure used by PROF_BF for locating the bound state energy eigenvalues. Before describing this procedure, it is useful to consider the behaviour of D(E) as function of energy. This is described next.

E1.8.2 Behaviour of D(E)

The behaviour of D(E) as a function of energy may be determined by considering solutions to the Schrödinger equation (Eq.E1.8.1), generated in the manner described above, at energies close to an eigenvalue. In the following it is assumed that the boundary conditions on solution values (Eqs.E1.8.2 and E1.8.3) are supplemented with boundary conditions on solution derivatives such that, before application of the scalings of Eqs.E1.8.5 and E1.8.9, the outwardly integrated solution has a positive derivative at R(0) and the inwardly integrated solution has a negative derivative at R(N).

Suppose a solution is obtained at an energy E which is just below that of the lowest eigenvalue, denoted E_0, and without loss of generality, the matching point R(m) is chosen to coincide with the first solution turning point in the inward direction so that

$$g_i'^{in}(R(m)) = 0. \qquad \text{(E1.8.15)}$$

After scaling via Eqs.E1.8.5 and E1.8.9 the solution values are matched at R(m) but, since $E < E_0$, the outwardly integrated part of the solution does not reach the (single) turning point and the derivative at the matching point, $g_i'^{out}(R(m))$, is positive. By Eqs.E1.8.14 and E1.8.15, D(E) is positive.

Now suppose that a solution is obtained at an energy E which is just above E_0 with the inwardly integrated part of the solution again being terminated at the first solution turning point so that Eq.E1.8.15 holds, and the outwardly integrated part having, as yet, no nodes. Since $E > E_0$, the outwardly integrated part of the solution reaches a turning point before R(m) and, after scaling via Eqs.E1.8.5 and E1.8.9, the derivative at the matching point, $g_i'^{out}(R(m))$, is negative; D(E) is now also negative.

Thus, increasing the energy E from below to above an eigenvalue results in the function D(E) changing sign from positive to negative. The energy at which D(E) is zero produces a solution whose inward and outward parts are continuous in value and derivative at R(m) and which therefore is an eigenfunction; this will occur at the eigenvalue energy $E = E_0$.

Now consider generating solutions of the Schrödinger equation (Eq.E1.8.1) at a series of energies E_i satisfying

$$E_0 < E_i < E_1 \qquad \text{(E1.8.16)}$$

where E_1 is the next highest eigenvalue after E_0, with each inward integration being terminated at the first solution turning point in the inward direction. At energies E_i just above E_0, there are no nodes in the outwardly integrated part of the solution, but as E_i increases towards E_1 (but remaining below it) a node will eventually appear in this part of the solution. Now the final solution value in the outward integration is negative, as is the derivative $g_i^{out}(R(m))$, and the scaling procedure (Eq.E1.8.9) has the effect of reversing the sign of all solution values of the outwardly integrated part. This leaves $g_i^{out}(R(m))$ positive and D(E) is now positive. Recall that at energies just above E_0, D(E) is negative; the change in sign of D(E) from negative to positive is a discontinuity in D(E) and does not signify the presence of an eigenvalue (E_i is still below E_1) but rather the introduction of an additional node into the solution. Changes in sign of D(E) from negative to positive (in the direction of increasing energy) therefore indicate a move from one vibrational quantum number to the next highest.

In summary, D(E) as defined by Eq.E1.8.14 is a function which oscillates between positive and negative values. Energies for which D(E) simultaneously satisfies the conditions

$$D(E) = 0, \qquad \text{(E1.8.17)}$$

$$\frac{dD(E)}{dE} < 0 \qquad \text{(E1.8.18)}$$

are the eigenvalue energies of bound states. Nodes of D(E) for which dD(E)/dE is positive are discontinuities and do not indicate eigenvalues but rather the appearance of an extra node in the solution g(R) and a transition to the next highest vibrational quantum number.

E1.8.3 Location of Rotationless (K = 0) Bound States via D(E)

The properties of the D(E) function identified above may be used to locate the energy eigenvalues of the rotationless (K = 0) bound states. The approach is to calculate D(E) for a series of trial energies within the excited state interatomic potential well and then to search this D(E) curve for nodes at which D(E) has a negative gradient with respect to E.

These nodes, by virtue of the conditions given in Eqs.E1.8.17 and E1.8.18, identify the energy eigenvalues $E_{V,K}$.

The calculation of D(E) for a given energy requires generating solutions, and solution derivatives, of the Schrödinger equation (Eq.E1.8.1). Schemes for obtaining these are given in the next two sections, followed by a description of how the D(E) curve is constructed and searched for the energy eigenvalues.

E1.8.3.1 Solving the Schrödinger Equation

In atomic units, the radial Schrödinger equation (Eq.E1.8.1) is of the form

$$\frac{d^2g(R)}{dR^2} + 2\mu \left[E - V(R) - \frac{K(K+1)}{2\mu R^2} \right] g(R) = 0. \qquad \text{(E1.8.19)}$$

Defining the quantities

$$U(R) = 2\mu \left[V(R) + \frac{K(K+1)}{2\mu R^2} \right], \qquad \text{(E1.8.20)}$$

$$E' = 2\mu E, \qquad \text{(E1.8.21)}$$

the Schrödinger equation may be written as

$$\frac{d^2g(R)}{dR^2} + \left[E' - U(R) \right] g(R) = 0. \qquad \text{(E1.8.22)}$$

A suitable procedure for obtaining numerical solutions of Eq.E1.8.22 on the solution grid {R(I)} is the integration scheme defined by

$$Y_I = s^2 (U_{I-1} - E') g_{I-1} + 2Y_{I-1} - Y_{I-2} \qquad \text{(E1.8.23)}$$

for integrations in the outward direction (direction of increasing R) and a modified form of this, i.e.,

$$Y_I = s^2 (U_{I+1} - E') g_{I+1} + 2Y_{I+1} - Y_{I+2} \qquad \text{(E1.8.24)}$$

for integrations in the inward direction (direction of decreasing R), where

$$Y_I = \left[1 - \left(\frac{s^2}{12}\right)(U_I - E') \right] g_I , \qquad \text{(E1.8.25)}$$

$$g_I \equiv g(R(I)), \qquad \text{(E1.8.26)}$$

$$U_I \equiv U(R(I)), \qquad \text{(E1.8.27)}$$

and s is the separation of radial points on the solution grid {R(I)}. This scheme, usually attributed to Numerov, is derived in Appendix E4 of this annex.

Recall from §E1.8.1 that the procedure for calculating D(E) is to integrate the Schrödinger equation in the inward direction first to some matching point R(m) and then to follow this by an integration in the outward direction to the same point R(m). The value of D(E) then follows from the difference in first derivatives of the two solution parts at R(m). The only constraint on the choice of R(m) is that it should be kept away from nodes in the solution g(R) in order to avoid potential numerical overflows during the scalings via Eqs.E1.8.5 and E1.8.9. A convenient way of ensuring this is to choose R(m) during the first (inward) integration to be close to the first turning point in the solution g(R) being generated. The second (outward) integration then uses this R(m) as its terminating point.

The implementation of the inward and outward integration schemes in PROF_BF consists of the following steps. For the inward integration:

Step 1 Initialise logical flag:
NO_TURNING_POINT =.FALSE.

Step 2 Set the initial g_I values:
$g_N = 0,$
$g_{N-1} = \varepsilon.$

Step 3 Calculate the initial Y_I values:
$Y_N = 0,$
$Y_{N-1} = \left[1 - \left(\frac{s^2}{12}\right)(U_{N-1} - E') \right] g_{N-1} .$

Step 4 **FOR** each successive radial point on the solution grid in the direction of decreasing R (I = N-2, 0):

Calculate Y_I :

$$Y_I = s^2 (U_{I+1} - E') g_{I+1} + 2Y_{I+1} - Y_{I+2} .$$

Calculate g_I :

$$g_I = Y_I / \left[1 - \left(\frac{s^2}{12}\right)(U_I - E') \right] .$$

Test for the first turning point in the solution:

IF $g_I < g_{I+1}$ **THEN**

Set the index of the matching point:

$$m = I + 1.$$

Calculate the scaled solution values:

$$g_I \leftarrow \frac{g_I}{g_m}; \quad I = m, N.$$

EXIT

ENDIF

Test the current solution magnitude and re-scale the calculated solution if necessary:

IF $|g_I| > g_{max}$ **THEN**

$$g_J \leftarrow \frac{g_J}{g_{max}}; \quad J = I, N.$$

Prevent numerical underflow:

FOR each g_J , J = I, N

IF $|g_J| < \varepsilon$ **THEN**

$$g_J \leftarrow 0.$$

ENDIF

ENDFOR

Recalculate the Y values:

$$Y_I = \left[1 - \left(\frac{s^2}{12}\right)(U_I - E') \right] g_I ,$$

$$Y_{I+1} = \left[1 - \left(\frac{s^2}{12}\right)(U_{I+1} - E') \right] g_{I+1} .$$

ENDIF

Test for the condition of no turning point:

IF I = 0 **THEN**

Set NO_TURNING_POINT = .TRUE.

EXIT

ENDIF

ENDFOR

There are number of points to note about this integration algorithm. Firstly, it is found in practice that for energies close to the minimum of the excited state potential well, inward integrations of the Schrödinger equation fail to produce any turning point in the solution g(R). To indicate the occurrence of this condition a logical flag, NO_TURNING_POINT, is used. This is initialised to .FALSE. in the first step of the algorithm. If the inward integration proceeds as far as the first solution grid point (R(0)) without a turning point being detected, this flag is set .TRUE. and the integration is halted. The flag is used in the construction of the D(E) curve to be described later in §E1.8.3.3.

Secondly, the Numerov integration scheme is not self-starting, the first two solution values, g_N and g_{N-1} being required as input. Since the integration is performed in the direction of decreasing R, setting g_N to zero approximates the boundary condition of Eq.E1.8.3. The second value, g_{N-1}, is arbitrary, its value simply determining the overall scaling of subsequent solution values. A small positive value of $\epsilon = 10^{-10}$ was chosen.

Thirdly, prior to its use, the integration algorithm requires the U_I quantities to have been calculated for the excited state interatomic potential and angular momentum quantum number K at each radial point on the solution grid {R(I)}.

Finally, the scaling of the solution induced by the value of g_{N-1} could, in practice, lead to numerical overflow if the starting point for integration, R_N, is far inside the classically inaccessible region created by the interatomic potential where the magnitude of the solution is extremely small. However, since the Schrödinger equation is homogeneous in g(R), it is acceptable to re-scale the solution by a constant whenever necessary. Therefore, in order to avoid numerical overflow, the magnitude of the solution being generated at the end of each integration step is monitored. If the magnitude of the value just calculated, g_I, exceeds some pre-set (positive) tolerance, denoted g_{max} (taken to be $1/\epsilon$), all the (non-zero) solution values determined in the integration so far are re-scaled downwards by dividing each by g_{max}. Then, in order to prevent numerical underflow in subsequent re-scalings, any (re-scaled) solution value with a magnitude less than ϵ is set to zero. The last two Y values, Y_I and Y_{I+1}, are then recalculated to reflect the new scaling of g_I and g_{I+1} ready for the next integration step. This re-scaling process ensures that the magnitude of the non-zero solution values in {g(R(I)} are maintained in the range $[\epsilon, 1/\epsilon]$ thus preventing numerical overflow or underflow.

For the outward integration, the steps are similar:

Step 1 Set the initial g_I values:

$g_0 = 0$,

$g_1 = \epsilon$.

Step 2 **Calculate the initial Y_I values:**

$$Y_0 = 0,$$

$$Y_1 = \left[1 - \left(\frac{s^2}{12}\right)(U_1 - E') \right] g_1 .$$

Step 3 **FOR each successive radial point on the solution grid in the direction of increasing R, up to the matching point (I = 2, m):**

Calculate Y_I :

$$Y_I = s^2 (U_{I-1} - E') g_{I-1} + 2Y_{I-1} - Y_{I-2} .$$

Calculate g_I :

$$g_I = Y_I / \left[1 - \left(\frac{s^2}{12}\right)(U_I - E') \right] .$$

Test the current solution magnitude and re-scale the calculated solution if necessary:

IF $|g_I| > g_{max}$ **THEN**

$$g_J \leftarrow \frac{g_J}{g_{max}}; \quad J = 0, I.$$

Prevent numerical underflow:

FOR each g_J , J = 0, I

IF $|g_J| < \varepsilon$ **THEN**

$g_J \leftarrow 0.$

ENDIF

ENDFOR

Recalculate the Y values:

$$Y_I = \left[1 - \left(\frac{s^2}{12}\right)(U_I - E') \right] g_I ,$$

$$Y_{I-1} = \left[1 - \left(\frac{s^2}{12}\right)(U_{I-1} - E') \right] g_{I-1} .$$

ENDIF

ENDFOR

Step 4 **Calculate the scaled solution values:**

$$g_I \leftarrow \frac{g_I}{g_m}; \quad I = 0, m.$$

EXIT

The choice of the initial solution value, $g_0 = 0$, approximates the boundary condition E1.8.2 on g(R). As in the inward integration scheme, the magnitude of the solution values is monitored throughout the outward integration and these values are re-scaled when necessary in order to prevent numerical overflow or underflow.

The result of applying the inward integration scheme, followed by the outward integration scheme, to the Schrödinger equation (Eq.E1.8.22) is an array {g(I)} of solution values matched in magnitude at the point R(m). In order to obtain D(E), the solution derivatives at the matching point are also required; the method of calculating these is described next.

E1.8.3.2 The Solution Derivatives

The array {g(I)} contains the series of values $g_0 \ldots g_{m-1}$ calculated by the outward integration scheme and the values $g_{m+1} \ldots g_N$ calculated by the inward integration scheme. The value of g_m is the same for both integrations and is equal to unity.

The first derivative of the outwardly integrated part of the solution, evaluated at the matching point R(m), is obtained by a six-point differentiation formula (Abramowitz and Stegun (1972), Table 25.2) using the calculated solution values $g_{m-5} \ldots g_m$:

$$g'^{out}(R(m)) \equiv \frac{1}{120s} \sum_{j=0}^{5} A_j \, g_{j+m-5} + O(s^6) \qquad \text{(E1.8.28)}$$

where the coefficients A_j are

$$\begin{array}{lll} A_0 = -24 & A_1 = 150 & A_2 = -400 \\ A_3 = 600 & A_4 = -600 & A_5 = 274 \end{array} \qquad \text{(E1.8.29)}$$

and s is the separation of radial points on the solution grid {R(I)}; the error term $O(s^6)$ is neglected. The first derivative of the inwardly integrated part of the solution, evaluated at the matching point R(m), is obtained by a similar formula using the calculated solution values $g_m \ldots g_{m+5}$:

$$g'^{in}(R(m)) \equiv \frac{1}{120s} \sum_{j=0}^{5} B_j \, g_{j+m} + O(s^6) \qquad \text{(E1.8.30)}$$

where the coefficients B_j are

$$\begin{array}{lll} B_0 = -274 & B_1 = 600 & B_2 = -600 \\ B_3 = 400 & B_4 = -150 & B_5 = 24. \end{array} \qquad \text{(E1.8.31)}$$

The error term $O(s^6)$ is again neglected. The integration and differentiation schemes described above allow D(E) to be calculated for any energy within the excited state interatomic potential well. The following sections describe how these schemes are

combined into a procedure for generating a D(E) curve and the subsequent analysis of the curve which yields the energy eigenvalues.

E1.8.3.3 Generating the D(E) curve

The D(E) curve is a set of $D(E_i)$ values calculated at a series of energies E_i, spanning the excited state interatomic potential well, in the range $V_{min} < E_i < 0$. The procedure for generating the D(E) curve consists of the following eight steps:

Step 1 With K = 0, calculate the U_I quantities required for Numerov integration:

$U_I \equiv U(R(I)) = 2\mu\ VEX(I)\ ;\qquad I = 0, N$

where VEX is the array holding the excited state interatomic potential.

Step 2 Initialise the energy variable:

$E_i = V_{min} + \Delta E\ ;\qquad i = 1$

where the increment $\Delta E = \dfrac{|V_{min}|}{n}$ for some integer n.

Step 3 Calculate E':

$E' = 2\mu\ E_i$.

Step 4 Integrate the Schrödinger equation (Eq.E1.8.22) in the inward direction from R(N) using the Numerov scheme (Eq.E1.8.24).

IF there is no turning point found in the solution
(NO_TURNING_POINT = .TRUE.) **THEN**
    Increment the energy variable:
    $E_i \leftarrow E_i + \Delta E$.
    Return to Step 3.
ELSE
    Scaled solution values are $g_m ... g_N$; matching point is R(m).
ENDIF

Step 5 Integrate the Schrödinger equation (Eq.E1.8.22) in the outward direction from R(0) to R(m) using the Numerov scheme (Eq.E1.8.23).
Scaled solution values are $g_0 ... g_m$.

Step 6 Calculate the solution derivatives at R(m) via the differentiation formulae (Eqs.E1.8.28 and E1.8.30).

Step 7 Calculate $D(E_i)$ via Eq.E1.8.14.

Step 8 Increment the energy variable:

$i \leftarrow i + 1$,

$E_i = E_{i-1} + \Delta E$,

and loop until the top of the potential well is reached:

IF $E_i \geq 0$ **THEN**

Number of energies in D(E) curve, $n_e = i - 1$.

EXIT

ELSE

Return to Step 3.

ENDIF

The output of this procedure is a D(E) curve evaluated at the energies $E_1 ... E_{n_e}$ across the potential well. By virtue of the check performed in Step 4, the first energy E_1 will be the lowest energy that produces a turning point in the solution g(R). The separation of energies at which D(E) is calculated, ΔE, is defined in terms of the potential well depth, V_{min}, and an integer, n; a value of n = 50 is chosen initially but this may be increased during the analysis if necessary (see §E1.8.3.4 below). The next section describes how this D(E) curve is analysed to determine the rotationless bound state energy eigenvalues $E_{V,0}$.

E1.8.3.4 Locating the Eigenvalues $E_{V,0}$

The eigenvalues $E_{V,0}$ are the energies at which the D(E) curve generated above is zero and simultaneously has a negative gradient with respect to E. The D(E) curve is defined by the set of values $D(E_i)$, i=1, n_e, with $E_1 < E_2 ... < E_{n_e-1} < E_{n_e} < 0$. To locate the required nodes of D(E), this set is searched in the direction of increasing energy for pairs of energies (E_j, E_{j+1}) between which a sign change of D(E) from positive to negative occurs, each such pair of energies bounding an eigenvalue. Binary chopping between E_j and E_{j+1} is then used to obtain an accurate value of the eigenvalue. To illustrate this, the following quantities are defined:

$$\begin{aligned} E^+ &\equiv E_j \qquad (D(E^+) > 0), \\ E^0 &\equiv E_{V,0} \qquad (D(E^0) = 0), \\ E^- &\equiv E_{j+1} \qquad (D(E^-) < 0) \end{aligned} \tag{E1.8.32}$$

where the eigenvalue $E_{V,0}$ satisfies

$$E^+ < E_{V,0} < E^- . \qquad \text{(E1.8.33)}$$

A first estimate of the eigenvalue is given by the mid-point between the energies E^+ and E^-,

$$E^0_{est} = \frac{E^+ + E^-}{2} \qquad \text{(E1.8.34)}$$

and the value of $D(E^0_{est})$ is calculated via integration of the Schrödinger equation (Eq.E1.8.22), and differentiation of the resulting solution, as described in the previous section. The value E^0_{est} is then used to replace either E^+ or E^- depending on which of $D(E^+)$ or $D(E^-)$ has the same sign as $D(E^0_{est})$: if $D(E^0_{est})$ is positive, E^+ is replaced by the estimate E^0_{est}; if $D(E^0_{est})$ is negative, E^- is replaced by E^0_{est}. A new estimate of the eigenvalue is then obtained by Eq.E1.8.34 and the above process is repeated until the relative difference between the bounding energies E^+ and E^- is less than some pre-set tolerance δ (a value of $\delta = 10^{-6}$ was chosen), i.e., until the condition

$$2\frac{E^- - E^+}{|E^- + E^+|} \leq \delta \qquad \text{(E1.8.35)}$$

is satisfied. The energy eigenvalue $E_{V,0}$ is then taken to be the mean of E^+ and E^-. Repeating this procedure for each pair of energies (E_j, E_{j+1}) found in the D(E) curve satisfying the conditions of Eq.E1.8.32 generates the set of eigenvalue energies $\{E_{V,0}\}$.

To ensure that no bound state eigenvalues are missed in this search, a check is kept on the number of nodes appearing in the Schrödinger equation solutions g(R) corresponding to each eigenvalue. The lowest eigenvalue should correspond to a solution g(R) with no nodes; the next highest eigenvalue to a solution with one node, and so on. As each eigenvalue is located, the number of nodes in the corresponding solution g(R) is checked to ensure that it is exactly one greater than that appearing in the solution corresponding to the previously located eigenvalue (or equal to zero if the first eigenvalue is being considered). If this condition is not satisfied, it indicates that the energy grid used to calculate the D(E) curve is too coarse and that a smaller energy increment ΔE is required.

In this situation, the current analysis is abandoned and a new D(E) curve is generated using a smaller energy increment ΔE half the size of the original value (the value of n is doubled - see §E1.8.3.3). The starting point of this new D(E) curve is taken to be at the energy $E_{V,0} + \Delta E$, where $E_{V,0}$ is the last eigenvalue located corresponding to an eigenfunction with the correct number of nodes. The analysis of this D(E) curve is as

described above, with additional D(E) curves being generated at finer grid spacings as necessary, until the set of resulting eigenvalue energies correspond to solutions g(R) with the correct sequence of nodes. The eigenvalues thus located correspond to energies $E_{0,0}$, $E_{1,0}$....$E_{V_{max},0}$ of the rotationless bound states.

In the scheme used to calculate D(E), the highest energy at which D(E) is generated is at $E_{n_e} = -\Delta E$. To ensure that no bound states which may lie in the range $[-\Delta E, 0]$ are missed, another D(E) curve is now calculated over this energy range. The energy increment for this curve is taken to be

$$\Delta E \leftarrow \frac{\Delta E}{n} \qquad \text{(E1.8.36)}$$

where n is the value adopted for the last D(E) curve calculated. The lowest energy in the new D(E) curve is taken to be at $E_{V_{max},0} + \Delta E$, just above the last eigenvalue located. This curve is analysed in the same way as the previous D(E) curves and any additional bound state eigenvalues located are added to the original set $\{E_{V,0}\}$. Further D(E) curves are generated over increasingly smaller energy ranges near the top of the potential well until no additional eigenvalues are found, at which point the analysis is complete and the entire set of rotationless eigenvalues has been found.

Having located the eigenvalues $\{E_{V,K}\}$ for K = 0, the next step is to locate the rotational bound state eigenvalues $E_{V,K}$ for K > 0. This is described in the next section.

E1.8.4 Location of Rotational (K>O) Bound States via D(E)

One method of locating the rotational bound states would be to calculate successive D(E) curves for K = 1, 2, 3..., analysing each curve in the manner described above for K = 0. There is, however, considerable computational effort involved in this approach: each D(E) curve requires a minimum of 50 integrations of the Schrödinger equation (Eq.E1.8.22) with at least two curves being generated for each K value.

A more efficient method, which avoids having to calculate entire D(E) curves, exploits the fact that the rotational states associated with a particular vibrational quantum number V are more closely spaced in energy than the rotational states (with the same K) of different V, i.e.,

$$E_{V,K+1} - E_{V,K} \ll E_{V+1,K} - E_{V,K} \qquad \text{(E1.8.37)}$$

resulting in $E_{V,K+1}$ being bounded by

$$E_{V,K} < E_{V,K+1} \ll E_{V+1,K} . \qquad \text{(E1.8.38)}$$

This suggests that the rotationless state eigenvalues $\{E_{V,0}\}$ already located may be used as lower bound estimates of the eigenvalues $\{E_{V,1}\}$. Generating appropriate upper bounds on the $\{E_{V,1}\}$ will allow the binary chopping procedure described in the previous section to be used to locate the K = 1 eigenvalues without calculating the entire D(E) curve. To illustrate the method, the location of the $\{E_{V,1}\}$ eigenvalues is described below.

A lower bound on a particular eigenvalue $E_{V,1}$ is given by the corresponding eigenvalue for K = 0, i.e., $E_{V,0}$. Using the notation of Eq.E1.8.32, the energy $E_{V,0}$ is identified with the lower bound E^+:

$$E^+ \equiv E_{V,0} \qquad (D(E^+) > 0). \qquad \text{(E1.8.39)}$$

To obtain an upper bound on $E_{V,1}$, an energy increment ΔE is defined by

$$\Delta E = \frac{(E_{V+1,0} - E_{V,0})}{n}; \quad 0 \le V < V_{max}$$
$$= \frac{|E_{V_{max},0}|}{n}; \quad V = V_{max} \qquad \text{(E1.8.40)}$$

where n is an integer; a value of n = 20 is chosen initially, but this may be increased during the analysis if necessary, as explained below. A trial upper bound energy E^- is then given by

$$E^- = E^+ + \Delta E. \qquad \text{(E1.8.41)}$$

With K = 1 and E = E', the Schrödinger equation (Eq.E1.8.22) is integrated to provide a value for $D(E^-)$. For E^- to be a valid upper bound, $D(E^-)$ must be negative. If this is so, the binary chopping procedure described in the previous section is invoked on the pair of energies (E^+, E^-) and the eigenvalue $E_{V,1}$ is located. If $D(E^-)$ is positive, the replacement

$$E^+ \leftarrow E^- \qquad \text{(E1.8.42)}$$

is made, the energy E^- is incremented via

$$E^- \leftarrow E^- + \Delta E \qquad \text{(E1.8.43)}$$

and the calculation of $D(E^-)$ is repeated. The replacement of Eq.E1.8.42 and incrementing of E^- by Eq.E1.8.43 are repeated until $D(E^-)$ is negative, at which point binary chopping is invoked on (E^+, E^-) to locate $E_{V,1}$.

A potential problem with this method is that between the lower bounds $E_{V,0}$ and $E_{V+1,0}$ (with V less than the maximum value, V_{max}) D(E) changes sign from positive (at the energy $E = E_{V,0}$) to negative (across energy $E = E_{V,1}$) and back to positive (before $E_{V+1,0}$) when the additional node appears in the solution g(R) corresponding to $E_{V+1,0}$. It is possible therefore that if the energy increment ΔE used in Eq.E1.8.43 is too large, the negative region of D(E) may be missed altogether. This condition is indicated by E^- reaching the value $E_{V+1,0}$ without producing a negative value of $D(E^-)$. In this situation, the search for an upper bound on $E_{V,1}$ is abandoned and repeated with a smaller ΔE (the value of n in Eq.E1.8.40 is doubled). ΔE is adjusted in this way until a search produces a negative $D(E^-)$ between $E_{V,0}$ and $E_{V+1,0}$. This value of ΔE is then retained and used to initiate subsequent searches for rotational eigenvalues, but it will be further reduced as and when necessary. In the special case of V equal to the maximum value, V_{max}, the search for an upper bound energy may also fail to produce a negative value of $D(E^-)$. This occurs when E^- reaches zero with $D(E^-)$ still positive and this is taken as indicating that there are no further rotational bound states associated with this value of V.

The procedure described above, applied to each of the rotationless bound state eigenvalues $E_{0,0}, E_{1,0}...E_{V_{max},0}$ in turn, generates the set of K = 1 eigenvalues $\{E_{V,1}\}$. In a similar manner, the $\{E_{V,1}\}$ eigenvalues just calculated are then used as lower bounds for the K = 2 eigenvalues, the above procedure leading to the set $\{E_{V,2}\}$; these eigenvalues in turn are used to generate the set $\{E_{V,3}\}$, and so on. The general form of the procedure for determining a single rotational bound state eigenvalue $E_{V,K}$ is summarised by the following 6 steps:

Step 1 Set the lower bound on $E_{V,K}$:

$$E^+ = E_{V,K-1}\,.$$

Step 2 Define the energy increment:

IF $V = V^c_{max}$ **THEN**

$$\Delta E = \frac{|E_{V,K-1}|}{n}\,.$$

ELSE

$$\Delta E = \frac{(E_{V+1,K-1} - E_{V,K-1})}{n}\,.$$

ENDIF

Step 3 Set a trial upper bound on $E_{V,K}$:

$$E^- = E^+ + \Delta E.$$

Step 4 Calculate $D(E^-)$ by integrating the Schrödinger equation (Eq.E1.8.22) with angular momentum K and $E = E^-$.

Step 5

IF $D(E^-) < 0$ **THEN**

Invoke binary chopping on (E^+, E^-) leading to the eigenvalue $E_{V,K}$.

EXIT

ELSE

$E^+ \leftarrow E^-$.

$E^- \leftarrow E^- + \Delta E$.

ENDIF

Step 6 Check E^- :

IF $V = V^c_{max}$ and $E^- > 0$ **THEN**

No further rotational bound states exist for this V.

EXIT

ELSEIF $E^- \geq E_{V+1,K-1}$ **THEN**

Negative region of $D(E^-)$ has been missed; reduce ΔE and repeat the search:

$n \leftarrow n/2$.

Return to Step 1.

ELSE

Return to Step 4.

ENDIF

The output of this procedure is either the rotational bound state eigenvalue $E_{V,K}$ or an indication (via Step 6) that no rotational eigenvalues exist for this V with angular momenta greater than (K-1).

Note that this general procedure uses a quantity V^c_{max} . This is the current value of the highest vibrational quantum number V for which rotational bound states may exist. It is well known that lower values of V have more associated rotational bound states than higher values of V. Denoting the maximum value of K associated with a particular V as $K_{max}(V)$, these quantities satisfy

$$K_{max}(V_{max}) \leq K_{max}(V_{max}-1) \leq \ldots \leq K_{max}(1) \leq K_{max}(0). \qquad \text{(E1.8.44)}$$

For $K = 0$, $V^c_{max} = V_{max}$. As K increases, at some point it will exceed $K_{max}(V_{max})$:

$$K_{max}(V_{max}) < K < K_{max}(V_{max}-1). \qquad \text{(E1.8.45)}$$

The quantum number V_{max} has no associated rotational bound states for this, or any greater, K and the quantity V^c_{max} now becomes equal to V_{max}-1. Further increases in K progressively reduce the number of V quantum numbers which need to be considered during the search for rotational bound states, the value of V^c_{max} indicating the current highest value of V that is to be used at any stage in the analysis.

The location of all $E_{V,K}$ eigenvalues for K > 0 is summarised in the following four step procedure:

Step 1 Initialise variables:

$V^c_{max} = V_{max}$,

K = 1.

Step 2 Calculate the U_I quantities required for Numerov integration:

$$U_I = 2\mu VEX(I) + \frac{K(K+1)}{R(I)^2}; \quad I = 0, N.$$

Step 3 **FOR** V = 0, V^c_{max}

Apply P($E_{V,K}$).

IF $E_{V,K}$ located **THEN**

Add $E_{V,K}$ to eigenvalue set {$E_{V,K}$}.

ELSE

No further rotational bound states exist for this V: decrement V^c_{max} :

$V^c_{max} \leftarrow V^c_{max}$ -1.

IF $V^c_{max} < 0$ **THEN**

All rotational bound states have been located.

EXIT

ENDIF

ENDIF

ENDFOR

Step 4 Increment K and loop:

K ← K + 1.

Return to Step 2.

Here, $P(E_{V,K})$ appearing in Step 3 denotes the 6 step procedure described earlier for locating a single rotational eigenvalue $E_{V,K}$.

E1.9 Step 6: The Main Program Loop

Section E1.8 above described procedures for locating the energy eigenvalues $E_{V,K}$ of bound states of alkali-rare gas core motion that are supported by the excited state interatomic potential. This eigenvalue determination is Step 5 of the computational procedure of PROF_BF outlined in §E1.3. The next step in this procedure, Step 6, constitutes the main loop of the program in which the bound-free emission intensity $I_{BF}(\lambda_n, T_m)$ is calculated to within a multiplicative constant. The loop is driven by the set of bound state eigenvalues $\{E_{V,K}\}$, the actions performed by the loop being applied to each eigenvalue in turn. These actions are described below.

E1.9.1 Normalised Bound State Eigenfunctions

Corresponding to an energy eigenvalue $E_{V,K}$ is a solution (eigenfunction) of the radial Schrödinger equation (Eq.E1.8.1) denoted $g^{V,K}(R)$. A numerical representation of the eigenfunction is obtained by the procedures described in §E1.8.3.1, i.e., a pair of numerical integrations of Eq.E1.8.1, one in the inward direction followed by one in the outward direction, using the Numerov scheme. The representation consists of (N+1) solution values, denoted $g_i(I)$ ($\equiv g_i(R(I))$), on the solution grid $\{R(I)\}$.

The required normalisation of bound state eigenfunctions is such that

$$\int_0^\infty \left[g_i^{V,K}(R) \right]^2 dR = 1. \qquad \text{(E1.9.1)}$$

The normalisation of the numerical representation of the eigenfunction is thus achieved by calculating the quantity

$$c = \int_{R(0)}^{R(N')} \left[g_i(I) \right]^2 dR \qquad \text{(E1.9.2)}$$

where N' is chosen such that g_i (N'-1) is the outermost non-zero solution point, and then scaling the original solution values via

$$g_i(I) \leftarrow \frac{g_i(I)}{c^{1/2}}; \quad I = 0, N'-1 \qquad \text{(E1.9.3)}$$

with the eigenfunction being zero for $R(N') \le R \le R(N)$.

The integral in Eq.E1.9.2 is evaluated piece-wise using an 11-point Newton-Cotes integration formula defined by (Abramowitz and Stegun (1972), Eq.25.4.20)

$$\int_{R(I)}^{R(I+10)} f(R)\,dR = \frac{5s}{299376}\Big\{\, 16067(f_I + f_{I+10}) + 106300(f_{I+1} + f_{I+9}) - 48525(f_{I+2} + f_{I+8}) + 272400(f_{I+3} + f_{I+7}) - 260550(f_{I+4} + f_{I+6}) + 427368 f_{I+5} \,\Big\} + O(s^{13}) \qquad \text{(E1.9.4)}$$

where

$$f(R) = \left[g_i^{V,K}(R) \right]^2, \qquad \text{(E1.9.5)}$$

$$f_I \equiv f(R(I)) = \left[g_i(I) \right]^2 \qquad \text{(E1.9.6)}$$

and s is the separation of radial points on the solution grid {R(I)}. The error term $O(s^{13})$ is neglected.

For an integration over the solution grid, from R(0) to R(N'), the grid is divided into M 11-point domains, with

$$M = \left[\frac{N'}{10} \right]_{int} \qquad \text{(E1.9.7)}$$

where 'int' denotes integer division. If N' is not a multiple of 10, a final $(M+1)^{th}$ domain is added; this contains fewer than 11 points, the number being given by (N'-10M+1). The integral of f(R) is then calculated over each of the first M domains via Eq.E1.9.4 leading to the quantities

$$I_j = \int_{R(10(j-1))}^{R(10j)} f(R)\,dR; \quad j = 1, M. \qquad \text{(E1.9.8)}$$

If there exists a final domain with fewer than 11 points, the following are defined:

$$f_I = f(R(I)) ; \quad I = 10M, N',$$
$$f_I = 0 ; \quad I = N'+1, 10(M+1) \qquad \text{(E1.9.9)}$$

and the integral of f(R) over this domain, denoted I_{M+1}, is calculated via Eq.E1.9.4. The normalisation constant c of Eq.E1.9.2 is then obtained via

$$c = \int_{R(0)}^{R(N')} \left[g_i(I) \right]^2 dR = \sum_{j=1}^{M'} I_j \qquad \text{(E1.9.10)}$$

where the upper summation limit M' equals M if N' is a multiple of 10, and equals (M+1) otherwise. The normalised bound state eigenfunction then follows from the scaling of Eq.E1.9.3.

E1.9.2 The Bound-Free Matrix Elements

Having obtained the normalised eigenfunction $g_i^{V,K}(R)$ corresponding to the bound state eigenvalue $E_{V,K}$, the next stage is to calculate the matrix elements $S_{if}(V,K)$ connecting this bound state to the continuum of the ground state. $S_{if}(V,K)$ is given by

$$S_{if}(V,K) = \left| \int_0^{\infty} g_i^{V,K}(R)\, D_{\Lambda',\Lambda}(R)\, g_f^{K}(R)\, dR \right|^2 \qquad \text{(E1.9.11)}$$

where $D_{\Lambda',\Lambda}(R)$ is the dipole transition moment for the transition between the excited and ground states and $g_f^K(R)$ is the normalised eigenfunction describing the relative radial motion of the alkali-rare gas cores under the influence of the ground state interatomic potential. This eigenfunction is a solution of the radial Schrödinger equation

$$\frac{d^2 g_f^K(R)}{dR^2} + \frac{2\mu}{\hbar^2}\left[E_f - V_f(R) - \frac{\hbar^2 K(K+1)}{2\mu R^2} \right] g_f^K(R) = 0 \qquad \text{(E1.9.12)}$$

where $V_f(R)$ is the final (ground) state interatomic potential and E_f is the energy of the continuum state.

The energy E_f is related to the excited (bound) state eigenvalue $E_{V,K}$ and the wavelength λ of radiation emitted during the bound-free transition via conservation of energy, i.e.,

$$h\nu = E_{V,K} - E_f + h\nu_0 \qquad \text{(E1.9.13)}$$

where ν is the frequency of the radiation emitted in the alkali resonance line wing and ν_0 is the frequency of the unperturbed resonance line given by (see §E1.4, Table E1.1)

$$h\nu_0 = \text{EAUP} - \text{EXUP}. \qquad \text{(E1.9.14)}$$

Both energies $E_{V,K}$ and E_f are measured relative to the atomic alkali resonance level energies. In atomic units,

$$h\nu = \frac{2\pi\alpha^{-1}}{\lambda_{a_0}} = \frac{2\pi\alpha^{-1}}{\lambda_{\text{Å}}}\left[\frac{1\ a_0}{1\ \text{Å}}\right] = \frac{455.63421}{\lambda_{\text{Å}}} \qquad \text{(E1.9.15)}$$

where α is the fine structure constant and the ratio (1 a_0 / 1 Å) converts wavelength units from a_0 to Å. Hence, for the eigenvalue energy $E_{V,K}$, the energy of the ground state E_f which results in emission of radiation at wavelength $\lambda_{\text{Å}}$ (i.e., wavelength measured in Å) due to a bound-free transition is given by

$$E_f = E_{V,K} + h\nu_0 - \frac{455.63421}{\lambda_{\text{Å}}}. \qquad \text{(E1.9.16)}$$

For bound-free transitions, E_f must be positive. If Eq.E1.9.16 produces a negative value of E_f for some wavelength $\lambda_{\text{Å}}$, this simply indicates that transitions out of the bound state of energy $E_{V,K}$ cannot give rise to emitted radiation at this wavelength.

A single bound state eigenvalue $E_{V,K}$ thus leads to, via Eq.E1.9.16, a set of ground state eigenvalues denoted $E_f(\lambda_n)$, one eigenvalue for each wavelength specified in the input data to PROF_BF (see §E1.4, Table E1.1):

$$E_f(\lambda_n) = E_{V,K} + h\nu_0 - \frac{455.63421}{\text{FLAMDA(n)}}; \quad n = 1, \text{NLAMDA}. \qquad \text{(E1.9.17)}$$

Corresponding to each $E_f(\lambda_n)$ is a normalised free state eigenfunction $g_f^K(R)$, the calculation of which is described next.

E1.9.2.1 Normalised Free State Eigenfunctions

With the boundary condition

$$g_f^K(R) \rightarrow 0\,; \quad R \rightarrow 0, \qquad \text{(E1.9.18)}$$

solutions of the Schrödinger equation (Eq.E1.9.12) are obtained via numerical integration using the Numerov scheme described in §E1.8.3. The integration procedure is identical to that described for integrations in the outward direction (direction of increasing R) used for obtaining bound state eigenfunctions (see §E1.8.3.1) with the following exceptions:

(i) the U_I quantities are now calculated with the ground state interatomic potential and the angular momentum K of the bound state:

$$U_I = 2\mu VGR(I) + \frac{K(K+1)}{R(I)^2}; \quad I = 0, N; \qquad \text{(E1.9.19)}$$

(ii) the quantity E' is given by

$$E' = 2\mu E_f(\lambda_n); \qquad \text{(E1.9.20)}$$

(iii) the end point of the integration is set to the outermost point of the solution grid {R(I)}:

$$m = N; \qquad \text{(E1.9.21)}$$

(iv) the solution value scaling (Step 4) is not required.

The output of the integration procedure is a numerical representation of the free state eigenfunction $g_f^K(R)$, as yet un-normalised, consisting of (N+1) solution values, denoted $g_f(I)$ ($\equiv g_f(R(I))$), on the solution grid {R(I)}. The eigenvalue corresponding to this eigenfunction is $E_f(\lambda_n)$.

The normalisation of the free state eigenfunction is obtained by considering its asymptotic behaviour. Three radial domains may be identified depending on the relative magnitudes of $E_f(\lambda_n)$, $V_f(R)$ and the centrifugal potential energy term involving K appearing in the Schrödinger equation (Eq.E1.9.12). In the first domain, $V_f(R)$ is not negligible and the solution $g_f^K(R)$ depends on the form of $V_f(R)$; in the second domain, $V_f(R)$ can be neglected but the centrifugal term cannot. In this domain, the Schrödinger equation (Eq.E1.9.12) becomes (in atomic units)

$$\frac{d^2 g_f^K(R)}{dR^2} + 2\mu \left[E_f(\lambda_n) - \frac{K(K+1)}{2\mu R^2} \right] g_f^K(R) = 0. \qquad \text{(E1.9.22)}$$

The most general solution of this equation is

$$g_f^K(R) = A_K kR[\cos(\eta_K) j_K(kR) - \sin(\eta_K) n_K(kR)] \qquad \text{(E1.9.23)}$$

where A_K = an arbitrary constant,
η_K = the elastic scattering phase shift,
$j_K(kR)$ = the spherical Bessel function of the first kind,
$n_K(kR)$ = the spherical Bessel function of the second kind,
$k = (2\mu E_f(\lambda_n))^{1/2}$.

In the third domain, both $V_f(R)$ and the centrifugal potential term are negligible and the solution $g_f^K(R)$ is obtained from the asymptotic forms of the Bessel functions:

$$j_K(kR) \rightarrow \frac{1}{kR} \cos(kR - \tfrac{1}{2}(K+1)\pi) ; \quad R \rightarrow \infty, \qquad \text{(E1.9.24)}$$

$$n_K(kR) \rightarrow \frac{1}{kR} \sin(kR - \tfrac{1}{2}(K+1)\pi) ; \quad R \rightarrow \infty, \qquad \text{(E1.9.25)}$$

so that

$$g_f^K(R) \rightarrow A_K \sin(kR - \tfrac{1}{2}K\pi + \eta_K) ; \quad R \rightarrow \infty. \qquad \text{(E1.9.26)}$$

The required normalisation of $g_f^K(R)$ is such that the solution is asymptotically a unit modulus sine wave. An expression for the constant A_K is now obtained in terms of quantities which may be calculated directly from the numerical solution of the Schrödinger equation, $\{g_f(I)\}$. Knowledge of A_K then permits the required normalisation of $g_f^K(R)$ via scaling. The formulation of this expression for A_K is as follows: assume that $g_f^K(R)$ has its most general form, given by Eq.E1.9.23, and define the quantity ρ by

$$\rho = kR. \qquad \text{(E1.9.27)}$$

Then

$$g_f^K(\rho) = A_K \rho[\cos(\eta_K) j_K(\rho) - \sin(\eta_K) n_K(\rho)]. \qquad \text{(E1.9.28)}$$

The solution derivative with respect to ρ is then

$$g'^{K}_{f}(\rho) = A_K\rho[\cos(\eta_K)j'_K(\rho) - \sin(\eta_K)n'_K(\rho)] + A_K[\cos(\eta_K)j_K(\rho) - \sin(\eta_K)n_K(\rho)] \qquad \text{(E1.9.29)}$$

The logarithmic derivative of $g^{K}_{f}(\rho)$ is then given by

$$\frac{g'^{K}_{f}(\rho)}{g^{K}_{f}(\rho)} = \frac{\cos(\eta_K)j'_K(\rho) - \sin(\eta_K)n'_K(\rho)}{\cos(\eta_K)j_K(\rho) - \sin(\eta_K)n_K(\rho)} + \frac{1}{\rho}. \qquad \text{(E1.9.30)}$$

The logarithmic derivative of the eigenfunction with respect to R is then obtained (using Eq.E1.9.27) as

$$\frac{g'^{K}_{f}(R)}{g^{K}_{f}(R)} = k\frac{g'^{K}_{f}(\rho)}{g^{K}_{f}(\rho)}. \qquad \text{(E1.9.31)}$$

Now the quantity $\gamma_K(R)$ is defined via

$$\gamma_K(R) = \frac{g'^{K}_{f}(R)}{g^{K}_{f}(R)} - \frac{1}{R}. \qquad \text{(E1.9.32)}$$

Using Eqs.E1.9.30 and E1.9.31, this may be written as

$$\gamma_K(R) = k\frac{[\cos(\eta_K)j'_K(\rho) - \sin(\eta_K)n'_K(\rho)]}{[\cos(\eta_K)j_K(\rho) - \sin(\eta_K)n_K(\rho)]} \qquad \text{(E1.9.33)}$$

which, by re-arrangement, gives an expression for the phase shift η_K:

$$\eta_K = \tan^{-1}\left\{\frac{\gamma_K(R)j_K(\rho) - kj'_K(\rho)}{\gamma_K(R)n_K(\rho) - kn'_K(\rho)}\right\}. \qquad \text{(E1.9.34)}$$

The point of this analysis is that the quantity $\gamma_K(R)$ defined in Eq.E1.9.32 can be obtained directly from the numerical representation of the eigenfunction at any radial point on the solution grid {R(I)}. By Eq.E1.9.34, a value for the phase shift η_K may then be calculated (the Bessel functions and their derivatives are known analytically) from which the constant A_K may be evaluated via Eq.E1.9.23:

$$A_K = \frac{g_f^K(R)}{kR\left[\cos(\eta_K) j_K(kR) - \sin(\eta_K) n_K(kR)\right]} . \qquad \text{(E1.9.35)}$$

The details of this evaluation are as follows: the first step is to calculate $\gamma_K(R)$ from the numerical representation of the eigenfunction at some radial point on the solution grid. A suitable radial point is the end point R(N) provided that this does not correspond to an eigenfunction node, in which case the previous analysis is invalid. If this is the case, the preceding solution values $g_f(N-1)$, $g_f(N-2)$... are considered in turn, the first non-zero point found (in the direction of decreasing R) being taken as the one at which to evaluate $\gamma_K(R)$. For the purposes of the following discussion, the radial point chosen by the method described above is denoted by R(M).

The first derivative of the solution at R(M) is determined in the same way as derivatives were obtained at the end points of outward integrations in the search for bound state eigenvalues (see §E1.8.3.2), i.e., by a six-point differentiation formula using the calculated solution values $g_f(M-5)...g_f(M)$:

$$g'_f(M) \cong \frac{1}{120s} \sum_{j=0}^{5} A_j \, g_f(j+M-5) \qquad \text{(E1.9.36)}$$

where the coefficients A_j are given in Eq.E1.8.29 and the error term $O(s^6)$ has been neglected. A numerical value for $\gamma_K(R)$ at the grid point R(M) then follows from Eq.E1.9.32:

$$\gamma_K(R(M)) = \frac{g'_f(M)}{g_f(M)} - \frac{1}{R(M)} . \qquad \text{(E1.9.37)}$$

To determine the phase shift η_K, values for the Bessel functions and their first derivatives are now required. For $K < 2$, the functions are obtained from their analytical forms:

$$K = 0: \qquad j_0(\rho) = \frac{\sin(\rho)}{\rho} \; ; \qquad n_0(\rho) = \frac{-\cos(\rho)}{\rho} , \qquad \text{(E1.9.38)}$$

$$K = 1: \qquad j_1(\rho) = \frac{\sin(\rho)}{\rho^2} - \frac{\cos(\rho)}{\rho} = \frac{1}{\rho} j_0(\rho) + n_0(\rho),$$

$$n_1(\rho) = \frac{-\cos(\rho)}{\rho^2} - \frac{\sin(\rho)}{\rho} = \frac{1}{\rho} n_0(\rho) - j_0(\rho). \qquad \text{(E1.9.39)}$$

For $K \geq 2$, recursion relations are used with the $K = 0, 1$ values as starting values:

$$K \geq 2: \qquad j_K(\rho) = \frac{2K-1}{\rho} j_{K-1}(\rho) - j_{K-2}(\rho),$$

$$n_K(\rho) = \frac{2K-1}{\rho} n_{K-1}(\rho) - n_{K-2}(\rho). \qquad \text{(E1.9.40)}$$

Similarly for the Bessel function derivatives: for $K = 0$, the derivatives are obtained from their analytical forms:

$$K = 0: \qquad j'_0(\rho) = \frac{\cos(\rho)}{\rho} - \frac{\sin(\rho)}{\rho^2} = -\frac{1}{\rho} j_0(\rho) - n_0(\rho),$$

$$n'_0(\rho) = \frac{\sin(\rho)}{\rho} + \frac{\cos(\rho)}{\rho^2} = -\frac{1}{\rho} n_0(\rho) + j_0(\rho). \qquad \text{(E1.9.41)}$$

For $K \geq 1$, recursion relations are used:

$$K \geq 1: \qquad j'_K(\rho) = j_{K-1}(\rho) - \frac{K+1}{\rho} j_K(\rho), \qquad \text{(E1.9.42)}$$

$$n'_K(\rho) = n_{K-1}(\rho) - \frac{K+1}{\rho} n_K(\rho).$$

Using these relations, the Bessel functions and their derivatives are calculated for the argument $\rho_M (= kR(M))$ and the angular momentum K of the ground state eigenfunction. The phase shift then follows via

$$\eta_K = \tan^{-1}\left\{\frac{\gamma_K(R(M))j_K(\rho_M) - kj'_K(\rho_M)}{\gamma_K(R(M))n_K(\rho_M) - kn'_K(\rho_M)}\right\}. \qquad \text{(E1.9.43)}$$

All the necessary quantities are now known to permit a value for the constant A_K to be determined:

$$A_K = \frac{g_f(M)}{kR(M)\left[\cos(\eta_K)j_K(\rho_M) - \sin(\eta_K)n_K(\rho_M)\right]}. \qquad \text{(E1.9.44)}$$

The normalised free state eigenfunction is then obtained by the scaling

$$g_f(I) \leftarrow \frac{g_f(I)}{|A_K|}; \quad I = 0, N. \tag{E1.9.45}$$

E1.9.2.2 Calculating the Matrix Element

The previous sections have shown how the normalised bound state eigenfunction $g_i^{V,K}(R)$, corresponding to the eigenvalue $E_{V,K}$, and the normalised free state eigenfunction $g_f^K(R)$, corresponding to the eigenvalue $E_f(\lambda_n)$ are obtained. With these solutions, the matrix element $S_{if}(V,K)$, defined by Eq.E1.9.11, may now be evaluated.

The first step is to calculate the integral

$$I = \int_0^\infty g_i^{V,K}(R)\, D_{\Lambda',\Lambda}(R)\, g_f^K(R)\, dR\,. \tag{E1.9.46}$$

This is done piece-wise over the solution grid {R(I)}, from R(0) to (R(N'), where R(N') is the radial extent of the (non-zero) excited state eigenfunction $\{g_i(I)\}$, using the 11-point Newton-Cotes integration formula given by Eq.E1.9.4, where now

$$f(R) = g_i^{V,K}(R)\, D_{\Lambda',\Lambda}(R)\, g_f^K(R), \tag{E1.9.47}$$

$$f_I \equiv f(R(I)) = g_i(I)\,.\,DTM(I)\,.\,g_f(I)\,; \quad I = 0, N' \tag{E1.9.48}$$

and DTM is the array holding the dipole transition moment (see §E1.7). The calculation proceeds as described in §E1.9.1, producing the set of domain integrals

$$I_j = \int_{R(10(j-1))}^{R(10j)} f(R)\, dR\,; \quad j = 1, M' \tag{E1.9.49}$$

and the integral in Eq.E1.9.46 is then given by

$$I = \sum_{j=1}^{M'} I_j\,. \tag{E1.9.50}$$

The required matrix element then follows via

$$S_{if}(V,K) = I^2. \tag{E1.9.51}$$

E1.9.2.3 Incrementing the Tote

The matrix element $S_{if}(V,K)$ calculated above connects the bound state with eigenvalue $E_{V,K}$ to the free state with eigenvalue $E_f(\lambda_n)$. A transition between these two states gives rise to emission of radiation at the single wavelength FLAMDA(n). The contribution (to within a constant factor) that this transition makes to the total bound-free emission intensity, $I_{BF}(\lambda,T)$, at the wavelength FLAMDA(n) is now saved by incrementing the elements of the tote FIBF corresponding to the wavelength FLAMDA(n) and each of the temperatures specified in the input data to PROF_BF (see §E1.4, Table E1.1):

$$\text{FIBF(n,m)} \leftarrow \text{FIBF(n,m)} + \Big[\text{FLAMDA(n)}^{-4} \,.\, \text{TEMP(m)}^{-3/2} \,.\, (2K+1)E_f(\lambda_n)^{-1/2} \times S_{if}(V,K)\exp(-E_{V,K}/\,k \,.\, \text{TEMP(m)})\Big] \;;\quad \text{m} = 1, \text{NTEMP} \,. \qquad \text{(E1.9.52)}$$

Matrix elements connecting the bound state of energy $E_{V,K}$ with each of the free states of energy $E_f(\lambda_n)$ defined by Eq.E1.9.17 are calculated in turn and the tote FIBF incremented as above. When all the $E_f(\lambda_n)$ have been considered, the tote contains, to within a multiplicative constant, the contribution to the total bound-free emission intensity, as a function of wavelength and temperature, arising from transitions out of the single bound state of energy $E_{V,K}$. This procedure is summarised as follows:

Step 1 Calculate the normalised bound state eigenfunction $g_i^{V,K}(R)$ corresponding to eigenvalue $E_{V,K}$.

Step 2

FOR n = 1, NLAMDA

Calculate the energy of the free state appropriate for emission at wavelength FLAMDA(n):

$$E_f(\lambda_n) = E_{V,K} + h\nu_0 - \frac{455.63421}{\text{FLAMDA(n)}} \,.$$

IF $E_f(\lambda_n) \geq 0$ **THEN**

Calculate the normalised free state eigenfunction $g_f^K(R)$ corresponding to eigenvalue $E_f(\lambda_n)$.

Calculate the matrix element $S_{if}(V,K)$ connecting the bound and free states.

Increment the tote elements FIBF(n,m) ; m = 1, NTEMP.

ENDIF

ENDFOR

Note that any $E_f(\lambda_n)$ that are negative are rejected as being physically unacceptable - the excited state with energy $E_{V,K}$ simply cannot contribute via bound-free transitions at these wavelengths.

Repeating this procedure for the complete set of bound state eigenvalues $\{E_{V,K}\}$ results in the tote FIBF holding the quantity

$$I'_{BF}(\lambda,T) = \lambda^{-4}\, T^{-3/2} \sum_{V\,K} (2K+1)\, E_i^{-1/2} S_{if}(V,K) \exp(-E_{V,K}/kT) \qquad \text{(E1.9.53)}$$

for each wavelength and temperature specified in the input data to PROF_BF. This is the total bound-free emission intensity to within a multiplicative constant.

E1.10 Step 7: Calculating the Bound-Free Emission Intensity

The penultimate step in the computational procedure of PROF_BF is to calculate the desired bound-free emission intensity, $I_{BF}(\lambda,T)$, given by Eq.E1.1.1. This is given by scaling the quantity currently held in the tote FIBF:

$$I_{BF}(\lambda,T) = 1.76526 \times 10^{14}\, \omega\mu^{-1}\, I'_{BF}(\lambda,T)\,. \qquad \text{(E1.10.1)}$$

The elements of the tote are therefore adjusted as follows:

FOR n = 1, NLAMDA
  FOR m = 1, NTEMP
    FIBF(n,m) ← $1.76526 \times 10^{14}\, \omega\mu^{-1}$ FIBF(n,m).
  ENDFOR
ENDFOR

The tote FIBF now contains the quantity $I_{BF}(\lambda,T)$.

E1.11 Step 8: Output the Calculation Results

The final action of PROF_BF is to write the results of the calculation described in §§E1.4 through E1.10 to the output file. The data written to this file consist of the following quantities:

(i) a copy of the input data for PROF_BF (see §E1.4);

(ii) the bound states located. For each state the following quantities are output:

- the vibrational and rotational quantum numbers V,K;
- the energy eigenvalue $E_{V,K}$;
- the value of D(E) and the bounds E^+, E^- at the end of binary chopping;
- the number of nodes appearing in the eigenfunction associated with eigenvalue $E_{V,K}$;

(iii) the calculated bound-free emission intensity $I_{BF}(\lambda,T)$ at the wavelengths FLAMDA(n), n = 1, NLAMDA and the temperatures TEMP(m), m = 1, NTEMP.

This completes the functional description of program PROF_BF.

Appendix E2 Functional Description of Program PROF_QBF

E2.1 Introduction

PROF_QBF is a computer program written in FORTRAN-77 and running on an HP9050 computer under the HP-UX (UNIX) operating system. It consists of 955 lines of source code occupying 26.0K of storage; the executable module occupies 131.3K.

The purpose of PROF_QBF is to calculate the contribution to the alkali resonance line wing emission intensity arising from quasibound-free transitions given by (see §7.2, Eq.7.2.6)

$$I_{QBF}(\lambda,T) = 1.76526\times10^{14}\,\omega\lambda_A^{-4}\,T^{-3/2}\mu^{-1}\sum_{r\,K}(2K+1)\,E_f^{-1/2}S_{if}(r,K)\exp(-E_{r,K}/kT). \qquad \text{(E2.1.1)}$$

The dependence of $I_{QBF}(\lambda,T)$ on the alkali-rare gas interatomic potentials is through the eigenvalues $E_{r,K}$ and E_f, and the eigenfunctions contained in the matrix element $S_{if}(r,K)$:

$$S_{if}(r,K) = \pi\Gamma_{r,K}\left|\int_0^\infty g_i^{r,K}(R)\,D_{\Lambda'\Lambda}(R)\,g_f^{K}(R)\,dR\right|^2. \qquad \text{(E2.1.2)}$$

The eigenfunctions $g_i^{rK}(R)$ and $g_f^{K}(R)$ describe the relative radial motion of the alkali and rare gas cores under the influence of the excited and ground state interatomic potentials respectively. In the context of quasibound-free transitions, the eigenfunction $g_i^{rK}(R)$ describes the initial state of core motion - a quasibound (resonance) state of energy $E_{r,K}$ and half-width $\Gamma_{r,K}$ - and the eigenfunction $g_f^{K}(R)$ describes the final state of core motion - a continuum state of energy E_f. The quasibound-free contribution $I_{QBF}(\lambda,T)$ is obtained by summing functions of matrix elements connecting all quasibound states supported by the excited state interatomic potential with the continuum of the ground state.

A single run of PROF_QBF performs this summation for a combination of

(i) one alkali-rare gas system (one of LiHe, LiNe, NaHe or NaNe in the present study);

(ii) one type of interatomic potential (either model potential or pseudopotential);

(iii) one type of electronic transition (either $A^2\Pi - X^2\Sigma$ or $B^2\Sigma - X^2\Sigma$)

at a given set of wavelengths and temperatures. The current implementation of PROF_QBF has restrictions on the last two quantities, namely, a maximum of 60 wavelengths and 5 temperatures.

E2.2 Input/Output Data Files

The input data used by PROF_QBF are identical to those used by program PROF_BF. The organisation of the data into a number of separate datasets is described in §E1.2.1 of Appendix E1; the content of each dataset is specified in §E1.2.2 of Appendix E1. On any single run of the program, PROF_QBF reads data from just one of these files.

A single run of PROF_QBF creates one output disc file holding the results of the calculation for a particular combination of system, interatomic potential type and electronic transition. The output files are named using a convention similar to that used in the PROF_BF case:

Output File Name = system | potential type | transition | qbf.out (E2.2.1)

where

system = one of {LiHe, LiNe, NaHe, NaNe},
potential type = M for model potentials
= P for pseudopotentials,
transition = A for $A^2\Pi - X^2\Sigma$
= B for $B^2\Sigma - X^2\Sigma$.

The content of the output file is given in §E2.11 following a description of the calculation performed by PROF_QBF.

E2.3 Computational Procedure of PROF_QBF

The computational procedure for evaluating Eq.E2.1.1 consists of eight major steps as follows:

Step 1 Read appropriate input data.
Define a set of wavelengths $\{\lambda_n\}$ and temperatures $\{T_m\}$ at which to calculate the quasibound-free emission intensity.

Step 2 Initialise the main tote:
FOR each wavelength in $\{\lambda_n\}$
FOR each temperature in $\{T_m\}$
$I_{QBF}(\lambda_n, T_m) \leftarrow 0.0$
ENDFOR
ENDFOR

Step 3 Define a suitable solution grid upon which to construct the eigenfunctions $g_i^{r,K}(R)$ and $g_f^K(R)$.

Step 4 Interpolate the interatomic potentials and dipole transition moments read in Step 1 for values on the solution grid defined in Step 3.

Step 5 Calculate the energies $E_{r,K}$ of all quasibound (resonance) states of core motion supported by the excited state interatomic potential.

Step 6 **FOR** each quasibound state of core motion located
Calculate the resonance half-width $\Gamma_{r,K}$.
Calculate the normalised eigenfunction $g_i^{r,K}(R)$ corresponding to energy $E_{r,K}$.

FOR each wavelength in $\{\lambda_n\}$
Calculate the energy of the free state, $E_f(\lambda_n)$, supported by the ground state interatomic potential appropriate for emission of radiation at wavelength λ_n.
Calculate the normalised eigenfunction $g_f^K(R)$ corresponding to energy $E_f(\lambda_n)$.
Calculate the matrix element $S_{if}(r,K)$.
Increment the main tote:
FOR each temperature in $\{T_m\}$

$$I_{QBF}(\lambda_n, T_m) \leftarrow I_{QBF}(\lambda_n, T_m) + \lambda_n^{-4} T_m^{-3/2} (2K+1) E_f^{-1/2}(\lambda_n) S_{if}(r,K) \exp(-E_{r,K}/kT_m).$$

ENDFOR
ENDFOR
ENDFOR

Step 7 Calculate the quasibound-free contribution:

FOR each wavelength in $\{\lambda_n\}$

FOR each temperature in $\{T_m\}$

$I_{QBF}(\lambda_n,T_m) \leftarrow 1.76526\times10^{14}\omega\mu^{-1}I_{QBF}(\lambda_n,T_m)$.

ENDFOR

ENDFOR

Step 8 Write the results of the calculation to the output file.

Comparison of this procedure with the computational procedure of program PROF_BF, given in §E1.3 of Appendix E1, shows that the structure of PROF_QBF is identical to that of PROF_BF. The only difference between the programs is that in PROF_BF the main program loop (Step 6) is driven by the set of bound states supported by the excited state interatomic potential whereas in PROF_QBF this loop is driven by the set of quasibound states supported by the same interatomic potential. Many of the numerical techniques used by PROF_BF are therefore used by PROF_QBF and to avoid unnecessary repetition, reference will be made to Appendix E1 where appropriate.

The remaining sections of the appendix describe the detailed implementation of the computational procedure of PROF_QBF outlined above.

E2.4 Step 1 : Read Input Data

On starting program PROF_QBF three items are requested from the user:

(i) the alkali-rare gas system for which the quasibound-free contribution is to be calculated (LiHe, LiNe, NaHe or NaNe);

(ii) a single character denoting the type of interatomic potentials to be used (M for model potentials, P for pseudopotentials);

(iii) a single character denoting the electronic transition to be used (A for $A^2\Pi - X^2\Sigma$, B for $B^2\Sigma - X^2\Sigma$).

The first two items are used to construct, in accordance with the convention given in Eq.E1.2.1 of Appendix E1, the name of the file holding the input dataset; the file is then opened for reading. Next, all three items are used to construct, in accordance with the convention given in Eq.E2.2.1, the name of the output file which will hold the results of the calculation performed by PROF_QBF; this file is then created and opened for writing.

PROF_QBF then reads the main input data from the open dataset. The content of the dataset and the program variables used to hold these data are the same as for PROF_BF and are listed in §E1.4 of Appendix E1.

Following this, the statistical weight ω is set to the value appropriate for the requested electronic transition, i.e.,

$$\omega = \frac{2}{3} \text{ for } A^2\Pi - X^2\Sigma \qquad \text{(E2.4.1)}$$
$$= \frac{1}{3} \text{ for } B^2\Sigma - X^2\Sigma.$$

E2.5 Step 2 : Initialise Tote

PROF_QBF uses a single tote in which to accumulate the contributions to the total quasibound-free emission intensity arising from each of the quasibound states of core motion supported by the excited state interatomic potential. This tote is a matrix with generic element $I_{QBF}(\lambda_n, T_m)$ which, on completion of PROF_QBF execution, will hold the quasibound-free emission intensity at wavelength λ_n and temperature T_m. The tote is implemented as a FORTRAN array FIQBF(n,m) with index n running from 1 to NLAMDA and index m running from 1 to NTEMP. In this step, the matrix is initialised by setting each element to zero.

E2.6 Step 3 : Define the Solution Grid

The next step in the PROF_QBF procedure is to create the solution grid upon which the radial eigenfunctions $g_i^{rK}(R)$ and $g_f^{K}(R)$ are to be generated. PROF_QBF uses the same solution grid {R(I)} as used by PROF_BF, that is, (N+1) radial points defined by

$$\begin{aligned} &R(0) = RI(1), \\ &R(I) = R(0) + (s \times I)\,; \quad I = 1, N-1, \\ &R(N) = RI(NIV) \end{aligned} \qquad \text{(E2.6.1)}$$

where the separation of grid points, s, has the value 0.02 au and RI(1), RI(NIV) are, respectively, the first and last points of the radial grid {RI(I)} upon which the interatomic potentials and dipole transition moments are defined in the input data.

E2.7 Step 4 : Interpolate Interatomic Potential Data

The interatomic potentials and dipole transition moments, defined as input data on the grid {RI(I)}, are obtained on the solution grid {R(I)} using 4-point Lagrange interpolation as described in §E1.7 of Appendix E1.

The output of the interpolation procedure is an excited state interatomic potential held in array VEX (equal to the $A^2\Pi$ potential if the requested electronic transition is $A^2\Pi - X^2\Sigma$, and equal to the $B^2\Sigma$ potential if the $B^2\Sigma - X^2\Sigma$ transition is requested), a ground state interatomic potential held in array VGR (equal to the $X^2\Sigma$ potential) and a dipole transition moment, corresponding to the requested electronic transition, held in array DTM.

E2.8 Step 5 : Location of Quasibound States

The next step in the computational procedure of PROF_QBF is to determine the set of quasibound states of alkali-rare gas core motion that are supported by the excited state interatomic potential. In the following sections, a method for locating the energies and widths of these resonances is described.

E2.8.1 Indicators of Quasibound States

The relative radial motion of the alkali-rare gas cores under the influence of the excited state interatomic potential is described by a solution of the Schrödinger equation (in atomic units)

$$\frac{d^2 g_i(R)}{dR^2} + 2\mu \left[E - V_i(R) - \frac{K(K+1)}{2\mu R^2} \right] g_i(R) = 0 \qquad \text{(E2.8.1)}$$

where $V_i(R)$ is the excited state interatomic potential and E is the (positive) energy of motion. At small R, the boundary condition on $g_i(R)$ is

$$g_i(R) \rightarrow 0 \; ; \quad R \rightarrow 0, \qquad \text{(E2.8.2)}$$

and at large R, since the energy of the state is positive, the solution is asymptotically a sine wave:

$$g_i(R) \rightarrow A_K \sin(kR - \tfrac{1}{2}K\pi + \eta_K)\,; \quad R \rightarrow \infty \qquad \text{(E2.8.3)}$$

where A_K = an arbitrary constant,
η_K = the elastic scattering phase shift,
$k = (2\mu E)^{1/2}$.

For non-zero angular momentum the effective potential energy seen by the alkali-rare gas cores is the sum of $V_i(R)$ and a centrifugal contribution, denoted $V_i^{eff}(R)$, given by

$$V_i^{eff}(R) = V_i(R) + \frac{K(K+1)}{2\mu R^2}. \qquad \text{(E2.8.4)}$$

For those interatomic potentials $V_i(R)$ possessing an attractive potential well, the effective potential exhibits a repulsive barrier at relatively large R and it is this barrier which is responsible for the existence of quasibound (resonance) states of relative core motion. Three features of eigenfunction behaviour (in the energy regime where three classical turning points exist) are found useful for locating the energies of quasibound states. These features are:

(i) *Eigenfunction magnitude* - at most positive energies below the barrier peak, the eigenfunction magnitude over the potential well region (i.e., inside the centrifugal barrier) is small relative to the eigenfunction magnitude in the external region (i.e., outside the barrier). In small energy intervals, however, the eigenfunction inside the barrier is found to have a large magnitude relative to the external solution and takes on the character of a bound state eigenfunction. Unlike true bound state eigenfunctions, which decay to zero at large R, these quasibound state eigenfunctions eventually become oscillatory. The key feature of this behaviour is that the eigenfunction magnitude inside the barrier (the 'internal magnitude'), relative to the eigenfunction magnitude outside the barrier (the 'external magnitude'), is a maximum at the resonance energy $E_{r,K}$.

(ii) *Number of solution nodes in the internal region* - in the direction of increasing R, a quasibound state eigenfunction passes through a number of nodes in the region inside the barrier (the 'internal region'). After the last node, it passes through a maximum, decays to a small value in the region of the potential barrier, eventually increasing again and becoming oscillatory. At energies just above the resonance value, $E_{r,K}$, an additional node appears in the eigenfunction in the internal region, indicating a transition to the next highest quasibound state. The energy at which this additional node first appears in the eigenfunction provides an indicator of the resonance energy regime.

(iii) *Eigenfunction phase shift* - in the neighbourhood of a resonance, the behaviour of the scattering phase shift $\eta_K(E)$ is given by the Breit-Wigner one level formula,

$$\eta_K(E) = \eta'_K(E) - \tan^{-1}\left[\frac{\Gamma_{r,K}}{2(E - E_{r,K})}\right] \qquad \text{(E2.8.5)}$$

where $\eta'_K(E)$ is the background phase shift (for scattering in the absence of the resonance) and $\Gamma_{r,K}$ is the energy half-width of the resonance. As the energy E approaches the resonance value, $E_{r,K}$, from below, the $\tan^{-1}$ function goes from 0 to $-\pi/2$ and thence from $-\pi/2$ to $-\pi$. Thus $\eta_K(E)$ rapidly increases by π as the energy goes through the resonance value. The quantity $\Gamma_{r,K}$ is a measure of the energy range over which the rapid phase shift variation takes place, i.e., the (energy) width of the resonance.

Taken together, these three features of eigenfunction behaviour permit the resonance energies $E_{r,K}$ to be determined. The procedure for this is described below; the calculation of the resonance half-width $\Gamma_{r,K}$ is discussed after this, in §E2.9.1.

E2.8.2 Locating the Resonance Energies $\{E_{r,K}\}$

The approach adopted for locating the resonance energies, $\{E_{r,K}\}$ is to calculate the scattering phase shift $\eta_K(E)$, together with a count of the number of 'internal' eigenfunction nodes (i.e., nodes in the 'internal region'), denoted n(E), for a series of trial energies over the energy range in which resonances may be supported. The n(E) curve is then searched for changes (by unity) in the number of internal nodes, indicating the energy regions near resonance and providing upper bounds on the $\{E_{r,K}\}$. In these identified regions, the $\eta_K(E)$ curve is searched for changes (by π) providing lower bounds on the $\{E_{r,K}\}$. A search is then made between the upper and lower energy bounds on each of the $E_{r,K}$ for a maximum in the internal magnitude of the eigenfunction; the energy at which the maximum occurs is taken as the resonance energy $E_{r,K}$.

The details of this calculation are given in the following sections, beginning with a discussion of the calculation of $\eta_K(E)$ and n(E).

E2.8.2.1 Calculating $\eta_K(E)$ and n(E)

A method for calculating $\eta_K(E)$ has already been described in the context of normalising free state eigenfunctions (see §E1.9.2.1 of Appendix E1). Direct application of this

approach, however, poses a problem - the phase shifts are determined by this method only to within a multiple of π. To locate resonances, it is necessary to be able to detect rapid changes in $\eta_K(E)$ of order π and this requires that the phase shifts be determined on an absolute scale, i.e., the appropriate multiple of π must be found in addition to $\eta_K(E)$. This is achieved by calculating a solution of the Schrödinger equation (Eq.E2.8.1) and comparing the number of nodes in this solution with the number of nodes appearing in the solution that would be obtained if the scattering (non-centrifugal) part of the potential were absent.

The first step then is to calculate the principal value of the phase shift, i.e., the value to within a multiple of π : this is denoted $\eta_K^*(E)$. For given values of angular momentum K and energy E, the Schrödinger equation (Eq.E2.8.1) is integrated numerically on the solution grid {R(I)} in the outward direction (direction of increasing R) using the Numerov scheme described in §E1.8.3.1 of Appendix E1; the boundary condition of Eq.E2.8.2 is used to start the integration.

The integration is allowed to proceed until the radial variable reaches the position of the centrifugal barrier peak, denoted R_{max}^{eff}, at which point the integration is temporarily suspended. The number of eigenfunction nodes in the internal region ($0 < R \leq R_{max}^{eff}$), denoted n(E), is then determined and the integration is resumed.

At each subsequent eigenfunction node, the integration is again temporarily suspended and a value of the phase shift $\eta_K^*(E)$ is calculated at the node. The radial position of the node is determined via 4-point Lagrange interpolation as follows: the last four calculated solution values, denoted $g_i(I-3)...g_i(I)$, are used. The corresponding solution grid points are R(I-3)...R(I) with the position of the (i^{th})node, denoted r_i, satisfying

$$R(I-1) \leq r_i < R(I). \qquad \text{(E2.8.6)}$$

The (interpolated) position of the node is then given by

$$r_i = \sum_{m=I-3}^{I} l_m R(m) + O(s^4) \qquad \text{(E2.8.7)}$$

where

$$l_m = \prod_{\substack{j=I-3 \\ j\neq m}}^{I} \left\{ \frac{g_i(j)}{g_i(j) - g_i(m)} \right\} \qquad \text{(E2.8.8)}$$

and s is the separation of grid points in {R(I)}; the error term $O(s^4)$ is neglected. If the non-centrifugal part of the potential $V_i(R)$ were negligible for all $R \geq r_i$, the solution of the Schrödinger equation over this range would have the form (see Appendix E1, §E1.9.2.1)

$$g_i(R) = A_K kR\left[\cos(\eta_K) j_K(kR) - \sin(\eta_K) n_K(kR)\right] \qquad \text{(E2.8.9)}$$

and the value of the phase shift associated with the node at r_i is obtained from

$$\eta_K^{*\,i} = \tan^{-1}\left[\frac{j_K(kr_i)}{n_K(kr_i)}\right] \qquad \text{(E2.8.10)}$$

with the phase shift satisfying

$$-\frac{\pi}{2} < \eta_K^{*\,i} \leq \frac{\pi}{2}. \qquad \text{(E2.8.11)}$$

The Bessel functions required to evaluate Eq.E2.8.10 are obtained from their analytic forms, with recursion where necessary (see §E1.9.2.1 of Appendix E1).

Following this determination of the phase shift, the integration is resumed and the above phase shift calculation is repeated at each successive node of the solution being generated until convergence of the phase shift value is achieved, indicated by

$$\left|\eta_K^{*\,i} - \eta_K^{*\,i-1}\right| < \varepsilon, \qquad \text{(E2.8.12)}$$

where ε is a pre-defined tolerance (a value of $\varepsilon = 10^{-4}$ rad was chosen), or the end of the solution grid {R(I)} is reached. In the latter case, the last phase shift calculated is taken as the best estimate achievable. The integration is then terminated.

The output of this procedure is the principal value of the phase shift evaluated at the i^{th} node of the solution. If the first node at which a phase shift is calculated is assigned the label i = n(E)+1, the value of label i associated with the last phase shift is the number of nodes in the solution in the range $0 < R \leq r_i$.

Having obtained the principal value of the phase shift, the next step is to determine the appropriate multiple of π to be added to the principal value in order to obtain the absolute value of the phase shift. This is found by comparing the eigenfunction calculated above with the solution of the Schrödinger equation (Eq.E2.8.1) in the absence of the scattering potential (obtained by setting $V_i(R)$ to zero). In the latter case, the solution, denoted $\bar{g}_i(R)$, is given by Eq.E2.8.9 with $\eta_K = 0$, i.e.,

$$\bar{g}_i(R) = A_K k R j_K(kR). \qquad \text{(E2.8.13)}$$

This solution is generated on the solution grid {R(I)} over the same radial range that $g_i(R)$ was calculated, $0 \le R \le r_i$. For K = 0 and 1, $\bar{g}_i(R)$ is computed directly from the analytic form of the Bessel function; for higher K, the Bessel function is obtained by applying the appropriate recursion relations at each radial point.

When $\bar{g}_i(R)$ has been calculated, the number of solution nodes appearing in the radial range ($0 \le R \le r_i$) is counted and denoted $\bar{i}$. The absolute value of the phase shift, $\eta_K(E)$, is then obtained via

$$\eta_K(E) = \eta_K^{*i} + (i - \bar{i} - 1)\pi; \quad \eta_K^{*i} > 0 \qquad \text{(E2.8.14)}$$

$$= \eta_K^{*i} + (i - \bar{i})\pi; \quad \eta_K^{*i} \le 0.$$

The calculation described above produces the quantities $\eta_K(E)$ and n(E) for a single energy. Generating the required $\eta_K(E)$ and n(E) curves is simply a matter of repeating the calculation for a series of energy values E_i. The procedure for this (for a given value of K) is summarised in the following 8 steps.

Step 1 Calculate the effective potential energy on the solution grid {R(I)}:

$$\text{VEFF(I)} = \text{VEX(I)} + \frac{K(K+1)}{2\mu R(I)^2}; \quad I = 0, N$$

where VEX is the array holding the excited state interatomic potential.

Step 2 Locate the minimum value of the effective potential energy and the centrifugal barrier position and height:

IF VEFF is monotonically decreasing with R **THEN**

No resonances exist for this, or any greater, K.

EXIT

ELSE

Denote the effective potential minimum by VEFF_MIN.

Denote the centrifugal barrier height by VEFF_MAX.

Denote the radial position of the centrifugal barrier peak by REFF_MAX.

ENDIF

Step 3 Calculate the U_I quantities required for Numerov integration:

$$U_I \equiv U(R(I)) = 2\mu VEFF(I) ; \quad I = 0, N.$$

Step 4 Initialise the energy variable:

$$E_i = E_{min} + \Delta E ; \quad i = 1$$

where

$$E_{min} = MAX(VEFF\_MIN, 0),$$

$$\Delta E = \frac{VEFF\_MAX - E_{min}}{m} \quad \text{for some integer m.}$$

Step 5 Calculate E':

$$E' = 2\mu E_i.$$

Step 6 Integrate the Schrödinger equation (Eq.E2.8.1) in the outward direction from R(0) using the Numerov scheme, calculating $n(E_i)$ and principal phase shift values at solution nodes until $\eta_K^*(E_i)$ has converged or R(N) is reached.

Step 7 Calculate the absolute phase shift value $\eta_K(E_i)$.

Step 8 Increment the energy variable:

$i \leftarrow i + 1$,

$E_i = E_{i-1} + \Delta E$,

and loop until the centrifugal barrier peak is reached:

IF $E_i >$ VEFF_MAX **THEN**

Number of energies in $\eta_K(E)$ curve is $n_e = i - 1$.

EXIT

ELSE

Return to Step 5.

ENDIF

The outputs of this procedure are $\eta_K(E)$ and n(E) curves evaluated at the energies $E_1 ... E_{n_e}$. The separation of the energies E_i is defined in terms of an integer m in Step 4 above; a value of m = 50 is chosen initially, but this may be increased during the analysis of these curves if necessary, as explained below.

The energy regimes of resonance are now located via a two step process, firstly by an analysis of the n(E) curve and secondly by an analysis of the $\eta_K(E)$ curve. A final iterative scheme is then used to converge on the resonance energies.

In the first step, the n(E) curve is searched, in the direction of increasing energy, for all successive pairs of energies (E_i, E_{i+1}) between which n(E) changes value. If no such pair exist (a situation detectable in advance of the search by the condition $n(E_1) = n(E_{n_e})$), then no resonances exist for this value of K in the range $[E_1, E_{n_e}]$. Alternatively, a change in n(E) by unity between E_i and E_{i+1} indicates the presence of a resonance, the energy E_{i+1} representing an upper bound on the resonance energy. If the change in n(E) between any pair of energies is found to be greater than unity, this indicates that the energy grid $\{E_i\}$ is too coarse: more than one resonance exists between E_i and E_{i+1}. In this case, the current analysis is abandoned and the calculation of n(E) and $\eta_K(E)$ is repeated with a smaller energy increment (the value of integer m set in Step 4 above is doubled). This process is repeated until the change in n(E) between any two energies E_i and E_{i+1} is, at most, unity.

Each pair of energies (E_i, E_{i+1}) for which $n(E_{i+1}) = n(E_i)+1$ is then analysed in the second step of this procedure as follows: an upper bound on the resonance energy $E_{r,K}$ is given by E_{i+1}. To obtain a lower bound on $E_{r,K}$, the $\eta_K(E)$ curve is searched, from energy E_{i+1} and in the direction of decreasing energy, for an energy $E_{i'}$ such that

$$\eta_K(E_{i+1}) - \eta_K(E_{i'}) > \pi. \qquad \text{(E2.8.15)}$$

The energy $E_{i'}$ then represents a lower bound on $E_{r,K}$. The upper and lower bounds on $E_{r,K}$ are then denoted E_U and E_L respectively. Thus $E_{r,K}$ satisfies the condition

$$E_L < E_{r,K} < E_U. \qquad \text{(E2.8.16)}$$

The final stage of the analysis is to invoke the 'internal magnitude' of the eigenfunction. This is defined by

$$IM(E) = \int_{R(0)}^{REFF\_MAX} [g_i(R)]^2 \, dR \qquad \text{(E2.8.17)}$$

where R(0) denotes the first point of the solution grid {R(I)} and REFF_MAX is the radial position of the centrifugal potential barrier peak; the eigenfunction $g_i(R)$ is normalised at large R to a unit modulus sine wave. IM(E) is a maximum at the resonance energy $E_{r,K}$. The approach is therefore to calculate IM(E) for a series of energies between the upper and lower bound energies (E_U and E_L) identified above and to search this curve for its maximum value. To do this, the energy range $[E_L, E_U]$ is divided into a number of intervals of size ΔE given by

$$\Delta E = \frac{E_U - E_L}{m'} \qquad \text{(E2.8.18)}$$

where m' is an integer and an energy grid $\{E_j\}$ is then given by

$$\begin{aligned} E_1 &= E_L, \\ E_j &= E_{j-1} + \Delta E, \\ E_{m'+1} &= E_U. \end{aligned} \qquad \text{(E2.8.19)}$$

At the energy E_j, the Schrödinger equation (Eq.E2.8.1) is integrated numerically on the solution grid {R(I)} in the outward direction using the Numerov scheme described in §E1.8.3.1 of Appendix E1; the boundary condition (Eq.E2.8.2) is used to start the integration. Principal values of the eigenfunction phase shift are calculated at successive solution nodes (external to the centrifugal potential barrier) until convergence of the phase shift value is attained, as described previously. When this is achieved, the eigenfunction has the form

$$g_i(R) = A_K kR[\cos(\eta_K) j_K(kR) - \sin(\eta_K) n_K(kR)] \qquad \text{(E2.8.20)}$$

where $k = (2\mu E_j)^{1/2}$, and any (non-zero) solution point $g_i(I)$ ($\equiv g_i(R(I))$) in this radial regime may then be used to determine the constant A_K via

$$A_K = \frac{g_i(I)}{kR(I)\left[\cos(\eta_K)j_K(kR(I)) - \sin(\eta_K)n_K(kR(I))\right]} \qquad \text{(E2.8.21)}$$

where the Bessel functions for the current value of K are obtained either from their analytic forms, or by recursion, as appropriate (see Appendix E1, §E1.9.2.1).

The eigenfunction, normalised to a unit modulus sine wave at large R, is then obtained on the solution grid over the range $R(0) \leq R \leq R(N')$ by the scaling

$$g_i(I) \leftarrow \frac{g_i(I)}{|A_K|}; \quad I = 0, N' \qquad \text{(E2.8.22)}$$

where R(N') = REFF_MAX.

The internal magnitude of the eigenfunction $IM(E_j)$ is then calculated. The integral in Eq.E2.8.17 is evaluated piece-wise using the 11-point Newton-Cotes integration formula described in §E1.9.1 of Appendix E1.

Repeating this procedure for each E_j defined by Eq.E2.8.19 results in an IM(E) curve evaluated between the upper and lower bounds of $E_{r,K}$. This curve is searched for the energy at which IM(E) reaches its maximum value; this energy is denoted E_m. The two grid points surrounding E_m, i.e., E_{m-1} and E_{m+1}, are then taken as new lower and upper energy bounds respectively by making the replacements

$$\begin{aligned} E_L &\leftarrow E_{m-1}, \\ E_U &\leftarrow E_{m+1}, \end{aligned} \qquad \text{(E2.8.23)}$$

and the calculation of IM(E) is repeated between these new bounds, yielding further values of E_L and E_U. Additional IM(E) curves are generated, and the above analysis repeated, until the relative difference between the bounding energies E_L and E_U is less than some pre-set tolerance δ (a value of $\delta = 10^{-6}$ was chosen), i.e., until the condition

$$2\left[\frac{E_U - E_L}{E_U + E_L}\right] \leq \delta \qquad \text{(E2.8.24)}$$

is satisfied. The resonance energy $E_{r,K}$ is then taken to be the mean of E_L and E_U.

In this way, all the resonances supported by the excited state interatomic potential, for a given value of angular momentum K, are located. Repeating this analysis for K = 1, 2, 3...

until the effective potential energy becomes monotonically decreasing with R yields the set of quasibound state energies $\{E_{r,K}\}$.

E2.9 Step 6 : The Main Program Loop

The previous section described procedures for locating the energies $E_{r,K}$ of quasibound states of alkali-rare gas core motion that are supported by the excited state interatomic potential. This constitutes Step 5 of the computational procedure of PROF_QBF outlined in §E2.3. The next step in this procedure, Step 6, constitutes the main loop of the program in which the quasibound-free emission intensity $I_{QBF}(\lambda_n,T_m)$ is calculated to within a multiplicative constant. The loop is driven by the set of quasibound state energies $\{E_{r,K}\}$, the actions performed by the loop being applied to each resonance energy in turn. These actions are now described.

E2.9.1 Calculating the Resonance Half-Width, $\Gamma_{r,K}$

Associated with each resonance, of energy $E_{r,K}$, is a half-width $\Gamma_{r,K}$ giving a measure of the energy extent of the resonance. This quantity is calculated from the approximate relationship (Sando and Dalgarno (1971))

$$\left[\frac{E_{r,K}}{2\mu}\right]^{1/2} \cong \Gamma_{r,K} \int_0^{R_b} \left[g_i(R)\right]^2 dR \qquad \text{(E2.9.1)}$$

where atomic units are used throughout and the eigenfunction $g_i(R)$ is assumed to be normalised at large R to a unit modulus sine wave. The quantity R_b is the radial dimension of the effective potential well.

The first step in obtaining a value for the resonance width is to calculate the eigenfunction $g_i(R)$. With energy $E_{r,K}$ and the corresponding value of angular momentum K, the Schrödinger equation (Eq.E2.8.1) is integrated numerically on the solution grid $\{R(I)\}$, with the boundary condition of Eq.E2.8.2, in the outward direction using the Numerov scheme. The constant A_K required for normalising the eigenfunction to a unit modulus sine wave at large R is obtained in the same way as that used in the context of calculating the internal magnitude of eigenfunctions described in §E2.8.2.1.

Before normalising the eigenfunction, it is appropriate to determine the quantity R_b since, in order to calculate $\Gamma_{r,K}$ via Eq.E2.9.1, the normalised eigenfunction is required only over the range $0 \le R \le R_b$. The value adopted for R_b is the point at which the eigenfunction starts to increase again after its exponential decay to a small value in the region of the potential barrier. To locate this point, the second classical turning point (in

the direction of increasing R) of the effective interatomic potential is found. This turning point is bounded on the solution grid {R(I)} by two successive points, R(J) and R(J+1), such that

$$VEFF(J) \le E_{r,K} \le VEFF(J+1) \qquad \text{(E2.9.2)}$$

where VEFF is the array holding the effective (excited state) interatomic potential. In the region of the turning point, the eigenfunction is decaying exponentially in the direction of increasing R. The magnitude of successive solution values (in the direction of increasing R) are considered, starting with $g_i(J)$, until a pair of values satisfying the condition

$$\left|g_i(N')\right| < \left|g_i(N'+1)\right| \qquad \text{(E2.9.3)}$$

is found indicating that the solution is starting to increase again. The radial grid point corresponding to $g_i(N')$, i.e., R(N') is then taken as the value of R_b.

The eigenfunction, normalised to a unit modulus sine wave at large R, is then obtained on the solution grid over the range $R(0) \le R \le R(N')$, by the scaling

$$g_i(I) \leftarrow \frac{g_i(I)}{\left|A_K\right|}; \quad I = 0, N' \qquad \text{(E2.9.4)}$$

using the value of the constant A_K determined earlier.

The quantity

$$c = \int_{R(0)}^{R(N')} \left[g_i(I)\right]^2 dR, \qquad \text{(E2.9.5)}$$

approximating the integral appearing in Eq.E2.9.1, is then evaluated piece-wise using the 11-point Newton-Cotes integration formula described in §E1.9.1 of Appendix E1. The resonance half-width is then calculated via

$$\Gamma_{r,K} \equiv \frac{1}{c}\left[\frac{E_{r,K}}{2\mu}\right]^{1/2}. \qquad \text{(E2.9.6)}$$

E2.9.2 The Re-normalised Quasibound State Eigenfunction

Because of its resonant behaviour, the magnitude of the eigenfunction corresponding to the resonance energy $E_{r,K}$ is large in the 'internal region' ($R < R_b$) in comparison to the external solution in the region $R > R_b$. The eigenfunction is thus assumed to be essentially a bound state function and to be zero for $R > R_b$; then the required normalisation of the eigenfunction is such that

$$\int_0^{R_b} \left[g_i(R) \right]^2 dR = 1. \qquad \text{(E2.9.7)}$$

The integral in this equation has already been evaluated during the calculation of the resonance half-width (see Eq.E2.9.5) and so the re-normalised quasibound state eigenfunction is obtained immediately via the scaling

$$g_i(I) \leftarrow \frac{g_i(I)}{c^{1/2}}; \quad I = 0, N' \qquad \text{(E2.9.8)}$$

with

$$g_i(I) = 0; \quad I = N'+1, N. \qquad \text{(E2.9.9)}$$

E2.9.3 The Quasibound-Free Matrix Elements

Having obtained the normalised eigenfunction $g_i^{r,K}(R)$ corresponding to the quasibound state energy $E_{r,K}$, the next step in the computational procedure of PROF_QBF is to calculate the matrix elements $S_{if}(r,K)$ connecting this resonance to the continuum of the ground state. $S_{if}(r,K)$ is given by

$$S_{if}(r,K) = \pi \Gamma_{r,K} \left| \int_0^{\infty} g_i^{r,K}(R)\, D_{\Lambda' \Lambda}(R)\, g_f^{K}(R)\, dR \right|^2 \qquad \text{(E2.9.10)}$$

where $D_{\Lambda' \Lambda}(R)$ is the dipole transition moment for the transition between the excited and ground states, and $g_f^K(R)$ is the normalised eigenfunction describing the relative radial motion of the alkali-rare gas cores under the influence of the ground state interatomic potential. This eigenfunction is a solution of the radial Schrödinger equation

$$\frac{d^2 g_f^K(R)}{dR^2} + \frac{2\mu}{\hbar^2}\left[E_f - V_f(R) - \frac{\hbar^2 K(K+1)}{2\mu R^2} \right] g_f^K(R) = 0 \qquad \text{(E2.9.11)}$$

where $V_f(R)$ is the ground state interatomic potential and E_f is the energy of the continuum state.

As described in §E1.9.2 of Appendix E1 for the bound-free emission case, the single resonance energy $E_{r,K}$ leads to a set of ground state energy eigenvalues $E_f(\lambda_n)$; these energies are determined by the set of NLAMDA wavelengths FLAMDA(n) specified in the input data to PROF_QBF at which the quasibound-free emission intensity is to be calculated and are given by (cf. Eq.E1.9.17 of Appendix E1)

$$E_f(\lambda_n) = E_{r,K} + h\nu_0 - \frac{455.63421}{\text{FLAMDA(n)}}; \quad n = 1, \text{NLAMDA}. \qquad \text{(E2.9.12)}$$

For quasibound-free transitions $E_f(\lambda_n)$ must be positive. If Eq.E2.9.12 produces a negative value of $E_f(\lambda_n)$ for some wavelength FLAMDA(n), this simply indicates that transitions out of the resonant state of energy $E_{r,K}$ cannot give rise to emitted radiation at this wavelength.

Corresponding to each of the energies $E_f(\lambda_n)$ is a normalised free state eigenfunction $g_f^K(R)$; this solution is obtained numerically via the same methods used in the bound-free case, described in §E1.9.2.1 of Appendix E1, and is denoted $\{g_f(I)\}$.

With the normalised excited (quasibound) state eigenfunction $g_i^{r,K}(R)$, corresponding to the energy $E_{r,K}$, and a normalised free state eigenfunction $g_f^K(R)$, corresponding to the energy $E_f(\lambda_n)$, the integral in Eq.E2.9.10,

$$I = \int_0^\infty g_i^{r,K}(R)\, D_{\Lambda',\Lambda}(R)\, g_f^K(R)\, dR, \qquad \text{(E2.9.13)}$$

may be evaluated. This is done piece-wise over the solution grid $\{R(I)\}$, from R(0) to R(N'+1), where R(N') corresponds to the last non-zero solution value (see Eqs.E2.9.8 and E2.9.9), using the 11-point Newton-Cotes integration formula described in §E1.9.1 of Appendix E1, where now

$$f(R) = g_i^{r,K}(R)\, D_{\Lambda',\Lambda}(R)\, g_f^{K}(R), \qquad \text{(E2.9.14)}$$

$$f_I \equiv f(R(I)) = g_i(I)\,.\,DTM(I)\,.\,g_f(I)\,; \quad I = 0, N'+1, \qquad \text{(E2.9.15)}$$

and DTM is the array holding the dipole transition moment. The calculation proceeds as described in §E1.9.1 of Appendix E1, producing the set of domain integrals

$$I_j = \int_{R(10(j-1))}^{R(10j)} f(R)\, dR\,; \quad j = 1, M' \qquad \text{(E2.9.16)}$$

and the integral in Eq.E2.9.13 is then given by

$$I = \sum_{j=1}^{M'} I_j\,. \qquad \text{(E2.9.17)}$$

The required matrix element then follows via

$$S_{if}(r,K) = \pi\Gamma_{r,K} I^2. \qquad \text{(E2.9.18)}$$

E2.9.4 Incrementing the Tote

The matrix element $S_{if}(r,K)$ calculated above connects the quasibound state with energy $E_{r,K}$ to the free state with eigenvalue $E_f(\lambda_n)$. A transition between these two states gives rise to emission of radiation at the single wavelength FLAMDA(n). The contribution (to within a constant factor) that this transition makes to the total quasibound-free emission intensity, $I_{QBF}(\lambda,T)$, at the wavelength FLAMDA(n) is now saved by incrementing the elements of the tote FIQBF corresponding to the wavelength FLAMDA(n) and each of the temperatures specified in the input data to PROF_QBF:

$$\begin{aligned} FIQBF(n,m) \leftarrow FIQBF(n,m) + \Big[& FLAMDA(n)^{-4}\,.\,TEMP(m)^{-3/2}\,.\,(2K+1)E_f(\lambda_n)^{-1/2} \\ & \times S_{if}(r,K)\exp(-E_{r,K}/k\,.\,TEMP(m))\Big]\,; \\ & m = 1, NTEMP \end{aligned} \qquad \text{(E2.9.19)}$$

Matrix elements connecting the quasibound state of energy $E_{r,K}$ with each of the free states of energy $E_f(\lambda_n)$ are calculated in turn and the tote FIQBF is incremented as above. When all the $E_f(\lambda_n)$ have been considered, the tote contains, to within a multiplicative

constant, the contribution to the total quasibound-free emission intensity, as a function of wavelength and temperature, arising from transitions out of the single quasibound state of energy $E_{r,K}$. This procedure is summarised below.

Step 1 Calculate the resonance half-width $\Gamma_{r,K}$ and the normalised eigenfunction $g_i^{r,K}(R)$ corresponding to the energy $E_{r,K}$.

Step 2 **FOR** n = 1, NLAMDA

Calculate the energy of the free state appropriate for emission at the wavelength FLAMDA(n):

$$E_f(\lambda_n) = E_{r,K} + h\nu_0 - \frac{455.63421}{\text{FLAMDA(n)}}.$$

IF $E_f(\lambda_n) \geq 0$ **THEN**

Calculate the normalised free state eigenfunction $g_f^K(R)$ corresponding to the eigenvalue $E_f(\lambda_n)$.

Calculate the matrix element $S_{if}(r,K)$ connecting the quasibound and free states.

Increment the tote elements FIQBF(n,m) ;

m = 1, NTEMP.

ENDIF

ENDFOR

Note that any $E_f(\lambda_n)$ that are negative are rejected as being physically unacceptable: the excited state with energy $E_{r,K}$ simply cannot contribute via quasibound-free transitions at these wavelengths.

Repeating this procedure for the complete set of quasibound state energies $\{E_{r,K}\}$ results in the tote FIQBF holding the quantity

$$I'_{QBF}(\lambda,T) = \lambda^{-4} T^{-3/2} \sum_{r\,K} (2K+1)\, E_f^{-1/2} S_{if}(r,K) \exp(-E_{r,K}/kT) \qquad \text{(E2.9.20)}$$

for each wavelength and temperature specified in the input data to PROF_QBF. This is the total quasibound-free emission intensity to within a multiplicative constant.

E2.10 Step 7: Calculating the Quasibound-Free Emission Intensity

The penultimate step in the computational procedure of PROF_QBF is to calculate the desired quasibound-free emission intensity, $I_{QBF}(\lambda,T)$, given by Eq.E2.1.1. This is given by scaling the quantity currently held in the tote FIQBF:

$$I_{QBF}(\lambda,T) = 1.76526 \times 10^{14}\, \omega\mu^{-1}\, I'_{QBF}(\lambda,T). \qquad \text{(E2.10.1)}$$

The elements of the tote are therefore adjusted as follows:

FOR n = 1, NLAMDA
  FOR m = 1, NTEMP
    FIQBF(n,m) ← $1.76526 \times 10^{14}\, \omega\mu^{-1}$ FIQBF(n,m).
  ENDFOR
ENDFOR

The tote FIQBF now contains the quantity $I_{QBF}(\lambda,T)$.

E2.11 Step 8: Output the Calculation Results

The final action of PROF_QBF is to write the results of the calculation described in §§E2.4 through E2.10 to the output file. The data written to this file consist of the following quantities:

(i) a copy of the input data for PROF_QBF (see §E2.4);

(ii) the value of the angular momentum quantum number K for which the effective excited state interatomic potential first becomes monotonically decreasing with increasing R;

(iii) the number of quasibound states (resonances) located;

(iv) the quasibound states located. For each state the following quantities are given:
- the rotational quantum number K;
- the resonance energy $E_{r,K}$;
- the resonance half-width $\Gamma_{r,K}$;
- the number of nodes appearing in the eigenfunction associated with the eigenvalue $E_{r,K}$;

(v) the calculated quasibound-free emission intensity $I_{QBF}(\lambda,T)$ at the wavelengths FLAMDA(n), n = 1, NLAMDA and the temperatures TEMP(m), m = 1, NTEMP.

This completes the functional description of program PROF_QBF.

Appendix E3 Functional Description of Program PROF_FF

E3.1 Introduction

PROF_FF is a computer program written in FORTRAN-77 and running on an HP9050 computer under the HP-UX (UNIX) operating system. It consists of 900 lines of source code occupying 26.6K of storage; the executable module occupies 133.8K.

The purpose of PROF_FF is to calculate the contribution to the alkali resonance line wing emission intensity arising from free-free transitions given by (see §7.2, Eq.7.2.7)

$$I_{FF}(\lambda,T) = 7.94646\times10^{13}\,\omega\lambda_A^{-4}\,T^{-3/2}\mu^{-1/2}$$

$$\times\int_0^{\infty}\sum_K (2K+1)\,E_f^{-1/2}E_i^{-1/2}(E_f - E_i)^{-2}S_{if}(K)\exp(-E_i/kT)\,dE_i\,. \qquad \text{(E3.1.1)}$$

The dependence of $I_{FF}(\lambda,T)$ on the alkali-rare gas interatomic potentials is through the eigenvalues E_i and E_f, and the eigenfunctions contained in the matrix element $S_{if}(K)$:

$$S_{if}(K) = \left|\int_0^{\infty} g_i^K(R)\,\Delta V(R)\,D_{\Lambda',\Lambda}(R)\,g_f^K(R)\,dR\right|^2. \qquad \text{(E3.1.2)}$$

The eigenfunctions $g_i^K(R)$ and $g_f^K(R)$ describe the relative radial motion of the alkali and rare gas cores under the influence of the excited and ground state interatomic potentials respectively. In the context of free-free transitions, both the initial state of core motion, described by eigenfunction $g_i^K(R)$, and the final state of core motion, described by eigenfunction $g_f^K(R)$, are continuum states of energy E_i and E_f respectively. The free-free contribution $I_{FF}(\lambda,T)$ is obtained by summing, via the integral in Eq.E3.1.1, functions of matrix elements connecting the continuum of the excited state with that of the ground state.

A single run of PROF_FF performs this summation for a combination of

(i) one alkali-rare gas system (one of LiHe, LiNe, NaHe or NaNe in the present study);

(ii) one type of interatomic potential (either model potential or pseudopotential);

(iii) one type of electronic transition (either $A^2\Pi - X^2\Sigma$ or $B^2\Sigma - X^2\Sigma$)

at a given set of wavelengths and temperatures. The current implementation of PROF_FF has restrictions on the last two quantities, namely, a maximum of 60 wavelengths and 5 temperatures. It is also important to note that, for any particular combination of alkali-rare gas system, interatomic potential type and electronic transition type, program PROF_QBF, described in Appendix E2, must be run *before* running PROF_FF. The reason for this will become evident later.

E3.2 Input/Output Data Files

The input data used by PROF_FF are identical to those used by program PROF_BF. The organisation of the data into a number of separate datasets is described in §E1.2.1 of Appendix E1; the content of each dataset is specified in Appendix E1, §E1.2.2. On any single run of the program, PROF_FF reads data from just one of these files.

In addition to these main input data files, PROF_FF also requires access to the output files generated by program PROF_QBF in order to read, as input data, the energies and half-widths of resonances located by that program; the use of these quantities in PROF_FF is described later, in §E3.9. The appropriate PROF_QBF output file to be used is identified by the naming convention given in Eq.E2.2.1 of Appendix E2; the content of this output file is specified in §E2.11 of Appendix E2.

A single run of PROF_FF creates one output disc file holding the results of the calculation for a particular combination of system, interatomic potential type and electronic transition. The output files are named using a convention similar to that used in the PROF_BF and PROF_QBF cases:

$$\text{Output File Name} = \text{system} \mid \text{potential type} \mid \text{transition} \mid \text{ff.out} \qquad \text{(E3.2.1)}$$

where

system = one of {LiHe, LiNe, NaHe, NaNe},
potential type = M for model potentials
= P for pseudopotentials,
transition = A for $A^2\Pi - X^2\Sigma$
= B for $B^2\Sigma - X^2\Sigma$.

The content of the output file is given in §E3.13 following a description of the calculation performed by PROF_FF.

E3.3 Computational Procedure of PROF_FF

The expression for the free-free emission intensity may be written in the form

$$I_{FF}(\lambda,T) = A(\lambda,T) \int_0^{\infty} F(E_i,\lambda) \exp(-E_i/kT)\, dE_i \qquad \text{(E3.3.1)}$$

where

$$A(\lambda,T) = 7.94646\times10^{13}\, \omega\lambda_A^{-4} T^{-3/2}\mu^{-1/2}, \qquad \text{(E3.3.2)}$$

$$F(E_i,\lambda) = \sum_K (2K+1)\, E_f^{-1/2}E_i^{-1/2}(E_f - E_i)^{-2}S_{if}(K). \qquad \text{(E3.3.3)}$$

The integral over the excited state energies is a consequence of the fact that the excited states form a continuum in the free-free case as opposed to a discrete set of states found in the bound-free and quasibound-free cases. A transformation of the variable of integration allows the integral to be evaluated by Gauss-Laguerre quadrature as follows: let

$$\varepsilon_i = \frac{E_i}{kT} \qquad \text{(E3.3.4)}$$

so that

$$d\varepsilon_i = \frac{dE_i}{kT}; \qquad \text{(E3.3.5)}$$

then

$$I_{FF}(\lambda,T) = A(\lambda,T) \int_0^{\infty} kT\, F(kT\varepsilon_i,\lambda) \exp(-\varepsilon_i)\, d\varepsilon_i \qquad \text{(E3.3.6)}$$

$$\equiv A(\lambda,T) \sum_{q=1}^{p} w(q;p)\, kT\, F(kT\varepsilon_i(q;p),\lambda) + R_p$$

where the weights, $w(q;p)$, and abscissae, $\varepsilon_i(q;p)$, are obtained from tabulations as a function of p (Abramowitz and Stegun (1972), Table 25.9); the remainder term, R_p, is

neglected. The set of excited state energies to be used are then given in terms of the abscissae via

$$E_i(q;p) = kT\varepsilon_i(q;p)\,; \quad q = 1, p. \tag{E3.3.7}$$

The computational procedure for evaluating Eq.E3.3.6 consists of 10 major steps as follows:

Step 1 Read appropriate input data.
Define a set of wavelengths $\{\lambda_n\}$ and temperatures $\{T_m\}$ at which to calculate the free-free emission intensity.

Step 2 Initialise the main tote:
FOR each wavelength in $\{\lambda_n\}$
  FOR each temperature in $\{T_m\}$
    $I_{FF}(\lambda_n, T_m) \leftarrow 0.0$
  ENDFOR
ENDFOR

Step 3 Define a suitable solution grid upon which to construct the eigenfunctions $g_i^K(R)$ and $g_f^K(R)$.

Step 4 Interpolate the interatomic potentials and dipole transition moments read in Step 1 for values on the solution grid defined in Step 3.
Calculate the difference potential $\Delta V(R)$ on the solution grid.

Step 5 Set the temperature to be used:
Temperature = T_m; $m = 1$.

Step 6 Determine the number of Gauss-Laguerre quadrature points, p, for the current temperature T_m.
Calculate the corresponding excited state energies:
$E_i(q;p) = kT_m\varepsilon_i(q;p)\,; \quad q = 1, p.$

Step 7 **FOR** each quadrature point $E_i(q;p)$

Calculate the set of ground state energies, $\{E_f(\lambda_n)\}$, appropriate for emission of radiation at the wavelengths $\{\lambda_n\}$.

Calculate the set of quantities $\{F(E_i(q;p),\lambda_n)\}$, corresponding to the wavelengths $\{\lambda_n\}$.

Increment the main tote:

FOR each wavelength in $\{\lambda_n\}$

$I_{FF}(\lambda_n,T_m) \leftarrow I_{FF}(\lambda_n,T_m) + w(q;p)kT_mF(E_i(q;p),\lambda_n)$.

ENDFOR

ENDFOR

Step 8 **IF** not all temperatures considered **THEN**

$m \leftarrow m + 1$.

Temperature = T_m.

Return to Step 6.

ENDIF

Step 9 Calculate the free-free contribution:

FOR each wavelength in $\{\lambda_n\}$

FOR each temperature in $\{T_m\}$

$I_{FF}(\lambda_n,T_m) \leftarrow 7.94646\times10^{13}\,\omega\lambda_n^{-4}T_m^{-3/2}\mu^{-1/2}I_{FF}(\lambda_n,T_m)$.

ENDFOR

ENDFOR

Step 10 Write the results of the calculation to the output file.

The details of how each of these steps is implemented in PROF_FF are described in the remaining sections of this appendix.

E3.4 Step 1 : Read Input Data

On starting program PROF_FF three items are requested from the user:

(i) the alkali-rare gas system for which the free-free contribution is to be calculated (LiHe, LiNe, NaHe or NaNe);

(ii) a single character denoting the type of interatomic potentials to be used (M for model potentials, P for pseudopotentials);

(iii) a single character denoting the electronic transition to be used (A for $A^2\Pi - X^2\Sigma$, B for $B^2\Sigma - X^2\Sigma$).

The first two items are used to construct, in accordance with the convention given in Eq.E1.2.1 of Appendix E1, the name of the file holding the main input dataset; this file is opened for reading. Next, all three items are used to construct, in accordance with the convention given in Eq.E2.2.1 of Appendix E2, the name of the output file created by program PROF_QBF for the requested combination of alkali-rare gas system, potential type and transition type; this file is opened for reading. Finally, all three items are again used to construct, in accordance with the convention given in Eq.E3.2.1, the name of the output file which will hold the results of the calculation performed by PROF_FF; this file is then created and opened for writing.

PROF_FF then reads the main input data from the open dataset. The content of the dataset and the program variables used to hold these data are the same as for programs PROF_BF and PROF_QBF and are listed in §E1.4 of Appendix E1.

Next, PROF_FF reads the resonance data from the open PROF_QBF output file. The content of this file is specified in §E2.11 of Appendix E2; the particular data items read from the file, and the program variables used to hold these data, are listed in Table E3.1.

Following this, the statistical weight ω is set to the value appropriate for the requested electronic transition, i.e.,

$$\begin{aligned} \omega &= \frac{2}{3} \quad \text{for } A^2\Pi - X^2\Sigma \\ &= \frac{1}{3} \quad \text{for } B^2\Sigma - X^2\Sigma. \end{aligned} \tag{E3.4.1}$$

E3.5 Step 2 : Initialise Tote

PROF_FF uses a tote in which to accumulate the contributions to the total free-free emission intensity arising from each of the p Gauss-Laguerre quadrature points used to approximate the integral over excited state energies. This tote is a matrix with generic element $I_{FF}(\lambda_n, T_m)$ which, on completion of PROF_FF execution, will hold the free-free emission intensity at wavelength λ_n and temperature T_m. The tote is implemented as a FORTRAN array FIFF(n,m) with index n running from 1 to NLAMDA and index m running from 1 to NTEMP. In this step, the matrix is initialised by setting each element to zero.

Table E3.1 Additional Input Data for Program PROF_FF

FORTRAN Variable Name	Description of Data Held
NRES	Number of quasibound (resonance) states located by previous run of program PROF_QBF.
ERES(I)	Array of NRES values specifying the energies of the resonances.
GAMMA(I)	Array of NRES values specifying the energy half-widths of the resonances.

E3.6 Step 3 : Define the Solution Grid

The next step in the PROF_FF procedure is to create the solution grid upon which the radial eigenfunctions $g_q^K(R)$ and $g_f^K(R)$ are to be generated. PROF_FF uses the same solution grid {R(I)} as used by programs PROF_BF and PROF_QBF, i.e., (N+1) radial points defined by

$$\begin{aligned} &R(0) = RI(1), \\ &R(I) = R(0) + (s \times I)\,; \quad I = 1, N - 1, \\ &R(N) = RI(NIV) \end{aligned} \qquad \text{(E3.6.1)}$$

where the separation of grid points, s, has the value 0.02 au and RI(1), RI(NIV) are, respectively, the first and last points of the radial grid {RI(I)} upon which the interatomic potentials and dipole transition moments are defined in the input data.

E3.7 Step 4 : Interpolate Interatomic Potential Data

The interatomic potentials and dipole transition moments, defined as input data on the grid {RI(I)}, are obtained on the solution grid {R(I)} using 4-point Lagrange interpolation as described in §E1.7 of Appendix E1.

The output of the interpolation procedure is an excited state interatomic potential held in array VEX (equal to the $A^2\Pi$ potential if the requested electronic transition is $A^2\Pi - X^2\Sigma$, and equal to the $B^2\Sigma$ potential if the $B^2\Sigma - X^2\Sigma$ transition is requested), a ground state interatomic potential held in array VGR (equal to the $X^2\Sigma$ potential) and a dipole transition moment, corresponding to the requested electronic transition, held in array DTM.

Following the interpolation of the interatomic potential data, the difference potential, $\Delta V(R)$, is calculated on the solution grid and stored in the array VDIFF:

$$\text{VDIFF(I)} = \text{VEX(I)} - \text{VGR(I)} ; \quad \text{I} = 0, \text{N}. \qquad \text{(E3.7.1)}$$

E3.8 Step 5 : Initialise Temperature

In the calculation of the bound-free and quasibound-free emission intensities, the same set of excited state energies, namely the bound state and quasibound state energies, apply to each temperature considered, leading to matrix elements $S_{if}(V,K)$ and $S_{if}(r,K)$ which are independent of temperature. The temperature dependence of the emission intensity appears late in the calculation (after the matrix element generation) as a simple multiplicative factor (see Step 6 in each of the computational procedures of PROF_BF (Appendix E1, §E1.3) and PROF_QBF (Appendix E2, §E2.3)). This convenience does not hold for the free-free emission intensity calculation: the excited state energies $E_i(q;p)$ to be used are a function of the temperature chosen, by virtue of Eq.E3.3.7, and $I_{FF}(\lambda,T)$, given in Eq.E3.3.6, must be evaluated separately for each individual temperature specified in the PROF_FF input data.

The current step, Step 5, is the start of the temperature loop, with the temperature to be used initialised to the first input data value TEMP(1).

E3.9 Step 6 : Determining the Excited State Energies, $E_i(q;p)$

The range of excited state energies over which the free-free emission contribution is to be evaluated is all the positive energies (see Eq.E3.3.1). This energy range may contain a number of orbiting resonances leading to a quasibound-free emission component superimposed on the 'background' free-free emission. The quasibound-free contribution is taken into account by the procedures implemented via program PROF_QBF specified in Appendix E2. To avoid distortion of the free-free emission calculation by these

resonances, it is necessary to choose a set of excited state energies $E_i(q;p)$ which are well removed from any resonance energy.

For a given temperature T_m, the energies $E_i(q;p)$ are fixed by the Gauss-Laguerre abscissae $\varepsilon_i(q;p)$ via

$$E_i(q;p) = kT_m\varepsilon_i(q;p)\,; \quad q = 1, p. \qquad \text{(E3.9.1)}$$

The only control available over the values of the $E_i(q;p)$ is the choice of p, the quadrature order. The purpose of Step 6 is to select an appropriate value of p and thence the energies $E_i(q;p)$.

The procedure adopted is to initially select the largest value of p for which weights and abscissae are tabulated (this is p = 15 (see Abramowitz and Stegun (1972), Table 25.9)) and to calculate the excited state energies $E_i(q;p)$ on the basis of the abscissae $\varepsilon_i(q;p)$ via Eq.E3.9.1. Each of the $E_i(q;p)$ is then compared with the positions of the resonances supported by the current excited state interatomic potential which were located by the previous run of program PROF_QBF to determine if a coincidence with a resonance exists. For the present purpose, a coincidence is assumed to exist if the condition

$$E_{r,K} - 3\Gamma_{r,K} \le E_i(q;p) \le E_{r,K} + 3\Gamma_{r,K} \qquad \text{(E3.9.2)}$$

is satisfied for any resonance. Here, $E_{r,K}$ is the resonance energy and $\Gamma_{r,K}$ is the resonance half-width. If such a coincidence is detected for any $E_i(q;p)$, the value of p is rejected and replaced with a new value. The above procedure is repeated, with alternative values of p as necessary, until a set of $E_i(q;p)$ is found which does not coincide with any resonance; this set of excited state energies is then adopted as suitable for the evaluation of the free-free emission contribution at the current temperature T_m via Eq.E3.3.6; this check of the $E_i(q;p)$ against the energies of resonances is applied at each temperature separately.

The order in which values of p are considered is first to try p = 15 and, if this value is unsuccessful, to then follow with p = 12, 10, 9 and 8; in practice, however, it was never found necessary to use a value of p less than 12.

E3.10 Step 7 : Gauss-Laguerre Quadrature

Step 7 is a program loop that evaluates the integral over excited state energies appearing in Eq.E3.3.1 using the Gauss-Laguerre quadrature given by Eq.E3.3.6. This procedure thus calculates the free-free emission intensity $I_{FF}(\lambda,T)$ to within a multiplicative factor.

The loop is driven by the set of energies $E_i(q;p)$ determined in Step 6 above, the actions performed by the loop being applied to each $E_i(q;p)$ in turn. These actions are described below.

E3.10.1 Ground State Energies

As described in §E1.9.2 of Appendix E1 for the bound-free emission case, the single excited state energy $E_i(q;p)$ leads to a set of ground state energy eigenvalues, $E_f(\lambda_n)$, determined by the set of NLAMDA wavelengths FLAMDA(n), specified in the input data to PROF_FF, at which the free-free emission intensity is to be calculated. These energies are given by (cf. Eq.E1.9.17 of Appendix E1)

$$E_f(\lambda_n) = E_i(q;p) + h\nu_0 - \frac{455.63421}{\text{FLAMDA(n)}}; \quad n = 1, \text{NLAMDA}. \qquad \text{(E3.10.1)}$$

For free-free transitions, $E_f(\lambda_n)$ must be positive. The first action of Step 7 is to calculate the set $\{E_f(\lambda_n)\}$ for the given wavelengths.

E3.10.2 Calculating the $F(E_i(q;p),\lambda)$

The next stage is to calculate the quantities $F(E_i(q;p),\lambda)$ for each of the NLAMDA wavelengths. For a particular wavelength λ_n,

$$F(E_i(q;p),\lambda_n) = \sum_K (2K+1)\, E_i(q;p)^{-1/2} E_f(\lambda_n)^{-1/2} (E_f(\lambda_n) - E_i(q;p))^{-2} S_{if}(K) \qquad \text{(E3.10.2)}$$

where the matrix element is

$$S_{if}(K) = \left| \int_0^\infty g_i^K(R)\, \Delta V(R)\, D_{\Lambda',\Lambda}(R)\, g_f^K(R)\, dR \right|^2. \qquad \text{(E3.10.3)}$$

The eigenfunction $g_i^K(R)$ is a solution of the radial Schrödinger equation

$$\frac{d^2 g_i^K(R)}{dR^2} + \frac{2\mu}{\hbar^2}\left[E_i(q;p) - V_i(R) - \frac{\hbar^2 K(K+1)}{2\mu R^2} \right] g_i^K(R) = 0 \qquad \text{(E3.10.4)}$$

where $V_i(R)$ is the excited state interatomic potential. Similarly, the eigenfunction $g_f^K(R)$ is a solution of the radial Schrödinger equation

$$\frac{d^2 g_f^K(R)}{dR^2} + \frac{2\mu}{\hbar^2}\left[E_f(\lambda_n) - V_f R) - \frac{\hbar^2 K(K+1)}{2\mu R^2} \right] g_f^K(R) = 0 \qquad \text{(E3.10.5)}$$

where $V_f(R)$ is the ground state interatomic potential. The boundary condition on each eigenfunction is

$$g_i^K(R) \to 0\,; \quad R \to 0, \qquad \text{(E3.10.6)}$$

$$g_f^K(R) \to 0\,; \quad R \to 0. \qquad \text{(E3.10.7)}$$

The expression for $F(E_i(q;p),\lambda_n)$, given by Eq.E3.10.2, contains a summation over the angular momentum quantum number K. In the bound-free and quasibound-free cases, summations over K were limited by the finite number of bound and quasibound excited states. In the free-free case there is no such limit and the summation extends, in principle, to infinity. In practice, however, the summation is found to be convergent and may be truncated after a finite number of terms. The procedure for calculating, for a single wavelength λ_n, the contribution to the sum arising from a single value of K consists of the following 4 steps:

Step 1 Calculate the excited state eigenfunction: with energy $E_i(q;p)$, the given value of K and the boundary condition of Eq.E3.10.6, the Schrödinger equation (Eq.E3.10.4) is integrated numerically on the solution grid {R(I)} in the outward direction, from R(0) to R(N), using the Numerov integration scheme described in §E1.8.3.1 of Appendix E1. This produces a numerical representation of the eigenfunction $g_i^K(R)$, denoted $\{g_i(I)\}$. The eigenfunction describes a free state of alkali-rare gas core motion; it is therefore normalised to a unit modulus sine wave at large R using the procedure described in §E1.9.2.1 of Appendix E1.

Step 2 Calculate the ground state eigenfunction: with energy $E_f(\lambda_n)$, the given value of K and the boundary condition of Eq.E3.10.7, the Schrödinger equation (Eq.E3.10.5) is integrated numerically on the solution grid {R(I)} in the outward direction, from R(0) to R(N), using the Numerov scheme. This produces a numerical representation of the eigenfunction $g_f^K(R)$

denoted $\{g_f(I)\}$. This eigenfunction is normalised to a unit modulus sine wave at large R in the same way as is the excited state eigenfunction $\{g_i(I)\}$.

Step 3 Evaluate the matrix element $S_{if}(K)$: the integral appearing in Eq.E3.10.3, i.e.,

$$I = \int_0^{\infty} g_i^K(R)\, \Delta V(R)\, D_{\Lambda',\Lambda}(R)\, g_f^K(R)\, dR, \qquad \text{(E3.10.8)}$$

is evaluated piece-wise over the solution grid $\{R(I)\}$ from R(0) to R(N) using the 11-point Newton-Cotes integration formula described in §E1.9.1 of Appendix E1, where now

$$f(R) = g_i^K(R)\, \Delta V(R)\, D_{\Lambda',\Lambda}(R)\, g_f^K(R), \qquad \text{(E3.10.9)}$$

$$f_I \equiv f(R(I)) = g_i(I)\,.\,VDIFF(I)\,.\,DTM(I)\,.\,g_f(I)\;;\;\; I = 0, N \qquad \text{(E3.10.10)}$$

and VDIFF, DTM are the arrays holding the difference potential (see Eq.E3.7.1) and the dipole transition moment respectively. The calculation proceeds as described in §E1.9.1 of Appendix E1, producing the set of domain integrals

$$I_j = \int_{R(10(j-1))}^{R(10j)} f(R)\, dR\;; \quad j = 1, M' \qquad \text{(E3.10.11)}$$

and the integral in Eq.E3.10.8 is then given by

$$I = \sum_{j=1}^{M'} I_j\,. \qquad \text{(E3.10.12)}$$

The required matrix element follows via

$$S_{if}(K) = I^2. \qquad \text{(E3.10.13)}$$

Step 4 Calculate the contribution, denoted $F(E_i(q;p),\lambda_n,K)$, to the summation arising from the given value of K:

$$F(E_i(q;p),\lambda_n,K) = (2K+1)\, E_i(q;p)^{-1/2} E_f(\lambda_n)^{-1/2} (E_f(\lambda_n) - E_i(q;p))^{-2} S_{if}(K). \qquad \text{(E3.10.14)}$$

The procedure described by Steps 1-4 above apply to a single wavelength λ_n. Since the excited state eigenfunction is applicable to all wavelengths, the procedure for calculating the $F(E_i(q;p),\lambda_n,K)$ for all NLAMDA wavelengths (for a given value of K) consists of applying Step 1 and then repeating Steps 2-4 for n = 1, NLAMDA.

The procedure described above determines a single term in the summation over K for each wavelength λ_n. To calculate $F(E_i(q;p),\lambda_n)$, given by Eq.E3.10.2, the terms $F(E_i(q;p),\lambda_n,K)$ are evaluated, via Step 1 - Step 4 above, for successive values of K, starting with K = 0, until the sum of these terms has converged for each wavelength λ_n. Convergence of the sum for a particular λ_n is assumed to have been obtained when 10 consecutive terms are found satisfying the condition

$$F(E_i(q;p),\lambda_n,K') \le \delta \sum_{K=0}^{K'} F(E_i(q;p),\lambda_n,K) \qquad \text{(E3.10.15)}$$

where δ is a pre-set tolerance (a value of $\delta = 10^{-6}$ was chosen). The sum on the rhs of Eq.E3.10.15 is then taken to be the value of $F(E_i(q;p),\lambda_n)$.

The procedure for calculating the $F(E_i(q;p),\lambda)$ is summarised by the following 4 steps:

Step 1 Initialise the tote and the convergence flags:

FOR each wavelength in $\{\lambda_n\}$

$F(E_i(q;p),\lambda_n) \leftarrow 0.0$

CONVERGED(n) = **.FALSE.**

ENDFOR

Initialise K:

K = 0.

Step 2 Calculate the normalised eigenfunction $g_i^K(R)$ corresponding to the energy $E_i(q;p)$.

Step 3

FOR each wavelength in $\{\lambda_n\}$
IF $E_f(\lambda_n) \geq 0$ **THEN**
IF .NOT. CONVERGED(n) **THEN**
Calculate the normalised eigenfunction $g_f^K(R)$ corresponding to the energy $E_f(\lambda_n)$.
Calculate the matrix element $S_{if}(K)$.
Increment the tote:
$F(E_i(q;p),\lambda_n) \leftarrow F(E_i(q;p),\lambda_n) +$
$(2K+1)\, E_i(q;p)^{-1/2} E_f(\lambda_n)^{-1/2} (E_f(\lambda_n) - E_i(q;p))^{-2} S_{if}(K)$.
Check for convergence of $F(E_i(q;p),\lambda_n)$.
IF $F(E_i(q;p),\lambda_n)$ converged **THEN**
CONVERGED(n) = **.TRUE.**
ENDIF
ENDIF
ENDIF
ENDFOR

Step 4

Loop over K until the $F(E_i(q;p),\lambda_n)$ have converged for all λ_n:
IF any $F(E_i(q;p),\lambda_n)$ has not converged **THEN**
$K \leftarrow K + 1$.
Return to Step 2.
ELSE
EXIT
ENDIF

Note that the convergence criterion is applied to summations over K for each wavelength separately. Once convergence of the summation for a particular wavelength is attained, this wavelength is subsequently ignored in Step 3.

E3.10.3 Incrementing the Tote

The final action of the loop in Step 7 of the computational procedure of PROF_FF is to save the contribution to the Gauss-Laguerre quadrature arising from the current quadrature point $E_i(q;p)$ by incrementing the elements of the main tote FIFF corresponding to the current temperature and each of the wavelengths:

$$FIFF(n,m) \leftarrow FIFF(n,m) + w(q;p).k.TEMP(m).F(E_i(q;p),\lambda_n)\ ; \quad n = 1, NLAMDA. \tag{E3.10.16}$$

Repeating the calculation described in §§E3.10.1 through E3.10.3 for each of the p excited state energies $E_i(q;p)$ results in the tote FIFF holding the quantity

$$I'_{FF}(\lambda,T) = \sum_{q=1}^{p} w(q;p)\, kT\, F(E_i(q;p),\lambda)$$

$$\equiv \int_0^{\infty} F(E_i,\lambda)\, \exp(-E_i/kT)\, dE_i \qquad \text{(E3.10.17)}$$

for all temperatures in $\{T_m\}$ up to, and including, the current temperature TEMP(m), and for each wavelength in $\{\lambda_n\}$. This is the total free-free emission intensity to within a multiplicative factor.

E3.11 Step 8 : Re-initialise Temperature

This step is the end of the temperature loop begun in Step 5. It simply increments the index m identifying the current temperature in $\{T_m\}$ and sets the value of the current temperature to TEMP(m). Program control is then passed back to Step 6 for the calculation of $I'_{FF}(\lambda,T)$ at this new temperature. The temperature loop is executed repeatedly until all temperatures specified in the input data to PROF_FF have been considered, at which point program control passes to Step 9.

E3.12 Step 9 : Calculating the Free-Free Emission Intensity

The penultimate step in the computational procedure of PROF_FF is to calculate the desired free-free emission intensity, $I_{FF}(\lambda,T)$, given by Eq.E3.3.1. This is obtained by scaling the quantity currently held in the tote FIFF:

$$I_{FF}(\lambda,T) = 7.94646\times10^{13}\, \omega\lambda^{-4}\, T^{-3/2}\mu^{-1/2} I'_{FF}(\lambda,T). \qquad \text{(E3.12.1)}$$

The elements of the tote are therefore adjusted as follows:

FOR n = 1, NLAMDA
  FOR m = 1, NTEMP
    FIFF(n,m) ← $7.94646\times10^{13}\, \omega$ FLAMDA(n)$^{-4}$ TEMP(m)$^{-3/2}$ $\mu^{-1/2}$ × FIFF(n,m).
  ENDFOR
ENDFOR

The tote FIFF now contains the quantity $I_{FF}(\lambda,T)$.

E3.13 Step 10 : Output the Calculation Results

The final action of PROF_FF is to write the results of the calculation described in §§E3.4 through E3.12 to the output file. The data written to this file consist of the following quantities:

(i) a copy of the input data for PROF_FF (see §E3.4);

(ii) the quasibound states (resonances) located by PROF_QBF for the current alkali-rare gas system and excited state interatomic potential. For each state the following quantities are given:
- the rotational quantum number K;
- the resonance energy $E_{r,K}$;
- the resonance half-width $\Gamma_{r,K}$;

(iii) the order of the Gauss-Laguerre quadrature used. For each temperature the following quantities are given:
- the temperature TEMP(m);
- the number of quadrature points (p) used for TEMP(m);

(iv) the calculated free-free emission intensity $I_{FF}(\lambda,T)$ at the wavelengths FLAMDA(n), n = 1, NLAMDA and the temperatures TEMP(m), m = 1, NTEMP.

This completes the functional description of program PROF_FF.

Appendix E4 The Numerov Integration Scheme

E4.1 Introduction

The Numerov integration scheme is used by all three quantum mechanical line profile programs (PROF_BF, PROF_QBF and PROF_FF) to obtain numerical solutions of the radial Schrödinger equation

$$\frac{d^2g(R)}{dR^2} = 2\mu \left[E - V(R) - \frac{K(K+1)}{2\mu R^2} \right] g(R) = 0. \qquad \text{(E4.1.1)}$$

The purpose of this appendix is to provide a derivation of this integration scheme.

E4.2 Derivation of the Numerov Integration Scheme

A numerical solution of Eq.E4.1.1 is to be constructed on the solution grid defined by the radial points {R(I)}. Suppose that the solution is known at the points R(I-2) and R(I-1), and denote these solution values by g_{I-2} and g_{I-1} respectively, where

$$g_J \equiv g(R(J)). \qquad \text{(E4.2.1)}$$

The starting point for determining the solution value at the next radial point, g_I, is to construct Taylor series expansions for the solution value and for the solution second derivative, i.e.,

$$g_{I-2} = g_{I-1} - sg^{(1)}_{I-1} + \frac{s^2}{2!} g^{(2)}_{I-1} - \frac{s^3}{3!} g^{(3)}_{I-1} + \frac{s^4}{4!} g^{(4)}_{I-1} - \ldots, \qquad \text{(E4.2.2)}$$

$$g_I = g_{I-1} + sg^{(1)}_{I-1} + \frac{s^2}{2!} g^{(2)}_{I-1} + \frac{s^3}{3!} g^{(3)}_{I-1} + \frac{s^4}{4!} g^{(4)}_{I-1} + \ldots, \qquad \text{(E4.2.3)}$$

for the solution values, and

$$g^{(2)}_{I-2} = g^{(2)}_{I-1} - sg^{(3)}_{I-1} + \frac{s^2}{2!} g^{(4)}_{I-1} - \frac{s^3}{3!} g^{(5)}_{I-1} + \frac{s^4}{4!} g^{(6)}_{I-1} - \ldots, \qquad \text{(E4.2.4)}$$

$$g^{(2)}_I = g^{(2)}_{I-1} + sg^{(3)}_{I-1} + \frac{s^2}{2!} g^{(4)}_{I-1} + \frac{s^3}{3!} g^{(5)}_{I-1} + \frac{s^4}{4!} g^{(6)}_{I-1} + \ldots, \qquad \text{(E4.2.5)}$$

for the solution second derivatives. Here, s denotes the separation of the radial points on the grid {R(I)}. Adding Eqs.E4.2.2 and E4.2.3 gives

$$g_{I-2} + g_I = 2\left[\, g_{I-1} + \frac{s^2}{2!} g^{(2)}_{I-1} + \frac{s^4}{4!} g^{(4)}_{I-1} + \frac{s^6}{6!} g^{(6)}_{I-1} + \ldots \,\right], \qquad \text{(E4.2.6)}$$

and adding Eqs.E4.2.4 and E4.2.5 gives

$$g^{(2)}_{I-2} + g^{(2)}_I = 2\left[\, g^{(2)}_{I-1} + \frac{s^2}{2!} g^{(4)}_{I-1} + \frac{s^4}{4!} g^{(6)}_{I-1} + \frac{s^6}{6!} g^{(8)}_{I-1} + \ldots \,\right]. \qquad \text{(E4.2.7)}$$

Multiplying Eq.E4.2.7 by $\frac{s^2}{12}$ and subtracting the resulting expression from Eq.E4.2.6 gives

$$g_{I-2} + g_I - \frac{s^2}{12}(g^{(2)}_{I-2} + g^{(2)}_I) = 2g_{I-1} + \frac{5s^2}{6} g^{(2)}_{I-1} - \frac{s^6}{240} g^{(6)}_{I-1} + \ldots, \qquad \text{(E4.2.8)}$$

i.e.,

$$(g_{I-2} - 2g_{I-1} + g_I) - \frac{s^2}{12}(g^{(2)}_{I-2} + 10g^{(2)}_{I-1} + g^{(2)}_I) = -\frac{s^6}{240} g^{(6)}_{I-1} + \ldots . \qquad \text{(E4.2.9)}$$

The Numerov integration scheme is obtained by neglecting the rhs of Eq.E4.2.9, i.e., all terms of order 6 and above. Using the Schrödinger equation, Eq.E4.1.1, the second derivatives may be written in the form

$$g^{(2)}_I = (U_I - E')\, g_I \qquad \text{(E4.2.10)}$$

where

$$U_I \equiv U(R(I)) = 2\mu\left[\, V(R(I)) - \frac{K(K+1)}{2\mu R(I)^2} \,\right], \qquad \text{(E4.2.11)}$$

$$E' = 2\mu E, \qquad \text{(E4.2.12)}$$

so that Eq.E4.2.9 may be re-written as

$$g_{I-2}\left(1 - \frac{s^2}{12}(U_{I-2} - E')\right) + g_I\left(1 - \frac{s^2}{12}(U_I - E')\right) - g_{I-1}\left(2 + \frac{5s^2}{6}(U_{I-1} - E')\right) = 0. \qquad \text{(E4.2.13)}$$

Defining the quantity Y_I via

$$Y_I = (1 - \frac{s^2}{12}(U_I - E'))\, g_I \,, \qquad \text{(E4.2.14)}$$

Eq.E4.2.13 becomes

$$Y_I = s^2 (U_{I-1} - E')\, g_{I-1} + 2Y_{I-1} - Y_{I-2} \quad . \qquad \text{(E4.2.15)}$$

This is the Numerov integration scheme.

Appendix E5 Functional Description of Program PROF_QS

E5.1 Introduction

PROF_QS is a computer program written in FORTRAN-77 and running on an HP9050 computer under the HP-UX (UNIX) operating system. It consists of 591 lines of source code occupying 17.8K of storage; the executable module occupies 128.1K.

The purpose of PROF_QS is to calculate the alkali resonance line wing emission intensity via the quasistatic theory given by (see §7.2, Eq.7.2.10)

$$I_{QS}(\lambda(R),T) = 4\pi R^2 \omega \left[\frac{\lambda(\infty)}{\lambda(R)}\right]^4 D_{\Lambda'\Lambda}(R)^2 \left|\frac{d(c/\lambda(R))}{dR}\right|^{-1} \exp\left[-\frac{(V_i(R) - V_i(\infty))}{kT}\right]. \qquad (E5.1.1)$$

A single run of PROF_QS calculates $I_{QS}(\lambda(R),T)$ for a combination of

(i) one alkali-rare gas system (one of LiHe, LiNe, NaHe or NaNe in the present study);

(ii) one type of interatomic potential (either model potential or pseudopotential);

(iii) one type of electronic transition (either $A^2\Pi - X^2\Sigma$ or $B^2\Sigma - X^2\Sigma$)

at a given set of wavelengths and temperatures. The current implementation of PROF_QS has restrictions on the last two quantities, namely, a maximum of 60 wavelengths and 5 temperatures.

E5.2 Input/Output Data Files

The input data used by PROF_QS are contained within the same datasets used by the quantum mechanical emission intensity programs PROF_BF, PROF_QBF and PROF_FF. The organisation of the data into these datasets is described in Appendix E1, §E1.2.1; the content of each dataset is specified in Appendix E1, §E1.2.2. On any single run of the program, PROF_QS reads data from just one of these files.

A single run of PROF_QS creates one output disc file holding the results of the calculation for a particular combination of system, interatomic potential type and

electronic transition. The output files are named using a convention similar to that used in the quantum mechanical programs:

$$\text{Output File Name} = \text{system} \mid \text{potential type} \mid \text{transition} \mid \text{qs.out} \qquad \text{(E5.2.1)}$$

where

system = one of {LiHe, LiNe, NaHe, NaNe},
potential type = M for model potentials
= P for pseudopotentials,
transition = A for $A^2\Pi - X^2\Sigma$
= B for $B^2\Sigma - X^2\Sigma$.

The content of the output file is given in §E5.13 following a description of the calculation performed by PROF_QS.

E5.3 Computational Procedure of PROF_QS

The basic assumption of the quasistatic theory is that emission of radiation at a wavelength λ originates from an electronic transition that occurs whilst the internuclear separation is R so that

$$\frac{hc}{\lambda(R)} = V_i(R) - V_f(R) \equiv \Delta V(R) \qquad \text{(E5.3.1)}$$

where the interatomic potentials $V_i(R)$ and $V_f(R)$ are those of the initial (excited) and final (ground) electronic states respectively. These potentials are measured on an absolute energy scale so that the unperturbed alkali resonance line has an energy given by

$$\frac{hc}{\lambda(\infty)} = V_i(\infty) - V_f(\infty) \equiv \Delta V(\infty). \qquad \text{(E5.3.2)}$$

In atomic units, Eq.E5.3.1 yields

$$\lambda(R) = \frac{2\pi c}{\Delta V(R)} \qquad \text{(E5.3.3)}$$

and

$$\frac{d(c/\lambda(R))}{dR} = \frac{1}{2\pi}\frac{d\Delta V(R)}{dR}. \qquad \text{(E5.3.4)}$$

The quasistatic emission intensity (Eq.E5.1.1) may then be written in the form

$$I_{QS}(\lambda(R),T) = 8\pi^2 R^2 \omega \left[\frac{\Delta V(R)}{\Delta V(\infty)}\right]^4 D_{\Lambda'\Lambda}(R)^2 \left|\frac{d\Delta V(R)}{dR}\right|^{-1} \exp\left[-\frac{(V_i(R) - V_i(\infty))}{kT}\right]. \qquad \text{(E5.3.5)}$$

It is this expression that is evaluated by PROF_QS. The computational procedure used consists of 10 major steps as follows:

Step 1 Read appropriate input data.
Define a set of wavelengths $\{\lambda_n\}$ and temperatures $\{T_m\}$ at which to calculate the quasistatic emission intensity.

Step 2 Initialise the main tote:
FOR each wavelength in $\{\lambda_n\}$
FOR each temperature in $\{T_m\}$
$I_{QS}(\lambda_n,T_m) \leftarrow 0.0$
ENDFOR
ENDFOR

Step 3 Define a suitable radial grid upon which to evaluate $I_{QS}(\lambda(R),T)$.

Step 4 Interpolate the interatomic potentials and dipole transition moments read in Step 1 for values on the radial grid defined in Step 3.

Step 5 Calculate the difference potential $\Delta V(R)$ on the radial grid.
Calculate the emission wavelengths corresponding to $\Delta V(R)$.

Step 6 Calculate the difference potential derivative $\frac{d\Delta V(R)}{dR}$ on the radial grid.

Step 7 Calculate $I_{QS}(\lambda(R),T_m)$ on the radial grid for each temperature T_m.

Step 8 **FOR** each temperature in $\{T_m\}$
Interpolate $I_{QS}(\lambda(R),T_m)$ for values at the wavelengths $\{\lambda_n\}$, giving $I_{QS}(\lambda_n,T_m)$.
ENDFOR

Step 9 **IF requested transition is $B^2\Sigma - X^2\Sigma$ THEN**
Calculate the position of the blue wing satellite.
ENDIF

Step 10 **Write the results of the calculation to the output file.**

The details of how each of these steps is implemented in PROF_QS are described in the remaining sections of this appendix.

E5.4 Step 1 : Read Input Data

On starting program PROF_QS three items are requested from the user:

(i) the alkali-rare gas system for which the quasistatic emission intensity is to be calculated (LiHe, LiNe, NaHe or NaNe);

(ii) a single character denoting the type of interatomic potentials to be used (M for model potentials, P for pseudopotentials);

(iii) a single character denoting the electronic transition to be used (A for $A^2\Pi - X^2\Sigma$, B for $B^2\Sigma - X^2\Sigma$).

The first two items are used to construct, in accordance with the convention given in Eq.E1.2.1 of Appendix E1, the name of the file holding the input dataset; the file is then opened for reading. Next, all three items are used to construct, in accordance with the convention given in Eq.E5.2.1, the name of the output file which will hold the results of the calculation performed by PROF_QS; this file is then created and opened for writing.

PROF_QS then reads the main input data from the open dataset. The content of the dataset and the program variables used to hold these data are the same as for the quantum mechanical emission intensity programs and are listed in §E1.4 of Appendix E1. [Note: the last entry in the input dataset, the reduced mass of the alkali-rare gas system, is not required for the quasistatic calculation; it is not, therefore, read from the open dataset by PROF_QS.] Following this, the statistical weight ω is set to the value appropriate for the requested electronic transition, i.e.,

$$\begin{aligned} \omega &= \frac{2}{3} \quad \text{for } A^2\Pi - X^2\Sigma \\ &= \frac{1}{3} \quad \text{for } B^2\Sigma - X^2\Sigma. \end{aligned} \tag{E5.4.1}$$

E5.5 Step 2 : Initialise Tote

PROF_QS uses a tote in which to accumulate contributions to the quasistatic emission intensity at each wavelength and temperature specified in the input data. This tote is a matrix with generic element $I_{QS}(\lambda_n,T_m)$ which, on completion of PROF_QS execution, will hold the quasistatic emission intensity at wavelength λ_n and temperature T_m. The tote is implemented as a FORTRAN array FIQS(n,m) with index n running from 1 to NLAMDA and index m running from 1 to NTEMP. In this step, the matrix is initialised by setting each element to zero.

E5.6 Step 3 : Define the Radial Grid

The next step in the PROF_QS procedure is to create the radial grid upon which to evaluate $I_{QS}(\lambda(R),T)$ given by Eq.E5.3.5. PROF_QS uses the same radial grid {R(I)} as used by the quantum mechanical programs, i.e., (N+1) radial points defined by

$$\begin{aligned} &R(0) = RI(1), \\ &R(I) = R(0) + (s \times I)\,; \quad I = 1, N - 1, \\ &R(N) = RI(NIV) \end{aligned} \tag{E5.6.1}$$

where the separation of grid points, s, has the value 0.02 au and RI(1), RI(NIV) are, respectively, the first and last points of the radial grid {RI(I)} upon which the interatomic potentials and dipole transition moments are defined in the input data.

E5.7 Step 4 : Interpolate Interatomic Potential Data

The interatomic potentials and dipole transition moments, defined as input data on the grid {RI(I)}, are obtained on the radial grid {R(I)} using 4-point Lagrange interpolation as described in §E1.7 of Appendix E1.

The output of the interpolation procedure is an excited state interatomic potential held in array VEX (equal to the $A^2\Pi$ potential if the requested electronic transition is $A^2\Pi - X^2\Sigma$, and equal to the $B^2\Sigma$ potential if the $B^2\Sigma - X^2\Sigma$ transition is requested), a ground state interatomic potential held in array VGR (equal to the $X^2\Sigma$ potential) and a dipole transition moment, corresponding to the requested electronic transition, held in array DTM.

E5.8 Step 5 : The Difference Potential and Emission Wavelengths

The next step is to calculate the difference potential $\Delta V(R)$, and to determine the corresponding emission wavelengths, at each radial grid point in {R(I)}.

The difference potential $\Delta V(R)$ is given by Eq.E5.3.1, i.e.,

$$\Delta V(R) = V_i(R) - V_f(R) \qquad \text{(E5.8.1)}$$

where the excited and ground state interatomic potentials, $V_i(R)$ and $V_f(R)$ respectively, are measured on an absolute energy scale. The interpolated potentials held in arrays VEX and VGR (see §E5.7 above) are measured relative to their respective separated atom limits; the difference potential, denoted VDIFF, is thus given in terms of VEX and VGR at each radial point in {R(I)} by

$$\text{VDIFF(I)} = \text{VEX(I)} - \text{VGR(I)} + \text{EAUP} - \text{EXUP}\,; \quad \text{I} = 0, \text{N} \qquad \text{(E5.8.2)}$$

where EAUP and EXUP are the energies of the alkali atomic states connected to the $A^2\Pi/B^2\Sigma$ and $X^2\Sigma$ molecular states respectively. The difference potential at infinite separation , $\Delta V(\infty)$, is represented by the variable VDINF given by

$$\text{VDINF} = \text{EAUP} - \text{EXUP}. \qquad \text{(E5.8.3)}$$

The difference potential $\Delta V(R)$ corresponds, via Eq.E5.3.1, to an emission wavelength $\lambda(R)$ given by

$$\lambda(R) = \frac{hc}{\Delta V(R)}. \qquad \text{(E5.8.4)}$$

In atomic units,

$$\lambda_{a_0}(R) = \frac{2\pi\alpha^{-1}}{\Delta V(R)} \qquad \text{(E5.8.5)}$$

where α is the fine structure constant. For wavelengths measured in Å, this becomes

$$\lambda_{Å}(R) = \frac{2\pi\alpha^{-1}}{\Delta V(R)}\left[\frac{1\ a_0}{1\ Å}\right] = \frac{455.63421}{\Delta V(R)}. \qquad \text{(E5.8.6)}$$

The final action of Step 5 is to calculate the emission wavelengths given by Eq.E5.8.6 at each radial grid point in {R(I)}; these are stored in the array FLAMR:

$$\text{FLAMR(I)} = \frac{455.63421}{\text{VDIFF(I)}}; \quad \text{I} = 0, \text{N.} \qquad \text{(E5.8.7)}$$

E5.9 Step 6 : Calculating the Difference Potential Derivatives

In this step, the derivative of the difference potential with respect to R, $\frac{d\Delta V(R)}{dR}$, is calculated at each radial grid point in {R(I)}. For the first 5 radial points, R(0)...R(4), the derivative is calculated by a six-point differentiation formula (Abramowitz and Stegun (1972), Table 25.2) and stored in the array DVDIFR:

$$\text{DVDIFR(I)} \equiv \frac{d\Delta V(R(I))}{dR} \cong \frac{1}{120s} \sum_{j=0}^{5} A_j \, \text{VDIFF(j+I)} + O(s^6); \quad I = 0, 4 \qquad \text{(E5.9.1)}$$

where the coefficients A_j are

$$A_0 = -274 \qquad A_1 = 600 \qquad A_2 = -600 \qquad \text{(E5.9.2)}$$
$$A_3 = 400 \qquad A_4 = -150 \qquad A_5 = 24$$

and s is the separation of radial points on the grid {R(I)}. The error term $O(s^6)$ is neglected. At the remaining grid points, R(5)...R(N), the derivative is obtained by a similar differentiation formula:

$$\text{DVDIFR(I)} \equiv \frac{d\Delta V(R(I))}{dR} \cong \frac{1}{120s} \sum_{j=0}^{5} B_j \, \text{VDIFF(j+I-5)} + O(s^6); \quad I = 5, N \qquad \text{(E5.9.3)}$$

where the coefficients B_j are

$$B_0 = -24 \qquad B_1 = 150 \qquad B_2 = -400 \qquad \text{(E5.9.4)}$$
$$B_3 = 600 \qquad B_4 = -600 \qquad B_5 = 274.$$

The error term $O(s^6)$ is again neglected. All the quantities required for evaluating $I_{QS}(\lambda(R),T)$ have now been obtained and this calculation is performed next.

E5.10 Step 7 : Calculating $I_{QS}(\lambda(R),T)$

Step 7 calculates the quasistatic emission intensity $I_{QS}(\lambda(R),T)$ given by Eq.E5.3.5 at each radial grid point in {R(I)} and at each temperature specified in the input data of PROF_QS. The emission intensity is stored in an array FIQSR with generic element FIQSR(I,m) where index I runs from 0 to N, corresponding to each radial grid point, and index m runs from 1 to NTEMP, corresponding to each temperature. The elements are calculated by the following procedure:

FOR each radial grid point, I = 0, N

$$c = 8\pi^2.R(I)^2.\omega.\left[\frac{VDIFF(I)}{VDINF}\right]^4.DTM(I)^2.DVDIFR(I)^{-1}.$$

FOR each temperature, m = 1, NTEMP

$$FIQSR(I,m) = c.\exp\left[-\frac{VEX(I)}{k.TEMP(m)}\right].$$

ENDFOR

ENDFOR

E5.11 Step 8 : Interpolating the Emission Intensity

The result of Step 7 above is the quasistatic emission intensity arising from each value of internuclear separation R on the radial grid {R(I)}, and at each of the required temperatures, stored in the array elements FIQSR(I,m). The wavelengths of emission at each internuclear separation are stored in the corresponding array elements FLAMR(I), calculated in Step 5. It is now necessary to interpolate this emission intensity to obtain intensity values at the wavelengths FLAMDA(n), n = 1, NLAMDA, specified in the input data of PROF_QS.

The interpolation procedure must take account of the fact that the difference potential $\Delta V(R)$ may be a non-monotonic function of R (as, for example, it is for the $B^2\Sigma - X^2\Sigma$ electronic transition). This results in emission at certain wavelengths arising from more than one value of R; all values of R giving rise to emission at a particular wavelength must be accounted for and their contributions summed. The method adopted for performing the interpolation is described below for a single wavelength FLAMDA(n) and temperature TEMP(m).

For convenience, the wavelength FLAMDA(n) is denoted by λ_n and the wavelength FLAMR(I) is denoted by $\lambda(R(I))$. The set of wavelengths $\{\lambda(R(I))\}$ is searched, in the direction I=1, N, for a consecutive pair of wavelengths $(\lambda(R(I)), \lambda(R(I-1)))$ satisfying the condition

$$\mathbf{MIN}(\lambda(R(I)),\lambda(R(I-1))) \leq \lambda_n \leq \mathbf{MAX}(\lambda(R(I)),\lambda(R(I-1))). \qquad \text{(E5.11.1)}$$

The MIN and MAX functions are required because the search procedure must allow for the wavelengths being an increasing function of R in some regions and a decreasing function of R in others. If such a pair of wavelengths is found, linear interpolation is performed between them to obtain the emission intensity at wavelength λ_n and temperature T_m from this region of R:

$$I_{QS}(\lambda_n,T_m) = FIQSR(I,m) - \left[\frac{\lambda(R(I)) - \lambda_n}{\lambda(R(I)) - \lambda(R(I-1))}\right][FIQSR(I,m) - FIQSR(I-1,m)]. \qquad \text{(E5.11.2)}$$

The tote holding the quasistatic emission intensity is then incremented:

$$FIQS(n,m) \leftarrow FIQS(n,m) + I_{QS}(\lambda_n,T_m). \qquad \text{(E5.11.3)}$$

The search of $\{\lambda(R(I))\}$ is then resumed and the above procedure repeated for all occurrences of condition E5.11.1. The result is a tote element FIQS(n,m) containing the quasistatic emission intensity at wavelength λ_n and temperature T_m accumulated from all contributing R values.

The procedure for considering all wavelengths in $\{\lambda_n\}$ and temperatures in $\{T_m\}$ is as follows:

FOR each λ_n, n = 1, NLAMDA
  FOR each $\lambda(R(I))$, I = 1, N
    IF $\mathbf{MIN}(\lambda(R(I)),\lambda(R(I-1))) \leq \lambda_n \leq \mathbf{MAX}(\lambda(R(I)),\lambda(R(I-1)))$ **THEN**

$$c = \left[\frac{\lambda(R(I)) - \lambda_n}{\lambda(R(I)) - \lambda(R(I-1))}\right]$$

      FOR each T_m, m = 1, NTEMP
        FIQS(n,m) ← FIQS(n,m)
          + FIQSR(I,m) - c[FIQSR(I,m) - FIQSR(I-1,m)].
      ENDFOR
    ENDIF
  ENDFOR
ENDFOR

The tote elements FIQS(n,m) now contain the quasistatic emission intensity at the wavelengths $\{\lambda_n\}$ and temperatures $\{T_m\}$ specified in the input data to PROF_QS.

E5.12 Step 9 : Locating the Blue Wing Satellite

This step is executed only if the requested electronic transition is $B^2\Sigma - X^2\Sigma$. Its purpose is to calculate the position of the blue wing satellite arising from the extremum (maximum) in the $B^2\Sigma - X^2\Sigma$ difference potential.

The radial region in which the satellite occurs is located by searching the array of difference potential values, VDIFF, for three values satisfying the condition

$$\text{VDIFF(I-1)} < \text{VDIFF(I)} > \text{VDIFF(I+1)}. \qquad \text{(E5.12.1)}$$

The radial position of the satellite is obtained by the least squares fitting of a quadratic function of R, i.e.,

$$\Delta V(R) = a + bR + cR^2, \qquad \text{(E5.12.2)}$$

to the array points VDIFF(I-1), VDIFF(I) and VDIFF(I+1). The coefficients a, b and c of the quadratic are solutions of the simultaneous equations (Mack (1969), Eq.12.10)

$$\begin{aligned} an + b\sum R(J) + c\sum R(J)^2 &= \sum \text{VDIFF(J)}, \\ a\sum R(J) + b\sum R(J)^2 + c\sum R(J)^3 &= \sum [R(J).\text{VDIFF(J)}], \\ a\sum R(J)^2 + b\sum R(J)^3 + c\sum R(J)^4 &= \sum [R(J)^2.\text{VDIFF(J)}] \end{aligned} \qquad \text{(E5.12.3)}$$

where n is the number of data points (in this case n = 3) and the summations are carried out over the index J, from J = I - 1 to J = I +1.

Denoting

$$\rho^N \equiv \sum R(J)^N; \qquad V \equiv \sum \text{VDIFF(J)}; \qquad \text{(E5.12.4)}$$

$$\rho V \equiv \sum [R(J).\text{VDIFF(J)}]; \qquad \rho^2 V \equiv \sum [R(J)^2.\text{VDIFF(J)}]$$

the quadratic coefficients a, b and c are given by the determinants

$$a=\frac{1}{D}\begin{vmatrix} V & \rho & \rho^2 \\ \rho V & \rho^2 & \rho^3 \\ \rho^2 V & \rho^3 & \rho^4 \end{vmatrix}; \quad b=\frac{1}{D}\begin{vmatrix} n & V & \rho^2 \\ \rho & \rho V & \rho^3 \\ \rho^2 & \rho^2 V & \rho^4 \end{vmatrix}; \quad c=\frac{1}{D}\begin{vmatrix} n & \rho & V \\ \rho & \rho^2 & \rho V \\ \rho^2 & \rho^3 & \rho^2 V \end{vmatrix} \tag{E5.12.5}$$

where

$$D=\begin{vmatrix} n & \rho & \rho^2 \\ \rho & \rho^2 & \rho^3 \\ \rho^2 & \rho^3 & \rho^4 \end{vmatrix}. \tag{E5.12.6}$$

Each of these determinants may be expanded to give forms for the quadratic coefficients amenable to direct calculation:

$$a=\frac{1}{D}\left\{V\begin{vmatrix} \rho^2 & \rho^3 \\ \rho^3 & \rho^4 \end{vmatrix}-\rho\begin{vmatrix} \rho V & \rho^3 \\ \rho^2 V & \rho^4 \end{vmatrix}+\rho^2\begin{vmatrix} \rho V & \rho^2 \\ \rho^2 V & \rho^3 \end{vmatrix}\right\},$$

$$b=\frac{1}{D}\left\{n\begin{vmatrix} \rho V & \rho^3 \\ \rho^2 V & \rho^4 \end{vmatrix}-V\begin{vmatrix} \rho & \rho^3 \\ \rho^2 & \rho^4 \end{vmatrix}+\rho^2\begin{vmatrix} \rho & \rho V \\ \rho^2 & \rho^2 V \end{vmatrix}\right\}, \tag{E5.12.7}$$

$$c=\frac{1}{D}\left\{n\begin{vmatrix} \rho^2 & \rho V \\ \rho^3 & \rho^2 V \end{vmatrix}-\rho\begin{vmatrix} \rho & \rho V \\ \rho^2 & \rho^2 V \end{vmatrix}+V\begin{vmatrix} \rho & \rho^2 \\ \rho^2 & \rho^3 \end{vmatrix}\right\},$$

$$D=n\begin{vmatrix} \rho^2 & \rho^3 \\ \rho^3 & \rho^4 \end{vmatrix}-\rho\begin{vmatrix} \rho & \rho^3 \\ \rho^2 & \rho^4 \end{vmatrix}+\rho^2\begin{vmatrix} \rho & \rho^2 \\ \rho^2 & \rho^3 \end{vmatrix}.$$

The determinants in Eq.E5.12.7 are then calculated directly via the general definition of the determinant, i.e.,

$$\begin{vmatrix} d_1 & d_2 \\ d_3 & d_4 \end{vmatrix}=d_1d_4-d_3d_2. \tag{E5.12.8}$$

Having obtained the quadratic coefficients, the satellite position is given by the extremum of Eq.E5.12.2, i.e., the internuclear separation R_s at which

$$\frac{d\Delta V(R)}{dR}=b+2cR_s=0. \tag{E5.12.9}$$

Hence,

$$R_s = -\frac{b}{2c}. \qquad \text{(E5.12.10)}$$

The value of the difference potential at R_s is

$$\Delta V(R_s) = a + bR_s + cR_s^2 \qquad \text{(E5.12.11)}$$

from which the satellite wavelength λ_s (in Å) follows via Eq.E5.8.6:

$$\lambda_s = \frac{455.63421}{\Delta V(R_s)}. \qquad \text{(E5.12.12)}$$

E5.13 Step 10 Output the Calculation Results

The final action of PROF_QS is to write the results of the calculation described in §§E5.4 through E5.12 to the output file. The data written to this file consist of the following quantities:

(i) a copy of the input data for PROF_QS (see §E5.4);

(ii) the wavelength of the blue wing satellite (if the requested electronic transition is $B^2\Sigma - X^2\Sigma$);

(iii) the calculated quasistatic emission intensity $I_{QS}(\lambda,T)$ at the wavelengths FLAMDA(n), n = 1, NLAMDA and the temperatures TEMP(m), m = 1, NTEMP.

This completes the functional description of program PROF_QS.

Annex F

The Implementation of the Line Core Broadening Model

Appendix F1 Functional Description of Program IMPACT

F1.1 Introduction

IMPACT is a computer program written in FORTRAN-77 and running on an HP9050 computer under the HP-UX (UNIX) operating system. It consists of 824 lines of source code occupying 26.3K of storage; the executable module occupies 145.9K.

The purpose of IMPACT is to calculate the width (W/N) and shift (d/N) of the alkali resonance line, broadened by collisions with rare gas atoms, in the impact approximation. These parameters are given by (see §7.3, Eq.7.3.1)

$$\frac{W}{N} + i\frac{d}{N} = 2\pi \int_0^\infty vf(v)\,dv \int_0^\infty \rho\Pi(\rho)\,d\rho \qquad \text{(F1.1.1)}$$

where f(v) is a Maxwellian distribution of velocities and $\Pi(\rho)$ is defined by

$$\Pi(\rho) = 1 - \sum_{\substack{m_i m_f \\ M}} \frac{< j_f\, l\, m_f\, M \mid j_i\, m_i >^2}{(2j_i + 1)} < j_f\, m_f \mid S_f^{-1} \mid j_f\, m_f > < j_i\, m_i \mid S_i \mid j_i\, m_i > \qquad \text{(F1.1.2)}$$

where ρ is the impact parameter. In addition, IMPACT uses the S matrices generated for evaluating Eq.F1.1.1 to calculate cross sections for the fine structure state changing transitions within the excited state multiplet given by (see §7.3, Eq.7.3.2)

$$\sigma_{j_i \to j'_i} = 2\pi \int_0^\infty \rho P_{j_i \to j'_i}(\rho)\,d\rho \qquad \text{(F1.1.3)}$$

where

$$P_{j_i \to j'_i}(\rho) = \frac{1}{(2j_i + 1)} \sum_{m_i m'_i} \left| < j'_i\, m'_i \mid S_i \mid j_i\, m_i > \right|^2. \qquad \text{(F1.1.4)}$$

The dependence of the line broadening parameters and the state changing cross sections on the alkali-rare gas interatomic potentials is through the S matrix elements of Eqs.F1.1.2 and F1.1.4. In addition, the matrix elements are dependent on the relative

velocity of the colliding atoms and results in W, $\dot{d}$ and $\sigma_{j_i \to j'_i}$ also exhibiting a temperature dependence.

A single run of IMPACT evaluates Eqs.F1.1.1 and F1.1.3 for a combination of

(i) one alkali-rare gas system (one of LiHe, LiNe, NaHe or NaNe in the present study);

(ii) one type of interatomic potential (either model potential or pseudopotential)

at a given set of temperatures. The current implementation of IMPACT has a restriction on the last quantity, namely, a maximum of 10 temperatures.

F1.2 Input/Output Data Files

F1.2.1 Overview of Input Files

The input data required by IMPACT are organised in the same way as for the line profile programs described in Annex E, i.e., into four pairs of datasets, each dataset being stored in a separate disc file on the HP9050 computer system. Each pair of datasets relates to one of the alkali-rare gas systems under investigation; within each pair, one dataset includes interatomic potentials calculated by the model potential method, the other includes interatomic potentials calculated by the pseudopotential method. To identify the datasets, each is named according to the convention given in Eq.E1.2.1 of Appendix E1. On any single run of the program, IMPACT reads data from just one of these files.

[Note: although the names used for the input datasets of program IMPACT are identical to those used for the input datasets of the line wing programs (PROF_BF, PROF_QBF, PROF_FF and PROF_QS) the former datasets are distinct from the latter, being held in a separate directory on the HP9050 computer system.]

All eight input files have the same basic data structure containing the following quantities:

(i) the number of input values, denoted NIV, used to specify each of the interatomic potentials and the radial grid on which these are represented;

(ii) the internuclear separations R(I), I = 1, NIV, at which the interatomic potentials have been calculated by Peach;

(iii) the $A^2\Pi$, $B^2\Sigma$ and $X^2\Sigma$ interatomic potentials at each R(I);

(iv) the number of temperatures, denoted NTEMP, at which the broadening parameters and state changing cross sections are to be calculated;

(v) the NTEMP temperatures;

(vi) the reduced mass of the alkali-rare gas system;

(vii) the fine structure splitting of the alkali excited state;

(viii) the maximum radius of influence (see §F1.7.2.1);

(ix) the number of integration points, as a function of impact parameter, to be used in calculating the S matrices (see §F1.7.2.1);

(x) the grid of impact parameter values to be used (see §F1.5).

The temperatures and the fine structure splitting of the alkali excited state are measured in degrees Kelvin and cm^{-1} respectively; all other data are expressed in atomic units. In addition, the interatomic potentials are measured relative to their respective separated atom limits (the alkali atomic state energies).

F1.2.2 Overview of Output Files

A single run of IMPACT creates one output disc file holding the results of the calculation for a particular combination of system and interatomic potential type. To identify the output files, each is named using the following convention:

Output File Name = system | potential type | im.out (F1.2.1)

where

system = one of {LiHe, LiNe, NaHe, NaNe},
potential type = M for model potentials
= P for pseudopotentials.

The content of the output file is given in §F1.10 following a description of the calculation performed by IMPACT.

F1.3 Computational Procedure of IMPACT

The expression for the resonance line width and shift (Eq.F1.1.1) contains an integration over all relative velocities, weighted by a Maxwellian distribution, f(v). In order to keep the execution time of IMPACT on the HP9050 computer down to a practical level, the integral over relative velocities is replaced by a single velocity - the rms velocity, denoted V_{rms} - given by

$$V_{rms} = \left[\frac{3kT}{\mu}\right]^{1/2} \qquad \text{(F1.3.1)}$$

where k is Boltzmann's constant, T is the temperature and μ is the reduced mass of the colliding atoms. Eq.F1.1.1 is then replaced by

$$\frac{W}{N} + i\frac{d}{N} = 2\pi V_{rms} \int_0^\infty \rho\Pi(\rho)\, d\rho \qquad \text{(F1.3.2)}$$

with $\Pi(\rho)$ given by Eq.F1.1.2. With this modification, the computational procedure of IMPACT consists of 7 major steps as follows:

Step 1 Read appropriate input data.
Define a set of temperatures $\{T_m\}$ at which to calculate the widths, shifts and state changing cross sections.

Step 2 Construct the grid of impact parameter values $\{\rho(I)\}$.

Step 3 Set the temperature to be used:
Temperature = T_m ; m = 1.
Calculate the rms velocity corresponding to T_m.

Step 4 **FOR** each impact parameter in $\{\rho(I)\}$
Calculate $S_i(\rho(I))$ and $S_f(\rho(I))$, the S matrices for the initial (excited) and final (ground) states of the alkali atom respectively.

Calculate $\rho(I)\Pi(\rho(I))$ for the D1 and D2 resonance line components.

Calculate $\rho(I)P_{1/2\rightarrow 3/2}(\rho(I))$ and $\rho(I)P_{3/2\rightarrow 1/2}(\rho(I))$.
ENDFOR

Step 5 Integrate $\rho(I)\Pi(\rho(I))$ over ρ for the D1 and D2 resonance line components.
Integrate $\rho(I)P_{1/2\rightarrow 3/2}(\rho(I))$ and $\rho(I)P_{3/2\rightarrow 1/2}(\rho(I))$ over ρ.
Calculate W and d for the D1 and D2 resonance line components.
Calculate $\sigma_{1/2\rightarrow 3/2}$ and $\sigma_{3/2\rightarrow 1/2}$.

Step 6 **IF** not all temperatures considered **THEN**
Re-set the temperature variable:
$m \leftarrow m + 1$.
Temperature = T_m.
Calculate the rms velocity corresponding to T_m.
Return to Step 4.
ENDIF

Step 7 Write the results of the calculation to the output file.

The details of how each of these steps is implemented in IMPACT are described in the remaining sections of this appendix.

F1.4 Step 1 : Read Input Data

On starting program IMPACT two items are requested from the user:

(i) the alkali-rare gas system for which the widths, shifts and fine structure state changing cross sections are to be calculated (LiHe, LiNe, NaHe or NaNe);

(ii) a single character denoting the type of interatomic potentials to be used (M for model potentials, P for pseudopotentials).

These items are used to construct, in accordance with the convention given in Eq.E1.2.1 of Appendix E1, the name of the file holding the input dataset; the file is then opened for reading. Next, the same two items are used to construct, in accordance with the convention given in Eq.F1.2.1, the name of the output file which will hold the results of the calculation performed by IMPACT; this file is then created and opened for writing.

IMPACT then reads the main input data from the open dataset. The content of the dataset is specified in §F1.2.1; for future reference, the program variables used to hold these data are listed in Table F1.1. The interatomic potentials used by IMPACT are listed in Appendix B1; each curve is specified at 82 values of the internuclear separation covering the range 2 - 40 au. The temperatures and reduced mass appropriate to each alkali-rare

Table F1.1 Input Data for Program IMPACT

FORTRAN Variable Name	Description of Data Held
NIV	Number of input values for the internuclear separations and interatomic potentials.
RI(I)	Array of NIV values specifying the internuclear separations at which the interatomic potentials are available.
VAI(I)	Array of NIV values, one value for each RI(I), specifying the $A^2\Pi$ interatomic potential.
VBI(I)	Array of NIV values, one value for each RI(I), specifying the $B^2\Sigma$ interatomic potential.
VXI(I)	Array of NIV values, one value for each RI(I), specifying the $X^2\Sigma$ interatomic potential.
NTEMP	Number of temperatures to be used in the calculation.
TEMP(m)	Array of NTEMP temperature values.
FMU	Reduced mass of the alkali-rare gas system.
OMEGA	Fine structure splitting of the alkali atom excited state.
RMAX	Maximum radius of influence (see §F1.7.2.1).
NREG	Number of impact parameter regions of constant granularity with respect to the S matrix calculation (see §F1.7.2.1).
RLOW(K)	Array of NREG values specifying the lower limit of each impact parameter region with respect to the S matrix calculation (see §F1.7.2.1).
RUPP(K)	Array of NREG values specifying the upper limit of each impact parameter region with respect to the S matrix calculation (see §F1.7.2.1).
NINPT(K)	Array of NREG values specifying the number of integration points to be used for the S matrix calculation in each impact parameter region (see §F1.7.2.1).
MREG	Number of impact parameter regions of constant granularity with respect to the impact parameter grid (see §F1.5).
SLOW(I)	Array of MREG values specifying the lower limit of each impact parameter region with respect to the impact parameter grid (see §F1.5).
SUPP(I)	Array of MREG values specifying the upper limit of each impact parameter region with respect to the impact parameter grid (see §F1.5).
STEP(I)	Array of MREG values specifying the step length to be used within each impact parameter region with respect to the impact parameter grid (see §F1.5).

gas system are given in Table 7.6 of §7.3 and Table E1.3 of Appendix E1 respectively; the values of the fine structure splitting in the excited state of Li and Na are 0.3372 cm^{-1} and 17.1963 cm^{-1} respectively. The values of the remaining input data are specified in the section of this appendix quoted in Table F1.1.

Following this, the fine structure splitting parameter, ω, is converted from units of cm^{-1} to atomic units of energy (cf. Eq.E1.9.15 of Appendix E1):

$$\omega(au) = 455.63421 \times 10^{-8}\, \omega\,(cm^{-1}) \qquad \text{(F1.4.1)}$$

F1.5 Step 2 : Define the Impact Parameter Grid

The next step is to define the impact parameter grid to be used. This is the set of values $\{\rho(I)\}$ at which the quantities $\Pi(\rho)$ and $P_{j_i \rightarrow j'_i}(\rho)$ of Eqs.F1.1.2 and F1.1.4 are calculated for subsequent evaluation of Eqs.F1.3.2 and F1.1.3. A number of trial evaluations of $\Pi(\rho)$ and $P_{j_i \rightarrow j'_i}(\rho)$ (using the methods to be described in §F1.7) showed that, for small impact parameters, both quantities vary quite rapidly with ρ whilst at larger ρ the quantities vary more smoothly with ρ. This behaviour is exploited in IMPACT by defining an impact parameter grid with a variable step length, starting with closely spaced grid points for the smaller ρ values and with the grid points becoming progressively more separated as ρ increases. The appropriate separation of grid points as a function of impact parameter was determined by carrying out numerous trial integrations of $\rho\Pi(\rho)$ over small ranges of ρ (of size between 0.5 and 1 au) placed at various impact parameters between 3 au and 36 au. Each integration was repeated with several different step sizes in ρ (ranging from 0.005 au up to 0.20 au), the step size appropriate for the particular impact parameter considered being taken as the largest value that maintained numerical stability in the value of the integral of $\rho\Pi(\rho)$. Here, numerical stability was judged to be maintained from one step size to another if the value of the integral changed by less than ~1%.

The results of these investigations for the four alkali-rare gas systems considered in the present study are summarised in Table F1.2 for the model potential interaction curves and in Table F1.3 for the pseudopotential curves. These calculations were carried out at a relatively low temperature (200K) since the step size requirements were found to be less stringent (i.e., larger step sizes were capable of maintaining numerical stability) for any given ρ as the temperature increases. The values shown in Tables F1.2 and F1.3 were used for all temperatures greater than 200K.

Table F1.2 Impact Parameter Step Sizes : Model Potentials

	Step Size (au)			
Range of ρ (au)	LiHe	LiNe	NaHe	NaNe
3.5 - 4.0	0.01	0.01	0.01	0.01
4.5 - 5.0	0.01	0.01	0.01	0.01
5.5 - 6.0	0.01	0.01	0.01	0.01
6.5 - 7.0	0.01	0.01	0.01	0.01
7.5 - 8.0	0.05	0.05	0.01	0.01
8.5 - 9.0	0.05	0.05	0.05	0.05
9.5 - 10.0	0.05	0.05	0.05	0.05
10.5 - 11.0	0.05	0.05	0.05	0.05
11.0 - 12.0	0.10	0.10	0.10	0.10
15.0 - 16.0	0.10	0.10	0.10	0.10
19.0 - 20.0	0.10	0.10	0.10	0.10
23.0 - 24.0	0.10	0.10	0.10	0.10
27.0 - 28.0	0.10	0.10	0.10	0.10
31.0 - 32.0	0.10	0.10	0.10	0.10
35.0 - 36.0	0.10	0.10	0.10	0.10

The dependence of the step size on ρ indicates that the impact parameter grid may be constructed from a small number of regions, each of a constant step size. Each such region is bounded by a lower limit in ρ, denoted SLOW(I), and an upper limit in ρ, denoted SUPP(I); within the region, the step size to be used is denoted STEP(I); the number of such regions used is denoted by MREG. The values adopted for these parameters, on the basis of the results shown in Tables F1.2 and F1.3, are given in Table F1.4 for the model potential curves and in Table F1.5 for the pseudopotential curves. These parameters are supplied as input data to program IMPACT (see §F1.4 and Table F1.1).

Table F1.3 Impact Parameter Step Sizes : Pseudopotentials				
	Step Size (au)			
Range of ρ (au)	LiHe	LiNe	NaHe	NaNe
3.5 - 4.0	0.01	0.01	0.01	0.01
4.5 - 5.0	0.01	0.01	0.01	0.01
5.5 - 6.0	0.01	0.01	0.01	0.01
6.5 - 7.0	0.01	0.01	0.01	0.01
7.5 - 8.0	0.05	0.01	0.01	0.01
8.5 - 9.0	0.05	0.05	0.01	0.01
9.5 - 10.0	0.05	0.05	0.05	0.05
10.5 - 11.0	0.05	0.05	0.05	0.05
11.0 - 12.0	0.10	0.10	0.10	0.10
15.0 - 16.0	0.10	0.10	0.10	0.10
19.0 - 20.0	0.10	0.10	0.10	0.10
23.0 - 24.0	0.10	0.10	0.10	0.10
27.0 - 28.0	0.10	0.10	0.10	0.10
31.0 - 32.0	0.10	0.10	0.10	0.10
35.0 - 36.0	0.10	0.10	0.10	0.10

In terms of these grid parameters, the set of values $\{\rho(I)\}$ is then constructed by the following procedure:

```
I = 0
ρ(I) = SLOW(1)
FOR K = 1, MREG
        FOR J = 1, N(K)
                I ← I + 1
                ρ(I) = SLOW(K) + [J × STEP(K)]
        ENDFOR
        I ← I + 1
        ρ(I) = SUPP(K)
ENDFOR
```

Here, N(K) is the number of grid points in each of the MREG regions (excluding the end points of the region) given by

Table F1.4 Grid Parameters : Model Potentials

System	MREG	SLOW(I) (au)	SUPP(I) (au)	STEP(I) (au)
LiHe	3	3.0	8.0	0.01
		8.0	12.0	0.05
		12.0	38.0	0.10
LiNe	3	3.0	8.0	0.01
		8.0	12.0	0.05
		12.0	38.0	0.10
NaHe	3	3.0	9.0	0.01
		9.0	12.0	0.05
		12.0	38.0	0.10
NaNe	3	3.0	9.0	0.01
		9.0	12.0	0.05
		12.0	38.0	0.10

$$N(K) = \left[\frac{SUPP(K) - SLOW(K)}{STEP(K)} \right]_{nint} - 1 ; \quad K = 1, MREG \qquad (F1.5.1)$$

where 'nint' denotes conversion to the nearest integer. The total number of points in the grid, denoted N, is then

$$N = MREG + 1 + \sum_{K} N(K). \qquad (F1.5.2)$$

F1.6 Step 3 : Initialise Temperature

This step is the start of the temperature loop and consists simply of initialising the temperature variable to the first input data value, TEMP(1), and calculating the rms velocity corresponding to this temperature:

Table F1.5 Grid Parameters : Pseudopotentials

System	MREG	SLOW(I) (au)	SUPP(I) (au)	STEP(I) (au)
LiHe	3	3.0	8.0	0.01
		8.0	12.0	0.05
		12.0	38.0	0.10
LiNe	3	3.0	9.0	0.01
		9.0	12.0	0.05
		12.0	38.0	0.10
NaHe	3	3.0	10.0	0.01
		10.0	12.0	0.05
		12.0	38.0	0.10
NaNe	3	3.0	10.0	0.01
		10.0	12.0	0.05
		12.0	38.0	0.10

$$v = \left[\frac{3kTEMP(1)}{\mu}\right]^{1/2}. \qquad \text{(F1.6.1)}$$

F1.7 Step 4 : Main Program Loop

Step 4 of the computational procedure of IMPACT constitutes the main loop of the program in which the quantities $\rho\Pi(\rho)$ and $\rho P_{j_i \to j'_i}(\rho)$ are calculated for each impact parameter in the set $\{\rho(I)\}$ constructed in the previous step. $\Pi(\rho)$ and $P_{j_i \to j'_i}(\rho)$ are expressed in terms of the S matrices of the collision and, in §6.4, the principle of the method by which these matrices are obtained was described, involving the solution of time-dependent differential equations for the expansion coefficients of the alkali valence electron eigenfunction. In practice, these equations are more easily solved by a change of variable from the time, t, to the angle ϕ which measures the rotation of the internuclear axis throughout the collision. This change of variable is described first and is then followed by the procedures used to solve the ϕ-dependent equations to obtain the required S matrices which lead subsequently to the calculation of the quantities $\Pi(\rho)$ and $P_{j_i \to j'_i}(\rho)$.

F1.7.1 Change of Variable

The time-dependent equations for the expansion coefficients of the alkali valence electron eigenfunction are given in §6.4 by Eqs.6.4.15, 6.4.16 and 6.4.19, reproduced below.

$$
\begin{aligned}
i\frac{da_1(t)}{dt} &= \tilde{V}\,a_1(t) - \frac{f}{3\sqrt{2}}e^{-i\omega t}\,a_2(t) + \frac{f}{\sqrt{6}}e^{-i\omega t-2i\phi}\,a_3(t)\\
i\frac{da_2(t)}{dt} &= -\frac{f}{3\sqrt{2}}e^{i\omega t}\,a_1(t) + (\tilde{V}-\frac{f}{6})\,a_2(t) - \frac{f}{2\sqrt{3}}e^{-2i\phi}\,a_3(t) \qquad \text{(F1.7.1)}\\
i\frac{da_3(t)}{dt} &= \frac{f}{\sqrt{6}}e^{i\omega t+2i\phi}\,a_1(t) - \frac{f}{2\sqrt{3}}e^{2i\phi}\,a_2(t) + (\tilde{V}+\frac{f}{6})\,a_3(t)
\end{aligned}
$$

$$
\begin{aligned}
i\frac{da_4(t)}{dt} &= \tilde{V}\,a_4(t) + \frac{f}{3\sqrt{2}}e^{-i\omega t}\,a_5(t) - \frac{f}{\sqrt{6}}e^{-i\omega t+2i\phi}\,a_6(t)\\
i\frac{da_5(t)}{dt} &= \frac{f}{3\sqrt{2}}e^{i\omega t}\,a_4(t) + (\tilde{V}-\frac{f}{6})\,a_5(t) - \frac{f}{2\sqrt{3}}e^{2i\phi}\,a_6(t) \qquad \text{(F1.7.2)}\\
i\frac{da_6(t)}{dt} &= -\frac{f}{\sqrt{6}}e^{i\omega t-2i\phi}\,a_4(t) - \frac{f}{2\sqrt{3}}e^{-2i\phi}\,a_5(t) + (\tilde{V}+\frac{f}{6})\,a_6(t)
\end{aligned}
$$

$$
i\frac{db_1(t)}{dt} = V_{X^2\Sigma}\,b_1(t) \qquad \text{(F1.7.3)}
$$

where

$$
\tilde{V} = \frac{2}{3}V_{A^2\Pi} + \frac{1}{3}V_{B^2\Sigma}\,, \qquad \text{(F1.7.4)}
$$

$$
f = V_{B^2\Sigma} - V_{A^2\Pi}\,, \qquad \text{(F1.7.5)}
$$

ω is the fine structure splitting of the alkali excited state, ϕ is the angle measuring the rotation of the internuclear axis (see Figure 6.1 of §6.2) and t is the time; $V_{A^2\Pi}$, $V_{B^2\Sigma}$ and $V_{X^2\Sigma}$ denote the $A^2\Pi$, $B^2\Sigma$ and $X^2\Sigma$ interatomic potentials respectively.

The relationship between t and ϕ is obtained with the aid of the straight path trajectory assumption (see §6.2) from which

$$\mathbf{R} = \rho + \mathbf{v}t \tag{F1.7.6}$$

where **R** is the internuclear vector and **v** is the relative velocity. The geometry resulting from this assumption is shown in Figure F1.1 (cf. Figure 6.1) from which

$$\sin(\phi - \pi/2) = -\cos(\phi) = \frac{\mathbf{v}t}{\mathbf{R}}, \tag{F1.7.7}$$

$$\cos(\phi - \pi/2) = \sin(\phi) = \frac{\rho}{\mathbf{R}}. \tag{F1.7.8}$$

These equations yield

$$t = -\frac{\mathbf{R}}{\mathbf{v}}\cos(\phi) = -\frac{\rho}{\mathbf{v}}\cot(\phi) \tag{F1.7.9}$$

so that

$$dt = \frac{\rho}{\mathbf{v}\sin^2(\phi)}d\phi = \frac{\mathbf{R}^2}{\mathbf{v}\rho}d\phi. \tag{F1.7.10}$$

Hence

$$\frac{d}{dt} = \frac{\mathbf{v}\rho}{\mathbf{R}^2}\frac{d}{d\phi}. \tag{F1.7.11}$$

With this relationship, and the first expression for the time, t, in Eq.F1.7.9, the time-dependent equations (Eqs.F1.7.1- F1.7.3) may be written, in matrix notation, as

$$\frac{d\mathbf{a}(\phi)}{d\phi} = \mathbf{A}(\phi)\,\mathbf{a}(\phi), \tag{F1.7.12}$$

$$\frac{d\mathbf{a}'(\phi)}{d\phi} = \mathbf{A}'(\phi)\,\mathbf{a}'(\phi), \tag{F1.7.13}$$

$$\frac{d\mathbf{b}(\phi)}{d\phi} = -\frac{i\mathbf{R}^2}{\mathbf{v}\rho}\mathbf{V}_{X^2\Sigma}\,\mathbf{b}(\phi) \tag{F1.7.14}$$

where

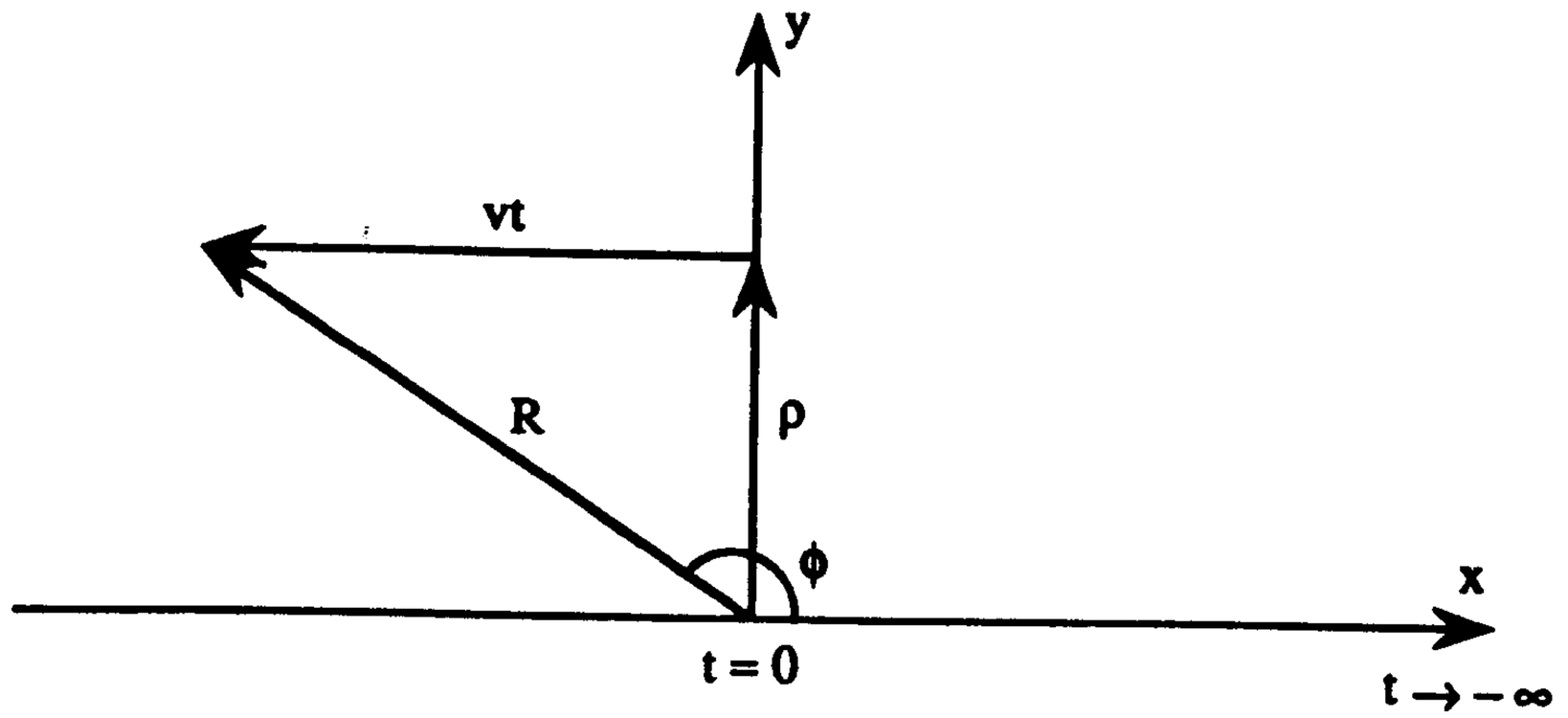

Figure F1.1 : Geometry of the Straight Path Trajectory

$$\mathbf{a}(\phi) = \begin{bmatrix} a_1(\phi) \\ a_2(\phi) \\ a_3(\phi) \end{bmatrix} \tag{F1.7.15}$$

$$\mathbf{a}'(\phi) = \begin{bmatrix} a'_1(\phi) \\ a'_2(\phi) \\ a'_3(\phi) \end{bmatrix} \equiv \begin{bmatrix} a_4(\phi) \\ a_5(\phi) \\ a_6(\phi) \end{bmatrix} \tag{F1.7.16}$$

$$\mathbf{A}(\phi) = -\frac{iR^2}{v\rho} \begin{bmatrix} \tilde{V} & -\frac{f}{3\sqrt{2}} e^{-i\zeta} & \frac{f}{\sqrt{6}} e^{-i\zeta-2i\phi} \\ -\frac{f}{3\sqrt{2}} e^{i\zeta} & \tilde{V} - \frac{f}{6} & -\frac{f}{2\sqrt{3}} e^{-2i\phi} \\ \frac{f}{\sqrt{6}} e^{i\zeta+2i\phi} & -\frac{f}{2\sqrt{3}} e^{2i\phi} & \tilde{V} + \frac{f}{6} \end{bmatrix} \tag{F1.7.17}$$

$$\mathbf{A}'(\phi) = -\frac{iR^2}{v\rho} \begin{bmatrix} \tilde{V} & \frac{f}{3\sqrt{2}} e^{-i\zeta} & -\frac{f}{\sqrt{6}} e^{-i\zeta+2i\phi} \\ \frac{f}{3\sqrt{2}} e^{i\zeta} & \tilde{V} - \frac{f}{6} & -\frac{f}{2\sqrt{3}} e^{2i\phi} \\ -\frac{f}{\sqrt{6}} e^{i\zeta-2i\phi} & -\frac{f}{2\sqrt{3}} e^{-2i\phi} & \tilde{V} + \frac{f}{6} \end{bmatrix} \tag{F1.7.18}$$

and

$$\zeta = -\frac{\omega R\cos(\phi)}{v}. \qquad \text{(F1.7.19)}$$

Note also that the subscript on the ground state expansion coefficient of Eq.F1.7.14 has been dropped because $b_1(\phi)$ is identical to $b_2(\phi)$ (see §6.4).

In principle, the coupled equations for the excited state (Eqs.F1.7.12 and F1.7.13) are each to be solved three times in succession (i = 1, 2, 3), each time adopting the boundary conditions

$$a_i(0) = \delta_{ik}\,; \qquad k = 1, 2, 3, \qquad \text{(F1.7.20)}$$

$$a'_i(0) = \delta_{ik}\,; \qquad k = 1, 2, 3, \qquad \text{(F1.7.21)}$$

and, in each case, the values of the expansion coefficients at $\phi = \pi$ constitute a single column in each of the two partitions of the S_l matrix. In practice, the three integrations of the equations may be performed simultaneously by replacing the column vectors $\mathbf{a}(\phi)$ and $\mathbf{a}'(\phi)$ by square matrices, denoted by $\mathbf{y}(\phi)$ and $\mathbf{y}'(\phi)$ respectively, where

$$\mathbf{y}(\phi) = \begin{bmatrix} y_{11}(\phi) & y_{12}(\phi) & y_{13}(\phi) \\ y_{21}(\phi) & y_{22}(\phi) & y_{23}(\phi) \\ y_{31}(\phi) & y_{32}(\phi) & y_{33}(\phi) \end{bmatrix} \equiv \begin{bmatrix} a_1(\phi) & a_1(\phi) & a_1(\phi) \\ a_2(\phi) & a_2(\phi) & a_2(\phi) \\ a_3(\phi) & a_3(\phi) & a_3(\phi) \end{bmatrix} \qquad \text{(F1.7.22)}$$

$$\mathbf{y}'(\phi) = \begin{bmatrix} y'_{11}(\phi) & y'_{12}(\phi) & y'_{13}(\phi) \\ y'_{21}(\phi) & y'_{22}(\phi) & y'_{23}(\phi) \\ y'_{31}(\phi) & y'_{32}(\phi) & y'_{33}(\phi) \end{bmatrix} \equiv \begin{bmatrix} a'_1(\phi) & a'_1(\phi) & a'_1(\phi) \\ a'_2(\phi) & a'_2(\phi) & a'_2(\phi) \\ a'_3(\phi) & a'_3(\phi) & a'_3(\phi) \end{bmatrix} \qquad \text{(F1.7.23)}$$

and replacing the boundary conditions of Eqs.F1.7.20 and F1.7.21 by the conditions

$$\mathbf{y}(0) = \mathbf{y}'(0) = \mathbf{I} \qquad \text{(F1.7.24)}$$

where $\mathbf{I}$ is the identity matrix. The solutions of the equations

$$\frac{d\mathbf{y}(\phi)}{d\phi} = \mathbf{A}(\phi)\,\mathbf{y}(\phi), \qquad \text{(F1.7.25)}$$

$$\frac{d\mathbf{y}'(\phi)}{d\phi} = \mathbf{A}'(\phi)\,\mathbf{y}'(\phi), \qquad \text{(F1.7.26)}$$

evaluated at $\phi = \pi$ are then directly equivalent to the partitions of the S_l matrix:

$$y(\pi) = S^{(i)}, \tag{F1.7.27}$$

$$y'(\pi) = S'^{(i)}. \tag{F1.7.28}$$

Here, $S^{(i)}$ is the upper left partition and $S'^{(i)}$ is the lower right partition of the S_l matrix which has the structure given by Eq.F1.7.29 below.

$$S_l = \begin{array}{c|cccccc} & (a_1) & (a_2) & (a_3) & (a'_1) & (a'_2) & (a'_3) \\ & |\tfrac{1}{2}\ -\tfrac{1}{2}> & |\tfrac{3}{2}\ -\tfrac{1}{2}> & |\tfrac{3}{2}\ \tfrac{3}{2}> & |\tfrac{1}{2}\ \tfrac{1}{2}> & |\tfrac{3}{2}\ \tfrac{1}{2}> & |\tfrac{3}{2}\ -\tfrac{3}{2}> \\ \hline (a_1)\ <\tfrac{1}{2}\ -\tfrac{1}{2}| & S^{(i)}_{11} & S^{(i)}_{12} & S^{(i)}_{13} & 0 & 0 & 0 \\ (a_2)\ <\tfrac{3}{2}\ -\tfrac{1}{2}| & S^{(i)}_{21} & S^{(i)}_{22} & S^{(i)}_{23} & 0 & 0 & 0 \\ (a_3)\ <\tfrac{3}{2}\ \tfrac{3}{2}| & S^{(i)}_{31} & S^{(i)}_{32} & S^{(i)}_{33} & 0 & 0 & 0 \\ (a'_1)\ <\tfrac{1}{2}\ \tfrac{1}{2}| & 0 & 0 & 0 & S'^{(i)}_{11} & S'^{(i)}_{12} & S'^{(i)}_{13} \\ (a'_2)\ <\tfrac{3}{2}\ \tfrac{1}{2}| & 0 & 0 & 0 & S'^{(i)}_{21} & S'^{(i)}_{22} & S'^{(i)}_{23} \\ (a'_3)\ <\tfrac{3}{2}\ -\tfrac{3}{2}| & 0 & 0 & 0 & S'^{(i)}_{31} & S'^{(i)}_{32} & S'^{(i)}_{33} \end{array} \tag{F1.7.29}$$

The rows and columns of matrix S_l are labelled with the $|\ j\ m\ >$ atomic states over which the alkali valence electron eigenfunction is expanded, together with the expansion coefficient associated with each state.

The single equation for the ground state (Eq.F1.7.14) is to be solved once only with the boundary condition

$$b(0) = 1 \tag{F1.7.30}$$

and the solution value at $\phi = \pi$ yields both elements of the S_f matrix:

$$b(\pi) = S^{(f)}_{11} = S^{(f)}_{22}. \tag{F1.7.31}$$

The S_f matrix has the structure given by Eq.F1.7.32 below.

$$S_f = \begin{array}{c|cc} & (b_1) & (b_2) \\ & |\tfrac{1}{2}\ \tfrac{1}{2}> & |\tfrac{1}{2}\ -\tfrac{1}{2}> \\ \hline (b_1)\ <\tfrac{1}{2}\ \tfrac{1}{2}| & S^{(f)}_{11} & 0 \\ (b_2)\ <\tfrac{1}{2}\ -\tfrac{1}{2}| & 0 & S^{(f)}_{22} \end{array} \tag{F1.7.32}$$

The labelling of the rows and columns of S_f has the same interpretation as given for matrix S_i above.

This completes the change of variable from t to ϕ; the new forms of the expansion coefficient equations, given by Eqs.F1.7.25, F1.7.26 and F1.7.14, are the ones actually solved by program IMPACT.

The next section returns to Step 4 of the computational procedure of IMPACT and describes the actions performed by this program loop.

F1.7.2 Actions of Step 4 of IMPACT

Step 4 of program IMPACT consists of a loop over the impact parameters contained in the set $\{\rho(I)\}$. For each $\rho(I)$, the following actions are performed in sequence:

(i) The grid of ϕ values, $\{\phi(J)\}$, on which to solve the expansion coefficient equations, is constructed.

(ii) The internuclear separations, $\{R(J)\}$, corresponding to the angles $\{\phi(J)\}$, are calculated.

(iii) The interatomic potentials are interpolated for values corresponding to the internuclear separations $\{R(J)\}$.

(iv) A second grid of ϕ values, $\{\phi_h(J)\}$, corresponding to the mid-points between each pair of ϕ values in $\{\phi(J)\}$, is constructed. (The need for these quantities, and those calculated by (v) and (vi) below, will become clear when the integration scheme used to solve the expansion coefficient equations is described later, in §F1.7.2.7.)

(v) The internuclear separations, $\{RH(J)\}$, corresponding to the angles $(\phi_h(J)\}$, are calculated.

(vi) The interatomic potentials are interpolated for values corresponding to the internuclear separations $\{RH(J)\}$.

(vii) The expansion coefficient equations (Eqs.F1.7.25, F1.7.26 and F1.7.14) are integrated to obtain the matrices S_i and S_f.

(viii) The quantity $\rho(I)\Pi(\rho(I))$ is calculated for the D1 and D2 resonance line components.

(ix) The quantities $\rho(I)P_{1/2\rightarrow 3/2}(\rho(I))$ and $\rho(I)P_{3/2\rightarrow 1/2}(\rho(I))$ are calculated.

Each of these actions is described in detail in the following sections.

F1.7.2.1 Constructing the Grid {ϕ(J)}

The solution grid on which the expansion coefficient equations are solved is defined by a set of angular points $\{\phi(J)\}$, with index J running from 0 to a maximum value N. In principle, the first grid point, $\phi(0)$, corresponds to $\phi = 0$; in practice, this boundary condition is approximated by (see Figure F1.1)

$$\phi(0) = \sin^{-1}\left[\frac{\rho(I)}{RMAX}\right] \qquad \text{(F1.7.33)}$$

where $\rho(I)$ is the impact parameter and RMAX is the maximum radius of influence. RMAX is provided in the input data to IMPACT (see §F1.4 and Table F1.1) and the value adopted in all cases is 40 au, the maximum internuclear separation at which the interatomic potentials are available. Similarly, the final grid point, $\phi(N)$, corresponds, in principle, to $\phi = \pi$; in practice, this boundary condition is approximated by

$$\phi(N) = \pi - \phi(0). \qquad \text{(F1.7.34)}$$

Between these limits, the grid points are separated by a constant interval of size s defined by

$$s = \frac{\phi(N) - \phi(0)}{N}. \qquad \text{(F1.7.35)}$$

A number of trial evaluations of the quantity $\rho\Pi(\rho)$ (using the methods to be described below) showed that for small impact parameters, the value of N used in Eq.F1.7.35 needs to be large in order to maintain numerical stability in the value of $\rho\Pi(\rho)$ whilst as ρ increases, the value of N may be decreased without loss of accuracy. The appropriate value of N, as a function of impact parameter, was determined by carrying out numerous evaluations of $\rho\Pi(\rho)$ at various impact parameters between 3 au and 36 au. Each evaluation was repeated with several different values for N (ranging from 100 to 10000), the value of N chosen as appropriate for the impact parameter $\rho(I)$ being the smallest N that maintained numerical stability in the value of $\rho\Pi(\rho)$. Here, numerical stability was

judged to be maintained from one value of N to another if the value of $\rho\Pi(\rho)$ changed by less than ~1%.

The results of these investigations for the four alkali-rare gas systems considered in the present study are summarised in Table F1.6 for the model potential interaction curves and in Table F1.7 for the pseudopotential curves. These calculations were carried out at a relatively low temperature (200K) since the grid point spacing was found to be less stringent (i.e., a smaller value of N was capable of maintaining numerical stability) for any given ρ as the temperature increases. The values shown in Tables F1.6 and F1.7 were used for all temperatures greater than 200K.

The dependence of N on ρ indicates that a small number of impact parameter regions may be defined within each of which a particular value of N is appropriate. Each such region is bounded by a lower limit in ρ, denoted RLOW(K), and an upper limit in ρ, denoted RUPP(K); within the region, the value of N to be used is denoted NINPT(K); the number of such regions is denoted by NREG. The values adopted for these parameters, on the basis of the results shown in Tables F1.6 and F1.7, are given in Table F1.8 for the model potential curves and in Table F1.9 for the pseudopotential curves. It should be noted that for impact parameters on the boundary of two regions, where

$$\text{RUPP(K)} = \text{RLOW(K+1)}\ ; \quad \text{K} = 1, \text{NREG} - 1, \tag{F1.7.36}$$

the *lower* value of NINPT (i.e., NINPT(K+1)) is the one that is used to define the ϕ-grid. These parameters are supplied as input data to program IMPACT (see §F1.4 and Table F1.1).

With the value of N appropriate to the impact parameter $\rho(I)$, the angular grid points are generated by the procedure

FOR J = 1, N - 1
$\quad\quad \phi(J) = \phi(0) + [J \times s]$
ENDFOR

where s is given by Eq.F1.7.35 and, together with $\phi(0)$ and $\phi(N)$, these points define the set $\{\phi(J)\}$.

Table F1.6 Number of Angular Grid Points : Model Potentials

	Value of N			
ρ (au)	LiHe	LiNe	NaHe	NaNe
3.0	4000	4000	4000	8000
4.0	2000	2000	4000	4000
5.0	2000	2000	2000	4000
6.0	1000	1000	2000	4000
7.0	1000	1000	1000	1000
8.0	200	200	400	400
12.0	100	100	100	100
16.0	100	100	100	100
20.0	100	100	100	100
24.0	100	100	100	100
28.0	100	100	100	100
32.0	100	100	100	100
36.0	100	100	100	100

Table F1.7 Number of Angular Grid Points : Pseudopotentials

	Value of N			
ρ (au)	LiHe	LiNe	NaHe	NaNe
3.0	4000	8000	8000	8000
4.0	4000	8000	8000	8000
5.0	2000	4000	4000	8000
6.0	2000	2000	4000	4000
7.0	1000	1000	2000	2000
8.0	400	400	1000	2000
12.0	100	100	100	200
16.0	100	100	100	100
20.0	100	100	100	100
24.0	100	100	100	100
28.0	100	100	100	100
32.0	100	100	100	100
36.0	100	100	100	100

Table F1.8 Grid Parameters : Model Potentials

System	NREG	RLOW(K) (au)	RUPP(K) (au)	NINPT(K)
LiHe	5	3.0	4.0	4000
		4.0	6.0	2000
		6.0	8.0	1000
		8.0	12.0	200
		12.0	38.0	100
LiNe	5	3.0	4.0	4000
		4.0	6.0	2000
		6.0	8.0	1000
		8.0	12.0	200
		12.0	38.0	100
NaHe	5	3.0	5.0	4000
		5.0	7.0	2000
		7.0	8.0	1000
		8.0	12.0	400
		12.0	38.0	100
NaNe	5	3.0	4.0	8000
		4.0	7.0	4000
		7.0	8.0	1000
		8.0	12.0	400
		12.0	38.0	100

Table F1.9 Grid Parameters : Pseudopotentials

System	NREG	RLOW(K) (au)	RUPP(K) (au)	NINPT(K)
LiHe	5	3.0	5.0	4000
		5.0	7.0	2000
		7.0	8.0	1000
		8.0	12.0	400
		12.0	38.0	100
LiNe	6	3.0	5.0	8000
		5.0	6.0	4000
		6.0	7.0	2000
		7.0	8.0	1000
		8.0	12.0	400
		12.0	38.0	100
NaHe	5	3.0	5.0	8000
		5.0	7.0	4000
		7.0	8.0	2000
		8.0	12.0	1000
		12.0	38.0	100
NaNe	5	3.0	6.0	8000
		6.0	7.0	4000
		7.0	12.0	2000
		12.0	16.0	200
		16.0	38.0	100

F1.7.2.2 Calculating the Internuclear Separations {R(J)}

The next action is to calculate the internuclear separation R(J) corresponding to each of the rotation angles in $\{\phi(J)\}$. The straight path trajectory assumption yields the relationship between R and ϕ:

$$R = \frac{\rho}{\sin(\phi)}. \qquad \text{(F1.7.37)}$$

Since the angles in $\{\phi(J)\}$ are distributed symmetrically about the element $\phi(N/2)$, corresponding to $\phi = \pi/2$, only R values corresponding to angles between $\phi(0)$ and $\phi(N/2)$ need to be calculated explicitly. The remaining R values (for angles greater than $\phi(N/2)$) are obtained by symmetry from these calculated values. The calculation is summarised by the following procedure:

Step 1 Set the initial radial value:
$R(0) = RMAX.$

Step 2 Calculate some of the radial values explicitly:

FOR $J = 1, \frac{N}{2} - 1$

$$R(J) = \frac{\rho(I)}{\sin(\phi(J))}.$$

ENDFOR
$R(N/2) = \rho(I).$

Step 3 Use symmetry to obtain the remaining radial values:

$K = \frac{N}{2} - 1.$
FOR $J = \frac{N}{2} + 1, N$
$R(J) = R(K).$
$K \leftarrow K - 1.$
ENDFOR

The R(J) values generated by this procedure are denoted collectively by {R(J)}.

F1.7.2.3 Interpolating the Interatomic Potentials

Having generated the grid of internuclear separations {R(J)} it is now necessary to obtain the interatomic potentials, defined as input data on the grid {RI(I)} (see §F1.4 and Table F1.1), on this new grid. Through the correspondence between {R(J)} and {ϕ(J)}, this gives the interatomic potentials as a function of rotation angle ϕ required for the solution of the expansion coefficient equations (Eqs.F1.7.25, F1.7.26 and F1.7.14). The interatomic potentials on the grid {R(J)} are obtained from the potentials defined on the grid {RI(I)} via interpolation, using the 4-point Lagrange formula described in §E1.7 of Appendix E1.

Recall that to interpolate a function F, defined on the grid {RI(I)}, for a value at the point R(J), an interpolation grid is constructed consisting of four grid points RI(K)... RI(K+3) such that

$$RI(K) \leq R(J) \leq RI(K+3) \qquad \text{(F1.7.38)}$$

and then the value of the function F at R(J) is given by

$$F(R(J)) = \sum_{m=K}^{K+3} l_m(R(J))\ F(RI(m)) \qquad \text{(F1.7.39)}$$

where

$$l_m(R(J)) = \prod_{\substack{n=K \\ n\neq m}}^{K+3} \left\{ \frac{R(J) - RI(n)}{RI(m) - RI(n)} \right\}. \qquad \text{(F1.7.40)}$$

The steps for carrying out the interpolation of the interatomic potentials to obtain their values on the grid {R(J)} are then as follows:

Step 1 Initialise the interpolation grid:

$K = 1$.

Step 2 Calculate the initial grid constants:

$$C_m = \prod_{\substack{n=K \\ n\neq m}}^{K+3} (RI(m) - RI(n)) ; \qquad m = K, K+3.$$

Step 3 **FOR each radial point R(J), J = $\frac{N}{2}, \frac{N}{2} - 1, \ldots, 1, 0$**

Ensure R(J) is on the interpolation grid:

IF R(J) > RI(K+3) THEN

Re-set interpolation grid: K ← K + 3.

Ensure interpolation grid wholly contained within {RI(I)} :

IF K > NIV-3 THEN

K ← NIV-3.

ENDIF

Update the grid constants:

$$C_m = \prod_{\substack{n=K \\ n \neq m}}^{K+3} (RI(m) - RI(n)) ; \qquad m = K, K+3.$$

ENDIF

Calculate differences and $l_m(R(J))$:

$$D_m = \prod_{\substack{n=K \\ n \neq m}}^{K+3} (R(J) - RI(n)) ; \qquad m = K, K+3.$$

$$l_m(R(J)) = \frac{D_m}{C_m}; \qquad m = K, K+3.$$

Calculate the interpolated functions:

$$VA(J) = \sum_{m=K}^{K+3} l_m(R(J))\ VAI(m).$$

$$VB(J) = \sum_{m=K}^{K+3} l_m(R(J))\ VBI(m).$$

$$VX(J) = \sum_{m=K}^{K+3} l_m(R(J))\ VXI(m).$$

$$VT(J) = \frac{1}{3} VB(J) + \frac{2}{3} VA(J).$$

$$VF(J) = VB(J) - VA(J).$$

ENDFOR

Step 4 **Use symmetry to obtain the remaining values:**

$$\mathbf{K = \frac{N}{2} - 1.}$$

$$\mathbf{FOR\ J = \frac{N}{2} + 1, N}$$

$$\mathbf{VA(J) = VA(K).}$$
$$\mathbf{VB(J) = VB(K).}$$
$$\mathbf{VX(J) = VX(K).}$$
$$\mathbf{VT(J) = VT(K).}$$
$$\mathbf{VF(J) = VF(K).}$$
$$\mathbf{K \leftarrow K - 1.}$$

ENDFOR

The output of the interpolation procedure consists of the $A^2\Pi$, $B^2\Sigma$ and $X^2\Sigma$ interatomic potentials corresponding to the internuclear separations {R(J)} (and thence to the rotation angles {ϕ(J)}) held in the arrays VA, VB and VX respectively. The opportunity is also taken here to calculate and store the evaluations, at the separations {R(J)}, of the quantities $\tilde{V}$ and f of Eqs.F1.7.4 and F1.7.5; these are held in arrays VT and VF respectively. Note that because of the symmetry of the {R(J)} values about the point R(N/2), the above procedure performs interpolation explicitly only for the values R(0) through to R(N/2) in Step 3; the symmetry is exploited in Step 4 to obtain the interatomic potentials and associated functions corresponding to the remaining R(J) values.

F1.7.2.4 Constructing the Grid {ϕ_h(J)}

In addition to the values of the interatomic potentials corresponding to the rotation angles {ϕ(J)} calculated above, the integration scheme adopted to solve the expansion coefficient equations (to be described below in §F1.7.2.7) also requires the values of the interatomic potentials at the mid-point between each adjacent pair of rotation angles in {ϕ(J)}. This section, and the next two, describe procedures for calculating these values and are analogous to the previous three sections dealing with the major grid points {ϕ(J)}.

The mid-point between each adjacent pair of rotation angles in {ϕ(J)} is calculated by the following procedure:

FOR J = 0, N - 1

$$\phi_h(J) = \phi(J) + \frac{s}{2}.$$

ENDFOR

where the step length, s, is defined by Eq.F1.7.35. The $\phi_h(J)$ values generated are denoted collectively by $\{\phi_h(J)\}$.

F1.7.2.5 Calculating the Internuclear Separations {RH(J)}

The internuclear separation RH(J) corresponding to each of the rotation angles $\{\phi_h(J)\}$ is calculated by a procedure analogous to that used for calculating the set {R(J)}:

Step 1 Calculate some of the radial values explicitly:

FOR $J = 0, \frac{N}{2} - 1$

$$RH(J) = \frac{\rho(I)}{\sin(\phi_h(J))}.$$

ENDFOR

Step 2 Use symmetry to obtain the remaining radial values:

$K = \frac{N}{2} - 1.$
FOR $J = \frac{N}{2}, N - 1$
$RH(J) = RH(K).$
$K \leftarrow K - 1.$
ENDFOR

The RH(J) values generated by this procedure are denoted collectively by {RH(J)}.

F1.7.2.6 Interpolating the Interatomic Potentials

The interatomic potentials corresponding to the rotation angles $\{\phi_h(J)\}$ are obtained by an interpolation procedure analogous to that described in §F1.7.2.3:

Step 1 Initialise the interpolation grid:
$K = 1.$

Step 2 Calculate the initial grid constants:

$$C_m = \prod_{\substack{n=K \\ n \neq m}}^{K+3} (RI(m) - RI(n)); \qquad m = K, K+3.$$

Step 3 **FOR each radial point RH(J), J = $\frac{N}{2}$ - 1, $\frac{N}{2}$ - 2, ..., 1, 0**

Ensure RH(J) is on the interpolation grid:

IF RH(J) > RI(K+3) THEN

Re-set interpolation grid: K ← K + 3.

Ensure interpolation grid wholly contained within{RI(I)} :

IF K > NIV-3 THEN

K ← NIV-3.

ENDIF

Update the grid constants:

$$C_m = \prod_{\substack{n=K \\ n\neq m}}^{K+3} (RI(m) - RI(n)) ; \qquad m = K, K+3.$$

ENDIF

Calculate differences and l_m(RH(J)):

$$D_m = \prod_{\substack{n=K \\ n\neq m}}^{K+3} (RH(J) - RI(n)) ; \qquad m = K, K+3.$$

$$l_m(RH(J)) = \frac{D_m}{C_m}; \qquad m = K, K+3.$$

Calculate the interpolated functions :

$$VAH(J) = \sum_{m=K}^{K+3} l_m(RH(J))\ VAI(m).$$

$$VBH(J) = \sum_{m=K}^{K+3} l_m(RH(J))\ VBI(m).$$

$$VXH(J) = \sum_{m=K}^{K+3} l_m(RH(J))\ VXI(m).$$

$$VTH(J) = \frac{1}{3} VBH(J) + \frac{2}{3} VAH(J).$$

$$VFH(J) = VBH(J) - VAH(J).$$

ENDFOR

Step 4 **Use symmetry to obtain the remaining values:**

```
K = N/2 - 1.
FOR J = N/2, N - 1
        VAH(J) = VAH(K).
        VBH(J) = VBH(K).
        VXH(J) = VXH(K).
        VTH(J) = VTH(K).
        VFH(J) = VFH(K).
        K ← K - 1.
ENDFOR
```

The output of the interpolation procedure consists of the $A^2\Pi$, $B^2\Sigma$ and $X^2\Sigma$ interatomic potentials corresponding to the internuclear separations {RH(J)} (and thence to the rotation angles $\{\phi_h(J)\}$) held in the arrays VAH, VBH and VXH respectively. The quantities $\tilde{V}$ and f of Eqs.F1.7.4 and F1.7.5, evaluated at the separations {RH(J)}, are held in arrays VTH and VFH respectively.

F1.7.2.7 Solving the Expansion Coefficient Equations

The equations to be solved in order to obtain the S_i and S_f matrices are Eqs.F1.7.25, F1.7.26 and F1.7.14, reproduced below (see §F1.7.1 for the definition of parameters).

$$\frac{dy(\phi)}{d\phi} = A(\phi)\, y(\phi), \tag{F1.7.41}$$

$$\frac{dy'(\phi)}{d\phi} = A'(\phi)\, y'(\phi), \tag{F1.7.42}$$

$$\frac{db(\phi)}{d\phi} = -\frac{iR^2}{v\rho} V_{X^2\Sigma}\, b(\phi). \tag{F1.7.43}$$

The method adopted to solve these equations is a fourth order Runge-Kutta integration scheme. For the general equation

$$\frac{dy(\phi)}{d\phi} = F(\phi, y(\phi)) \tag{F1.7.44}$$

this scheme is defined by (Abramowitz and Stegun (1972), Eq.25.5.10)

$$y(\phi(J)) = y(\phi(J\text{-}1)) + \frac{1}{6}(k_1 + 2k_2 + 2k_3 + k_4) + O(s^5) \qquad \text{(F1.7.45)}$$

where

$$\begin{aligned} k_1 &= sF[\phi(J\text{-}1),\ y(\phi(J\text{-}1))], \\ k_2 &= sF[\phi(J\text{-}1) + \tfrac{1}{2}s,\ y(\phi(J\text{-}1)) + \tfrac{1}{2}k_1], \\ k_3 &= sF[\phi(J\text{-}1) + \tfrac{1}{2}s,\ y(\phi(J\text{-}1)) + \tfrac{1}{2}k_2], \\ k_4 &= sF[\phi(J\text{-}1) + s,\ y(\phi(J\text{-}1)) + k_3], \end{aligned} \qquad \text{(F1.7.46)}$$

and s is the step length between the ϕ grid points. The error term $O(s^5)$ is neglected. The implementation of this scheme for solving Eqs.F1.7.41 - F1.7.43 consists of the following 12 steps:

Step 1 Initialise the solution values:

$\mathbf{y}(\phi(0)) = \mathbf{I}$,

$\mathbf{y}'(\phi(0)) = \mathbf{I}$,

$b(\phi(0)) = 1$.

Calculate the initial interaction matrices, $\mathbf{A}(\phi(0))$ and $\mathbf{A}'(\phi(0))$.

Initialise the solution grid index:

$J = 1$.

Step 2 Calculate the k_1 quantities:

$$k_1(n,m) = s \sum_{p=1}^{3} A_{np}(\phi(J\text{-}1))\, y_{pm}(\phi(J\text{-}1)); \qquad n, m = 1, 2, 3.$$

$$k'_1(n,m) = s \sum_{p=1}^{3} A'_{np}(\phi(J\text{-}1))\, y'_{pm}(\phi(J\text{-}1)); \qquad n, m = 1, 2, 3.$$

$$k''_1 = -\frac{iR(J\text{-}1)^2}{v\rho(I)}\, s\, VX(J\text{-}1)\, b(\phi(J\text{-}1)).$$

Step 3 Calculate the interaction matrices at the mid-point rotation angle, i.e., quantities $\mathbf{A}(\phi_h(J\text{-}1))$ and $\mathbf{A}'(\phi_h(J\text{-}1))$.

Step 4 **Calculate the modified solution matrices:**

$$\bar{y}_{nm}(\phi(J\text{-}1)) = y_{nm}(\phi(J\text{-}1)) + \frac{1}{2} k_1(n,m)\,; \quad n, m = 1, 2, 3.$$

$$\bar{y}'_{nm}(\phi(J\text{-}1)) = y'_{nm}(\phi(J\text{-}1)) + \frac{1}{2} k'_1(n,m)\,; \quad n, m = 1, 2, 3.$$

$$\bar{b}(\phi(J\text{-}1)) = b(\phi(J\text{-}1)) + \frac{1}{2} k''_1\,.$$

Step 5 **Calculate the k_2 quantities:**

$$k_2(n,m) = s \sum_{p=1}^{3} A_{np}(\phi_h(J\text{-}1))\, \bar{y}_{pm}(\phi(J\text{-}1))\,; \quad n, m = 1, 2, 3.$$

$$k'_2(n,m) = s \sum_{p=1}^{3} A'_{np}(\phi_h(J\text{-}1))\, \bar{y}'_{pm}(\phi(J\text{-}1))\,; \quad n, m = 1, 2, 3.$$

$$k''_2 = -\frac{iRH(J\text{-}1)^2}{v\rho(I)}\, s\, VXH(J\text{-}1)\, \bar{b}(\phi(J\text{-}1)).$$

Step 6 **Re-set the modified solution matrices:**

$$\bar{y}_{nm}(\phi(J\text{-}1)) = y_{nm}(\phi(J\text{-}1)) + \frac{1}{2} k_2(n,m)\,; \quad n, m = 1, 2, 3.$$

$$\bar{y}'_{nm}(\phi(J\text{-}1)) = y'_{nm}(\phi(J\text{-}1)) + \frac{1}{2} k'_2(n,m)\,; \quad n, m = 1, 2, 3.$$

$$\bar{b}(\phi(J\text{-}1)) = b(\phi(J\text{-}1)) + \frac{1}{2} k''_2\,.$$

Step 7 **Calculate the k_3 quantities:**

$$k_3(n,m) = s \sum_{p=1}^{3} A_{np}(\phi_h(J\text{-}1))\, \bar{y}_{pm}(\phi(J\text{-}1))\,; \quad n, m = 1, 2, 3.$$

$$k'_3(n,m) = s \sum_{p=1}^{3} A'_{np}(\phi_h(J\text{-}1))\, \bar{y}'_{pm}(\phi(J\text{-}1))\,; \quad n, m = 1, 2, 3.$$

$$k''_3 = -\frac{iRH(J\text{-}1)^2}{v\rho(I)}\, s\, VXH(J\text{-}1)\, \bar{b}(\phi(J\text{-}1)).$$

Step 8 **Re-set the modified solution matrices:**

$$\bar{y}_{nm}(\phi(J-1)) = y_{nm}(\phi(J-1)) + k_3(n,m)\,; \quad n, m = 1, 2, 3.$$

$$\bar{y}'_{nm}(\phi(J-1)) = y'_{nm}(\phi(J-1)) + k'_3(n,m)\,; \quad n, m = 1, 2, 3.$$

$$\bar{b}(\phi(J-1)) = b(\phi(J-1)) + k''_3\,.$$

Step 9 **Calculate the interaction matrices at the current major grid point, i.e., quantities $A(\phi(J))$ and $A'(\phi(J))$.**

Step 10 **Calculate the k_4 quantities:**

$$k_4(n,m) = s \sum_{p=1}^{3} A_{np}(\phi(J))\, \bar{y}_{pm}(\phi(J-1))\,; \quad n, m = 1, 2, 3.$$

$$k'_4(n,m) = s \sum_{p=1}^{3} A'_{np}(\phi(J))\, \bar{y}'_{pm}(\phi(J-1))\,; \quad n, m = 1, 2, 3.$$

$$k''_4 = -\frac{iR(J)^2}{v\rho(I)}\, s\, VX(J)\, \bar{b}(\phi(J-1)).$$

Step 11 **Calculate the new solution values:**

$$y_{nm}(\phi(J)) = y_{nm}(\phi(J-1)) + \frac{1}{6}\,(k_1(n,m) + 2k_2(n,m) + 2k_3(n,m) + k_4(n,m));$$

$$n, m = 1, 2, 3.$$

$$y'_{nm}(\phi(J)) = y'_{nm}(\phi(J-1)) + \frac{1}{6}\,(k'_1(n,m) + 2k'_2(n,m) + 2k'_3(n,m) + k'_4(n,m));$$

$$n, m = 1, 2, 3.$$

$$b(\phi(J)) = b(\phi(J-1)) + \frac{1}{6}\,(k''_1 + 2k''_2 + 2k''_3 + k''_4).$$

Step 12 **Increment the grid index and loop until the end of the grid is reached:**

J ← J + 1.

IF J ≤ N THEN

    Return to Step 2.

ELSE

    EXIT

ENDIF

The interaction matrices $A(\phi)$ and $A'(\phi)$ used by this procedure are defined in Eqs.F1.7.17 and F1.7.18 respectively. Because these matrices are closely related to each other in form, not all their elements need to be calculated explicitly on each integration step. The calculation of the matrices $A(\phi(J))$ and $A'(\phi(J))$, required in Step 1 and Step 9 of the above procedure, is implemented as follows:

Step 1 Calculate constants c_1 and c_2:

$$c_1 = -\frac{iR(J)^2}{v\rho(I)}.$$

$$c_2 = -\frac{\omega R(J)\cos(\phi(J))}{v}.$$

Step 2 Calculate the elements of the interaction matrix $A(\phi(J))$:

$$A_{11}(\phi(J)) = c_1\ VT(J).$$
$$A_{12}(\phi(J)) = -\frac{c_1}{3\sqrt{2}} VF(J)\exp(-ic_2).$$
$$A_{13}(\phi(J)) = \frac{c_1}{\sqrt{6}} VF(J)\exp[-i(c_2 + 2\phi(J))].$$
$$A_{21}(\phi(J)) = -A_{12}(\phi(J))^*.$$
$$A_{22}(\phi(J)) = c_1\,(VT(J) - \frac{1}{6} VF(J)).$$
$$A_{23}(\phi(J)) = -\frac{c_1}{2\sqrt{3}} VF(J)\exp(-2i\phi(J)).$$
$$A_{31}(\phi(J)) = -A_{13}(\phi(J))^*.$$
$$A_{32}(\phi(J)) = -A_{23}(\phi(J))^*.$$
$$A_{33}(\phi(J)) = c_1\,(VT(J) + \frac{1}{6} VF(J)).$$

Step 3 Calculate the elements of the interaction matrix $A'(\phi(J))$:

$$A'_{11}(\phi(J)) = A_{11}(\phi(J)).$$
$$A'_{12}(\phi(J)) = -A_{12}(\phi(J)).$$
$$A'_{13}(\phi(J)) = -A_{13}(\phi(J))\exp(4i\phi(J)).$$
$$A'_{21}(\phi(J)) = -A_{21}(\phi(J)).$$
$$A'_{22}(\phi(J)) = A_{22}(\phi(J)).$$
$$A'_{23}(\phi(J)) = -A_{23}(\phi(J))^*.$$
$$A'_{31}(\phi(J)) = -A'_{13}(\phi(J))^*.$$
$$A'_{32}(\phi(J)) = -A'_{23}(\phi(J))^*.$$
$$A'_{33}(\phi(J)) = A_{33}(\phi(J)).$$

The calculation of the mid-point interaction matrices, $\mathbf{A}(\phi_h(J))$ and $\mathbf{A}'(\phi_h(J))$, required in Step 3 of the integration procedure, is implemented in an analogous way. The equations for these matrix elements are obtained from the above expressions following the replacements

$$\begin{aligned} &R(J) \leftarrow RH(J), \\ &\phi(J) \leftarrow \phi_h(J), \\ &VT(J) \leftarrow VTH(J), \\ &VF(J) \leftarrow VFH(J). \end{aligned} \tag{F1.7.47}$$

The final solution matrices emerging from the above integration scheme are $\mathbf{y}(\phi(N))$, $\mathbf{y}'(\phi(N))$ and $\mathbf{b}(\phi(N))$. The matrices $\mathbf{y}(\phi(N))$ and $\mathbf{y}'(\phi(N))$ are equivalent to the two partitions of the $\mathbf{S}_l$ matrix (see Eq.F1.7.29):

$$\mathbf{y}(\phi(N)) = \mathbf{S}^{(i)}, \tag{F1.7.48}$$

$$\mathbf{y}'(\phi(N)) = \mathbf{S}'^{(i)}, \tag{F1.7.49}$$

where the full $\mathbf{S}_l$ matrix has the structure

$$\mathbf{S}_l = \begin{bmatrix} \mathbf{S}^{(i)} & 0 \\ 0 & \mathbf{S}'^{(i)} \end{bmatrix}. \tag{F1.7.50}$$

The solution value $\mathbf{b}(\phi(N))$ gives both elements of the $\mathbf{S}_f$ matrix (see Eq. F1.7.32):

$$\mathbf{b}(\phi(N)) = S_{11}^{(f)} = S_{22}^{(f)} \tag{F1.7.51}$$

where the $\mathbf{S}_f$ matrix has the structure

$$\mathbf{S}_f = \begin{bmatrix} S_{11}^{(f)} & 0 \\ 0 & S_{22}^{(f)} \end{bmatrix}. \tag{F1.7.52}$$

F1.7.2.8 Calculating $\rho\Pi(\rho)$

Having obtained the required S matrices, the next action of program IMPACT is to calculate the quantity $\rho\Pi(\rho)$ for the current impact parameter $\rho(I)$. $\Pi(\rho)$ is given by (cf. Eq.F1.1.2)

$$\Pi(\rho) = 1 - \sum_{\substack{m_i m_f \\ M}} \frac{< j_f\, l\, m_f\, M \mid j_i\, m_i >^2}{(2j_i + 1)} < j_f\, m_f \mid S_f \mid j_f\, m_f >^* < j_i\, m_i \mid S_i \mid j_i\, m_i > \qquad \text{(F1.7.53)}$$

where use has been made of the symmetry relation (cf. Eq.6.5.5. of §6.5)

$$S_f^{-1} = S_f^* \,. \qquad \text{(F1.7.54)}$$

For the D1 component of the alkali resonance line ($^2P_{1/2} \rightarrow {}^2S_{1/2}$), the following values of the quantum numbers apply:

$$\begin{aligned} &l = 1, \\ &j_i = \tfrac{1}{2}, \quad m_i = \pm\tfrac{1}{2}, \\ &j_f = \tfrac{1}{2}, \quad m_f = \pm\tfrac{1}{2}. \end{aligned} \qquad \text{(F1.7.55)}$$

Noting that the vector coupling coefficients are zero unless $M = m_i - m_f$, $\Pi(\rho(I))$ for the D1 resonance line component is given by

$$\begin{aligned} \Pi(\rho(I))_{D1} = 1 - \tfrac{1}{2} \Big\{ & < \tfrac{1}{2}\, 1\, \tfrac{1}{2}\, 0 \mid \tfrac{1}{2}\, \tfrac{1}{2} >^2 < \tfrac{1}{2}\, \tfrac{1}{2} \mid S_f \mid \tfrac{1}{2}\, \tfrac{1}{2} >^* < \tfrac{1}{2}\, \tfrac{1}{2} \mid S_i \mid \tfrac{1}{2}\, \tfrac{1}{2} > \\ & + < \tfrac{1}{2}\, 1\, \tfrac{1}{2}\, -1 \mid \tfrac{1}{2}\, -\tfrac{1}{2} >^2 < \tfrac{1}{2}\, \tfrac{1}{2} \mid S_f \mid \tfrac{1}{2}\, \tfrac{1}{2} >^* < \tfrac{1}{2}\, -\tfrac{1}{2} \mid S_i \mid \tfrac{1}{2}\, -\tfrac{1}{2} > \\ & + < \tfrac{1}{2}\, 1\, -\tfrac{1}{2}\, 1 \mid \tfrac{1}{2}\, \tfrac{1}{2} >^2 < \tfrac{1}{2}\, -\tfrac{1}{2} \mid S_f \mid \tfrac{1}{2}\, -\tfrac{1}{2} >^* < \tfrac{1}{2}\, \tfrac{1}{2} \mid S_i \mid \tfrac{1}{2}\, \tfrac{1}{2} > \\ & + < \tfrac{1}{2}\, 1\, -\tfrac{1}{2}\, 0 \mid \tfrac{1}{2}\, -\tfrac{1}{2} >^2 < \tfrac{1}{2}\, -\tfrac{1}{2} \mid S_f \mid \tfrac{1}{2}\, -\tfrac{1}{2} >^* < \tfrac{1}{2}\, -\tfrac{1}{2} \mid S_i \mid \tfrac{1}{2}\, -\tfrac{1}{2} > \Big\}. \end{aligned} \qquad \text{(F1.7.56)}$$

The vector coupling coefficients are evaluated in the manner described in §D1.2 of Appendix D1, that is, by writing them in terms of 3-j symbols via Eq.D1.2.25 and manipulating these using symmetry relations (Eqs.D1.2.26 - D1.2.28) into forms which may be evaluated directly from standard tables (Edmonds (1957), Appendix 2, Table 2). The coefficients required evaluate as follows:

$$
\begin{aligned}
&\langle \tfrac{1}{2}\,1\,\tfrac{1}{2}\,0 \mid \tfrac{1}{2}\tfrac{1}{2}\rangle = \frac{1}{\sqrt{3}},\\
&\langle \tfrac{1}{2}\,1\,\tfrac{1}{2}\,-1 \mid \tfrac{1}{2}\,-\tfrac{1}{2}\rangle = \sqrt{\frac{2}{3}}\,,\\
&\langle \tfrac{1}{2}\,1\,-\tfrac{1}{2}\,1 \mid \tfrac{1}{2}\tfrac{1}{2}\rangle = -\sqrt{\frac{2}{3}}\,,\\
&\langle \tfrac{1}{2}\,1\,-\tfrac{1}{2}\,0 \mid \tfrac{1}{2}\,-\tfrac{1}{2}\rangle = -\frac{1}{\sqrt{3}}.
\end{aligned}
\qquad \text{(F1.7.57)}
$$

Using Eqs.F1.7.29 and F1.7.32 to relate the S matrix elements to the atomic | j m > states, and the correspondence between the S matrices and the solutions $y(\phi(N))$, $y'(\phi(N))$ and $b(\phi(N))$ given in Eqs.F1.7.48, F1.7.49 and F1.7.51, Eq.F1.7.56 may then be written as

$$
\begin{aligned}
\Pi(\rho(I))_{D1} &= 1 - \left\{ \frac{1}{6}b^{*}y'_{11} + \frac{1}{3}b^{*}y_{11} + \frac{1}{3}b^{*}y'_{11} + \frac{1}{6}b^{*}y_{11} \right\}\\
&= 1 - \frac{1}{2}b^{*}(y'_{11} + y_{11})
\end{aligned}
\qquad \text{(F1.7.58)}
$$

where

$$
\begin{aligned}
&y'_{11} \equiv y'_{11}(\phi(N)),\\
&y_{11} \equiv y_{11}(\phi(N)),\\
&b \equiv b(\phi(N)).
\end{aligned}
\qquad \text{(F1.7.59)}
$$

For the D2 component of the alkali resonance line ($^2P_{3/2} \rightarrow {}^2S_{1/2}$), the following values of the quantum numbers apply:

$$
\begin{aligned}
&l = 1,\\
&j_i = \tfrac{3}{2}, \quad m_i = \pm\tfrac{1}{2}, \pm\tfrac{3}{2},\\
&j_f = \tfrac{1}{2}, \quad m_f = \pm\tfrac{1}{2}.
\end{aligned}
\qquad \text{(F1.7.60)}
$$

Again with $M = m_i - m_f$, $\Pi(\rho(I))$ for the D2 resonance line component is given by

$$\Pi(\rho(I))_{D2} = 1 - \frac{1}{4}\Big\{ \langle \tfrac{1}{2}1\,\tfrac{1}{2}1 | \tfrac{3}{2}\tfrac{3}{2}\rangle^2 \langle \tfrac{1}{2}\tfrac{1}{2} | S_f | \tfrac{1}{2}\tfrac{1}{2}\rangle^* \langle \tfrac{3}{2}\tfrac{3}{2} | S_i | \tfrac{3}{2}\tfrac{3}{2}\rangle$$

$$+ \langle \tfrac{1}{2}1\,\tfrac{1}{2}0 | \tfrac{3}{2}\tfrac{1}{2}\rangle^2 \langle \tfrac{1}{2}\tfrac{1}{2} | S_f | \tfrac{1}{2}\tfrac{1}{2}\rangle^* \langle \tfrac{3}{2}\tfrac{1}{2} | S_i | \tfrac{3}{2}\tfrac{1}{2}\rangle$$

$$+ \langle \tfrac{1}{2}1\,\tfrac{1}{2}\,-1 | \tfrac{3}{2}-\tfrac{1}{2}\rangle^2 \langle \tfrac{1}{2}\tfrac{1}{2} | S_f | \tfrac{1}{2}\tfrac{1}{2}\rangle^* \langle \tfrac{3}{2}-\tfrac{1}{2} | S_i | \tfrac{3}{2}-\tfrac{1}{2}\rangle$$

$$+ \langle \tfrac{1}{2}1\,\tfrac{1}{2}-2 | \tfrac{3}{2}-\tfrac{3}{2}\rangle^2 \langle \tfrac{1}{2}\tfrac{1}{2} | S_f | \tfrac{1}{2}\tfrac{1}{2}\rangle^* \langle \tfrac{3}{2}-\tfrac{3}{2} | S_i | \tfrac{3}{2}-\tfrac{3}{2}\rangle$$

$$+ \langle \tfrac{1}{2}1\,-\tfrac{1}{2}2 | \tfrac{3}{2}\tfrac{3}{2}\rangle^2 \langle \tfrac{1}{2}-\tfrac{1}{2} | S_f | \tfrac{1}{2}-\tfrac{1}{2}\rangle^* \langle \tfrac{3}{2}\tfrac{3}{2} | S_i | \tfrac{3}{2}\tfrac{3}{2}\rangle$$

$$+ \langle \tfrac{1}{2}1\,-\tfrac{1}{2}1 | \tfrac{3}{2}\tfrac{1}{2}\rangle^2 \langle \tfrac{1}{2}-\tfrac{1}{2} | S_f | \tfrac{1}{2}-\tfrac{1}{2}\rangle^* \langle \tfrac{3}{2}\tfrac{1}{2} | S_i | \tfrac{3}{2}\tfrac{1}{2}\rangle$$

$$+ \langle \tfrac{1}{2}1\,-\tfrac{1}{2}0 | \tfrac{3}{2}-\tfrac{1}{2}\rangle^2 \langle \tfrac{1}{2}-\tfrac{1}{2} | S_f | \tfrac{1}{2}-\tfrac{1}{2}\rangle^* \langle \tfrac{3}{2}-\tfrac{1}{2} | S_i | \tfrac{3}{2}-\tfrac{1}{2}\rangle$$

$$+ \langle \tfrac{1}{2}1\,-\tfrac{1}{2}\,-1 | \tfrac{3}{2}-\tfrac{3}{2}\rangle^2 \langle \tfrac{1}{2}-\tfrac{1}{2} | S_f | \tfrac{1}{2}-\tfrac{1}{2}\rangle^* \langle \tfrac{3}{2}-\tfrac{3}{2} | S_i | \tfrac{3}{2}-\tfrac{3}{2}\rangle \Big\}. \quad \text{(F1.7.61)}$$

The vector coupling coefficients evaluate as follows:

$$\begin{aligned}
&\langle \tfrac{1}{2}1\,\tfrac{1}{2}1 | \tfrac{3}{2}\tfrac{3}{2}\rangle = 1, \\
&\langle \tfrac{1}{2}1\,\tfrac{1}{2}0 | \tfrac{3}{2}\tfrac{1}{2}\rangle = \sqrt{\frac{2}{3}}, \\
&\langle \tfrac{1}{2}1\,\tfrac{1}{2}\,-1 | \tfrac{3}{2}-\tfrac{1}{2}\rangle = \frac{1}{\sqrt{3}}, \\
&\langle \tfrac{1}{2}1\,\tfrac{1}{2}-2 | \tfrac{3}{2}-\tfrac{3}{2}\rangle = 0, \\
&\langle \tfrac{1}{2}1\,-\tfrac{1}{2}2 | \tfrac{3}{2}\tfrac{3}{2}\rangle = 0, \\
&\langle \tfrac{1}{2}1\,-\tfrac{1}{2}1 | \tfrac{3}{2}\tfrac{1}{2}\rangle = \frac{1}{\sqrt{3}}, \\
&\langle \tfrac{1}{2}1\,-\tfrac{1}{2}0 | \tfrac{3}{2}-\tfrac{1}{2}\rangle = \sqrt{\frac{2}{3}}, \\
&\langle \tfrac{1}{2}1\,-\tfrac{1}{2}\,-1 | \tfrac{3}{2}-\tfrac{3}{2}\rangle = 1,
\end{aligned} \quad \text{(F1.7.62)}$$

and then, in terms of the solutions $y(\phi(N))$, $y'(\phi(N))$ and $b(\phi(N))$, Eq.F1.7.61 may be written as

$$\Pi(\rho(I))_{D2} = 1 - \Big\{ \tfrac{1}{4}b^* y_{33} + \tfrac{1}{6}b^* y'_{22} + \tfrac{1}{12}b^* y_{22} + \tfrac{1}{12}b^* y'_{22} + \tfrac{1}{6}b^* y_{22} + \tfrac{1}{4}b^* y'_{33} \Big\}$$

$$= 1 - \frac{1}{4}b^*(y_{33} + y'_{22} + y_{22} + y'_{33}) \quad \text{(F1.7.63)}$$

where

$$y_{ij} \equiv y_{ij}(\phi(N)),$$
$$y'_{ij} \equiv y'_{ij}(\phi(N)), \qquad \text{(F1.7.64)}$$
$$b \equiv b(\phi(N)).$$

The action of the current step of program IMPACT is therefore to calculate the quantities

$$\rho(I)\Pi(\rho(I))_{D1} = \rho(I)\left[\, 1 - \frac{1}{2} b^*(y'_{11} + y_{11}) \,\right], \qquad \text{(F1.7.65)}$$

$$\rho(I)\Pi(\rho(I))_{D2} = \rho(I)\left[\, 1 - \frac{1}{4} b^*(y_{33} + y'_{22} + y_{22} + y'_{33}) \,\right]. \qquad \text{(F1.7.66)}$$

F1.7.2.9 Calculating $\rho P_{j_i \to j'_i}(\rho)$

The final action of Step 4 of the computational procedure of IMPACT (see §F1.3) is to calculate the quantities $\rho P_{j_i \to j'_i}(\rho)$ for the current impact parameter $\rho(I)$. $P_{j_i \to j'_i}(\rho)$ is given by Eq.F1.1.4, reproduced below

$$P_{j_i \to j'_i}(\rho) = \frac{1}{(2j_i + 1)} \sum_{m_i\, m'_i} \left| < j'_i\, m'_i \mid S_i \mid j_i\, m_i > \right|^2. \qquad \text{(F1.7.67)}$$

In terms of the solution matrices $y(\phi(N))$ and $y'(\phi(N))$, the required quantities are calculated from

$$\rho(I)P_{1/2 \to 3/2}(\rho(I)) = \frac{1}{2}\left\{ |y_{21}|^2 + |y_{31}|^2 + |y'_{21}|^2 + |y'_{31}|^2 \right\}, \qquad \text{(F1.7.68)}$$

$$\rho(I)P_{3/2 \to 1/2}(\rho(I)) = \frac{1}{4}\left\{ |y_{12}|^2 + |y_{13}|^2 + |y'_{12}|^2 + |y'_{13}|^2 \right\}. \qquad \text{(F1.7.69)}$$

Since the S_i matrix is symmetric,

$$y_{ij} = y_{ji}\,, \qquad \text{(F1.7.70)}$$

the transition probabilities obey the relation

$$P_{1/2 \to 3/2}(\rho(I)) = 2\, P_{3/2 \to 1/2}(\rho(I)). \qquad \text{(F1.7.71)}$$

The actions described in §§F1.7.2.1 - F1.7.2.9 are repeated for each impact parameter contained in the set {ρ(I)}. The termination of this loop completes the actions performed by Step 4 of the IMPACT computational procedure.

F1.8 Step 5 : Widths, Shifts and Fine Structure State Changing Cross Sections

The previous step, Step 4, calculates the quantity $\rho\Pi(\rho)$ for the D1 and D2 components of the alkali resonance line and the quantity $\rho P_{j_i \rightarrow j'_i}(\rho)$ for $j_i = \frac{1}{2}, j'_i = \frac{3}{2}$ and for $j_i = \frac{3}{2}, j'_i = \frac{1}{2}$, at each impact parameter on the grid {ρ(I)}. The purpose of Step 5 of program IMPACT is to integrate these quantities over the impact parameter and subsequently to calculate the widths, shifts and fine structure state changing cross sections for the current temperature. The method of evaluating the integrals over the impact parameter is considered first.

F1.8.1 Integrating Over the Impact Parameter

Recall from §F1.5 that the grid of impact parameters {ρ(I)} extends from the lower limit SLOW(1) to the upper limit SUPP(MREG) and is divided into MREG regions, each with its own particular step size. Over the i^{th} region, the integral of a general function f(ρ) (standing for any of the quantities $\rho\Pi(\rho)_{D1}$, $\rho\Pi(\rho)_{D2}$, $\rho P_{1/2\rightarrow 3/2}(\rho)$, $\rho P_{3/2\rightarrow 1/2}(\rho)$) is calculated piece-wise using the 11-point Newton-Cotes integration formula introduced in §E1.9.1 of Appendix E1 (see Eq.E1.9.4). For the present integration, this scheme takes the form

$$\int_{\rho(I)}^{\rho(I+10)} f(\rho)\, d\rho = \frac{5.STEP(i)}{299376} \Big\{ 16067(f_I + f_{I+10}) + 106300(f_{I+1} + f_{I+9}) - 48525(f_{I+2} + f_{I+8}) + 272400(f_{I+3} + f_{I+7}) - 260550(f_{I+4} + f_{I+6}) + 427368 f_{I+5} \Big\} + O(STEP(i)^{13}) \qquad (F1.8.1)$$

where

$$f_I \equiv f(\rho(I)) \qquad (F1.8.2)$$

and STEP(i) is the separation of the grid points within the i^{th} region; the error term $O(STEP(i)^{13})$ is neglected. The choice of step size and boundaries of each region (see Tables F1.4 and F1.5) ensures that all MREG regions can be divided into an integer number of 11-point domains, the end point of one domain coinciding with the first point of the next. The number of such domains in the i^{th} region, denoted N_i, is given by

$$N_i = \left[\frac{SUPP(i) - SLOW(i)}{10 \times STEP(i)} \right]_{nint} \qquad (F1.8.3)$$

where 'nint' denotes conversion to the nearest integer. The integral of $f(\rho)$ over the i^{th} region, denoted I(i), is calculated by the application of Eq.F1.8.1 to each of the N_i domains, yielding the quantities

$$I_j(i) = \int_{domain\ j} f(\rho)\, d\rho\ ; \quad j = 1, N_i\ , \qquad (F1.8.4)$$

and then

$$I(i) = \int_{SLOW(i)}^{SUPP(i)} f(\rho)\, d\rho = \sum_{j=1}^{N_i} I_j(i). \qquad (F1.8.5)$$

Repeating this procedure for all MREG regions yields the integral of $f(\rho)$ over the entire grid:

$$I = \int_{SLOW(1)}^{SUPP(MREG)} f(\rho)\, d\rho = \sum_{i=1}^{MREG} I(i). \qquad (F1.8.6)$$

In principle, the integral should extend from 0 to ∞ (see Eqs.F1.1.3 and F1.3.2). In practice, the upper limit of Eq.F1.8.6, SUPP(MREG) is taken to be 38 au; this is considered to be large enough to approximate the required limit since both $\Pi(\rho)$ and $P_{j_i \rightarrow j'_i}(\rho)$ are close to zero for this, and all greater, impact parameters. A correction term is, however, added to Eq.F1.8.6 to account for the non-zero lower limit. The function being integrated is assumed to be linear in the interval [0, SLOW(1)] and a quantity c, defined by

$$c = \frac{1}{2} \,.\, SLOW(1) \,.\, f(\rho(0)), \qquad (F1.8.7)$$

is added to the integral calculated above. Thus

$$\int_0^{\infty} f(\rho)\, d\rho \equiv I + c. \qquad (F1.8.8)$$

Carrying out the above procedure with $f(\rho)$ replaced successively by $\rho\Pi(\rho)_{D1}$, $\rho\Pi(\rho)_{D2}$, $\rho P_{1/2\rightarrow 3/2}(\rho)$ and $\rho P_{3/2\rightarrow 1/2}(\rho)$ yields the quantities

$$I_1 = \int_0^\infty \rho\Pi(\rho)_{D1}\, d\rho, \qquad \text{(F1.8.9)}$$

$$I_2 = \int_0^\infty \rho\Pi(\rho)_{D2}\, d\rho, \qquad \text{(F1.8.10)}$$

$$I_3 = \int_0^\infty \rho P_{1/2\rightarrow 3/2}(\rho)\, d\rho, \qquad \text{(F1.8.11)}$$

$$I_4 = \int_0^\infty \rho P_{3/2\rightarrow 1/2}(\rho)\, d\rho. \qquad \text{(F1.8.12)}$$

F1.8.2 Calculating the Broadening Constants and Cross Sections

The final action of Step 5 is to calculate the D1 and D2 line widths and shifts, and the two fine structure state changing cross sections. In terms of the integrals evaluated above, the width (W/N) and shift (d/N) of the D1 resonance line component are calculated by (cf. Eq.F1.3.2)

$$\left[\frac{W}{N}\right]_{D1} = 6.12620\,(\,2\pi v\ \mathrm{Re}[I_1]\,), \qquad \text{(F1.8.13)}$$

$$\left[\frac{d}{N}\right]_{D1} = 6.12620\,(\,2\pi v\ \mathrm{Im}[I_1]\,), \qquad \text{(F1.8.14)}$$

where v is the rms velocity appropriate to the current temperature and the numerical factor (6.12620) converts from atomic units to units of 10^{-9} rad s^{-1} $atom^{-1}$ cm^3. Similarly, the width and shift of the D2 resonance line component are calculated by

$$\left[\frac{W}{N}\right]_{D2} = 6.12620\,(\,2\pi v\ \mathrm{Re}[I_2]\,), \qquad \text{(F1.8.15)}$$

$$\left[\frac{d}{N}\right]_{D2} = 6.12620\,(\,2\pi v\ \mathrm{Im}[I_2]\,). \qquad \text{(F1.8.16)}$$

The fine structure state changing cross sections are then calculated by (cf. Eq.F1.1.3)

$$\sigma_{1/2\rightarrow 3/2} = 2.80029 \times 10^{-17}\ (2\pi I_3), \qquad \text{(F1.8.17)}$$

$$\sigma_{3/2\rightarrow 1/2} = 2.80029 \times 10^{-17}\ (2\pi I_4), \qquad \text{(F1.8.18)}$$

where the numerical factor (2.80029×10^{-17}) converts from atomic units to units of cm^2.

F1.9 Step 6 : End of Temperature Loop

This step is the end of the temperature loop. If the last temperature value supplied in the input data to IMPACT has not yet been considered, the temperature variable is re-set to the next input value and the rms velocity corresponding to this temperature is calculated. Program control then passes back to Step 4 of the computational procedure of IMPACT. If all input temperatures have been considered, program control passes to the final step, Step 7.

F1.10 Step 7 : Output the Calculation Results

The final action of IMPACT is to write the results of the calculation described in §§F1.4 through F1.9 to the output file. The data written to this file consist of the following quantities:

(i) a copy of the input data for IMPACT (see §F1.4);

(ii) for each temperature considered:
- the width and shift of the D1 resonance line component;
- the width and shift of the D2 resonance line component;
- the fine structure state changing cross section for $j_i = \frac{1}{2} \rightarrow j'_i = \frac{3}{2}$;
- the fine structure state changing cross section for $j_i = \frac{3}{2} \rightarrow j'_i = \frac{1}{2}$.

This completes the functional description of program IMPACT.

References

References

Abramowitz M. and Stegun I. A. 1972 *Handbook of Mathematical Functions*, 9th ed. (New York: Dover Publications, Inc.).

Ahmad-Bitar R., Lapatovich W. P. and Pritchard D. E. 1977 *Phys. Rev. Lett.* **39** 1657.

Allard N. and Kielkopf J. 1982 *Rev. Mod. Phys.* **54** 1103.

Baird J. P., Eckart M. J. and Sandeman R. J. 1979 *J. Phys. B* **12** 355.

Balling L. C., Wright J. J. and Havey M. D. 1982 *Phys. Rev. A* **26** 1426.

Baur J. F. and Cooper J. 1977 *J. Quant. Spectrosc. Radiat. Transfer* **17** 311.

Baylis W. E. 1969 *J. Chem. Phys.* **51** 2665.

Behmenburg W. 1964 *J. Quant. Spectrosc. Radiat. Transfer* **4** 177.

Behmenburg W. and Kohn H. 1964 *J. Quant. Spectrosc. Radiat. Transfer* **4** 163.

Bottcher C. 1973 *Chem. Phys. Lett.* **18** 457.

Bottcher C., Cravens T. C. and Dalgarno A. 1975 *Proc. R. Soc. London, Ser. A* **346** 157.

Bottcher C. and Dalgarno A. 1974 *Proc. R. Soc. London, Ser. A* **340** 187.

Bottcher C., Dalgarno A. and Wright E. L. 1973 *Phys. Rev. A* **7** 1606.

Burgess D. D. and Grindlay J. E. 1970 *Astrophys. J.* **161** 343.

Carrington C. G., Drummond D., Gallagher A. and Phelps A. V. 1973 *Chem. Phys. Lett.* **22** 511.

Chatham R. H., Gallagher A. and Lewis E. L. 1980 *J. Phys. B* **13** L7.

Copley G. H. 1976 *Can. J. Phys.* **54** 619.

Dalgarno A. and Sando K. M. 1973 *Comm. Atom. Mol. Phys.* **4** 29.

Dehmer P. and Wharton L. 1972 *J. Chem. Phys.* **57** 4821.

Deleage J. P., Kunth D., Testor G., Rostas F. and Roueff E. 1973 *J. Phys. B* **6** 1892.

Eckart M. J. 1975 *J. Phys. B* **8** 852.

Edmonds A. R. 1957 *Angular Momentum in Quantum Mechanics* (Princeton: Princeton University Press).

Elbel M., Koch A. and Schneider W. 1972 *Z. Phys.* **255** 14.

Elward-Berry J. and Berry M. J. 1980 *J. Chem. Phys.* **72** 4500.

Gallagher A. 1975A *Atomic Physics* **4** 559, Edited by G. Zu Putlitz, E. W. Weber and A. Winnacker (New York and London: Plenum Press).

Gallagher A. 1975B *Phys. Rev. A* **12** 133.

Gatland I. R., Morrison W. F., Ellis H. W., Thackston M. G. and McDaniel E. W. 1977 *J. Chem. Phys.* **66** 5121.

Gay J. C. and Schneider W. 1976 *Z. Phys.* **A278** 211.

Geltman S. 1969 *Topics in Atomic Collision Theory* (New York and London: Academic Press).

Granier R., Charton G. and Granier J. 1981 *J. Quant. Spectrosc. Radiat. Transfer* **26** 71.

Hanssen J., McCarroll R. and Valiron P. 1979 *J. Phys. B* **12** 899.

Harris M., Lwin N. and McCartan D. G. 1982 *J. Phys. B* **15** L831.

Havey M. D. 1983 *private communication.*

Havey M. D., Frolking S. E. and Wright J. J. 1980 *Phys. Rev. Lett.* **45** 1783.

Havey M. D., Frolking S. E., Wright J. J. and Balling L. C. 1981 *Phys. Rev. A* **24** 3105.

Hedges R. E. M., Drummond D. L. and Gallagher A. 1972 *Phys. Rev. A* **6** 1519.

Herman P. S. and Sando K. M. 1978 *J. Chem. Phys.* **68** 1153.

Inouye H. and Kita S. 1973 *J. Phys. Soc. Japan* **34** 1588.

Jordan J. A. and Franken P. A. 1966 *Phys. Rev.* **142** 20.

Jungen M. and Staemmler V. 1988 *J. Phys. B* **21** 463.

Kachru R., Mossberg T. W. and Hartmann S. R. 1980 *J. Phys. B* **13** L363.

Kielkopf J. F. 1980 *J. Phys. B* **13** 3813.

Kita S., Noda K. and Inouye H. 1975 *J. Chem. Phys.* **63** 4930.

Krauss M., Maldonado P. and Wahl A. C. 1971 *J. Chem. Phys.* **54** 4944.

Lapatovich W. P., Ahmad-Bitar R., Moskowitz P. E., Renhorn I., Gottscho R. A. and Pritchard D. E. 1980 *J. Chem. Phys.* **73** 5419.

Lee C. J., Havey M. D. and Meyer R. P. 1990 *to be published in Phys. Rev. A.*

Lewis E. L. 1980 *Phys. Rep.* **58.**

Lwin N. 1976 *Thesis,* University of Newcastle upon Tyne (unpublished).

Lwin N., McCartan D. G. and Lewis E. L. 1976 *J. Phys. B* **9** L161.

Lwin N., McCartan D. G. and Lewis E. L. 1977 *Astrophys. J.* **213** 599.

Mack C. 1969 *Essentials of Statistics for Scientists and Technologists* (London: Heinemann Educational Books Ltd.).

Masnou-Seeuws F., Philippe M. and Valiron P. 1978 *Phys. Rev. Lett.* **41** 395.

McCartan D. G. and Farr J. M. 1976 *J. Phys. B* **9** 985.

Merzbacher E. 1970 *Quantum Mechanics,* 2nd ed. (New York: John Wiley & Sons, Inc.).

N'Dede Ebby and Weniger S. 1978 *J. Quant. Spectrosc. Radiat. Transfer* **19** 247.

Nieuwesteeg K. J., Leegwater J. A., Hollander Tj. and Alkemade C. Th. J. 1987 *J. Phys. B* **20** 487.

Pascale J. and Olson R. E. 1976 *J. Chem. Phys.* **64** 3538.

Pascale J. and Vandeplanque J. 1974 *J. Chem. Phys.* **60** 2278.

Peach G. 1978 *J. Phys. B* **11** 2107.

Peach G. 1988 *private communication.*

Peach G. 1990 *private communication.*

Philippe M., Masnou-Seeuws F. and Valiron P. 1979 *J. Phys. B* **12** 2493.

Phillips W. D., Glaser C. L. and Kleppner D. 1977 *Phys. Rev. Lett.* **38** 1018.

Pitre J. and Krause L. 1967 *Can. J. Phys.* **45** 2671.

Roueff E. 1972 *J. Phys. B* **5** L79.

Roueff E. 1974 *J. Phys. B* **7** 185.

Roueff E. 1975 *J. Phys. B* **8** L429.

Sando K. M. and Chu S-I. 1988 *Adv. At. Mol. Phys.* **25** 133.

Sando K. M. and Dalgarno A. 1971 *Mol. Phys.* **20** 103.
Sando K. M. and Wormhoudt J. C. 1973 *Phys. Rev. A* **7** 1889.
Saxon R. P., Olson R. E. and Liu B. 1977 *J. Chem. Phys.* **67** 2692.
Sayer B., Ferray M. and Lozingot J. 1979 *J. Phys. B* **12** 227.
Scheel N. and Griffing V. 1962 *J. Chem. Phys.* **36** 1453.
Scheps R., Ottinger Ch., York G. and Gallagher A. 1975 *J. Chem. Phys.* **63** 2581.
Schiff L. I. 1968 *Quantum Mechanics*, 3rd ed. (Tokyo: McGraw-Hill Kogakusha, Ltd.).
Schneider W. 1971 *Z. Phys.* **248** 387.
Schneiderman S. B. and Michels H. H. 1965 *J. Chem. Phys.* **42** 3706.
Smith G. and Collins B. S. 1976 *J. Phys. B* **9** L117.
Szudy J. 1980 *Ann. Phys. Fr.* **5** 255.
Tellinghuisen J. 1979 *J. Chem. Phys.* **71** 1283.
Visticot J. P., Szudy J., Ferray M. and Sayer B. 1981 *J. Phys. B* **14** 4755.
Visticot J. P., Szudy J. and Sayer B. 1981 *J. Phys. B* **14** 2329.
Walkup R., Spielfiedel A., Ely D., Phillips W. D. and Pritchard D. E. 1981 *J. Phys. B* **14** 1953.
Weber E. W. and Jungmann K. 1981 *Phys. Lett.* **81A** 223.
York G., Scheps R. and Gallagher A. 1975 *J. Chem. Phys.* **63** 1052.
Zimmermann M. and Miles R. B. 1981 *J. Phys. B* **14** L85.